Western Australian School of Mines: Minerals, Energy and Chemical Engineering

Oil-Water-Rock Interactions and Their Implications for Water- and 1-Pentanol-Assisted Enhanced Oil Recovery in Carbonate Reservoirs

Nasser Saleh 'Amur Al Maskari
0000-0001-5021-7716

This thesis is presented for the Degree of
Doctor of Philosophy
of
Curtin University

February 2021

DECLARATION

To the best of my knowledge and belief this thesis contains no material previously published by any other person except where due acknowledgment has been made.

This thesis contains no material which has been accepted for the award of any other degree or diploma in any university.

Signature:

Date: 27th of August 2020

COPYRIGHT

I warrant that I have obtained, where necessary, permission from the copyright owners to use any third-party copyright material reproduced in the thesis (e.g. questionnaires, artwork, unpublished letters), or to use any of my own published work (e.g. journal articles) in which the copyright is held by another party (e.g. publisher, co-author).

Signature:

Date: 27th of August 2020

DEDICATION

I would like to dedicate my thesis to my dear parents, for their encouragement, and their prayers to see me as a successful and educated person.

To my beloved wife and my children for their greatest support and encouragement.

To all my brothers, sisters, friends, and all relatives in Oman, for their encouragement and support.

ACKNOWLEDGMENT

In The Name of Allah, The Most Gracious, The Most Merciful

First of all, I am thankful to Allah for all the success I have had during my studies. Then, I would like to highly express my utmost sincere appreciation and gratitude to my main supervisor Dr. Quan Xie (Sam) for his guidance, encouragement, and support during my PhD study. Because of his professional supervision, I successfully achieved my research objectives and successfully completed my PhD study. Also, his insightful comments and guidance helped me to develop my research skills, which is well noticeable by my publications in the peer-review journals. Also, I would like to extend my utmost sincere appreciation and gratitude to my co-supervisor Associate Professor Ali Saeedi for his guidance, encouragement, and support during my PhD study. I am happy and proud to be under their supervision.

I would like to acknowledge the scholarship and financial support from Petroleum Development Oman (PDO) during my PhD study.

During this research at Curtin University, I was fortunate to associate with many wonderful colleagues in the Petroleum Engineering Department, and I worked with some of them in some projects. I appreciate all the researchers (previous and current PhDs students) who have offered me their friendship, advice, and support during my PhD study.

Ultimately, I am thankful to Almighty Allah for all opportunities that I have had. In addition, I wish to express my sincere thanks and gratitude to my parents, brothers, sisters, friends, and all relatives in Oman, for their encouragement and their prayers to see me as a successful and educated person. Finally, I would like to especially express my deepest sincere appreciation and gratitude to my wife (Moza Al Maskari), my lovely daughters (Balqees, Al Yamamah, and Maryam), and sons (Saleh, and Ali), for their patience, understanding, support, and encouragement that helped me tremendously throughout the duration of my PhD study. I would like to acknowledge that without their help, love, and forbearance, this project would not have been done.

ABSTRACT

Crude oil price has suffered the biggest fall since the 1991 due to ongoing trade disputes, cutting back CO_2 emissions, together with the COVID 19 pandemic. However, given that the crude oil is the largest source of energy in the world, it will remain important with increasing energy demand due to the development of the world industrial sector. Nevertheless, there is a pressing need to develop cost-effective and environmentally friendly approaches to improve the oil recovery in particular in carbonate reservoirs. This is because more than 60% of the world crude oil was discovered in carbonate reservoirs, and approximately 40% or less of the original oil in place can be produced by the primary recovery stage and secondary recovery stage. Low salinity waterflooding (also called smart waterflooding) appears to be a viable means to enhance oil recovery from carbonate reservoirs by shifting the relative permeability curves to a lower residual oil saturation. This shift is mainly governed by wettability alteration process occurring at oil-brine-carbonate interfaces. While this process has been investigated from pore (μm)- to core-scale (cm), detailed understanding at nanoscale with respect to oil adhesion forces as a function of pH and oil composition remains unclear. This presents a tremendous impediment and uncertainty to manage and predict the performance of low salinity waterflooding.

This research aims to gain a deeper understanding of the controlling factor(s) of oil-brine-carbonate system wettability with a combination of multi-scale experimental, analytical, and geochemical modeling approaches. The effect of oil composition (e.g., non-polar oil, and acidic oil components), carbonate mineral impurities (e.g., clay-rich carbonate), and calcite dissolution process on the adhesion of oil-brine-carbonate system at nanoscale and sub-pore scale have been examined. Moreover, with new understanding from the above work, a novel alcohol-assisted enhanced oil recovery (EOR) means was proposed and investigated with multi-scale experimental and analytical approaches.

Results show that the increase of local pH during low salinity waterflooding reduces the adhesion forces between the oil components and carbonate (clay) surfaces due to the increase of electrostatic forces at the oil-brine and brine-carbonate (clay) interfaces, altering the wettability of carbonate system toward hydrophilicity. The results shed light on the significance of pH increase during low salinity water injection on adhesion of oil components ($-CH_3$ and –COOH) on carbonate (clay) surfaces, providing insights into wettability alteration process at nanoscale. In addition, surface roughness variation resulted from calcite dissolution process in low salinity water plays a negligible role in contact angle, confirming that contact angle measurement remains a valid approach to directly examine the wettability alteration process in the low salinity waterflooding.

Our results also show that intermediate carbon chain alcohol shifts the wettability of the oil−brine−carbonate system to less oil-wet or more water-wet, implying a greater hydrophilicity compared to other short carbon chain alcohols. In addition, the number of −OH functional group in an alcohol has a negligible effect on the contact angle, whereas increasing the length of the carbon chain likely increases the concentration of −OH at the oil−brine interfaces, which likely breaks the *in-situ* bridges between oil and calcite surfaces hence increasing hydrophilicity. Furthermore, coreflooding experiments show that wettability alteration process achieved by 1-pentanol alcohol at sub-pore level would trigger oil detachment, coalescence, transport and thus enhance oil recovery.

In conclusion, this research extends our knowledge of oil-brine-carbonate system wettability from core (cm)-, pore (μm)-scale to nanoscale, providing additional evidence with respect to oil adhesion as a function of oil composition and a local pH increase. Moreover, one of the more significant findings to emerge from this study is that 1-pentanol-assisted waterflooding would be a promising EOR means for carbonate reservoirs where low salinity water/freshwater is not available even for high temperature and high salinity reservoir conditions.

LIST OF PUBLICATIONS

Published papers forming part of the thesis as chapters:

1- **Al Maskari,** N.S., A. Sari, M.M. Hossain, A. Saeedi, and Q. Xie, Response of Non-Polar Oil Component on Low Salinity Effect in Carbonate Reservoirs: Adhesion Force Measurement Using Atomic Force Microscopy. Energies, 2020. 13(1): p. 77. https://doi.org/10.3390/en13010077.

2- **Al Maskari,** N.S., M. Almobarak, A. Saeedi, and Q. Xie, Influence of pH on Acidic Oil–Brine–Carbonate Adhesion Using Atomic Force Microscopy. Energy & Fuels, 2020. 34(11): p. 13750-13758. https://doi.org/10.1021/acs.energyfuels.0c02494 .

3- **Al Maskari**, N.S., Q. Xie, and A. Saeedi, Role of Basal-Charged Clays in Low Salinity Effect in Sandstone Reservoirs: Adhesion Force on Muscovite using Atomic Force Microscope. Energy & Fuels, 2019. 33(2): p. 756-764. https://pubs.acs.org/doi/10.1021/acs.energyfuels.8b03452.

4- **Al Maskari**, N.; Sari, A.; Saeedi, A.; Xie, Q. Influence of Surface Roughness on the Contact Angle due to Calcite Dissolution in an Oil–Brine–Calcite System: A Nanoscale Analysis Using Atomic Force Microscopy and Geochemical Modeling. Energy & Fuels, 2019. 33(5): p. 4219-4224. https://doi.org/10.1021/acs.energyfuels.9b00739.

5- **Al Maskari**, N.S., A. Saeedi, and Q. Xie, Alcohol-Assisted Waterflooding in Carbonate Reservoirs. Energy & Fuels, 2019. 33(11): p. 10651-10658. https://doi.org/10.1021/acs.energyfuels.9b02497.

6- **Al Maskari**, N.S., E. Arjomand, M. Almobarak, A. Saeedi, and Q. Xie, 1-Pentanol-Assisted Waterflooding in High Salinity Brine up to 140 °C in Carbonate Reservoirs. Energy & Fuels, 2020. 34(10): p. 12215-12224. https://doi.org/10.1021/acs.energyfuels.0c01953

TABLE OF CONTENTS

LIST OF FIGURES

LIST OF TABLES

NOMENCLATURE

Abbreviations

AFM	Atomic force microscopy
AN	Acid number
AR	Analytical reagent
BN	Base number
BPS	Bound product sum
CA	Contact angle
CEC	Cation exchange capacity
CEOR	Chemical enhanced oil recovery
CF	Core flooding
DLVO	Derjaguin, Landau, Verwey, and Overbeek
EOR	Enhance oil recovery
FB	Formation brine
FBP	Formation brine + 0.4 wt% of 1-pentanol
HS	High salinity
IFT	Interfacial tension
LS	Low salinity
LSW	Low salinity water
OOIP	Original oil in place
QCM	Quartz crystal microbalance
TDS	Total dissolved solid

Units

C	Coulombs
^{o}C	Degree Celsius

cc/min	Cubic centimeter per minute
C/(V.m)	Coulombs per volt metre
dyn/cm	Dyne per centimeter
g/cm^3	Gram per cubic centimeter
g/L	Gram per liter
h	Hour
J	Joule
J/K	Joule per kelvin
M	Molar
mM	millimolar
MPa	Mega Pascal
mg/g	milligram per gram
mol/mol	Mole per mole
mg/l	milligram per liter
mg KOH/g	milligram of potassium hydroxide per gram
m^2/g	Square metre per gram
MΩ	Megaohm
mol/L	Mole per liter
mV	millivolt
nm	Nanometer
nN	Nano-Newton
N/m	Newton per meter
pN	Pico-Newton
ppm	Part per million
psi	Pound per square inch

PV	Pore volume
wt%	Weight percent
μm	Micrometer
μmol	Micromole
μmol/m^2	Micromole per square metre

Symbols

A	Hamaker constant (J)
A_s	Constant range between 10^6 to 5×10^8 Pa.
e	Charge of electron (1.60×10^{-19} C)
$F_{adh}^{pH\ i}$	Adhesion force at pH (i)
ΔF_{adh}	Change in adhesion force
h	Distance between the two surfaces (m)
k	Debye length of aqueous solutions (m^{-1})
k_B	Boltzmann constant (1.381×10^{-23} J/K)
$K_{rw}(S_{orw})$	Water relative permeability at residual oil saturation
n_b	Total ion density in the bulk solution
R	Radius of sphere (m)
Ra	Average roughness
$RF_{Breakthrough}$	Recovery factor at breakthrough
RF_{Total}	Total recovery factor
r	Roughness factor
S_o	Oil saturation
S_{or}	Residual oil saturation
S_{wi}	Irreducible water saturation

T	Temperature in kelvin
z	Valence of the asymmetrical electrolyte solution
$\bar{z}$	Arithmetic average height

Greek Symbols

ζ	Zeta potential
ε	Vacuum permittivity (8.85×10^{-12} C/(V.m))
ε_o	Oil permittivity (2 C/(V.m))
ε_w	Water permittivity (78.3 C/(V.m))
ε_s	Rock permittivity (7 C/(V.m)).
ψ_1	Zeta potential of the brine-rock interface
ψ_2	Zeta potential of the oil-brine interface
λ_0	Decay length (range between 0.2 to 1 nm)
θ	Contact angle
$\prod_{(EDL)}$	Electric double layer forces (Pa)
$\prod_{(STR)}$	Structural forces (Pa)
$\prod_{(Total)}$	Total disjoining pressure (Pa)
$\prod_{(vdw)}$	Van der Waals forces (Pa)

Chapter 1. Introduction

1.1 Background

At the beginning of 2020, the geopolitical and geographical tensions together with the COVID 19 pandemic affect the crude oil price leading to the biggest fall in the crude oil price since 1991. However, the global energy demand continues to increase due to the development of the global industrial sector, thus increasing the importance of crude oil because it remains the largest energy source in the world. Therefore, there is a pressing need to improve oil production efficiency by developing cost-effective and environmentally friendly techniques to enhance oil recovery (EOR). Due to the fact that more than 60% of the world crude oil was discovered in carbonate reservoirs [1, 2], and approximately only 40% of original oil in place can be produced by the primary recovery stage and secondary recovery stage [3]. In the secondary recovery stage, saline water would be usually injected into the reservoir to maintain the reservoir pressure and thus improve oil recovery. However, in this process, the injected water may not be able to reduce the residual oil saturation and enhance oil recovery.

Since the inception of low salinity waterflooding in sandstone two decades ago (which is also called i.e., *LoSal flooding* [4-6], *Designer waterflooding* [7-9]), the same concept was used with an aim to enhance oil recovery from carbonate reservoirs, and also named a *Smart waterflooding*. [7, 10-17] The nature of the physics involved in this process is to reduce the residual oil saturation hence enhancing oil recovery through fluid-fluid-rock interactions.

Published work shows that low salinity water or smart water yields 5-30% additional oil recovery in carbonate reservoirs compared to conventional oil recovery [11, 14, 15, 18-24], with experimental evidence from contact angle [25-28], spontaneous imbibition [29-31], and forced imbibition (core flooding) experiments. While the low salinity waterflooding has been studied extensively in sandstone reservoirs with more than ten plausible mechanisms [11, 32-41], the controlling factor(s) of low salinity flooding in carbonate reservoirs remains incomplete, which present a substantial impediment for the implementation of low salinity flooding in carbonate reservoirs.

To constrain the uncertainties of low salinity waterflooding in carbonate reservoirs, a few mechanisms have been proposed, such as mineral dissolution (calcite and anhydrite) [15, 23, 42], change of carbonate surface charges [24, 43], a combination of the mineral dissolution and change of surface charge [44, 45], electrical double-layer theory [46-49], in-situ surfactant generation [50], and variations in interface viscoelasticity [7, 33, 36, 41, 51], and formation of micro dispersions [39, 52].

The above mechanisms can be categorized into three categories: (1) Fluid-fluid interactions, which include variations in interface viscoelasticity [7, 33, 36, 41, 51] and formation of micro-

dispersions [39, 52] mechanisms. In this classification, the suggested mechanisms point to the interaction between the oil and brine (fluid-fluid interaction) [53]. (2) Fluid-rock interactions – this includes mineral dissolution (calcite and anhydrite) [15, 23, 42] and *in-situ* surfactant generation [50] mechanisms. In this category, the low salinity effect was elucidated based on the brine-carbonate (fluid-rock) interaction with neglecting the effect of the oil composition on the wettability. (3) Fluid-fluid-rock interactions – this physiochemical process includes electrical double-layer theory [42, 48, 49, 54], adsorption of potential determining ions (PDI) [24, 55-57], and the surface complexation at oil-brine and brine-carbonate surfaces [58-61]. Publishes work also shows that oil-brine-carbonate interactions play an important role in wettability alteration, which has been identified as a key process to trigger incremental oil recovery.

Wettability alteration process likely shifts the oil relative permeability towards a lower residual oil saturation. [22, 23, 25, 34, 49, 62-65] This process will not only accelerate the oil production, but also lower the residual oil saturation. Several key factors have been reported to influence the wettability alteration of carbonate surfaces such as brine salinity and composition [21, 22, 25, 29, 48, 57, 60, 66], oil composition [21, 42, 48, 66-69], mineralogy of the rock surface [25, 66, 68-70], saturation history [49, 66, 69, 71], and system temperature [29, 42, 48, 66, 67]. However, few studies have been done to reveal the impact of oil-brine-carbonate interactions on fluids flow in porous media with a combination of multi-scale experimental techniques, i.e., nanoscale, sub-pore scale, and core scale. This provides a tremendous impediment to identify the scalable mechanism(s) which leads to oil detachment, coalescence, transport, and oil banking. Moreover, fewer works have been done to look beyond the new enhanced oil recovery (EOR) techniques based on the insights of oil-brine-rock interactions.

To be more specific, most of the studies elucidated the wettability alteration based on results obtained from the contact angle experiments, zeta potential measurements, spontaneous imbibition, and force flooding experiments, without understanding the wettability alteration at the nanoscale (the basic oil-brine-rock interactions). This presents a tremendous impediment to quantify the response of oil composition on the low salinity effect associated with wettability alteration. For example, published work indicates that crude oil components play an important role in the wettability of the oil-brine-carbonate system from contact angle [46, 61, 64, 68], surface complexation modeling [42, 58, 60, 61, 72], and core flooding experiments [15, 56, 73-75]. However, what is not yet clear is the impact of polar (e.g., $-COO^-$, $-NH^+$) and non-polar (e.g., $-CH_3$) on oil adhesion at pore surfaces with the presence of various brines in particular from the experimental point of view.

Moreover, while existing work confirms that mineralogy of carbonate rocks likely affects the oil-brine-carbonate system adhesion, no previous study has investigated the effect of impurities (clay-rich carbonate) on the low salinity effect. Furthermore, contact angle measurement has been widely used to assess the low salinity effect as a result of the wettability shift. However, there has been no reliable evidence that the calcite dissolution on substrates in low salinity water may [76] affect the contact angle results. This uncertainty generates concerns about wettability shift estimation through contact angle measurements during low salinity waterflooding in carbonate reservoirs. Taken together, more research is needed to better understand the controls of oil-brine-carbonate interactions pertaining to the wettability shift.

One source of weakness in low salinity waterflooding in carbonate reservoirs for EOR purpose is the lack of freshwater in some regions, such as the Middle East (host 70% of carbonate fields in the world), East of China, and offshore oil fields. Hence, research is urgently needed to enhance oil recovery from carbonate reservoirs where high salinity brine is the only available source. There is, therefore, a definite need for exploring new cost-effective, and environmentally friendly means in light of existing knowledge in oil-brine-carbonate interactions. Published work suggests that adsorption of the potential determining ions (Mg^{2+}, Ca^{2+}, and SO_4^{2-}) onto the carbonate leads to detachment of the acidic oil from the carbonate surface [15, 24, 55-57, 77], which results in wettability alteration thereby enhancing oil recovery. Also, surface complexation modeling shows that low salinity water breaks the electrostatic bridges between the opposite charges species on the carbonate surface ($>CO_3^-$, $>CaCO_3^-$, $>CaOH_2^+$, $>CO_3Ca^+$) and oil surface ($-COO^-$, $-NH^+$, $-COOCa^+$**)** [58, 60, 61, 72, 78]. Collectively together, these existing knowledge shed light on the wettability shift by breaking the bridges possibly through chemical additives, which may bridge the functional groups from oil surfaces and thus breaking the bonds between oil and rock surfaces. For this study, alcohol-based chemical additives were used to explore the possible wettability alteration on carbonate surfaces even at high salinity and high temperature conditions.

1.2 Research Objectives

This research aims to answer the following two main questions in the area of low salinity waterflooding in carbonate reservoirs.

1) Wettability alteration appears to be an important physicochemical process during the low salinity waterflooding in carbonate reservoirs. However, how do oil compositions (e.g., acid number and base number), calcite dissolution process affect the oil adhesion at the nanoscale and sub-pore scale? Also, how do these processes contribute to oil detachment, coalescence, and transport in porous media?

2) While low salinity waterflooding has been confirmed as an appealing EOR means, can we take advantage of the existing knowledge in oil-brine-carbonate interactions to explore the new EOR techniques for carbonate reservoirs where is a lack of low salinity water/fresh water, especially for high temperature and high salinity carbonate reservoirs?

To answer the questions outlined above, a combination of atomic force microscopy, zeta potential, contact angle, core flooding, and analytical modeling have been conducted to gain a better understanding of the wettability alteration process of the oil-brine-carbonate system from the nanoscale to core scale. Moreover, alcohol-assisted EOR techniques have been explored for EOR purposes in carbonate reservoirs even at high temperature and high pressure conditions with the following sub-objectives.

1. Elucidating the effect of water chemistry on adhesion force between the non-polar oil component and calcite surface by conducting atomic force microscopy (AFM) measurements.
2. Revealing the effect of water chemistry on adhesion force between polar oil components and calcite surface by conducting AFM measurements.
3. Detailing the effect of water chemistry on adhesion force between polar oil component and clay: implications for low salinity effect in clay-rich carbonate reservoirs.
4. Understanding the effect of calcite dissolution on the wettability of the oil-brine-calcite system at the sub-pore scale by testing the surface roughness using AFM and measuring the contact angle.
5. Shifting the wettability of carbonate towards hydrophilicity by adding alcohol-based chemical additives in brines.
6. Expanding the application of alcohol-assisted EOR to high temperature and salinity carbonate reservoir.

The main methodologies used in this research to achieve these research objectives are briefly listed as the following:

1. To achieve objective #1, the influence of brine chemistry on the interaction between non-polar oil component and calcite surface was investigated using AFM. In addition, to gain a better isotherm thermodynamic understanding, we measured the zeta potential of the oil-brine and brine-calcite interfaces, and calculated the disjoining pressure isotherm. Furthermore, the contact angle of the non-polar oil-brine-calcite system was measured to compare with AFM and disjoining pressure isotherm.
2. To achieve objective #2, AFM was used to study the impact of water chemistry on the adhesion force between the polar oil components and calcite. Additionally, the zeta potential of the oil-brine and brine-calcite interfaces was measured for the calculation

of disjoining pressure isotherm. Moreover, the contact angle of the polar oil-brine-calcite system was measured to compare with AFM and disjoining pressure isotherm.

3. To achieve objective #3, the effect of the brine chemistry on the interaction between oil components (polar and non-polar) and mica was investigated by measuring adhesion force using AFM, together with zeta potential measurements and disjoining pressure isotherm calculation.
4. To achieve objective #4, both AFM and contact angle experiments were conducted to study the effect of calcite dissolution on the contact angle of the oil-brine-calcite system at the sub-pore scale.
5. To achieve objective #5, the influence of adding a small percentage of different alcohols on the hydrophobicity of the oil-brine-calcite system was investigated by measuring the contact angle and zeta potential of oil-brine and brine-calcite interfaces.
6. To achieve objective #6, I measured the contact angles of oil droplets on calcite substrate in the presence of 1-pentanol in high and low salinity brines at different temperatures (60, 100, 140^{o}C), and pressure (10, 20, 30, 40 MPa). Subsequently, core flooding experiments were performed to examine the impact of the wettability alteration process at the sub-pore level, which would trigger oil detachment, coalescence, transport, and thus enhance oil recovery for high temperature and high salinity carbonate reservoirs.

1.3 Outline and Organisation

To achieve the above objectives, the following ten chapters were performed to elucidate the wettability alteration of the oil-brine-carbonate system from the nanoscale to the core scale. Chapter 1 & 2 present the research introduction and literature review. Chapter 3 demonstrates the research framework and the methodologies used to achieve the goals of this research. Then a combination of experimental (AFM, zeta potential, contact angle experiments) and analytical calculation (disjoining pressure isotherm) were obtained in Chapter 4-6. These Chapters cover the effect of the oil compositions and water chemistry on the wettability alteration of the oil-brine-carbonate system at the nanoscale and pore scale. Furthermore, the surface roughness and contact angle measurements were carried out to examine the impact of surface roughness on the contact angle due to calcite dissolution in an oil−brine−calcite system at sub-pore and pore-scale in Chapter 7. Moreover, the potential of adding a low concentration of alcohol to the injected water on increasing the hydrophilicity of the oil-brine-carbonate system was investigated in Chapter 8-9. Finally, Chapter 10 presents the overall conclusions and the recommendation for future work.

Chapter 2. Literature Review

2.1 Introduction

Two-thirds of the global oil's was discovered in the carbonate formations [1, 2], and less than 40% of the oil can be extracted by the primary stage (e.g., pressure depletion process) and secondary stage (e.g., water injection, gas injection) [3]. This means that more than 60% of oil remain at subsurface after the extraction. Therefore, the petroleum industry has been continuously working to find economically applicable techniques to enhance oil recovery, and thus meets the global energy demand with minimum environmental footprint. Since the inception of low salinity waterflooding in sandstone reservoirs two decades ago, a similar concept of waterflooding, e.g., smart waterflooding [10-16], low salinity waterflooding [18, 19, 64, 65, 79-84], engineered waterflooding [83, 85] has been proposed and examined with an aim to enhanced oil recovery from carbonate reservoirs. Published work shows that low salinity flooding likely yield 5-30% incremental oil recovery compared to conventional high salinity water injection (or formation brine reinjection) [11, 14, 15, 18, 19, 22, 23, 65].

To understand the physics behind the incremental oil recovery for managing and predicting the low salinity waterflooding performance, extensive laboratory work have been conducted, for example, contact angle [25-28], micro-model [7, 33, 39, 86, 87], spontaneous imbibition [29-31], and forced imbibition experiments (or core flooding) [14, 21, 49, 68]. Several published work show that fluid-fluid interactions likely contribute to additional oil recovery yielded by low salinity water [7, 33, 39, 87], experimental results, taken together, confirm that wettability alteration plays a main role in low salinity EOR-Effect. This is mainly achieved by disturbing the oil-brine-carbonate isotherm which has been interpreted using electrical double layer [46-49] and surface complexation modeling [42, 58-61, 72].

To elucidate the wettability alteration by low salinity flooding, a few mechanisms have been proposed, such as mineral dissolution (calcite and anhydrite) [15, 23, 42], chemical mechanism [11, 15, 24, 57, 88], electrical double layer expansion [46-49], and surface complexation [42, 58-61, 72] to characterize the wettability alteration process. However, these mechanisms have not been examined at a molecular level or nanoscale, presenting a tremendous impediment to capture the physics. To fill the gap and reduce the uncertainties of predicting the performance of low salinity waterflooding, the effect of the water chemistry on oil-brine-carbonate system wettability needs to be examined at the nanoscale together with thermodynamics isotherm investigation. This can be done by: 1) Using atomic force microscopy (AFM) to measure the adhesion force between different oil components and carbonate surface; 2) Analysing the thermodynamic isotherm of the system; 3) Elucidating the effect of low salinity water on

wettability at the sub-pore level by conducting contact angle measurements and understand the contribution of calcite dissolution on the wetting.

2.1.1 Mineralogy of Carbonate

Studying the mineralogy of the reservoir rocks is an essential step prior to the development of any oilfield, as it helps to understand the reservoir properties, avoid the formation damage of the reservoirs during the oil production, and provide useful information to enhance the oil recovery. Carbonate rocks host two thirds of the discovered oil in place [1, 2]. Therefore, understanding the mineralogy of carbonate reservoir rocks is one of the key factors to further unlock the existing huge Original Oil in Place (OOIP).

Carbonate rocks are sedimentary rocks and mainly composed of calcium carbonate ($CaCO_3$), and the common carbonate minerals are calcite ($CaCO_3$), aragonite ($CaCO_3$), and dolomite ($CaMg(CO_3)_2$). The calcite forms when the calcium carbonate ($CaCO_3$) crystalizes with a trigonal crystal structure, where the aragonite forms when the calcium carbonate ($CaCO_3$) crystalizes with an orthorhombic crystal structure. However, most of the aragonite minerals were changed spontaneously to calcite while it was buried and heated during the geological time, and thus calcite is the main component of the limestone and chalk reservoir rocks. In contrast, the dolomite rock is formed when the magnesium in the groundwater substitutes the calcium in the calcite crystal. However, the density of the carbonate minerals varies such as calcite (2.710 g/cm^3), aragonite (2.931 g/cm^3), and dolomite (2.866 g/cm^3) [89].

In addition, carbonate rocks sometimes contain calcium sulfate, hydrated calcium sulfate, and a small percentage of clays. In this work, the calcite is used to represent the carbonate rocks because it is the main component of carbonate reservoir rocks in addition to being commercially available as pure calcite crystals.

2.1.2 Wettability Alteration on Surfaces and in Carbonate Porous Media

Typically, different enhanced oil recovery techniques are used in the tertiary oil recovery stage to further unlock the remaining oil in place. In this context, altering the wettability of the reservoir rock or changing the fluid flow behaviour in the porous media are considered among the main mechanisms to reduce the residual oil saturation and to achieve the target of increasing the oil recovery factor.

The wettability of carbonate rock is a description of the selectivity of the carbonate surface to contact with oil or water in the oil-brine-carbonate system [90]. The carbonate wettability is considered oil-wet if the carbonate surface prefers oil, or it is water-wet if the rock surface prefers the water [91], and it could be a mixed-wet if the wettability changes from location to location within the same carbonate rock [91-95]. Several factors are influencing the wettability

of the carbonate surface, such as oil composition, brine chemistry (pH, salinity, and ions composition), rock mineralogy, saturation history, temperature and pressure conditions. However, wettability can be explained differently depending on the length scale, such as the molecular scale, sub-pore scale, pore scale, and core scale.

Wettability at the molecular scale (nanoscale, nm) is determined by adhesion between the rock, oil, and brine. The nature of the adhesion is determined by the sum of all the intermolecular forces that are acting between oil-brine, oil-rock, and brine-rock [96], where these forces could be attractive or repulsive depending on the distance between the molecules [96, 97]. However, the adhesion strength between one fluid (e.g., oil) and rock surface in the presence of the other fluid (e.g., brine) determines the nature of rock wettability. For example, the greater adhesion force between oil and calcite surface in the oil-brine-calcite system indicates that the calcite surface is more oil-wet, where the lower adhesion shows that the calcite surface is less oil-wet or more water-wet. Since the wettability at this scale length is mainly dependant on the intermolecular forces between molecules, the compositions of the oil, brine, and mineral, in addition to temperature and pressure are the major controlling factors of the wettability at this length scale.

At the sub-pore scale (from 0.1 to 1μm), the contact angle experiments are the direct tool to measure the wettability of the rock surfaces. Contact angle measurements can be achieved by imaging a drop of one fluid on the rock surface in the presence of the second fluid; the contact angle is measured between the fluid drop and rock surface through the denser fluid (which could be the drop or the bulk fluid). The contact angle reading distinguishes between the states of the wettability. The rock surface is considered as an oil-wet when the contact angle is greater than 90^o, where it is considered a water-wet when the contact angle is less than 90^o, and finally, the rock is intermediate-wet when the contact angle is 90^o [90, 98]. The estimation of the wettability in this scale is also affected by the surface's roughness and mineral heterogeneity. For example, the wettability alteration process from the flat surface would be greater than the pore surfaces with a certain level of surface roughness. Thus, wettability measurements in this scale may not represent the real system wettability [99-104].

Measuring the contact angles at the pore scale is another technique used to evaluate the wettability of the reservoir rock by using X-ray microtomography [105-107]. In this length scale, the contact angles are varied at different locations due to heterogeneity in surface minerals, surface roughness, saturation history, and also because of the fluid movement states (advancing and receding). However, the wettability of the system can be estimated from the contact angle distribution. For example, Alhammadi et al. [108] observed a shift in the distribution of the contact angles at the pore scale as a result of altering the wettability of the

rock by aging. But still, the contact angle's distribution in the pore-scale is not adequate to upscale the wettability alteration to the core-scale by prediction of the relative permeability curves [109].

The fluid distribution in the rock pores is another method to characterize the wettability at the pore scale. For instance, in a water-wet system, the oil clusters appear more spherical in shape when compared to oil-wet or mixed-wet systems, where the oil clusters appear with a flat shape [110, 111]. Moreover, it was found that in the mixed-wet systems, the oil form a layer on the rock surface and also between the interfaces of two brines, which result in the formation of a flow path for the oil in the pores [112]. However, the information on the fluid distribution and configurations at the pore scale is useful for deriving the relative permeability or estimation of capillary pressure [113, 114], and hence, upscaling the wettability alteration to the core-scale.

At core scale experiments, the wettability of the system is estimated through the relationship between the capillary pressure and saturation, which can be attained from the data of the spontaneous imbibition experiment. In particular, by attaining the forced part of the capillary pressure from the cumulative production of displaced fluid and waterfloods against time. However, several indices have been proposed to obtain the wettability of the system from the relationship between capillary pressure and saturation. The most used indices are the Amott and USBM index [115, 116]. However, apart from the wettability, there are other factors influencing the results of these experiments, such as interfacial tension, viscosity, and also flow dynamics [117-119], hence making it difficult to interpret the wettability. Also, the re-scaling of the Leverett J function has been used to characterize the wettability of the system by the prediction of the average contact angle [120, 121], but this technique fails to explain the mixed wettability.

In addition, the relative permeability curves have been used to estimate the wettability of the system through the water relative permeability endpoint, oil-layer drainage, and water relative permeability shape. For example, when the water relative permeability endpoint value is greater than 0.6, then it indicates that the system is oil-wet, where the system is mixed-wet for the values between 0.6 and 0.3, and it is water-wet for values less than 0.3. Whereas the k_{ro} near the endpoint describes the oil-layer drainage when the value of k_{ro} is less than 0.05, and there is a decrease in saturation at the same time. This indicates that the crude oil is flowing through a layer of oil, therefore the system is oil-wet or mixed-wet. Similarly, the system is oil-wet when there is a sharp rise in the k_{ro} and k_{ro} crossing the S_w at values less than 0.5. In contrast, the system is water-wet if the value of k_{rw} is less than 0.2 for $S_w = S_{wi} + 0.2$ [122].

Wettability alteration towards a more water-wet state is believed to be one of the main physiochemical processes behind the low salinity effect, which shifts oil relative permeability towards a lower residual oil saturation [22, 49, 62, 63], thus enhancing oil recovery. Therefore, in order to understand the controlling factors of the wettability alteration process in carbonate reservoirs, several explanations have been developed to predict and quantify the wettability alteration, such as mineral dissolution (calcite and anhydrite) [15, 23, 42], chemical mechanism [11, 15, 24, 57, 88], electrical double layer expansion [46-49], and surface complexation [42, 58-61, 72] to characterize the wettability alteration process. Generally, all the mechanisms are associated with oil-brine interaction or/and brine-rock interaction, or/and oil-brine-rock interactions. However, it appears that oil-brine-rock interactions are of paramount importance, which governs the in-situ wettability of reservoirs during low salinity water injection.

2.1.3 Brine-rock system

Exposure of the carbonate minerals to the low salinity brine causes carbonate mineral dissolution, such as the dissolution of calcite and anhydrite minerals, which occurs due to the following chemical reactions:

$$CaCO_3 + H^+ = Ca^{2+} + HCO_3^-$$

$$CaCO_3 + 2H^+ = Ca^{2+} + H_2CO_3$$

$$CaCO_3 + H_2CO_3 = Ca^{2+} + 2HCO_3^-$$

$$CaCO_3 + H_2O = Ca^{2+} + HCO_3^- + OH^-$$

$$CaSO_4 + 2H_2O = Ca^{2+} + SO_4^{2-} + 2H_2$$

Mineral dissolution is one of the fluid-rock interactions, which has been perceived as the main mechanism of the low salinity effect by generating in-situ ions that work as a wettability modifier. For example, Hiorth et al. [42] studied the impact of brine chemistry on carbonate surface charge and carbonate dissolution. They concluded that mineral dissolution is the controlling factor of the low salinity effect. In another work, Evje et al. [123] developed a mathematical model to predict the influence of brine-rock chemistry on the wettability alteration. Based on their mathematical model, Evje et al. [123] found a direct relationship between the wettability alteration and the change in the brine chemistry generated from calcite dissolution and precipitation. It is worth mentioning that calcite dissolution during low salinity flooding leads to increases in the local pH [20, 82, 124-126], and this pH increase most likely affects the oil−brine−carbonate interactions and hence wettability alteration. However, the low salinity water may not always cause the pH change at the core or reservoir scale due to the buffering effect.

Moreover, anhydrite ($CaSO_4$) dissolution was suggested as a key factor for the low salinity effect [15, 127, 128]. For example, Pu et al. [127] related the enhanced oil recovery during the low salinity flooding to the wettability alteration from weakly water-wet to more water-wet system as a result of anhydrite dissolution and the associated release of fine materials and dolomite crystals from the surfaces of the pores. In another work, Yousef et al. [23] found that injection of the low salinity brine enhanced the pore network connectivity due to the mineral dissolution in line with their NMR results. They concluded that a change of the surface charge causes the dissolution process and thus wettability alteration. Furthermore, other researchers believe that the presence of anhydrite in carbonate is the key for the low salinity effect [15, 128].

In contrast, other published work show that there is no relationship between the low salinity effect and dissolution of anhydrite in the oil-brine-carbonate system. For example, Jiang et al. [129] conducted spontaneous imbibition and coreflooding experiments to study the low salinity effect. They detected anhydrite dissolution during the low salinity flooding in the tertiary mode, but without measurable incremental recovery, and suggest that anhydrite dissolution may play a minor role in the low salinity effect. Also, Gandomkar et al. [126] conducted coreflooding experiments using limestone core samples to investigate the low salinity effect in secondary and tertiary modes. They reported no additional oil recovery in the tertiary mode, although they used limestone core samples containing anhydrite. In addition, Uetani et al. [130] performed spontaneous imbibition experiments to examine the role of the anhydrite on the low salinity effect in carbonate rock. They observed a low salinity effect in carbonate cores regardless of anhydrite content. Therefore, they confirm that anhydrite is not a must to be present in carbonate rocks to yield a low salinity effect.

2.1.4 Oil and Brine Fluids System

Apart from brine-rock interaction on low salinity effect, fluid-fluid interactions have also been examined to understand their contributions on incremental oil recovery during low salinity waterflooding. In particular, salting in and out effect, IFT reduction, and micro-dispersion are reviewed in the subsection below.

Salting in and out effect

The solubility of the hydrocarbon in water depends on the salinity, where increasing the salinity of an aqueous solution leads to a decrease in the solubility of hydrocarbon in the aqueous solution. This process is known as the salting-out effect. On the contrary, the solubility of hydrocarbon in the aqueous solution increases with decreasing the salinity, and this effect is known as salting in effect [11, 131].

When solving a hydrocarbon molecule in water, water molecules form a structure around the hydrophobic part through hydrogen bonds; this phenomenon allows hydrocarbon molecules to be soluble in water, although hydrocarbon molecule is hydrophobic. However, when adding salts, the salts ions break the hydrogen bonds between water molecules and hydrocarbon molecules, which results in a decrease in the hydrocarbon solubility, and thus the solubility of hydrocarbon decreases with increasing salinity [11].

Given that the ionic strength of the salt ions plays an important role in salting in effect, the monovalent ions (e.g., Na^+) have a lower impact than the divalent ions (e.g., Ca^{2+}, Mg^{2+}). Therefore, salting in effect contributes to the low salinity effect by increasing the solubility of oil in brine, hence desorption of oil from pores surface [11].

Reduction of the Interfacial Tension (IFT)

During secondary waterflooding, oil clusters are trapped in the porous media due to the capillary forces (called residual oil saturation, S_{or}). One of the effective methods to release this trapped oil and to reduce the residual oil saturation is reducing the interfacial tension (IFT) between the oil and brine interface. This process leads to a reduction in the capillary forces, and thus reduces the residual oil saturation and enhance the oil recovery, such as surfactant flooding. However, the interfacial tension between the oil and brine needs to be reduced to 10^{-2} dyn/cm to attain a reasonable residual oil reduction [132]. Literature shows that low salinity flooding could affect the interfacial tension between the oil and brine, due to the change in composition and salinity of the brine phase at the oil and brine interface. There are few published works which show that the low salinity water leads to a significant interfacial tension reduction between the oil and brine. [133, 134]. For instance, Al Harrasi et al. [18] found that one unit of the interfacial tension (1.0 dyn/cm) only reduced when diluting the formation brine one hundred times from 194450 ppm to 1944 ppm. Also, Al-Attar et al. [135] reported a reduction between 14-30 dyn/cm in the interfacial tension when lowering the salinity of two different formations brines. In addition, Yousef et al. [23] performed coreflooding experiments and a series of interfacial tension experiments to study the relation between oil-brine interaction and the enhancement of the oil recovery. They found that interfacial tension reduction was less than 10 dyn/cm, suggesting that low salinity waterflooding has a minor effect on interfacial tension between oil and brine. Therefore, the above authors, Al Harrasi et al. [18] Al-Attar et al. [135] and Yousef et al. [23] concluded that the interfacial tension of oil-brine plays a negligible role in the low salinity effect.

Micro-Dispersion Formation

The formation of the micro-dispersions is another fluid-fluid interaction mechanism proposed by some researchers to explain the wettability alteration of the reservoir rocks during the low salinity flooding [39, 52, 87]. Initially, Emadi et al. [86] provided the first visual evidence of the formation of the water micro-emulsion at the oil and brine interface during the low salinity flooding. They suggest that the formation of the water micro-emulsion during the low salinity water flooding leads to absorption of surface-active agents from the crude oil-brine interface to water micro-emulsion, which in return changes the oil-brine interface charge and consequently changes the charge of the fluids-rock interfaces, and thus altering the wettability of the carbonate rock. Furthermore, Mahzari et al. [52] conducted a series of fluid characterization experiments to study the oil-brine interactions. They reported that decreasing the salinity of the brine leads to the formation of water-in-oil dispersion spontaneously, which is in line with their colleague's previous work (Emad et al. [86]). Similarly, Sarvestani et al. [136] examined the influence of the water salinity on stabilization of the micro-emulsions droplets as one of the dominant mechanisms of the low salinity EOR. They found that lowering the salinity of the brine increases the stability of the micro-emulsion droplets, which could elucidate the growth in the pressure drop while injecting the low salinity water in their experiments. Generally, all the mechanisms based on the fluid-fluid interaction could contribute to the low salinity effect. However, more quantitative work remains to be done to quantify the contribution of such a process on incremental oil recovery during low salinity waterflooding in reservoirs.

2.1.5 Oil-Brine-Rock Interactions

To gain a deeper understanding of low salinity EOR-Effect, oil-brine-rock interactions have been examined to account for the incremental oil recovery through multi-scale experiments and geochemical modeling.

Potential Determining Ions (PDI)

Published works show that the presence of some divalent ions in the water is the key factor of releasing the adsorbed polar oil components (e.g., -COOH) from the carbonate surface in the oil-brine-carbonate system. For example, the divalent cations such as Ca^{2+}, Mg^{2+}, and SO_4^{2-} play an important role in the low salinity water EOR Effect, and they are also called potential determining ions (PDI) [55-57, 77]. These oil-brine-rock interactions have been examined with a combination of contact angle experiments, force flooding experiments, and spontaneous imbibition experiments. The experimental results indicate that adjusting the concentration of the potential determining ions in the brine affects the oil-brine-carbonate interaction and leads to the wettability alteration. For example, Austed et al. [55] found that the presence of the

SO_4^{2-} in seawater increases the oil recovery from the chalk core samples in spontaneous imbibition experiments. They propose that adsorption of the SO_4^{2-} (PDI) on the chalk surface lowers the positive charge at the chalk surface, thus releasing the adsorbed acidic oil components from the chalk surface. Also, Zhang et et al. [56] found that the presence of SO_4^{2-} in the brine results in an improvement in the oil recovery from chalk core in spontaneous imbibition experiments, confirming that wettability alteration occurs at the chalk surface. In another work, Strand et al. [57] used chromatographic techniques to study the impact of the presence of both Ca^{2+} and SO_4^{2-} on the oil-brine-carbonate system. They reported that raising the concentration of Ca^{2+} in the brine leads to an increase in adsorption of SO_4^{2-} ions at the surface of chalk. The authors suggest a possible mechanism to explain the contribution of the Ca^{2+} on the adsorption SO_4^{2-} on the carbonate surface, which results in changes in charge of carbonate surface, thus release of the polar oil components from the carbonate surface and enhance the oil recovery. Also, Mg^{2+} was identified as a potential determining ion which can raise the density of the positive charge on the calcite surface by replacing the Ca^{2+} at high temperatures.[77] However, the proposed mechanism for the Mg^{2+} is close to the mechanism suggested by Strand et al. [57].

Moreover, atomic force microscopy (AFM) has been used to investigate the impact of potential determining ions on the oil-brine-carbonate interactions. For instance, Generosi et al. [137] conducted AFM experiments to study the influence of the potential determining ions on the adhesion force between the oil and calcite surface. The authors concluded that the presence of SO_4^{2-} and Mg^{2+} ions reduced the adhesion force between the oil (CH_3-terminated tip) and calcite surface, thereby wettability alteration of calcite to less oil-wet. Also, the molecular dynamics simulation has been performed to explore the influence of the potential determining ions on adsorption of the polar oil components on carbonate. For example, Bai et al. [138] developed a molecular dynamics model to investigate the adsorption of polar oil components (acidic oil, $-COO^-$) on calcite, and thus the wettability of the calcite surface. The authors reported that the presence of the potential determining ions (Ca^{2+} and SO_4^{2-}) results in the release of the acidic oil component ($-COO^-$) from the calcite. They found that the negative SO_4^{2-} ion replaces the negative acidic oil component ($-COO^-$) from the calcite surface, and then the positive Ca^{2+} forms ion-pair with the negative acidic oil component ($-COO^-$) and thus detaching the acidic oil components from the calcite surface.

In conclusion, the most important potential ion is sulfate, which can be added to the low salinity brine or it can be generated from the dissolution of anhydrite minerals to yield the low salinity effect. However, sulfate is known as the main source of several operational problems. For instance, the presence of the sulfate increases the formation of scales such as barium sulfate ($BaSO_4$), calcium sulfate ($CaSO_4$), and strontium sulfate ($SrSO_4$), and these scales are

sources of problems in the oil fields operation [139-142]. Also, it was found that using brine with a high concentration of sulfate caused a reservoir souring issue [143], which is a big challenge in the petroleum industry. Therefore, it is important to fully understand the low salinity effect so the low salinity effect can be obtained without adding sulfate to the injected water and avoid all the problems associated with the presence of sulfate in injected water.

DLVO-Disjoining Pressure-Electrical Double Layer Forces

Placing calcite crystal in an aqueous solution results in an electrical field, which causes the unequable distribution of different charge ions in the nearness of the calcite surface. Counter ions in the solution move toward the surface due to the attraction force with the opposite charges at the calcite surface, forming a diffuse layer of charge. At the same time, the similarly charged ions in solution move away from the surface, due to the repulsion force with a similar charge at the calcite surface [144]. The surface charge and the diffuse layer together form the electrical double layer. The concentration of the counterions and co-ions is not distributed equally within the electrical double layer, thus developing a potential across the interface. The concentration of the counterions is higher in the adjacent solution and decreases as moving away from the calcite surface, while the concentration of co-ions increases when moving away from the calcite surface. Calcite surface adsorbs the closest counter ions, forming a fixed layer called Stern layer. This layer of fixed counter ions divided into the inner and outer stern layer or also called inner and outer Helmoltz layers [145]. However, the surface electrical potential at the location of shear or slip plane is known as the zeta potential of the surface and is usually measured by the electrophoresis technique. This zeta potential is highly dependent on several factors, such as the charge of the surface, pH, salinity, and composition of the aqueous solution.

The pH is strongly influencing the surface charge, due to the protonation and deprotonation of the surface sites [46], and the value of the pH, where the surface charge change from positive charge to negative charge, is called the Point of Zero Charge (PZC). Zeta potential values of the oil-brine and brine-calcite interfaces are used to calculate the electrical double layer forces, which is part of the Derjaguin, Landau, Verwey, and Overbeek (DLVO) theory as shown in Eq 2-1, where the positive and negative disjoining pressure represents repulsive and attractive forces between oil-brine and brine-calcite interfaces, respectively.

$$\prod_{(\mathrm{Total})} = \prod_{(\mathrm{vdw})} + \prod_{(\mathrm{EDL})} + \prod_{(\mathrm{STR})} \qquad \mathrm{Eq}\ 2-1$$

Researchers have used DLVO to interpret the low salinity effect on the contact angle/wettability/incremental oil recovery increase with different boundary conditions (constant charge, or constant potential boundaries). For example, Alshakhas et al. [47] used

DLVO to evaluate the effect of low salinity water on the oil-brine-carbonate interaction by conducting contact angle and coreflooding experiments. They reported that the low salinity effect was confirmed by the calculation of the surface forces, suggesting that surface forces in the double layer are responsible for the low salinity effect and additional oil recovery. In addition, Mahani et al. [146] used DLVO theory to calculate the interaction potential of the oil-brine-carbonate system and to compare its consistency with the contact angle measurements at high and low salinity values. They found that lowering the salinity reduces the attractive forces or increases the repulsion forces between the crude oil and carbonate (double layer expansion), thus wettability alteration from oil-wet to less oil-wet. Although DLVO may not be able to quantify the contact angle/wettability alteration, it is a reasonable quantitative practice to predict the trend of the wettability shift with the various oil-brine-rock system.

Electrical double layer forces play an important role in the total value of the disjoining pressure, and as previously mentioned above, that water chemistry is the main factor affecting the zeta potential, thus it is affecting the electrical double layer and, therefore, the total disjoining pressure. For that, some researchers have used zeta potential measurements to understand the effect of brine salinity on carbonate wettability alteration and oil recovery. For instance, Alotabi et al. [46] found that low salinity water increased the negativity of carbonate surface (dolomite and limestone), which led to double layer expansion, therefore wettability alteration on dolomite and limestone rocks to less oil-wet. Also, Alotabi et al. [147] investigated the influence of the ions types and salinity on the zeta potential of oil-brine and brine-limestone interfaces. They concluded that the zeta potential of the oil-brine-carbonate interfaces directly affects the wettability of the limestone and oil recovery. In addition, Mahani et al. [65] conducted contact angle and zeta potential measurements to study the influence of the brine chemistry on the wettability alteration of the oil-brine-carbonate system. They observed that wettability alteration occurs when low salinity water lowers the zeta potential of oil-brine-carbonate interfaces, concluding that surface charge change is possibly the main mechanism behind the low salinity effect in carbonate.

Surface Complexation Modeling

Surface species at the interface of oil/brine and brine/rock strongly affect the interactions of the oil/brine/rock system, thus contributing to the wettability of the system. Surface complexation modeling has been applied to understand the effect of water chemistry on a number of surface species at these interfaces. Also, oil consists of basic and acidic functional groups such as -NH, and $-COO^-$, where the base number and acid number demonstrate the concentration of these basic and acidic functional groups, respectively. The surface species of

the opposite charges from calcite and oil surfaces attracted to each other and created an electrostatic bridge, thus increase the oil-wetness. The number of the electrostatic bridges (bond product sum) between the oil and calcite surface species controls the strength of the electrostatic attraction thereby the oil-wetness [58]. The bond product sum is a function of oil composition [148-150], rock mineralogy [147], salinity [25, 151], and ionic strength [131, 152]. However, some researchers used surface complexation modeling to elucidate the influence of water chemistry on the surface species at the calcite surface. For example, Van Cappellen et al. [153] developed a surface complexation model of the carbonate-brine interface, which proposes the generation of >CaOH and $>CO_3H$ at the surface of calcite when exposed to water. Where the protonation/deprotonation of >CaOH and $>CO_3H$ calcite surface species enables the adsorption of anions and cations from the brine (e.g., CO_3^{2-}, SO_4^{2-}, and Ca^{2+}), thus generating a charge on the calcite surface [58]. The overall calcite surface charge can be calculated from the overall concentration of differently charged species. In addition, Mahani et al. [59] developed a surface complexation model to investigate the effect of pH and salinity on zeta potential of the brine-carbonate interface. Their surface complexation model demonstrated that increasing pH leads to the formation of surface species, which in return influence the overall surface charge, and thus the zeta potential of carbonate. In addition, they observed that carbonate surface charge is more sensitive to the pH at low salinity, suggesting that brine salinity plays an important role in the pH impact on zeta potential. Moreover, they found that lowering salinity increases the numbers of negative surface species, therefore reduces the overall positive charge of carbonate surface. However, their surface complexation model works for the brine-carbonate interface and cannot investigate the effect of brine chemistry on the oil-brine interface. Furthermore, Song et al. [154] conduct zeta potential experiments to investigate the effect of potential determining ions (Ca^{2+}, Mg^{2+}, SO_4^{2-}, CO_3^{2-}) on the brine-calcite interface. They also developed double layer surface complexation model to simulate the results of their experiments and to predict the wettability alteration. Their model predicts the zeta potential of calcite with different potential determining ions (Ca^{2+}, Mg^{2+}, SO_4^{2-}, CO_3^{2-}) accurately, but the role of the oil-brine interface was not considered in this model.

In parallel, other researchers used surface complexation modeling to elucidate the effect of water chemistry on both oil-brine-carbonate interfaces, thus characterizing the wettability alteration. For example, Brady et al. [58] established a surface complexation model to calculate the bond product sum (BPS), and to study its relationship with the wettability alteration. They suggested that decreasing the bond product sum indicates that the wettability of the oil-brine-carbonate system shifts toward less oil-wet, while increasing the bond product sum designates that the wettability of carbonate becomes more oil-wet. Also, Chen et al. [61] used surface

complexation modeling to study the factors influencing the wettability of the oil-brie-carbonate system. They reported that the surface complexation model predicts a similar trend of salinity effect on the wettability of contact angle results. In particular, they observed that lowering the salinity decreases the bond product sum. In addition, they found that lowering the salinity at pH <6 leads to an increase in the calcite oil-wetness for oil with a high base number, where reducing the salinity at pH>7 decreases calcite oil-wetness for oil with a high acid number. Furthermore, Xie et al. [60] performed contact angle experiments and geochemical modeling to examine the influence of pH on the oil-brine-calcite system. They found that the bond product sum concept predicts the trend of contact angle measurements, suggesting that pH is one of the controlling factors to govern the wettability of the carbonate system.

2.2 Identified Knowledge Gaps

2.2.1 Effect of Oil Compositions on Low Salinity Effect in Carbonate Reservoirs

Oil-brine-carbonate interactions play an important role in the carbonate reservoirs wettability alteration during low salinity flooding. To better understand the factor(s) controlling the wettability alteration process, the effect of brine chemistry on the oil-brine-carbonate interactions has been widely explored through experimental and numerical studies [11, 15, 18, 23-25, 29, 49, 55-57, 59, 88, 137, 155-159]. For instance, Austad et al. [15, 55, 88] and other researchers [11, 24, 29, 56, 57, 155-157] have found that the presence of the potential determining ions (Ca^{2+},SO_4^{2-}, and Mg^{2+}) would likely alter the wettability of the oil-brine-carbonate system toward less oil-wet, and thus increasing the oil recovery [18, 23, 25, 49, 59]. Also, previous studies show that reducing the salinity of the brine increases the hydrophilicity of the oil-brine-carbonate system, hence decreasing residual oil saturation. Furthermore, to gain a better understanding at the molecular level, quartz crystal microbalance (QCM) [158] and atomic force microscopy (AFM) [137, 159] have been used to investigate the influence of brine chemistry on the interaction between the polar oil and rock. For example, Joonaki et al. [158] used QCM to examine the impact of brine composition on the deposition of the asphaltene oil species on the rock surface at elevated temperature and pressure conditions. They found that brine salinity and composition play an important role in the deposition of the asphaltene oil species on the rock surface, thereby affecting the wettability of the oil-brine-rock system. In addition, Generosi et al. [137] used AFM to study the influence of the potential determining ions on the calcite wettability, although the pH effect was not investigated. They concluded that the presence of SO_4^{2-} and Mg^{2+} ions reduced the adhesion forces between CH_3-terminated tip and calcite substrate, and thus increasing the hydrophilicity of the oil-brine-carbonate system.

Apart from the effects of the brine composition on oil adhesion, the oil components also play an important role in the oil-brine-carbonate interaction. The published work shows that the polar oil composition (acid and base number) plays an important role in the wettability of the carbonate surface [70, 73, 160], by playing a part in the surface charge of the oil-brine interface [48, 146, 150, 161-163], double layer expansion [48, 138, 146, 150, 161-163], disjoining pressure [146, 150, 161-163], and formation of electrostatic bridges with the carbonate surface [48, 58, 60, 61, 164]. For example, contact angle, spontaneous imbibition, and core flooding experiments show that polar oil components play a crucial role in the oil-brine-carbonate interaction, and thus wettability of carbonate surface [15, 48, 55, 75, 165]. In addition, AFM has been used to study the influence of salinity on the adhesion force between the oil components and hydrophobic surfaces, although the pH effect was not investigated. For example, Liu et al. [166] used AFM to investigate the influence of the brine salinity on the interaction force between functional oil groups and hydrophobic surfaces. They found that the adhesion force between functional oil groups and hydrophobic surfaces decreases with the decrease of the brine salinity, and thus the wettability alteration of oil-brine-rock.

To better quantify and predict the wettability alteration process, surface complexation modeling has been implemented to model chemical surface species from oil and calcite surfaces, thus characterizing the adhesion of oil and calcite [32, 58-61, 164]. For example, Brady et al. [58] developed a surface complexation model to characterize the wettability of oil-brine-calcite using a bond product sum concept, which is equal to $[–COOCa^+]\ [>CO_3^-] + [–COOCa^+]\ [>CaCO_3^-] + [–NH^+]\ [>CO_3^-] + [–NH^+]\ [>CaCO_3^-] + [–COO^-]\ [>CaOH_2^+] + [–COO^-]\ [>CO_3Ca^+]$. They suggest that the potential adhesion between the polar oil and carbonate surface decreases with decreasing bond product (less oil-wet system), and the potential adhesion between the polar oil and carbonate surface increases with increasing bond product (more oil-wet system). However, the above geochemical models were proposed to characterize oil-brine-carbonate wettability in light of the interaction of polar oil groups ($–NH^+$ and $–COO^-$) on carbonate surfaces. Taken together, while there is a considerable investigation on the response of the polar oil components to the salinity effect, there are limited studies that have been carried out to investigate the response of the non-polar oil components to the wettability alteration during the low salinity flooding in the oil-brine-carbonate system, and fewer studies have been done to study the impact of the pH increases on the interactions between the oil components (non-polar & acidic oil) and carbonate surface at the molecular level, although low salinity flooding likely leads to the increase of the local pH in carbonate formations. It is worth noting that injecting low salinity water in carbonate leads to an increase of the local pH (up to 10) due to the calcite dissolution [20, 82, 124-126], and this pH increase most likely affects the oil-brine-carbonate interactions, hence wettability alteration.

Generally, the response of the non-polar oil species on wettability alteration as a function of salinity and pH remains unclear. Also, it is widely known how the brine chemistry affects the interaction between the polar oil and carbonate surface, but how the pH affects the interactions between the oil components (non-polar & acidic oil) and carbonate surface remains unclear. Therefore, to reduce ambiguity, in this work, adhesion force measurements using AFM and contact angle experiments have been conducted to study the response of the non-polar oil (-CH_3) and acidic oil (-COOH) species to the pH increase during low salinity water injection in carbonate reservoirs. Furthermore, we measured the zeta potential of oil-brine and brine-carbonate interfaces at different pH, and computed the disjoining pressure of the system to gain a deeper understanding of the isothermal thermodynamic of the pH effect on the interactions between the non-polar oil components and carbonate surfaces (Chapter 4 & 5).

2.2.2 Role of Clays on Low Salinity Effect: Implications for Clay-Rich Carbonate Rocks

Carbonate rocks are composed primarily of calcite ($CaCO_3$) (e.g., chalk or limestone), and with magnesium ($MgCO_3$) (e.g., dolomite). Also, some carbonates may contain anhydrite ($CaSO_4$), gypsum ($CaSO_4.2H_2O$), and a small percentage of clays minerals. The published works indicate that carbonate mineral plays a vital role in the wettability alteration during low salinity flooding. For example, Fernø et al. [167] used three different outcrop chalks in spontaneous imbibition experiments to investigate the influence of sulfate concentration on oil production. They found that the mineralogy sedimentations and compositional differences of the chalks play an essential role in response to the sulfate effects. Also, Romanuka et al. [79] found that dolomite and limestone core samples respond to the low salinity effects in spontaneous imbibition experiments, whereas chalk core samples did not give much response. Additionally, other studies suggested that anhydrite is the key factor for the low salinity effect in carbonate rocks [64, 127].

While the effect of carbonate mineralogy (chalk, limestone, dolomite, and anhydrite) has been investigated, there has been little investigation of the effect of the clay impurities in carbonate on the wettability of the carbonate. The published works found that clay minerals play an important role in the wettability of the sandstone rocks [4, 35, 168, 169], and linked the low salinity effect in sandstone to the presence of the clay minerals [4, 6, 40, 168, 170-177]. Although carbonate reservoir rocks contain a small percentage of clay (<5 wt%) [178, 179], this small percentage covers a significant percentage of the carbonate free surface in the pores [179]. This means that the clay impurities likely play a certain role in the low salinity effect. However, the effect of clay impurities on the oil adhesion in carbonate remains incomplete, which presents a tremendous impediment to understand the response of low salinity water in clay-rich carbonate reservoirs.

To provide a better understanding and to limit the uncertainties of the wettability alteration during low salinity flooding in particular for the clay-rich carbonate reservoirs, we performed an experimental investigation to understand the correlation between the pH and adhesion forces between oil components and clay surface. Also, to better understand the isotherm thermodynamic of the system, I conducted zeta potential measurements and computed the total disjoining pressure of the oil-brine and brine-clay interfaces at different pH (Chapter 6).

2.2.3 Variables and Influencing Factors for the Shift of Contact Angle

Wettability alteration during low salinity waterflooding in carbonate reservoirs has been identified as the main physicochemical processes [83, 168, 174]. The contact angle experiment is a simple and straightforward method to evaluate the effect of low salinity on the wettability alteration of the oil− brine−carbonate system. For instance, Yousef et al. [14] performed contact angle measurements to examine the impact of smart water on low salinity EOR effect in carbonate reservoirs. Their results show that initial connate water (213 000 ppm salinity) gives a contact angle of 90°, while the twice diluted seawater (29 000 ppm) and ten times diluted seawater (6000 ppm) give a contact angle of 80° and 69°, respectively, suggesting that reducing the salinity alters the wettability of the carbonate rock from intermediate-wet toward weakly water-wet. Alameri et al. [49] also conducted contact experiments to investigate the influence of the low salinity water on the wettability alteration of the oil-brine-carbonate system. Their results show that reducing the salinity of the seawater from 51 346 to 12 840 ppm reduces the contact angle from 133° to 117°, suggesting a less oil-wet system. Additionally, AlQuraishi et al. [64] reported that the contact angle of the oil−brine−carbonate system reduces from 98° to 65° when diluting the seawater 20 times, proposing that reducing the salinity can alter the wettability of the carbonate from intermediate-wet to more water-wet status. Furthermore, Awolayo et al. [27] found that reducing the salinity of the brine from 261 210 ppm (formation brine) to 48 280 ppm salinity (synthetic seawater) reduces the contact angle of the oil−brine−carbonate system from 135° to 120°. To understand the controlling factor(s) of wettability alteration as shown by contact angle decrease with reducing the salinity in carbonate reservoirs, electrical double layer theory [42, 49, 54], electrostatic bridging [15, 25, 77], and surface complexation modeling [58, 59] have been suggested and developed to predict the wettability alteration.

However, there are doubts with respect to the reliability of contact angle results to evaluate the wettability alteration process behind the low salinity effect. This is because calcite dissolution caused by the low salinity water during contact angle measurement may yield surface roughness variation, which may either overestimate or underestimate the wettability alteration process. As the published works show that changing the surface roughness affects the contact angle measurements in the oil−brine−rock system [180, 181]. For instance, AlRatrout et al.

[180] found that increasing surface roughness reduces the contact angle in the oil−brine−carbonate system. Additionally, Rücker (2018) concluded that surface roughness has a significant impact on the wettability alteration process, which influences the wettability measurements of the oil−brine−rock system [181]. However, to mitigate the uncertainties on the contact angle measurements, and understand if the surface roughness variation induced by calcite dissolution in the presence of low salinity water plays a certain role in contact angle measurements, an experimental and analytical study has been conducted in this research (Chapter 7).

2.2.4 Oil-Brine-Carbonate Interactions: Implications for Alcohol-Assisted Waterflooding

Low salinity waterflooding has been identified as a cost-effective and environmentally friendly means to enhance oil recovery in carbonate reservoirs, mainly by decreasing hydrophobicity. In this context, low salinity water injection would be considered as a viable means to enhance the oil recovery in harsh carbonate reservoir conditions (high temperature and high salinity), where the Chemical-Enhanced Oil Recovery (Chemical-EOR) approaches may not be able to handle economically at such critical conditions in particular at the period of low oil prices. However, the shortage of low salinity water sources in most locations (e.g., the Middle East countries, Western China, and the offshore oil fields) limits the application of this valuable EOR technology. For instance, more than 70% of carbonate fields in the world are located in the Middle East [2], where is a lack of freshwater or low salinity water. Accordingly, there is an imperative need to find alternative EOR techniques to improve the oil recovery in carbonate formations at high salinity and high temperature conditions, where the low salinity EOR and the existing Chemical-EOR techniques are not economically viable.

Published work indicates that adsorption of the potential determining ions (Mg^{2+}, Ca^{2+} and SO_4^{2-}) onto the carbonate causes the detachment of the acidic oil from the carbonate surface [15, 24, 55-57, 77], which leads to wettability alteration hence enhancing oil recovery. Also, surface complexation modeling shows that low salinity water likely breaks the electrostatic bridges between the opposite charges species on the oil surface ($-COO^-$, $-COOCa^+$, $-NH^+$) and carbonate surface ($>CaOH_2^+$, $>CO_3Ca^+$,$>CO_3^-$, $>CaCO_3^-$) [58, 60, 61, 72, 78]. Collectively together, these existing knowledge shed light on the wettability shift by breaking the bridges possibly through chemical additives, which may bridge the functional groups from oil surfaces and thus breaking the bonds between oil and rock surfaces.

In light of the existing knowledge from the low salinity effect on the oil-brine-carbonate interactions, alcohol-based chemical additives were used to explore the possible wettability alteration on carbonate surfaces even at high salinity and high temperature conditions.

Therefore, an experimental investigation was conducted to explore the possible wettability alteration process by adding a low concentration of alcohol-based chemicals into brines with various salinity levels (Chapter 8). Furthermore, I proved that the wettability alteration process achieved by 1-pentanol alcohol at the sub-pore level would trigger oil detachment, coalescence, transport and thus enhance oil recovery at high temperature and high salinity conditions (Chapter 9).

Chapter 3. Research Framework and Methodology

3.1 Research Framework

Figure 3-1 below shows the thesis's framework to address the knowledge gaps related to the oil-brine-carbonate interactions at different length scales such as nanoscale, sub-pore scale, and core scale. Initially, the research focuses on the effect of the low salinity on the oil-brine-carbonate interactions at the nanoscale (the yellow outlined boxes) by investigating the influence of the pH increases on the adhesion force between non-polar/polar oil functional groups and calcite surface, thus addressing gaps #1 and #2. Also, the research examines the influence of the mineral heterogeneity in carbonate on the low salinity effect. Particularly, the role of the clay impurities on the low salinity effect in clay-rich carbonate reservoirs. After that, the thesis studies the impact of low salinity brine on the oil-brine-carbonate interactions at the sub-pore scale (the blue outlined box). Specifically, the research aims to understand how the calcite dissolution caused by low salinity can affect the oil-brine-carbonate interactions at the sub-pore scale, thereby the contact angle measurements.

Later, based on the existing and gained knowledge of the low salinity effect on the oil-brine-carbonate interactions, the research explores alternative EOR techniques for reservoirs without access to low salinity water by adding alcohol to the formation brine to obtain a similar effect of low salinity on the oil-brine-interactions (the green outlined boxes). I studied the influence of different alcohols at the sub-pore scale to elucidate the alcohol-carbon chain's influence and the number of alcohol groups (-OH) on the oil-brine-carbonate system. I also investigated the impact of the brine salinity on the performance of alcohols. The research then examines the performance of alcohols at high temperature and high salinity at a sub-pore scale. Finally, the coreflooding experiments were performed to reveal the impact of the in-situ wettability alteration on oil detachment, coalescence, oil banking, and transport in the porous media.

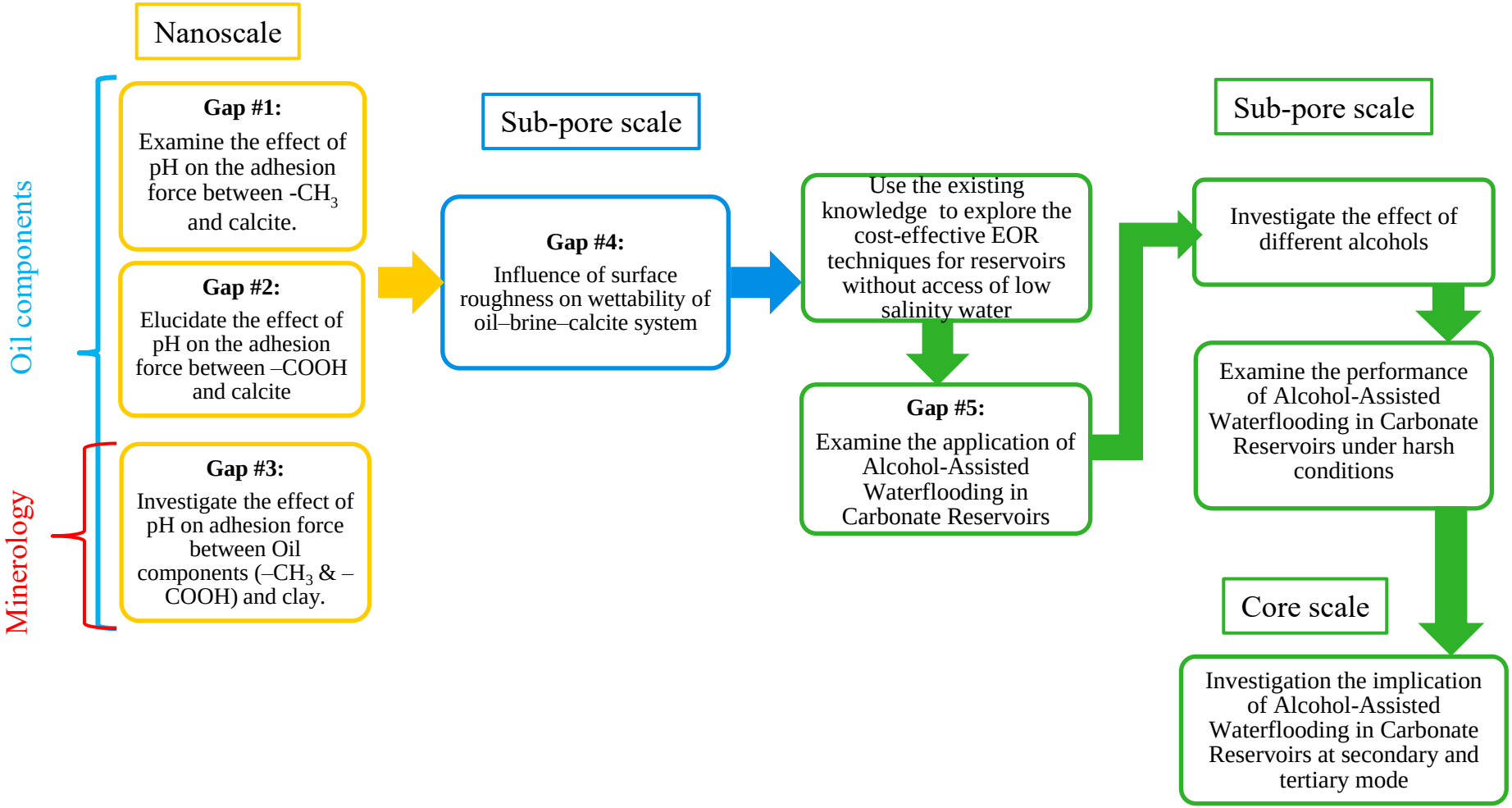

Figure 3-1: Research Framework

3.2 Methodology

To achieve the objectives of this research, I designed multi-scale experimental and analytical approaches to address the knowledge gaps with a combination of contact angle measurements (sessile drop method), zeta potential measurements, disjoining pressure isotherm analysis, geochemical modeling, and coreflooding experiments.

3.2.1 Understanding the Effect of Oil Compositions and Clays on Low Salinity Effect in Carbonate Reservoirs

The existing literature has shown that previous studies on the low salinity effect on oil-brine-carbonate systems have overlooked the response of the non-polar oil components on wettability alteration as a function of salinity and pH. In addition, there are very limited studies examining how the pH influences the interactions between the oil components (non-polar & acidic oil) and carbonate surface, especially at the molecular scale. Therefore, to address this issue, I designed the methodologies in Chapters # 4 & 5 and aimed to understand the impact of brine chemistry (pH) on the interaction between oil components (non-polar & acidic oil) and calcite surface, hereby the interaction of the oil-brine-carbonate system. To achieve this objective, I combined the contact angle, AFM, and zeta potential experiments with disjoining pressure calculation to investigate the pH effect on the oil-brine-carbonate system at the molecular-scale and sub-pore scale.

Firstly, I performed a suit of contact angle measurements to elucidate the pH's effect on the oil-brine-carbonate system at the sub-pore scale. In particular, I used the sessile drop method to conduct contact angle measurements by introducing a droplet of model oil (non-polar/polar) on calcite substrate in the presence of 10 000 ppm NaCl brine at different pH values (6.5, 9.5, and 11) at ambient conditions. It is worth mentioning that I used monovalent ion only in all the experiments with a focus on the pH effect. I did not use the divalent cations (e.g., Ca^{2+} & Mg^{2+}) due to their competition with H^{+}/OH^{-} to adsorb on calcite surfaces, which likely compensates for the impact of the pH effect on the oil-brine-calcite interactions.

Secondly, I used the AFM (WITec alpha 300 SAR) to investigate the effect of the pH on the oil-brine-carbonate interactions at the molecular scale by measuring the adhesion force between the oil components (non-polar/polar) and calcite surface in the presence of 10 000 ppm NaCl brine at different pH values (9.5 and 11) at ambient conditions. It is worth noting that I selected only high pH values for the adhesion force measurements (9.5 and 11) to avoid calcite dissolution, which may influence the adhesion measurements at the nanoscale.

Thirdly, to further understand the impact of the pH on the oil-brine-carbonate interactions, I measured the zeta potential of the oil-brine-calcite interfaces at the ambient conditions. However, the zeta potentials of oil-brine and brine-calcite interfaces were measured in the

presence of 10 000 ppm NaCl brine at different pH values (6.5, 9.5, and 11) using Malvern Zetasizer ZS Nano series equipment, and used the zeta potential results to calculate the disjoining pressure of the system. It is worth mentioning that the used AFM in this study can only handle the adhesion measurements at ambient conditions, and I aimed to use the impact of the pH on the adhesion force between acidic oil and calcite to interpret the impact of the pH on the contact angle, thereby the wettability of carbonate. All the experiments (AFM, contact angle, and zeta potential measurements) were conducted at ambient conditions.

While there are some uncertainties related to the experimental and calculation results in this methodology (e.g., AFM experiments at high pH, contact angle at pH 6.5, and boundary conditions used for the disjoining pressure calculations), I believe that the experiments and the disjoining pressure isotherm calculations together can provide an indication on the effect of the pH on the adhesion force and wettability alteration process.

Moreover, while the literature shows that clays play a critical role in the low salinity effect in the sandstone rock, there is a lack of research on how the oil-brine-clay interactions respond to the low salinity water effect in clay-rich carbonate reservoirs, especially at the molecular scale. Therefore, to reduce the ambiguity and to provide a better understanding of the wettability alteration during low salinity flooding in the clay-rich carbonate reservoirs, the methodology of Chapter # 6 was designed to elucidate the impact of the brine chemistry (pH) on the adhesion force between the oil components and clay (mica) in clay-rich carbonate reservoirs.

Initially, I used AFM to measure the adhesion force at the molecular level between oil components (non-polar and polar) and mica surface in the presence of 10 000 ppm NaCl brine at different pH (7 and 11) at ambient conditions. Then, I used Malvern Zetasizer ZS Nano series equipment to measure the zeta potential of the oil-brine-mica interfaces and evaluate the impact of the pH on the zeta potential of the oil-brine and brine-mica interfaces. However, the zeta potential measurements were conducted in the presence of the 10 000 ppm NaCl brine at pH 7 and 11 at ambient conditions. Furthermore, to further understand the isothermal thermodynamic of the system, I used zeta potential results to calculate the disjoining pressure of the oil-brine-mica system at pH 7 and 11. To avoid the complexity (e.g., ion exchange effect) and focus only on the pH effects, I used an aqueous NaCl solution in the adhesion force and zeta potential measurements.

3.2.2 Understanding the Variables and Influencing Factors for the Shift of Contact Angle

Placing calcite crystals in low salinity water causes a dissolution at the calcite surface, which results in variation in the surface roughness of the calcite surface at the sub-pore scale. This

phenomenon raises doubts about the reliability of contact angle results in the laboratories to evaluate the low salinity effects on the wettability alteration at the reservoir scale. This is because the surface roughness variation may lead to overestimating or underestimating the wettability alteration by low salinity water. Therefore, to limit the contact angle measurement uncertainty, the methodology in Chapter #7 was designed to elucidate the role of the surface roughness changes caused by calcite dissolution in the presence of LSW on the contact angle measurements at the sub-pore scale. To achieve this, I used two calcite samples in two different scenarios:

Scenario One: calcite sample #1 (AFM test) → contact angle measurement in high salinity (HS) brine → AFM test.

Initially, the AFM was used to measure the surface roughness of calcite sample #1. Then, the contact angle of the oil droplet on calcite sample #1 was measure in the presence of HS brine. Thereafter, the surface roughness of the calcite sample #1 was measured again using AFM to evaluate the change in the surface roughness.

Scenario Two: calcite sample #2 (AFM test) → contact angle measurement in low salinity (LS) brine → AFM test → contact angle measurement in HS brine → AFM test.

Firstly, the AFM was used to measure the surface roughness of calcite sample #2. Secondly, the contact angle of the oil droplet on calcite sample #2 was measured in the presence of LS brine. Thirdly, the surface roughness of the calcite sample #2 was measured again using AFM to evaluate the change in the surface roughness. Thereafter, the contact angle of the oil droplet on calcite sample #2 was conducted again in the presence of HS brine. Finally, AFM was used again to measure the surface roughness of the calcite sample #2 and evaluate the change in the surface roughness.

Moreover, a geochemical study was conducted through PHREEQC software to evaluate the calcite dissolution process in high and low salinity brines and correlate the results with the surface roughness variations.

3.2.3 Testing the Mechanisms of Alcohol-Assisted Waterflooding

Most of the discovered carbonate oil reservoirs are located in countries where are lack of freshwater resources (e.g., the Middle East), which consequently limits the application of the low salinity water injection as an enhanced oil recovery (EOR) method. Therefore, it is critical to find a new EOR technique to improve oil production in the traditional water flooding stage where the high salinity water is used. Therefore, the methodology in Chapter # 8 was designed to study the controlling factors of wettability alteration of the oil-brine-carbonate system by adding alcohols to the brine. To achieve this objective, I investigated the impact of the alcohol

carbon chain length and the number of hydroxy (−OH) functional groups on the contact angle of the oil−brine−carbonate system by adding different alcohols (ethanol, isopropanol, 1-pentanol, and glycerol) in high- and low-salinity brines at ambient conditions. Moreover, zeta potentials of brine−calcite and brine−oil interfaces at ambient conditions were measured with and without alcohols to elucidate the contact angle measurements on the basis of the thermodynamic isotherm. However, the brines used in all the experiments were formulated from NaCl and $CaCl_2$ salts only to represent the monovalent and divalent cations in the formation brine. The high salinity brine contains 1.00 mol/L NaCl and 0.01 mol/L $CaCl_2$, where the low salinity brine was prepared by diluting the high salinity brine 100 times by adding ultrapure water.

Whereas the methodology in Chapter # 9 was designed based on the results obtained from Chapter #8. In particular, the methodology was designed to investigate whether the wettability alteration obtained by adding alcohol (1-pentanol) at sub-pore level would trigger oil detachment, coalescence, transport, and thus enhance oil recovery in high temperature and high salinity carbonate reservoirs. To achieve this objective, firstly, I conducted contact angle experiments at the sub-pore scale to explore the impact of different temperatures (60, 100, 140^{o}C) and pressures (10, 20, 30, 40 MPa) on the oil-brine-carbonate interactions in the presence of 1-pentanol in high and low salinity brines. Secondly, four coreflooding experiments were performed at high temperature (140^{o}C) and high salinity (194450 ppm) at reservoir conditions to test the application of mixing a small percentage of 1-pentanol alcohol with the high salinity brine to improve the oil production in the secondary and tertiary waterflooding modes.

Note: the photographs of the used equipment in this research are provided in the appendix section.

Chapter 4. Response of Non-polar Component on Low Salinity Effect in Carbonate Reservoirs: Adhesion Force Measurement Using Atomic Force Microscopy*

4.1 Abstract

While the effect of polar-oil component on oil-brine-carbonate system wettability has been extensively investigated, there has been little quantitative analysis of the effect of non-polar components on system wettability, in particular as a function of pH. In this context, we measured the contact angle of non-polar oil on calcite surface in the presence of 10 000 ppm NaCl at pH values of 6.5, 9.5, and 11. We also measured the adhesion of non-polar oil group ($–CH_3$) and calcite using atomic force microscopy (AFM) under the same conditions of contact angle measurements. Furthermore, to gain a deeper understanding, we performed zeta potential measurements of the non-polar oil-brine and brine-calcite interfaces, and calculated the total disjoining pressure.

Our results show that the contact angle decreases from 125° to 78° with an increase in pH from 6.5 to 11. AFM measurements show that the adhesion force decreases with increasing pH. Zeta potential results indicate that an increase in pH would change the zeta potential of the non-polar oil-brine and calcite-brine interfaces towards more negative values, resulting in an increase of electrical double layer forces. The total disjoining pressure and results of AFM adhesion tests predict the same trend, showing that adhesion forces decrease with increasing pH. Our results show that the pH increase during low salinity waterflooding in carbonate reservoirs would lift off non-polar components, thereby lowering residual oil saturation. This physiochemical process can even occur in reservoirs with low concentration of polar components in crude oils.

4.2 Introduction

Carbonate reservoirs host roughly (>60%) of hydrocarbons (oil and gas) in the world [1], but only up to 40% of the oil can be recovered from the reservoirs [3]. The petroleum industry is therefore constantly working to develop economically feasible techniques to enhance oil recovery in order to meet the growing global demand for energy [182]. One technique that has attracted interest within the industry is low salinity waterflooding [83]. Extensive research has been done to show that lowering injected brine salinity can improve oil recovery from carbonate reservoir at secondary and tertiary mode from 5 to 30% of the original oil in place (OOIP) [11, 14, 15, 18, 19, 22, 23, 65]. Wettability alteration towards a more water-wet state is believed to be one of the main physiochemical processes behind the low salinity effect, which shifts oil relative permeability towards a lower residual oil saturation [22, 49, 62, 63], thus enhancing oil recovery. To understand the factors controlling the wettability alteration process in carbonate reservoirs, several explanations have been developed and proposed to

predict and quantify the wettability alteration, such as electrostatic bridging [15, 24, 25, 65, 77], electrical double layer [46, 48, 49, 54] and surface complexation modeling [58, 59].

To be more specific, the existing literature shows that the adsorption of the sulphate onto the pore surface would likely shift the surface charge from positive to negative, thus leading to a repulsion force between the oil (base and acidic functional groups) and carbonate pore surfaces [15]. Additionally, previous studies show that electrical double layer force also plays an important role in wettability alteration and release of the oil component from the carbonate surface [25, 46, 48, 49, 59]. For example, Mahani et al. [25] measured the zeta potential of the oil-brine and brine-carbonate (limestone) interfaces. They found that decreasing the salinity leads to an increase in the negative charge of the polar oil-brine and brine-carbonate (limestone) interfaces, suggesting a weaker electrostatic adhesion between the polar oil-brine and brine-carbonate (limestone) interfaces, and hence recession of the three-phase contact line. Furthermore, to gain a deeper understanding at the molecular level, atomic force microscopy (AFM) [159, 166] and quartz crystal microbalance (QCM) [158] have been used to examine the effect of brine chemistry on polar oil-rock adhesion. For example, Liu et al. [166] used AFM to study the effect of salinity on the adhesion force between functional oil groups and hydrophobic surfaces. They concluded that the electrical double layer was at least one of the controlling factors of adhesion forces, and thus the wettability of oil-brine-rock. In addition, Joonaki et al. [158] used QCM to investigate the impact of brine composition on the deposition of the asphaltene oil species on the rock surface at elevated temperature and pressure conditions. They found that brine composition and salinity play an important role in the deposition of the asphaltene oil species on the rock surface, thereby affecting the wettability of the oil-brine-rock system.

To better quantify and predict the wettability alteration process, surface complexation modeling has been implemented to model chemical surface species from oil and calcite surfaces thus characterizing the adhesion of oil and calcite [32, 58-61, 164]. For example, Brady et al. [58] developed a surface complexation model to characterize the wettability of oil-brine-calcite using a bond product sum concept, which is equal to $[-NH^+]\,[>CO_3^-] + [-NH^+]\,[>CaCO_3^-] + [-COOCa^+]\,[>CO_3^-] + [-COOCa^+]\,[>CaCO_3^-] + [-COO^-]\,[>CaOH_2^+] + [-COO^-]\,[>CO_3Ca^+]$. They suggest that the potential adhesion between the polar oil and carbonate surface increases with increasing bond product (more oil-wet system), and the potential adhesion between the polar oil and carbonate surface decreases with decreasing bond product (less oil-wet system). However, the above geochemical models were proposed to characterize oil-brine-carbonate wettability in light of the interaction of polar oil groups ($-NH^+$ and $-COO^-$) on carbonate surfaces. Few research have been done to draw on any

structured research into the response of non-polar oil on wettability alteration when low salinity waterflooding in carbonate reservoirs, and fewer works have been performed to investigate the effect of pH on the adhesion of non-polar oil and calcite, although local pH likely increases with low salinity waterflooding in carbonate reservoirs [20, 124, 125, 183]. For example, Generosi et al. [137] used AFM to investigate the effect of the potential determining ions on the calcite wettability although the pH effect was not examined. They found that the presence of Mg^{2+} and SO_4^{2-} ions decreased the adhesion forces between CH_3-terminated tip and calcite surface thus increasing hydrophilicity.

In conclusion, while the influence of polar oil components on wettability alteration has been extensively investigated, in particular in geochemical modeling and molecular-level force measurements, researchers have not treated the response of non-polar oil on wettability alteration in much detail. Also, we know that the binding/bridging between polar oil component-calcite surface would likely decrease with increasing pH, but how non-polar oil responds to the increase in pH remains unclear. We therefore hypothesized that non-polar oil would be lifted off from calcite surfaces due to the increase in pH during low salinity waterflooding. To test this hypothesis, we measured the contact angle of non-polar oil on the calcite surface in the presence of an aqueous ionic solution (10 000 ppm NaCl) at pH values of 6.5, 9.5, and 11. We also measured the adhesion of the non-polar oil group ($–CH_3$) and calcite using AFM under the same conditions of the contact angle measurement. Furthermore, to gain a deeper understanding of the isothermal thermodynamic, we performed zeta potential measurements of $–CH_3$-brine and brine-calcite interfaces, and calculated the total disjoining pressure using a sphere to flat thermodynamic model under constant potential condition.

4.3 Experimental Procedures

4.3.1 Materials

Brine

To validate our hypothesis and study the influence of pH on the adhesion force between non-polar oil and carbonate surface, we used NaCl salt (Analytical reagent, 99.9%) and ultrapure water (Resistivity 18.2 MΩ) to prepare NaCl brine with 10 000 ppm salinity. It is noteworthy that divalent cations (Ca^{2+} & Mg^{2+}) were not used in this study because of their competition with H^+/OH^- to adsorb on calcite surfaces, which likely compensates for the pH effect on non-polar oil [146]. Rather, the monovalent ion can better help us to focus on the pH effect. Also, to avoid any variation of the pH due to calcite dissolution during the measurements, a piece of calcite crystal was submerged in the solution for two days to reach calcite dissolution equilibrium. It is worth noting that calcite dissolution can reach equilibrium within 4 hours

[82]. Finally, we used 0.250 mol/L of hydrochloric acid and sodium hydroxide solutions to adjust the pH of the brine to 9.5 and 11.

Oil

Given that this work aims to understand the response of non-polar component on the adhesion at calcite surface with the presence of various brines, we used model oil compound containing $–CH_3$ groups to represent hydrocarbon functional groups [32, 184, 185]. In this work, we used Octadecane ($C_{18}H_{38}$) for contact angle measurements, and 1-Octadecanethiol ($C_{18}H_{38}S$) for AFM measurements. The strong chemisorption of the thiol group on the gold helps to represent the oil on the gold AFM tip [186, 187].

Calcite

To examine our hypothesis, we used calcite crystal (Iceland Spar from Ward's Science) as substrates for the contact angle measurements and the AFM experiments. To ensure the integrity of experimental measurements, and to avert the surface roughness effect on the contact angle and AFM measurements [188, 189], the calcite crystals were cleaved to obtain a new clean smooth calcite surface [60], then rinsed with deionized water saturated with calcite to remove any small calcite pieces. It is worth noting that we saturated the deionized water with calcite to prevent any effect on the new calcite surface during cleaning. Also, it is noteworthy that the surface roughness of the new calcite surface used in this work is in a range of 4 to 7 nm, which has been reported in our previous work [190].

Also, we prepared calcite powders with diameters in the range of 10 to 100 μm for the zeta potential measurements at the interface of brine-calcite as a function of pH (6.5, 9.5, and 11). The calcite powders were prepared using the following steps. Deionized water saturated with calcite was used to clean the calcite crystal. Then, the calcite crystal was kept in an oven at 60° to remove any adsorbed water at surfaces. Afterwards, mortar and pestle were used to crush the calcite crystal to fine powders [48].

4.4.2 Contact Angle Measurements

In this study, we used the sessile drop method (Figure 4-1) to measure the contact angle of non-polar oil in the presence of aqueous ionic solution (10 000 ppm NaCl) at pH values of 6.5, 9.5 and 11 on calcite crystal surfaces. Given that pressure likely plays a negligible role in the oil-brine-rock system interactions [191], we measured the contact angle at ambient pressure. Also, we performed the contact angle measurements at 27 °C to avoid any solidification of the non-polar oil (Octadecane). However, a clean and new calcite substrate was used in the contact angle experiments. The substrate was obtained by cleaving a clean calcite sample, which was then rinsed with ultrapure water pre-saturated with $CaCO_3$ to remove all the remaining small

pieces of calcite from the new surface. Afterward, the new calcite surface was placed into the wettability measurement cell which was pre-filled with NaCl solution. After that, a droplet of the non-polar oil was then introduced onto the calcite substrate using a syringe. The contact angle was monitored and recorded until the contact angle variation with time was negligible. It is worth noting that to solely focus on the pH effect on non-polar oil adhesion on calcite surfaces, and to compare contact angle results with adhesion force measured by atomic force microscopy, we did not use a porous carbonate rock to measure contact angle [192].

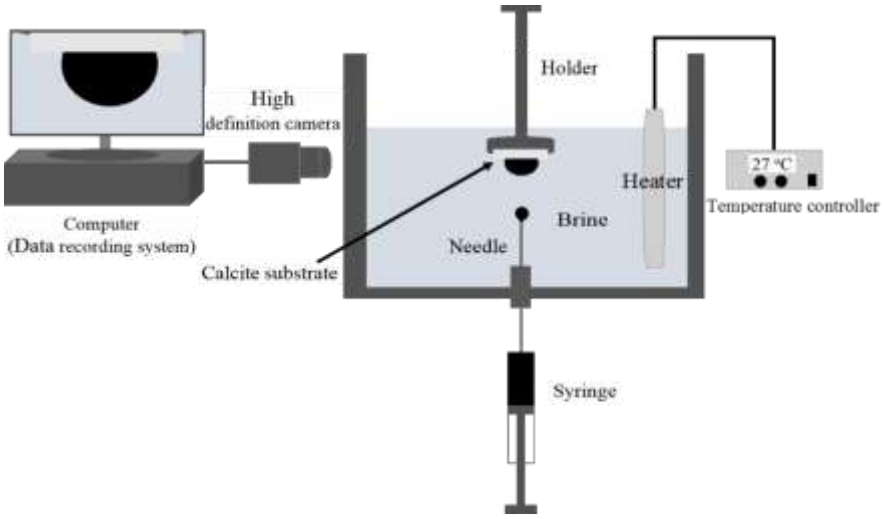

Figure 4-1. Schematic diagram of the contact angle test setup.

4.4.3 AFM Measurements

Atomic force microscopy (AFM) is an effective tool for directly measuring the adhesion force of the oil-brine-rock system [150, 159, 166, 193-197]. In this work, we used AFM (WITec alpha 300 SAR) to measure the adhesion force between the model oil compound and calcite in the presence of NaCl brine (10 000 ppm) at pH values of 9.5 and 11 at ambient conditions. It is worth noting that we did not measure the adhesion force at pH 6.5 due to the fact that calcite dissolution at the surface may significantly affect the oil-brine-calcite adhesion at nanoscale. To achieve realistic adhesion force results, we performed about one thousand force-distance measurements for each of the experiments with one thousand data points for each force-distance curve. The average value is reported in the results section. However, WITec ProjectFOUR software was used to collect the AFM experimental data. Also, we modified the MatLab program developed by Yu et al. [198], and used it to extract adhesion force data for multiple measurements at the same time.

To functionalize the model oil compound onto the AFM tip surface, in all the AFM experiments, we used the AFM tips (NPG-10 from Bruker Corporation) coated with gold and with a spring constant of 0.06 N/m. A chemical (1-Octadecanethiol, $C_{18}H_{38}S$) was used to functionalize the tip to represent the non-polar oil group ($–CH_3$) [197]. To successfully

functionalize the tip, we firstly used a plasma cleaner to clean the AFM tip for 30 min. Then, we immersed the AFM tip directly into ethanol at ambient temperature to minimize the gold oxide (Au_2O_3) that forms during the cleaning to metallic gold (Au) [199]. Thereafter, we submerged the AFM tip in 1mM of 1-Octadecanethiol ($C_{18}H_{38}S$) ethanol solution for one day. On the completion of the functionalization, the functionalized tip was washed by pure ethanol, and then dried by a stream of nitrogen gas prior to AFM measurements [200].

4.4.4 Zeta Potential Measurements

Electrical double layer force may play an important role in the wettability alteration of oil-brine-mineral systems [48, 201, 202], and this can be computed using the zeta potential of the oil-brine and brine-mineral interfaces. Thus, we used a Malvern Zetasizer ZS Nano series to measure the zeta potential of $–CH_3$-brine and brine-calcite interfaces at different pH values (6.5, 9.5, and 11). However, the zeta potential experiment methodologies are well demonstrated by Yang et al. [203]. It is worth noting that all the measurements were conducted at 27 °C, and the value of each zeta potential was taken from the average of four measurements.

4.4.5 Total Disjoining Pressure ($\Pi_{(Total)}$)

To expand our understanding of the isothermal thermodynamic, we calculated the intermolecular forces (IMF) between the non-polar oil-brine and brine-calcite interfaces using Derjaguin, Landau, Verwey, and Overbeek (DLVO) theory [204, 205].

$$\prod_{(\text{Total})} = \prod_{(\text{Van der Waals})} + \prod_{(\text{electric double layer})} + \prod_{(\text{structural})} \qquad \text{Eq } 4-1$$

To interpret the AFM adhesion measurements better, we used the sphere to flat geometry model to compute the total disjoining pressure at the constant potential condition [197]. It is worth noting that our previous study showed that the sphere to flat geometry model could better interpret the adhesion between the tip and flat substrate in AFM experiments compared to flat to flat geometry model [197].

Van der Waals forces

Van der Waals force is a long-range interaction, and it can be an attractive or repulsive force, depending on the sign of the calculated Hamaker constant [206]. In this research, the Van der Waals intermolecular force was an attractive force, and we computed the Van der Waals intermolecular force using the sphere to flat surface geometry model using the following model [206]:

$$\prod_{(\text{Van der Waals})} = -\frac{AR}{6h^2} \qquad \text{Eq } 4-1$$

where R is the sphere radius (m), h the film thickness between the tip and flat substrate (m), and A is the Hamaker constant (range between 10^{-21} to10^{-19}) calculated using equation 4-3, below [146]:

$$A = \frac{3}{4} k_B T \left(\frac{\varepsilon_o - \varepsilon_w}{\varepsilon_o + \varepsilon_w}\right) \times \left(\frac{\varepsilon_s - \varepsilon_w}{\varepsilon_s + \varepsilon_w}\right) \qquad \text{Eq } 4-3$$

where k_B is the Boltzman constant (1.381×10^{-23} J/K); T is the temperature in kelvin; ε_o is the permittivity of oil (2 C/(V.m)) [146]; ε_w is the permittivity of water (78.3 C/(V.m)), and ε_s is the permittivity of rock (7 C/(V.m)) [146].

Electric double layer forces

Electric double layer forces are a function of the surface charges and brine ionic strength, which strongly affects the total disjoining pressure [204]. It is noteworthy that we calculated electrostatic potential using the Debye-Huckel equation although some of our zeta potential values are a bit greater than 50 mV [207].

$$\prod_{(\text{Electric double layer})} = \frac{2\pi R \varepsilon \varepsilon_w k[\, 2\psi_1\psi_2 - (\psi_1^2 + \psi_2^2)e^{-kh}]}{(e^{+kh} - e^{-kh})} \qquad \text{Eq } 4-4$$

Where ψ_1 and ψ_2 are the zeta potential of the brine-calcite and $-CH_3$-brine interfaces, respectively; ε is the permittivity of vacuum (8.85×10^{-12} C/(V.m)); R is the radius of the sphere (m), and k is the Debye length of solution (m^{-1}).

The Debye length is computed using equation 4-5 below [204]:

$$k^{-1} = \sqrt{\frac{\varepsilon \varepsilon_w \, k_B T}{2e^2 z^2 n_b}} \qquad \text{Eq } 4-5$$

Where e is the electron charge (1.60×10^{-19} C); z is the valence of a symmetrical electrolyte solution; and n_b is the ion density in the bulk solution.

Structural forces

The structural forces are a short-range interaction (h < 5 nm) compared to the long-range interaction forces (Van der Waals and Electric double layer forces). In this research, the structural forces were attractive interaction (hydrophobic forces) [205, 208], and we computed these using equation 4-6, below [208]:

$$\prod_{(\text{structural})} = -A_s \exp\left(-\frac{h}{\lambda_0}\right) \qquad \text{Eq } 4-6$$

where A_s is the constant range between 10^6 to 5×10^8 Pa [209]; and λ_0 is the structural forces decay length range between 0.2 to 1 nm [209]. In our study, we assumed that $A_s = 10^8$ Pa [209] and the λ_0 = 0.3 nm [210, 211].

4.4 Results and Discussion

4.4.1 Effect of pH on the Contact Angle of the Non-Polar Oil-Brine-Calcite System

Our contact angle measurement (measured through the brine phase) shows that increasing the pH of the bulk brine leads to a decrease in the contact angle of the non-polar oil-brine-calcite system, indicating a more water-wet system. For example, Figure 4-2 shows that the contact angle of the non-polar oil-brine-calcite system decreases from 125° to 97° when pH increases from 6.5 to 9.5, and decreases further to 78° when the pH increases to 11. This is largely due to the fact that pH influences the magnitude and polarity of electrostatic forces at the non-polar oil-brine and brine-calcite interfaces [60, 61]. Our results are in agreement with Rezaei et al. [212], who reported that increasing the pH of n-decane (non-polar oil)-brine-calcite system from 5 to 10 reduces the contact angle from 148° to 51°, suggesting that the wettability of n-decane-brine-calcite system is dependent on pH. Alameri et al. [49], also reported a similar pH effect on the contact angle of the oil-brine-carbonate system. It is also worth noting that pH likely significantly affects the interaction of the polar-oil-brine-carbonate system, and thus contact angle and wettability. For example, Xie et al. [60], found that increasing the pH from 3 to 8 increased the contact angle of the oil-brine (Na_2SO_4)-carbonate system from 53° to 175°. Moreover, the trend of the contact angle variation with pH can be predicted by the concept of bond product sum [60, 61].

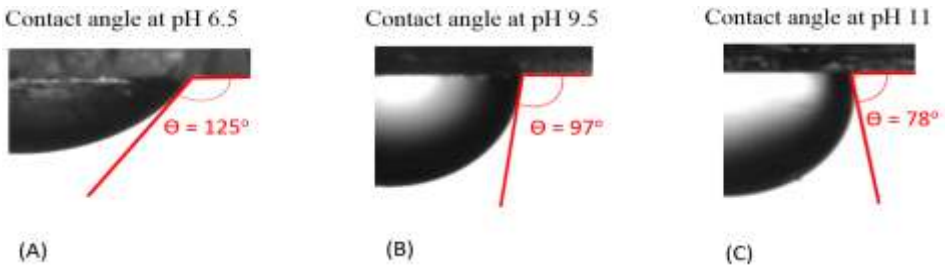

Figure 4-2. Contact of non-polar oil group (-CH_3) with calcite in presence of NaCl solution at (A) pH 6.5 (B) pH 9.5 and (C) pH 11.

4.4.2 Effect of pH on Non-Polar Oil-Calcite Interaction

The AFM results show that the adhesion force between non-polar-oil and calcite decrease with increasing pH (Figure 4-3 and 4-4), supporting our contact angle measurements and confirming that the increase of pH caused by low salinity injection likely prompts non-polar oil lifting off from pore surfaces. Figure 4-3 shows the average force-distance curves between non-polar oil group and calcite in the presence of sodium chloride brine (10 000 ppm salinity) at pH 9.5 and 11. The force-distance curves show that the adhesion forces of the non-polar oil group (–CH_3) decreases from about 9.2 to 2.8 nN (a 3-fold decrease) with an increase in pH

from 9.5 to 11. While few studies have been done to examine the impact of pH on non-polar calcite adhesion with the aid of AFM, our new results are in agreement with our previous work [197], where we found that increasing the pH from 7 to 11 would decrease the adhesion force five times (from 890 to 180 pN) between non-polar oil ($–CH_3$) and muscovite in the presence of sodium chloride brine with 10 000 ppm salinity. Also, Juhl et al. [207], found that increasing the pH from 2 to 8 decreased the adhesion force between non-polar oil ($–CH_3$) and muscovite from 1200 to 100 pN. Additionally, they noticed similar pH impact on the adhesion force between non-polar oil ($–CH_3$) and quartz. For example, in their measurements, when increasing the pH from 2 to 8 the adhesion force between the non-polar oil ($-CH_3$) and quartz decreased from 300 to ≈10 pN. Therefore, we tentatively conclude that increasing the pH increases the negative charges of the non-polar oil ($−CH_3$)-brine interface and brine-calcite interface thus giving rise to the electrical double layer force, which is discussed in the section below.

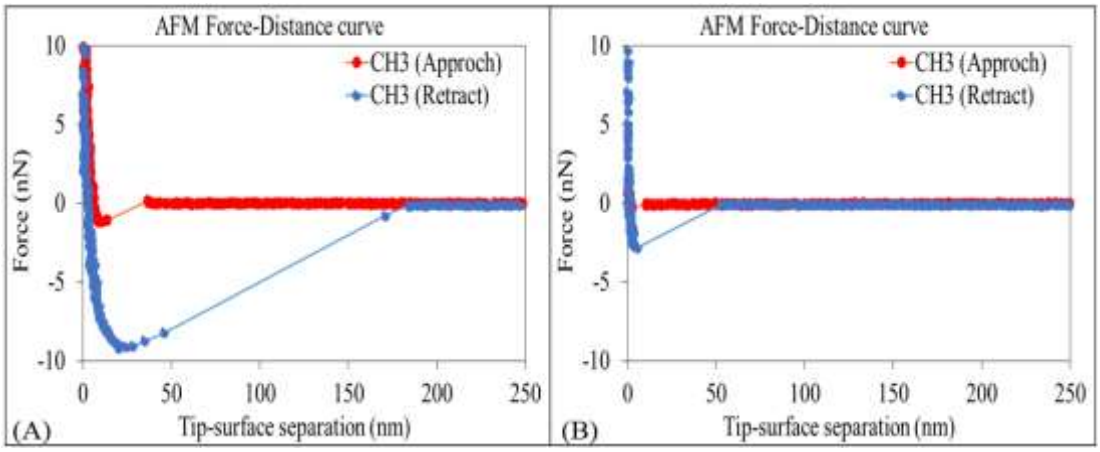

Figure 4-3. Average force-distance curves of non-polar oil group ($-CH_3$) and calcite in 10 000 ppm NaCl solution at (A) pH of 9.5 and (B) pH of 11.

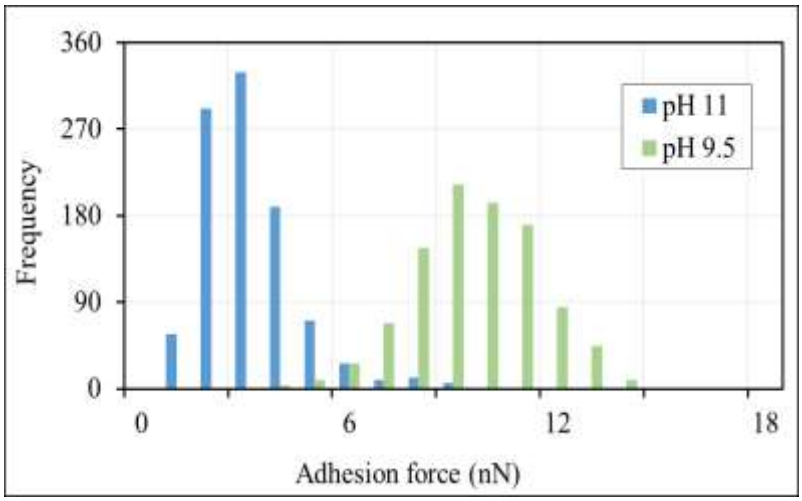

Figure 4-4. Histograms of adhesion forces between non-polar oil group (-CH_3) and calcite in 10 000 ppm NaCl solution at pH of 9.5 and pH of 11.

4.4.3 Effect of pH on Zeta Potential of Brine-Calcite and Non-Polar Oil-Brine Interfaces

The zeta potential of the brine-calcite interface is shifted in the negative direction with increasing pH (Figure 4-5), which is in line with previous works [213-215]. To be more specific, the zeta potential of the brine-calcite decreases from −8.0 mV to −12.0 mV with increasing pH from 6.5 to 9.5, and decreases further to −18.3 mV when increasing the pH to 11. This is consistent with the work of Thompson et al. [214], who found that increasing the pH from 9 to 11 decreased the zeta potential of the brine-calcite interface from −19 to −31 mV. Similarly, Siffert et al. [213], found that the zeta potential of NaCl brine (1mM)-calcite interface decreased from −2 to −22 mV when increasing pH from 9 to 11. Additionally, Vdovic et al. [215], reported that zeta potential of calcite in 1 mM NaCl brine decreased from −15 to −18 mV when increasing the pH from 9 to 10.5. However, the increase of zeta potential negativity with pH is mainly due to the deprotonation of the calcite surface sites and the increase in the negative calcite surface species $>CaO^-$ and $>CO_3^-$ according to the following geochemical reactions [54, 216]:

$$>CaOH^0 + OH^- = >CaO^- + H_2O$$

$$>CO_3H^0 + OH^- = >CO_3^- + H_2O$$

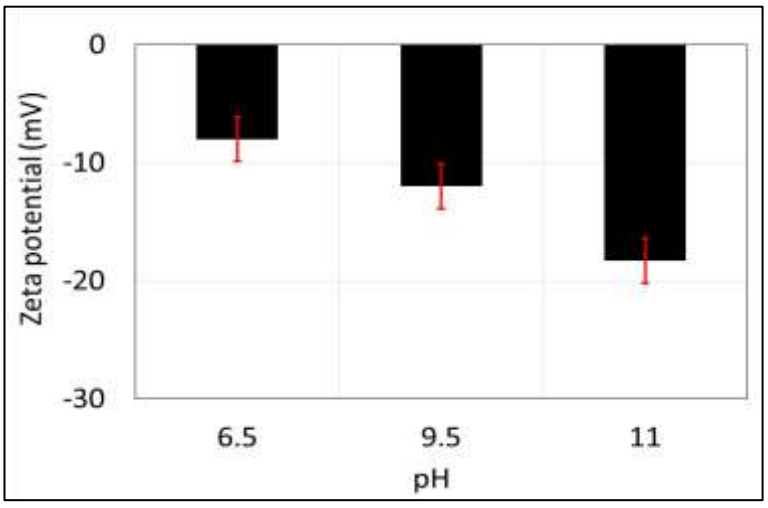

Figure 4-5. Zeta potential of calcite powder as a function of pH in 10 000 ppm of NaCl solution. Error bars represent the standard deviation.

Similar to the brine-calcite interface, increasing pH yields strongly negative zeta potential of non-polar oil (–CH_3)-brine interface. For example, increasing the pH from 6.5 to 9.5 (Figure 4-6) decreases the zeta potential of the non-polar oil (–CH_3)-brine interface from −35 to −45

mV, and it decreases further to −64 mV when increasing the pH to 11. This is consistent with the work of Jozef et al. [217], who observed that increasing the pH from 6 to 11 leads to a decrease in the zeta potential of the non-polar oil (C_6H_{14})-brine from −30 to −35 mV. Also, Marinova et al. [218], observed that raising the pH from 7 to 9 leads to a decrease in the zeta potential of the non-polar oil interface from −70 to −100 mV. Additionally, Beattie et al. [219], reported that zeta potential of the non-polar oil (hexadecane)-brine decreased from −95 to −125 mV when increasing the pH from 7 to 9.5. Taken together, the existing zeta potential of non-polar oil-brine implies that increasing pH leads to the adsorption of excess OH^- on the –CH_3 -brine interface, thus further shifting the zeta potential to be more negative [217-219].

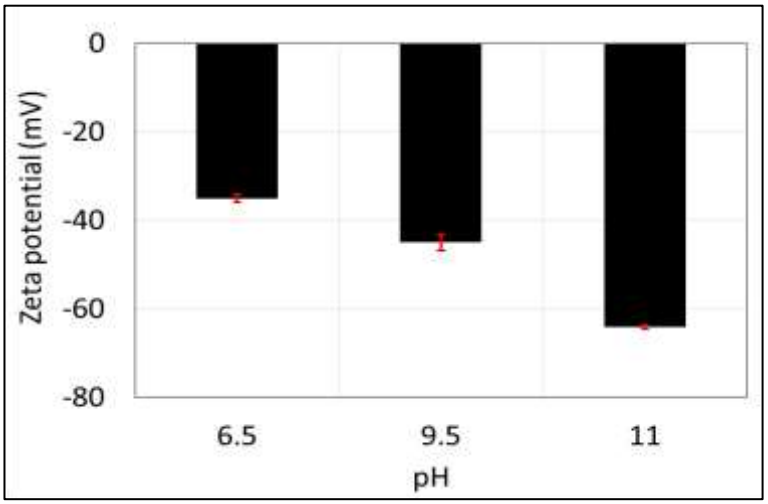

Figure 4-6. Zeta potential of non-polar oil group (-CH_3) as a function of pH in 10 000 ppm of NaCl solution. Error bars represent the standard deviation.

4.4.4 Effect of pH on Disjoining Pressure of the Sphere to Flat Model

To provide deeper thermodynamic insight into the experiments (e.g., contact angle, AFM adhesion force and zeta potential measurements), total disjoining pressure calculation was performed under constant potential conditions. It is worth noting that positive and negative disjoining pressure represents repulsive and attractive forces, respectively. Figure 4-7 shows that all pHs (6.5, 9.5, and 11) give negative disjoining pressure (Figure 4-7) in line with the AFM measurement. Additionally, the total disjoining pressure increases with increasing pH, suggesting greater repulsion in the non-polar oil-brine-calcite systems, which is in agreement with adhesion force results. For example, increasing the pH from 9.5 to 11 increases the repulsion of non-polar oil-brine-calcite systems in line with the AFM measurement.

In general, our results show that increases of pH during low salinity flooding in carbonate reservoirs lead to detachment of the non-polar oil components (the major oil components) from carbonate surface. This physicochemical process may not be modelled using the existing geochemical reactions because only the polar functional groups are captured in the

geochemical models [58, 61, 78]. However, our results show that the pH increase triggered by low salinity waterflooding may lead to the detachment of non-polar component. This implies that low salinity waterflooding may also be applied to carbonate reservoirs with low concentration of polar component such as low acid number and base number.

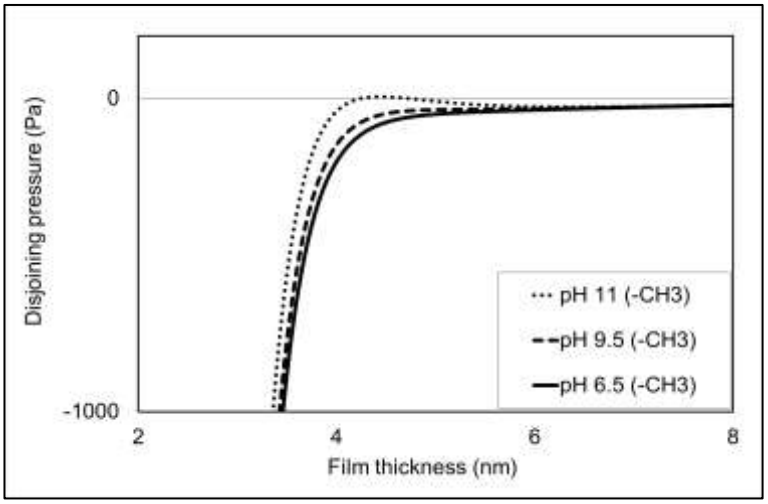

Figure 4-7. Total disjoining pressure under constant potential condition, versus interfacial separation of Calcite and non-polar oil with presence of NaCl solution at pH 6.5, 9.5 and 11.

4.5 Summary and Conclusions

Wettability alteration is believed to be a major physicochemical factor in the application of low salinity water injection in carbonate formations. The effect of polar oil components on wettability alteration has been extensively investigated as a function of pH, but researchers have not evaluated the response of non-polar oil on wettability alteration in much detail, although crude oils are rich in non-polar components. Therefore, we measured the contact angle of non-polar oil on the calcite surface in the presence of an aqueous ionic solution (10 000 ppm NaCl) at pH values of 6.5, 9.5, and 11. In addition, we used atomic force microscopy (AFM) to measure the adhesion of the non-polar oil group ($–CH_3$) and calcite at different pH. Furthermore, to gain a deeper understanding of the isothermal thermodynamic, we performed zeta potential measurements of non-polar oil ($–CH_3$)-brine and brine-calcite interfaces, and calculated the total disjoining pressure using a sphere to flat thermodynamic model under constant potential conditions.

Contact angle measurements showed that the contact angle decreases from 125° to 97° with increasing pH from 6.5 to 9.5, and decreases further, to 78°, when increasing the pH to 11, implying a more water-wet system. AFM adhesion force measurements between the non-polar oil group ($–CH_3$) and calcite showed that the adhesion force decreases with an increase in pH from 9.5 to 11. The zeta potential data measured indicate that an increase in pH would cause a change in the zeta potential of the non-polar oil ($–CH_3$)-brine and calcite-brine interfaces

towards more negative values which would then result in an increase in the electrical double layer force. The total disjoining pressure and results of AFM adhesion tests follow similar trends, showing that adhesion force decreases with increasing pH due to electrical double layer expansion thus leads to a water-wet system. Taken together, our results confirm that detachment of non-polar oil from carbonate rock continues to take place during low salinity water injection, although desorption of non-polar oil from carbonate could not be modeled using existing surface complexation models. Also, this work sheds further light on the significance of pH increase on non-polar oil-calcite adhesion during low salinity water injection, and provides insights into the quantification of carbonate reservoir wettability.

Chapter 5. Influence of pH on Acidic Oil-Brine-Carbonate Adhesion Using Atomic Force Microscopy*

5.1 Abstract

Wettability alteration seems to be the main physicochemical process during low salinity water injection in carbonate formations. A pH increase due to calcite dissolution during low salinity water injection may affect oil-brine-rock interaction and thereby wettability. However, far too little attention has been paid to quantifying the impact of such an pH increase on acidic oil-carbonate adhesion. Therefore, we measured contact angles between acidic oil (-COOH) and calcite crystal in the presence of 10 000ppm NaCl solutions at different pHs (6.5, 9.5 and 11) at ambient conditions. Furthermore, we used atomic force microscopy (AFM) to measure the adhesion force between acidic oil groups (–COOH) and calcite substrate at different pHs (9.5 and 11) at similar conditions of the contact angle experiments. Moreover, to confirm the contact angle and AFM results, we measured the zeta potential of oil-brine and calcite-brine interfaces at the same condition and calculated the thermodynamic isotherm disjoining pressure. disjoining pressure. Our results show that the contact angle reduces from 134 to 95° as the pH increases from 6.5 to 11, increasing hydrophilicity. Adhesion force measurements show that increasing pH reduces the adhesion force between the acidic oil and carbonate in line with contact angle results. Zeta potential results show that increasing the pH increases the negativity of the zeta potential of acidic oil−brine and calcite−brine interfaces, implying the increase of the electrical double layer force. Furthermore, the total disjoining pressure isotherm becomes less negative with increasing pH, implying an increase of hydrophilicity. Taken together, our results confirm that a local pH increase due to calcite dissolution during low salinity water injection would prevail in the wettability alteration process in particular for high acidic oil bearing carbonate reservoirs.

5.2 Introduction

Carbonate formations are considered to be the most important oil reserves because they host more than 60% of the world's oil [1]. Nevertheless, the primary oil recovery stage (i.e., pressure depletion process) and the secondary oil recovery stage (i.e., gas or water injection) produce less than 40% of original oil in place (OOIP) in total from the carbonate reservoirs [3]. Low salinity water flooding appears to be a cost-effective and environmentally friendly means to achieve the reservoir potential by accelerating oil production while reducing residual oil saturation. Extensive work has been conducted at multiscale to investigate the potency of the low salinity effect in carbonate formation such as micromodel experiments (calcite microfluidic chip) [220], contact angle experiments [14, 23, 25-28, 220], spontaneous imbibition experiments [11, 18, 29-31], and forced imbibition experiments [14, 18, 23, 30, 49, 68], which show 5-30% increase in oil recovery.

* *Reference: Al Maskari et al. (2020) in Energy & Fuels, 34(11): p. 13750-13758.*

The wettability alteration process has been confirmed as at least one of the dominant mechanisms during low salinity water flooding. Moreover, a few mechanisms have been proposed to decipher the wettability alteration process such as dissolution of anhydrite [15] and calcite [23, 42], change of the electrostatic charge of the carbonate surface [24, 43], combination of the charge change and dissolution mechanisms [44, 45], expansion of the electrical double layer [46, 49, 54, 163], generation of in situ surfactant, [50] variations in interface viscoelasticity [7, 33, 36, 41, 51], and formation of microdispersions [39, 52].
Generally, all the mechanisms are associated with fluid−fluid interaction, and/or fluid−rock interaction, and/or fluid-fluid−rock interactions. However, it appears that fluid−fluid−rock interactions are of paramount importance, which governs the in situ wettability of reservoirs during low salinity water injection. Published works show that polar oil components (e.g., acidic oil group and basic oil group) play a vital role in the wettability of the carbonate surface [15, 48, 55, 58, 60, 70, 73, 75, 165]. For instance, contact angle, spontaneous imbibition, and core flooding experiments show that the acidic oil component (−COOH) plays a crucial role in the low salinity effect on the oil−brine− carbonate interaction, and hence the wettability of carbonate surface [15, 48, 55, 70, 73, 75, 165]. In addition, atomic force microscopy (AFM) has been used to study the influence of salinity on the adhesion force between the acidic oil components and hydrophobic surfaces, although the pH effect was not investigated. For example, Liu et al. [166] used AFM to investigate the influence of the brine salinity on the interaction force between the oil components and hydrophobic surfaces. They found that reducing salinity decreases the adhesion force between acidic oil groups and hydrophobic surfaces, thus altering the wettability of the hydrophobic surfaces. Furthermore, the molecular dynamic modeling has been used to elucidate the effect of the salinity on the adsorption of the acidic oil species on the carbonate surface. For instance, Bai et al. [138] developed a new molecular dynamic model to study the wettability alteration on the carbonate surface by analyzing the adsorption of the carboxylate species ($R{-}COO^{-}$, acidic oil) on the calcite surface. They found that lowering the salinity of the water increases the distance between the carboxylate ($R{-}COO^{-}$) oil species and the calcite surface due to the double layer expansion and, thus, leads to detachment of the carboxylate ($R{-}COO^{-}$) oil species and increases the oil recovery. Also, they observed that the presence of SO_4^{2-} and Ca^{2+} ions in the brine lead to the detachment of the carboxylate ($R{-}COO^{-}$) oil species from the calcite surface. In particular, they found that SO_4^{2-} displaces carboxylate ($R{-}COO^{-}$) oil species from the calcite surface, while Ca^{2+} forms an ion pair with the carboxylate ($R{-}COO^{-}$) oil species, thereby detaching the oil from the calcite surface.

Published work also shows that injecting low salinity water in carbonate leads to an increase in the local pH (up to 10) due to calcite dissolution [20, 82, 124-126], and this pH increase

most likely affects the oil−brine−carbonate interactions and hence wettability alteration. It is worth noting that the low salinity water may not always trigger the pH change at the core or reservoir scale as a result of the buffering effect. For example, Al-Attar et al. [135] Adegbite et al. [221] and Zaeri et al. [222] report increase of ≤1 pH unit during the low salinity water injection in carbonate. However, the local pH increase at the brine−carbonate interface disturbs the oil−brine−carbonate geochemical equilibrium and thus breaks the bonds between oil and carbonate, which triggers the wettability alteration process [48, 58-61, 82]. In this context, the geochemical modeling [58-61], and the contact angle measurements [48, 60, 61, 212] have been conducted in the past few years to reveal the key factor(s) of the wettability shift process during low salinity water flooding, accounting for the contribution of pH toward wettability alteration. For instance, Brady et al. [58] developed a surface complexation model to predict the low salinity effect on the wettability of the carbonate system by calculating the bond product sum, which is equal to $[>CaOH_2^+][–COO^–]$ + $[>CO_3Ca^+][–COO^–]$+ $[>CO_3^–]$ $[–COOCa^+]$ + $[>CaCO_3^–][–COOCa^+]$ + $[>CO_3^–][–NH^+]$ + $[>CaCO_3^–][–NH^+]$. They propose that the potential adhesion between the carbonate surface and polar oil species reduces with decreasing the bond product sum (more water-wet system), and the potential adhesion between the carbonate surface and polar oil species increases with the increasing the bond product sum (more oil-wet system). However, they reported that increasing the pH causes a decrease in the concentration of the polar oil and calcite surface species (bond product sum), and thus shifts the wettability to less oil-wet and increase the oil recovery. Also, Xie et al. [60] investigated the effect of pH on the wettability of the oil-brine-carbonate system and the implication of low salinity water flooding by conducting contact angle measurements and geochemical modeling. They found that at low pH (< 5), the oil-brine-carbonate system usually shows a water-wet system, where at pH between 6.5 to 7.5 exhibits oil-wet system, suggesting that pH is one of the controlling factors to govern the wettability of carbonate system.

Contact angle measurements also show that pH plays an important role in the oil-brine-carbonate interactions, thus wettability alteration. For example, Rezaei Gomari et al. [212] conducted contact angle experiments to study the influence of brine chemistry on the acidic oil-brine-calcite interaction. They found that the adsorption of the acidic oil groups on the carbonate surface decreases with increasing the pH of the brine, and thus increases the hydrophilicity of the carbonate surface. In addition, Xie et al. [223] performed contact angle measurements to study the influence of brine chemistry and oil composition on the wettability of the calcite surface. They found that increasing the pH of the brine from 7 to 12 slightly decreases the contact angle, suggesting that increasing the pH reduces the adsorption of the acidic oil components ($–COO^–$) on the carbonate surface, thus shifting the wettability of the carbonate system to more water-wet. Moreover, Sari et al. [48] preformed contact angle

measurements to investigate the influence of the pH on the wettability of the oil-brine-carbonate system. They found that increasing the pH from 3 to 8 decreases the hydrophilicity. However, contradictions remain on the effect of the pH on the acidic oil-carbonate interactions, and the response of the acidic oil species on wettability alteration as a function of the pH remains unclear.

In conclusion, while there has been considerable investigation on the response of the acidic oil components to the salinity effect, there are limited experimental studies that have been carried out to investigate the impact of pH increases due to calcite dissolution on the adhesion force between the acidic oil components (-COOH) and carbonate surface at the molecular level. Therefore, in this work we aimed to experimentally measure the contact angle of pure acidic oil (-COOH) on the calcite crystal in the presence of 10 000ppm NaCl solutions at different pH values (6.5, 9.5, and 11) at ambient condition. Then, we used an atomic force microscope (AFM) to measure the adhesion force between acidic oil groups (–COOH) and calcite substrate at different pH values (9.5 and 11) at conditions similar to those for the contact angle experiments. Moreover, to decipher the AFM and contact angle results, we conducted zeta potential experiments and computed the disjoining pressure isotherm as a function of pH.

5.3 Experimental Methodology

5.3.1 Experimental Materials

Carbonate substrate

In this research, we used Iceland Spar calcite crystal to represent carbonate substrate in the adhesion force experiments (AFM) and contact angle experiments. Prior to all the AFM and contact angle experiments, the Iceland Spar calcite crystals were cleaved to gain a new clean calcite surface [60], which can help to eliminate the impact of surface roughness on the results of the experiments [188, 189]. Our previous work shows a surface roughness with a range of 4 to 7 nm on a new calcite surface, which plays a minor role in adhesion forces [190]. To remove small calcite particles from the new calcite substrate, deionized water equilibrated with $CaCO_3$ was used to rinse all the new calcite surfaces.

We also used Iceland Spar calcite crystal to prepare calcite powders for zeta potential experiments with diameters of the powder particles ranging from 10 to 100 µm. The steps of the preparation of the calcite powders were well explained in previous work [48, 224].

Brines

Given that we aimed to focus on the influence of pH on the wettability of acidic oil component-brine-carbonate, and divalent cations (Ca^{2+} and Mg^{2+}) may compensate the pH effect due to their adsorption on the calcite surface which in return will reduce the influence of H^+/OH^-

[146], the brine used in this research was prepared using monovalent ion (NaCl) at a concentration of 10 000 mg/L. The brine was prepared by dissolving the analytical reagent NaCl salt (99.9%) in ultrapure water with a resistivity of 18.2 MW. It is worth noting that 10 000 ppm NaCl gives the highest wettability alteration in carbonate in the presence of NaCl solution [225]. Furthermore, we placed a small piece of calcite in the NaCl brine for 2 days to avoid calcite dissolution during the experiments which most likely lead to pH variation. Finally, we obtained the desired brine pH (9.5, 11) by adding 0.250 M NaOH and HCl solutions. It is worth noting that when the brine has a pH < than 9, the dissolution process will take place and thus lead to unstable adhesion force measurements at the nanoscale. Therefore, in this study, high pH values were selected for the adhesion force measurements (9.5 and 11) to avoid the calcite dissolution which could influence the adhesion measurements at the nanoscale. In this case, we at least can obtain a realistic trend of the pH effect on the adhesion force between the acidic oil and the calcite surface, although the low salinity flooding in carbonate leads to a pH increase up to 10 [20, 82, 124-126].

Oil

To elucidate the impact of pH on the interaction between the acidic oil components and carbonate substrate, a model oil with a carboxylic functional group was used to represent the acidic oil component. The model oil used in the adhesion measurements was 11-mercaptoundecanoic acid ($C_{11}H_{22}O_2S$) with a purity of 100% [150, 166, 197, 201, 226], and undecanoic acid ($C_{11}H_{22}O_2$) with a purity of 98% was used for contact angle measurements. It is worth noting that strong chemisorption between the gold on the AFM tip and the thiol group in 11-mercaptoundecanoic acid ($C_{11}H_{22}O_2S$) would help to functionalize the tip with the model oil [186, 187]. Also, it is worthwhile to mention that we did not use non-polar model oil (e.g., n-decane) to dilute the TAN of the acidic oil used in the contact angle measurements. This is because we aim to compare the contact angle results with the AFM results, which requires functional groups to be modified onto the tip of the sensor. In addition, the effect of the acidic oil concentration becomes negligible after a certain level of $–COO^–$. This is because the calcite surface contains a limited number of surface species (e.g., $>CaOH_2^+$, $>CO_3Ca^+$) which can accommodate a similar number of $–COO^–$ oil components.

5.3.2 Contact Angle Experiments

The sessile drop procedure was conducted in this study to examine the impact of pH increases on the contact angle of the acidic oil drop on calcite substrate in the presence of the 10 000 mg/L NaCl brine. Given that the pH of the brine likely increases from 5 to 10 during the injection of low salinity water in carbonate due to the dissolution of the calcite [20, 82, 124-126], a variation of pH (6.5, 9.5, and 11) was used to examine the influence of pH on the

wettability of the acidic oil-brine-carbonate system. We selected pH 11 to run contact angle measurements to further examine the trend of the pH effect on wettability. However, to solely focus on the impact of pH on the adhesion between the acidic oil and calcite surface, and to compare contact angle results with the adhesion force measured by AFM, we performed all the contact angle experiments at ambient conditions. The procedure of the contact angle measurement was well described in our previous work [224]. It is worth mentioning that, in each contact angle experiment, we placed two acidic oil droplets on the calcite substrate and reported the average of the contact angle measurements after the equilibrium conditions were reached.

5.3.3 AFM Experiments

Given that atomic force microscopy (AFM) [150, 159, 166, 193-197] is a well-defined and controlled setup for adhesion force at the molecular level, we used WITec alpha AFM (300 SAR) to examine the impact of the pH on the interaction between the acidic oil component and the calcite substrate inside sodium chloride solution (10 000 mg/L) at different pHs (9.5 and 11). To achieve reliable interaction forces between the calcite surface and the acidic oil species, 300 adhesion measurements were obtained. The average value of the adhesion forces and the closest force−distance curve to it are presented under Results and Discussion. The data from the AFM measurement was collected by WITec ProjectFOUR software; thereafter we used the MatLab program to extract the adhesion force measurement data. It is worth noting that we used NPG-10 AFM tips from Bruker Corp. in all the AFM experiments, and the methods of functionalizing the AFM tip with the model oil are well documented in our previous works [197, 224].

5.3.4 Zeta Potential Measurements

We measured the zeta potential of calcite−brine and acidic oil−brine interfaces to investigate the impact of pH increases on the zeta potentials of these interfaces, and also to calculate the electrical double layer force. Malvern ZS series was used in this study to determine the zeta potentials of calcite−brine and acidic oil−brine interfaces at 6.5, 9.5, and 11 pH values. The steps of zeta potential measurements are explained in detail by Yang et al. [203]. All the zeta potential tests were performed at the same temperature as the contact angle experiments (27 °C), and the average of four results is reported under Results and Discussion.

5.4 Total Disjoining Pressure ($\Pi_{(Total)}$)

This section describes the computation of the Derjaguin, Landau, Verwey, and Overbeek (DLVO) theory, which can provide a deep understanding of the influence of pH increases on the intermolecular forces in the oil−brine−carbonate system [204]. All the meanings and units of the symbols in the equations are provided in the Nomenclature.

$$\prod_{(\text{Total})} = \prod_{(\text{vdw})} + \prod_{(\text{EDL})} + \prod_{(\text{STR})} \qquad \text{Eq } 5-1$$

We calculated the total disjoining pressure at constant potential assumption using a sphere on flat geometry model [197, 224], which provides a representative demonstration of the interaction between model oil on the AFM tip and the calcite surface in the AFM adhesion force measurements, in comparison to other geometry models such as the two flat surfaces model [197].

5.4.1 Van der Waals Forces ($\Pi_{(vdw)}$)

The first part of the total disjoining pressure is the van der Waals force, which is a long-range interaction force [206]. In this study, we used the following equation (eq 5-2) to calculate the van der Waals intermolecular force: [206]

$$\prod_{(\text{vdw})} = -\frac{AR}{6h^2} \qquad \text{Eq } 5-2$$

However, the sign of the Hamaker constant determines if the van der Waals force is a repulsive or attractive force [227], and eq 5-3 was used to calculate the Hamaker constant: [146]

$$A = \frac{3}{4}k_B T \left(\frac{\varepsilon_o - \varepsilon_w}{\varepsilon_o + \varepsilon_w}\right).\left(\frac{\varepsilon_s - \varepsilon_w}{\varepsilon_s + \varepsilon_w}\right) \qquad \text{Eq } 5-3$$

5.4.2 Electric Double Layer Forces ($\Pi_{(EDL)}$)

Electric double layer forces play an important role in the calculation of the total disjoining pressure [204], and this force is a function of the ionic strength of the solution and charges of the surfaces. It is worth knowing that some of our zeta potential measurements are slightly higher than 50 mV and we computed the electrostatic potential by the Debye−Hücke equation [207].

$$\prod_{(\text{EDL})} = \frac{2\pi R\varepsilon\varepsilon_w k[\,2\psi_1\psi_2 - (\psi_1^2 + \psi_2^2)e^{-kh}]}{(e^{+kh} - e^{-kh})} \qquad \text{Eq } 5-4$$

where eq 5-5 was used to calculate k (Debye length of solution): [204]

$$k^{-1} = \sqrt{\frac{\varepsilon\varepsilon_w\, k_B T}{2e^2 z^2 n_b}} \qquad \text{Eq } 5-5$$

5.4.3 Structural Forces ($\Pi_{(STR)}$)

The third part in eq 5-1 is a short-range structural force (h < 5 nm). Structural forces can be repulsive forces for the hydrophilic surface and attractive forces for the hydrophobic surface [205, 208]. In this study, the structural forces are attractive forces (negative sign in eq 5-6), and they are calculated by using eq 5-6: [208]

$$\prod_{(\mathrm{STR})} = -A_s \exp\left(-\frac{h}{\lambda_0}\right) \qquad \text{Eq } 5-6$$

5.5 Results and Discussion

5.5.1 Influence of pH on the Contact Angle

Contact angle experiments show that raising the pH of the NaCl brine lowers the contact angle of the acidic oil−brine−calcite system, implying an increase of hydrophilicity. For example, the contact angle results in Figure 5-1 demonstrate that raising the pH of the solution from 6.5 to 9.5 reduces the contact angle of the acidic oil droplets on the calcite substrate from 130° (strong oil-wet system) to 110° (less oil-wet system), and the contact angle of the acidic oil drop on the calcite substrate reduces further to 80° with raising the pH further to 11, implying wettability alteration of acidic oil−brine−carbonate from the strong oil-wet surface to a slightly water-wet surface. However, this is mostly because the magnitude and polarity of the electrostatic forces of calcite−brine and acidic oil−calcite interfaces are highly sensitive to the pH variation [60, 61]. The contact angle results are in line with those of Rezaei Gomari et al. [212] who found that adsorption of the oil carboxylic functional group on calcite is controlled by the pH of the bulk solution. For instance, Rezaei Gomari et al. [212] found that raising the pH of NaCl brine from 5 to 7 causes a reduction in the advancing contact angle of the stearic acid/n-decane/water/calcite system from 140 to 95°, and this reduction in the contact angle continues to reach 50° when the pH increases further to 10 (see Figure 4 in ref [212]). Also, they report that the contact angle of the stearic acid/n-decane/water/calcite system decreases from 108 to 82° when the pH of the $MgCl_2$ brine increases from 5 to 7, and the contact angle reduces further to 68° with raising the pH to 10 [212]. In addition, Xie et al. [223] observed a similar pH effect on the contact angle of the oil−brine−calcite system. They found that raising the pH of the brine from 7 to 12 decreases the contact angle of the oil−brine−calcite system, and they suggested that increasing the pH reduces the adsorption of the acidic oil components ($-COO^-$) on the calcite and, thus, shifts the wettability of the system to more water wet.

Also, it is worth mentioning that the basic oil components ($-NH^+$) behave oppositely with increasing pH. For example, Chen et al. [61] measured the contact angle of oil with a high base number on the calcite surface in the presence of brines with different pH values. Their results indicate that the contact angle increases from 50 to 81° with increasing the pH from 4.42 to 5.68 regardless of the salinity; thus increasing the pH decreases the hydrophilicity of the calcite surface.

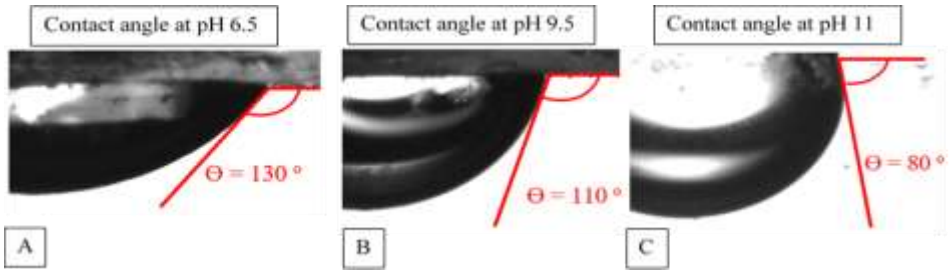

Figure 5-1: Contact angle of a drop of acidic oil on calcite substrate in sodium chloride (NaCl) solution at different pHs: (A) 6.5, (B) 9.5, and (C) 11.

However, the effect of pH on the contact angle can be interpreted from a geochemical perspective. For example, the pH increase of NaCl solution in the contact angle experiment likely reduces the [$–COO^-$] at the oil surfaces [76, 228], and decreases the [$>CaOH_2^+$] at the calcite crystal surface [229], hence reducing the electrostatic bridges between acidic oil and calcite surface species and shifting the wettability from strongly oil wet to a less oil-wet system. Also, elevating the pH in the contact angle experiment possibly increases the [$>CaCO_3^-$] at the calcite crystal surface [60, 61], which may increase the repulsion between the [$–COO^-$] at the oil surface and [$>CaCO_3^-$] at the calcite crystal surface [58]. Consequently, the contact angle of the acidic oil droplets on the carbonate reduces with pH, shifting the wettability of carbonate system from strongly oil-wet to a less oil-wet system.

In addition to the contact angle results, we found that raising the pH from 6.5 to 11 leads to a slight decrease in the interfacial tension (IFT) of the acidic oil-brine interface. For example, Figure 2 shows that increasing the pH from 6.5 to 11 decreases the interfacial tension from 11 to 8.5 mN/m; thereby the IFT plays a minor role in the wettability alteration. Also, this small reduction in the IFT confirms that saponification did not occur in the system at pH 11 as the saponification leads to a significant reduction in the IFT. However, the IFT results are in line with the work of Rezaei Gomari et al. [212] who found that increasing the pH from 5 to 10 causes a negligible effect on the IFT of short-chain acid (heptanoic acid) and suggested that acid dissociation was behind this phenomenon. It is worth noting that heptanoic acid and undecanoic acid (model oil used in this study) have the same dissociation constant of 4.8 [230].

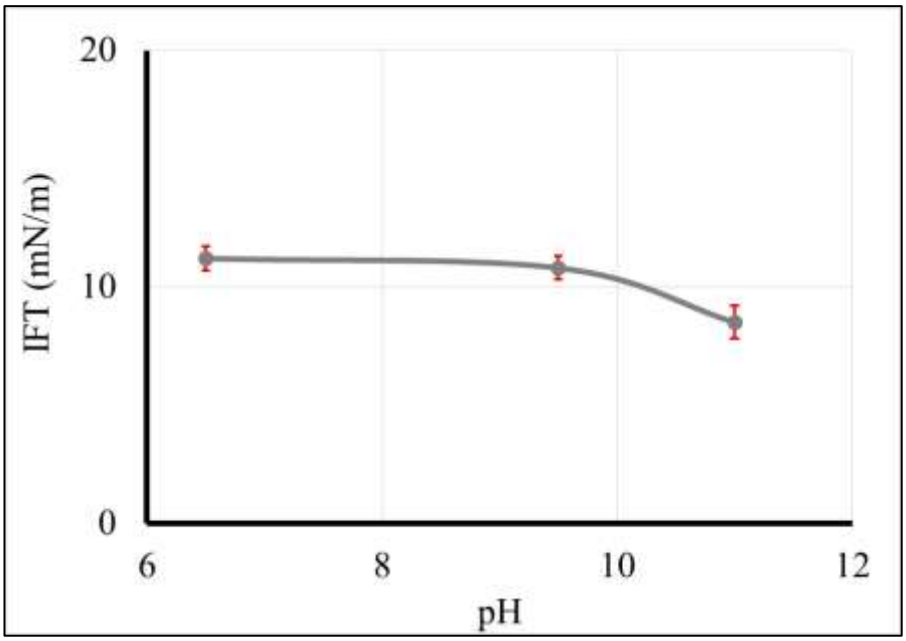

Figure 5-2: Effect of pH on the IFT of undecanoic acid−(NaCl) brine interface. Error bars show the standard deviation.

5.5.2 Influence of pH on Adhesion Force

AFM measurements show that elevating the pH reduces the adhesion forces between the acidic oil and carbonate substrate (Figures 5-3 and 5-4), suggesting an increase of hydrophilicity in line with contact angle measurements. For example, the average force-distance curves in Figure 5-3 show that the average adhesion force decreases from 1317 to 1034 pN (21.5% reduction of the adhesion force) when the pH of the brine is raised from 9.5 to 11. In addition, Figure 5-4 displays the frequency distribution histograms of adhesion force at pH 9.5 and 11, and it is evident that increasing the pH reduces the adhesion force between carboxylic oil species and calcite substrate. This reduction is mainly due to the fact that increasing the pH increases the negativity of the calcite−brine and acidic oil−brine interfaces, which in return increases the electrical double layer forces. Moreover, the adhesion force measurements are in line with the published work [7, 196, 197], For example, the calculation of the total disjoining pressure in our previous work [197] shows that raising the pH of the sodium chloride solution from 9.5 to 11 decreases the adhesion forces in the acidic oil−brine−rock system. Also, the core flooding experiment shows that injection of formation brine in the limestone core yields 40% OOIP combined with pH incremental from 5.2 to 6. When the pH further increases to 7.5 with the injection of the diluted seawater, the recovery factor increases to 32% original oil in place (OOIP) with a total oil recovery of 72% OOIP [20]. This confirms that desorption of acidic oil groups from the carbonate pore surface significantly contributes to the additional oil recovery during low salinity water flooding [82].

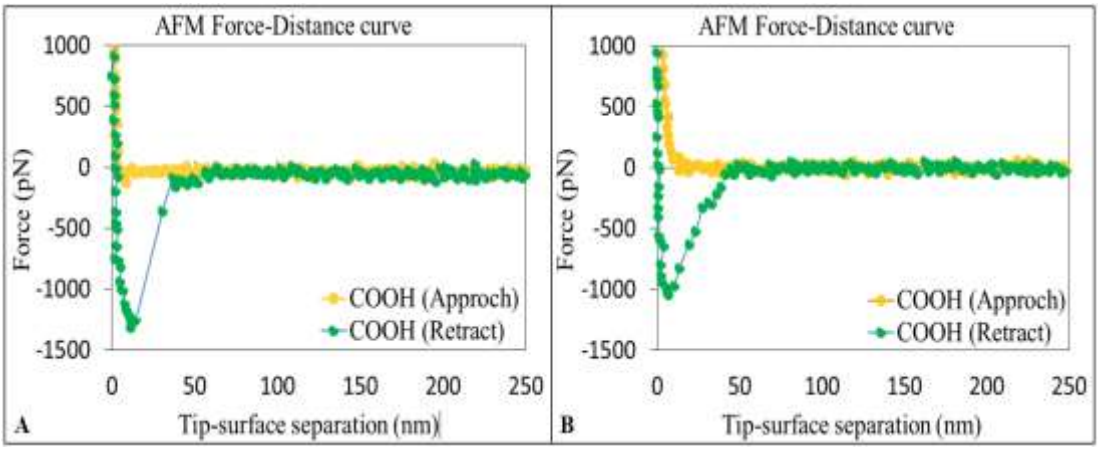

Figure 5-3: Force-distance curves measured between carboxylic oil species and calcite substrate inside sodium chloride (NaCl) solution at different pHs: (A) 9.5 and (B) 11.

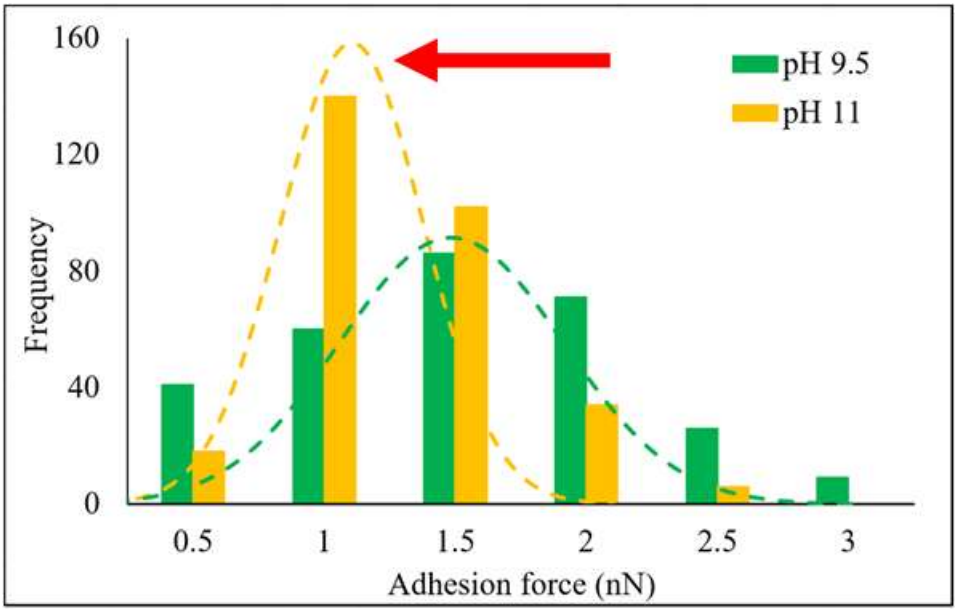

Figure 5-4: Frequency distribution histograms of adhesion force between carboxylic oil species and calcite substrate inside sodium chloride (NaCl) solution at pH 9.5 and 11(red arrow, trend of adhesion force with increasing pH). The wide distribution of the adhesion force does not indicate the uncertainty of the measurement but shows the different interactions between the acidic oil ($–COO^-$) and the different calcite surface species (e.g., $>CaOH_2^+$, $>CO_3Ca^+$) at the nanoscale.

5.5.3 Influence of pH on Zeta Potential

Acidic Oil-Brine Interface

Increasing the pH of the aqueous solution shifts the zeta potential of the acidic oil-brine interface to a strongly negative value in agreement with the literature [197]. The negativity of the zeta potential of the model oil used in this study is higher than that of the zeta potential of

crude oil and is mainly due to the higher content of the carboxylic oil group ($-COO^-$). For instance, the zeta potential of the acidic oil−brine interface reduces from −55 to −62 mV with raising the pH of the NaCl brine from 6.5 to 9.5. Further raising the pH of the brine to 11 reduces the zeta potential to −65 mV (Figure 5-5). This is mostly because elevating the pH of the brine causes deprotonation of the carboxylic functional group according to the reaction R-COOH = $R\text{-}COO^-$ + H^+, which is well supported by published literature [60, 76, 165]. For instance, Brady et al. [76] conducted geochemical modeling to investigate the impact of pH variation on the oil surface species. They found that raising the pH of sodium chloride brine from 4 to 9 causes an increase in the density of $-COO^-$ in the oil surface from 4 to 6 μmol/m^2, suggesting that at high pH values the oil surface charge would be predominated by the $-COO^-$ oil group.

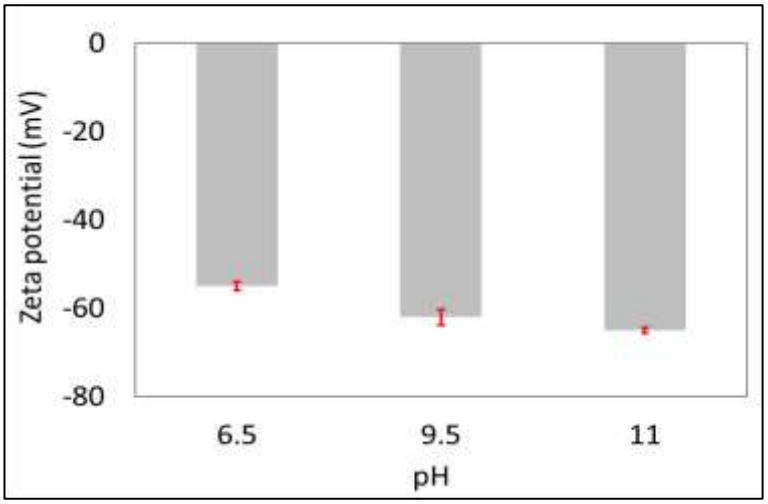

Figure 5-5: Zeta potential of acidic oil−(NaCl) brine at pH 6.5, 9.5, and 11. Error bars represent the standard deviation.

Calcite-Brine Interface

A similar pH effect was observed with the zeta potential of the calcite−brine interface in agreement with the literature [213-215]. For example, raising the pH of the sodium chloride brine from 6.5 to 9.5 reduces the zeta potential of the calcite−brine interface 4.0 mV units from −8.0 to −12 mV. Raising the pH of the sodium chloride brine to 11 reduces the zeta potential of the calcite−brine interface furthermore to −18.3 mV (Figure 5-6). This is in line with Siffert et al. [213] who reported that the zeta potential of the calcite−brine interface reduced −2 to −22 mV with raising the pH of the NaCl solution from 9 to 11. Likewise, Thompson et al. [214] found that the zeta potential of the calcite−brine interface reduces from −19 to −31 mV with raising the pH of the aqueous solution from 9 to 11. The experimental data confirms that the increase of pH promotes deprotonation of carbonate surface species such as >CaOH and

$>CO_3H$ and thus increases $>CaCO_3^-$ and $>CO_3^-$ [229], leading to a shift of the zeta potential of the calcite−brine interface toward a more negative value.

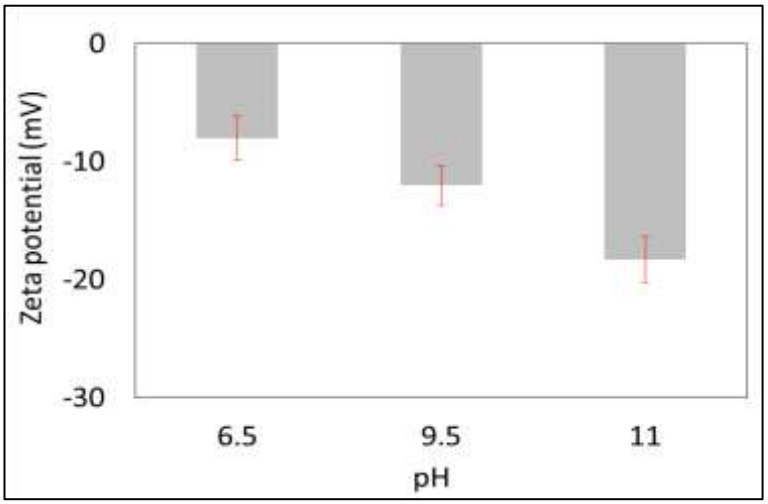

Figure 5-6: Zeta potential of calcite−(NaCl) brine at pH 6.5, 9.5, and 11. Error bars represent the standard deviation.

5.5.4 Influence of pH on Total Disjoining Pressure

To obtain a better understanding of the contact angle results, AFM results, and zeta potential results, the total disjoining pressure isotherm was calculated between the acidic oil−brine surface and the brine−calcite surface at the constant potential assumption. It is worthwhile to mention that negative and positive disjoining pressure values indicate attractive and repulsive forces, respectively. Our disjoining pressure calculation (Figure 5-7) shows that all the forces at all pH values are attractive forces (negative values), which is in line with the results obtained from the adhesion force experiments. Moreover, the disjoining pressure between the acidic oil− brine and calcite−brine interfaces increases with increasing pH, thus more repulsion forces. This is mainly due to the changes in the zeta potential of the acidic oil−brine and calcite−brine interfaces toward more negative values, which leads to an increase in the electrical double layer force. However, these increases in the repulsion forces with increasing the pH were in agreement with the contact angle and adhesion force measurements. For example, Figure 5-7 shows that repulsion forces rise with increasing pH of the system from 6.5 to 11, supporting Figure 5-1, which shows that the contact angle of an acidic oil droplet on calcite substrate shifts from a strongly oil wet system toward the less oil wet system with increasing the pH from 6.5 to 11. While the disjoining pressure at pH 11 remains negative over the water film thickness, the trend of the disjoining pressure isotherm shift with pH reveals that the increase of pH facilitates desorption of acidic functional groups from the carbonate surface, shifting wettability toward less oil wet. With a combination of contact angle measurements, AFM, zeta potential experiments, and disjoining pressure calculation, we

demonstrate that calcite dissolution may not directly contribute to the incremental oil recovery of low salinity water injection in carbonate reservoirs, but the pH increase as a result of calcite dissolution plays an important role to shift wettability and thus increase oil recovery.

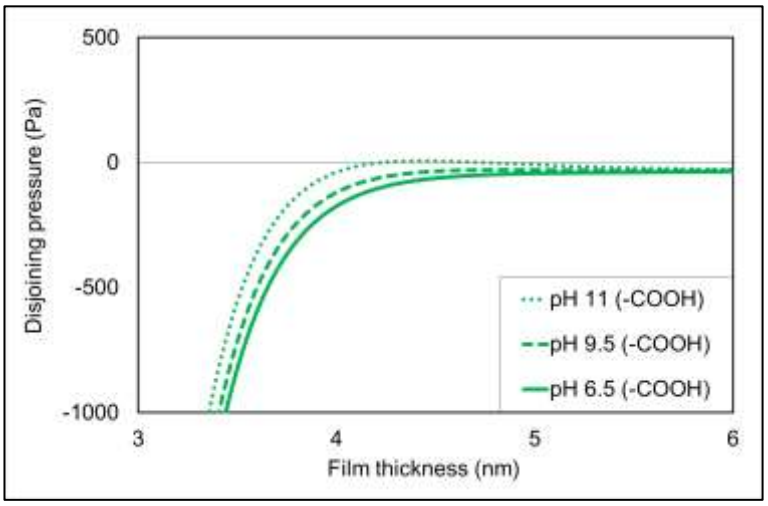

Figure 5-7: Disjoining pressure function of acidic oil (−COOH) and calcite in sodium chloride solution at different pHs (6.5, 9.5, and 11).

Generally, there are some uncertainties related to the experimental and calculation results in this study (e.g, contact angle at pH 6.5, AFM experiments at high pH, and boundary used for the disjoining pressure calculations). It is worth noting that we may not fully trust the absolute value of the results, but the experiments and the disjoining pressure isotherm calculations together underscore the importance of the pH on the adhesion force and wettability alteration process.

5.6 Summary and Conclusions

Wettability shift appears to be an important physicochemical process to trigger incremental oil recovery during low salinity water injection in carbonate formations. Oil components and pH together play a significant role in in situ wettability. While geochemical modeling together with contact angle measurement has been performed to understand the nature of the wettability alteration during low salinity water injection, there has been little experimental evidence associating acidic oil groups (−COOH) with wettability at a molecular level as a function of pH. Therefore, we hypothesize that the pH increase as a result of calcite dissolution during low salinity injection decreases the adhesion between the acidic oil group (−COOH) and carbonate pore surfaces, leading to detachment of the acidic oil from the carbonate pore surfaces and thus improving the oil recovery. To examine our hypothesis, we conducted contact angle measurements of an acidic oil (−COOH) drop on a calcite crystal inside (10 000 ppm) sodium chloride brine at different pH values (6.5, 9.5, and 11). Furthermore, we used

atomic force microscopy (AFM) to measure the adhesion force between acidic oil groups (−COOH) and the calcite substrate at different pHs (9.5 and 11) at similar conditions of the contact angle experiment. Moreover, we conducted zeta potential experiments to examine the impact of pH on the total disjoining pressure of the system against the AFM and contact angle results. Our contact angle results show that contact angle reduces from 134 to 117° with raising pH from 6.5 to 9.5, and the contact angle reduces furthermore to 95° with raising the pH to 11. Also, the AFM measurements support our contact angle results, showing that the adhesion force between the −COOH oil group and calcite reduces from 1.26 to 1.05 nN as the pH of the sodium chloride brine increases from 9.5 to 11. Zeta potential results show that raising the pH increases the negativity of the zeta potential of the acidic oil−brine and calcite−brine interfaces, thus elevating the electrical double layer force. Furthermore, the disjoining pressure calculation shows a shift of thermodynamic isotherm from strongly negative to less negative, supporting the results of AFM and contact angle experiments, confirming that the increase of pH caused by calcite dissolution during low salinity water injection contributes to wettability alteration and hence incremental oil recovery. This study sheds light on the significant influence of a local pH increase caused by calcite dissolution on the performance of low salinity water flooding in particular for high acidic oil bearing carbonate reservoirs.

Chapter 6. Role of Basal-Charged Clays in Sandstone and Clay-Rich Carbonate Reservoirs: Adhesion Force on Muscovite using Atomic Force Microscope*

6.1 Abstract

Low salinity waterflooding appears to be an important means to improved oil recovery in sandstone reservoirs. Wettability alteration has been identified as the main effect behind low salinity waterflooding due to the interaction of oil−brine−rock interfaces, where clay minerals play a significant role. While how edge-charged clays (kaolinite-bearing sandstone) contribute to wettability alteration during low salinity waterflooding has been well-studied, the role of basal charged clays (smectite, illite, and chlorite) in wettability alteration remains unclear. We previously confirmed that basal charged clays trigger pH increases (2 to 3) due to ion exchange with added impetus of mineral dissolution by means of geochemical modeling (Chen et al. Fuel 2018, 112−117). In this work, we hypothesized that the pH increase triggers negative zeta potential of both oil−brine and brine−clays, thus increasing double layer expansion, as well as hydrophilicity. To test our hypothesis, we measured adhesion force between functional groups ($-CH_3$ and −COOH) and muscovite using atomic force microscope (AFM) at pH of 7 and 11 with NaCl at a concentration of 10 000 mg/L NaCl. To gain a better isotherm thermodynamic understanding, we measured zeta potential of brine−muscovite and oil−brine and computed total disjoining pressure under constant potential condition using flat to flat and sphere to flat thermodynamic models. Zeta potential measurements show that increasing pH shifted the zeta potential of oil−brine and brine−muscovite to more negative values thus increasing the electrical double layer force. Our AFM measurements show that increasing pH from 7 to 11 indeed decreased 80% of the adhesion force for both functional groups. Total disjoining pressure calculation predicts the same trend as the AFM adhesion measurements. However, the sphere to flat thermodynamic model predicts a correct degree of decrease in adhesion force compared to AFM, implying that the sphere to flat model should be applied to interpret AFM results. Together, our results confirm that basal-charged clays can significantly contribute to low salinity effect due to electrical double layer expansion, thus expanding the application envelope of low salinity flooding in sandstone reservoirs bearing basal-charged clays.

6.2 Introduction

Oil will be an important energy source for the rest of the 21st century [231]. As global energy demand continues to increase, the petroleum industry is constantly striving to develop economically viable techniques to improve oil recovery to meet this growing demand. Manipulating injected water chemistry, namely *LoSal* flooding by BP [4, 5] *Smart Waterflooding* by its originators, Austad and co-workers, at the University of Stavanger, Saudi Aramco [17], and *Designer Waterflooding* by Shell [8, 9], has emerged as a cost-effective and

environmentally friendly means to enhanced oil recovery (EOR) in sandstone reservoirs [232, 233]. Since the inception of this EOR technique, several mechanisms have been proposed to describe how the low salinity water improves oil recovery, including fines mobilization [40], limited release of mixed-wet particles [40], increased pH and reduced interfacial tension (IFT) similar to alkaline flooding , multicomponent ion exchange [4, 6, 35], ion exchange , double layer expansion [30, 37, 234], salting-in [11], salting-out [34], osmotic pressure , formation of micro-dispersions [39, 52], and variations in interface viscoelasticity [7, 33, 36, 41, 51].

However, all these mechanisms consist of liquid−liquid and solid−liquid interactions, and the contribution of each of the interactions to the low salinity effect is still incomplete; especially, how liquid−liquid interaction affects the low salinity effect remains unclear although the snap-off effect may be suppressed during low salinity waterflooding [235, 236]. For instance, Bartels et al. [237] used glass micromodels to investigate the effect of clay presence, type of oil, and aging on the low salinity effect at pore scale. Their results show that crude oil triggers incremental oil recovery during low salinity waterflooding, suggesting that interaction of polar oil and solid likely governs the low salinity effect. In contrast, Sohrabi et al. [39] also conducted fluid characterization and micromodel experiments to study the mechanism of the low salinity effect at pore scale. They concluded that the micro-dispersion mechanism is behind the low salinity effect, and it is independent of the rock mineralogy. Rather, they believe that oil−brine interactions likely control the wettability. Analogously, Morin et al. [36] conducted microfluidic flow to mimic the pore-level flow dynamics, and their results suggest that the low salinity effect is dominated by liquid−liquid interfacial viscoelasticity. Similarly, Wang et al. [41] used a porous plate to study the effect of the low salinity water on capillary pressure hysteresis, and their results show that the low salinity EOR-effect is not only attributed to wettability alteration but also to liquid−liquid interactions.

While several mechanisms have been investigated, wettability alteration has been identified as the main effect to achieve incremental oil recovery during low salinity waterflooding [83, 168, 174]. Two mechanisms have been proposed to decipher the controlling factor(s) of the wettability alteration. One is the electrical double layer theory, which describes the interaction forces between oil/brine and brine/rock interfaces [9, 238, 239]. The other one is surface complexation modeling which quantifies the number of surface species at interfaces of oil−brine and brine−rock and thus electrostatic forces [72, 76]. Rock mineralogy, in particular, clay minerals (e.g., montmorillonite, chlorite, illite, and kaolinite) are important to both theories because clay mineral surface chemistry plays a significant role in oil−brine−rock interaction and thus wettability [4, 35, 168, 169]. For example, Alotaibi et al. [168] found that clay content in sandstone significantly altered the wettability to intermediate or water-wet. Also, Berg et al. [174] visualized detachment of oil drops from the montmorillonite clay

minerals in low salinity water. Lager et al. [4] reported that cation exchange between oil and clays is important to yield low salinity effect.

Kaolinite mineral has been identified as an important mineral to trigger low salinity effect. For example, Seccombe et al. [175] reported that incremental oil recovery increases with increasing kaolinite content during low salinity waterflooding in Endicott Field, Alaska. Also, core plugs bearing kaolinite achieved 4.5%, 5.5%, and 7.3% of the original oil in place (OOIP) during low salinity waterflooding [6, 40, 175]. Moreover, low salinity effect was observed at pore network in the presence of kaolinite [170-173, 176, 177]. For example, Robin et al. [176] concluded that sandstone wettability is dependent on kaolinite clay using cryo-scanning electron microscopy. Jerauld et al. [173] also showed that oil preferentially sticks to kaolinite compared to quartz and chert using micromodel and cryo-scanning-electron- microscope. To understand how kaolinite affects oil−brine−reservoir rock system wettability, Austad et al. [240] proposed a chemical model to qualitatively describe the interaction of the oil−brine−kaolinite system. Later, Brady et al. [76, 241] proposed a surface complexation model to decipher the controlling factor of wettability alteration during low salinity waterflooding. They computed surface species at oil and kaolinite surfaces and proposed a parameter, namely bound product sum (BPS), to quantify the electrostatic forces and thus wettability.

Existing reports however also show that kaolinite free sandstone core plugs yield incremental oil recovery during low salinity waterflooding. For example, core flooding experiments conducted by Austad et al. [240] with kaolinite free showed that low salinity waterflooding yields pH increase from 6.7 to 9.6. They concluded that low salinity water promotes the substitution of Ca^{2+} by H^{+} at the clay surfaces, thus leading to a local pH increase at pore surfaces. Similarly, Cissokho et al. [242] also observed a pH increase from 7.3 to 10 during low salinity water using kaolinite free sandstone core plugs. They suggested that ion exchange and calcite dissolution likely trigger the pH increase during the low salinity flooding. In addition, Al-Saedi et al. [243] observed a pH increase from 7.3 to 9.9 while injecting low salinity into chromatography column containing 95% quartz and 5% illite, and they also believed that this pH shift is largely due to ion exchange process. Also, Brady et al. [76] proposed a geochemical model to decipher the pH increase due to the ion exchange process between brine and clays, also between oil and clays. Furthermore, Chen et al. [244] performed geochemical modeling to quantify the pH increase against RezaeiDoust et al.'s core flooding experiments [131] containing basal-clays only, confirming that ion exchange between low salinity water and basal clays (clay-Na + H^{+} = clay-H + Na^{+}) yields a pH increase.

It is worth noting that low salinity water may not achieve a measurable pH shift from effluent with presence of edge charged clays (kaolinite) in core plugs. For example, Nasralla et al. [245] showed that kaolinite mixing with low salinity brine gives the lowest pH increase (0.4 in average), whereas basal charged clay (montmorillonite) gives the highest pH increase (2.1 in average). Our latest surface complexation modeling [246] also shows that edge charged clays (kaolinite) only gives pH increase less than 1 in low salinity water [246]. However, basal charged clays can yield pH increase up to 2.5 with ion exchange process. Moreover, Al-Saedi et al. [243] observed a low pH increase from 7.3 to 8 while flooding low salinity water into chromatography columns containing 95% quartz and 5% kaolinite. Yet, they observed the pH increase from 7.3 to 9.9 when the column contains 95% quartz and 5% illite. Moreover, a local pH increase [247] due to geochemical reactions may not be monitored from the effluent [240]. This is because the pH of the effluent brine can be affected by other factors such as rock mineralogy, brine composition, and oil composition [39].

The pH increase likely affects oil surface chemical species [60, 76] thus interfacial tension of oil and brine, but it has been confirmed that negligible interfacial tension (IFT) variation plays a minor role in capillary number and thus residual oil saturation [235]. For instances, Farooq et al. [248] showed that increasing the pH of the low salinity NaCl solution (1500 ppm) from 7 to 9 leads to decrease of the IFT from only 17 to 13 dyn/cm. In addition, they observed that IFT between the crude oil and diluted seawater (1500 ppm decreases from only 15 to 12 dyn/cm while increasing the pH from 7 to 9. Also, Serkan et al. [249] studied the influence of aqueous phase pH on the interfacial tension of acidic crude oil and synthetic oil. Similarly, their results showed that the aqueous pH increase from 7 to 9 decreases the IFT of the acidic crude oil from 17 to 16 dyn/cm. Moreover, AL-Saedi et al. [243] examined the effect of clay minerals (kaolinite and illite on functional groups adsorption using chromatography columns. They observed that with the presence of 5% kaolinite, low salinity water yields effluent pH increase from 7.3 to 8, whereas the concentration of CH_3COO^- in the effluent increases from 0.001 to 0.15 μmol due to the desorption process. Similarly, RezaeiDoust et al. [131] reported that increasing the pH of the low salinity solution from 5 to 9 leads to decrease of quinolone oil adsorption on kaolinite clay for about 4 mg/g kaolinite.

Moreover, our previous geochemical modeling shows that pH increase due to ion exchange and mineral dissolution like decreases the adsorption of oil on mineral surfaces. For example, Chen et al. [244] performed geochemical studies against RezaeiDoust et al.'s core flooding experiments [131]. The geochemical study shows that bridging number between oil and basal-charged clays decreases from 3.34 to 0.21 μmol/m^2 while increasing the pH of the reservoir brine from 5 to 10. However, we did observe a widespread in additional oil recovery at a given

bridging number (Figure 7 of ref 109), implying that electrical double layer may need to be included to account for low salinity effect in basal charged clays.

To provide a lens to better understand low salinity effect in basal charge clays, we hypothesized that basal charged clays triggers pH increase due to ion exchange, which in return leads to strongly negative zeta potential at both oil−brine and brine−clay interfaces, thus increasing double layer expansion and hydrophilicity. To test our hypothesis, we measured adhesion force between functional groups (−CH_3 and −COOH) and muscovite using atomic force microscope (AFM) at pH of 7 and 11 with NaCl at a concentration of 10 000 mg/L NaCl. To gain a better isotherm thermodynamic understanding, we measured zeta potential of brine−muscovite and oil−brine and computed total disjoining pressure under constant potential condition using surface−surface and sphere−surface thermodynamic models.

6.3 Experimental procedures

6.3.1 Materials

Brines

To test our hypothesis and understand the effect of pH on oil−brine−rock adhesion force, we synthesized aqueous ionic solution NaCl with a concentration of 10 000 ppm using ultrapure water (resistivity 18.2 MΩ) and NaCl salt (AR, 99.9%). It is worth noting that divalent cations can facilitate the ion exchange process thus affecting system wettability [32]. To focus on the effect of an electrical double layer on the oil−brine−muscovite system, we only used aqueous NaCl solution in this study. Moreover, the pH of the solution was adjusted to 7 and 11 using 0.250 M sodium hydroxide (NaOH) and 0.250 M hydrochloric acid (HCl) solutions. We decided to manually adjust pH to 7 and 11 to test our hypothesis for two reasons. First, existing reports show that pH increase during low salinity waterflooding can reach up to pH unit of 3. For example, a pH increase of 2−3 was observed from four core flooding experiments (bearing with basal-charged clays) during the low salinity waterflooding [131]. Similar pH increase was also observed by Zhang et al. [250] who showed a pH increase of 2−3 during low salinity waterflooding. Likewise, Xie et al. [234] observed a pH increase from 6 to 9 during low salinity water injection. Second, the pH increase during AFM measurements cannot reach to pH unit of 3 due to the limited specific surface area. For example, the specific reactive surface area of the experimental substrate for the brine−muscovite is around 0.003225 m^2/g, which is much lower than brine−muscovite powers (100 m^2/g) [251, 252] representative of in situ reservoir condition.

Oil

Oil composition is important to affect oil−brine−rock interaction and thus wettability. Model compounds containing $-CH_3$ and −COOH groups were used to represent hydrocarbon functional groups [32, 184, 185]. Therefore, we used 1-octadecanethiol ($C_{18}H_{38}S$) and 11-mercaptoundecanoic acid ($C_{11}H_{22}O_2S$) to represent $-CH_3$ and −COOH oil groups, respectively.

Muscovite

To examine our hypothesis, muscovite sheets (supplied by wards scientific) were used as substrates for the AFM experiments and zeta potential measurements. This is because that structurally muscovite is characterized as a 2:1 clay mineral, one unity of muscovite consists of one octahedral aluminum layer located between two tetrahedral silica layers. Although, illite and smectite are 2:1 clay similar to muscovite and chlorite consisting of muscovite structure units bonded by a brucite layer. However, also, muscovite has the same range of cation exchange capacity (CEC) as these basal charged clays. Moreover, muscovite is a main constituent of different formed minerals which widely exist in sandstone reservoirs [253]. More importantly, muscovite is an ideal and common basal-clay for atomic force microscopy experiments because muscovite cleavage gives a clean and smooth basal-plan, which minimizes the surface roughness effect on adhesion force measurements [254].

6.3.2 Zeta Potential Measurements

Electrical double layer force may significantly affect the oil−brine−mineral system wettability, which can be calculated using zeta potential at oil−brine and brine−mineral surfaces. Therefore, we measured the zeta potential of oil− brine and brine−muscovite using Malvern Zetasizer ZS Nano series at different pH (7 and 11). The procedures of the zeta potential measurements are well described by Yang et al. [203].

6.3.3 AFM Measurements

To test our hypothesis that pH increase due to the ion exchange likely decreases the adhesion force between oil and basal-charged clays, we used atomic force microscopy (WITec alpha 300 SAR) to measure adhesion force of model compounds and muscovite at pH of 7 and 11 at ambient condition. The data of the AFM experiments were collected using WITec ProjectFOUR software, and then, the adhesion force data was extracted by using a modified MatLab code provided by Yu et al. [198].

To measure the adhesion force, AFM tips were functionalized. AFM tips (NPG-10) supplied by Bruker Corporation were used in all AFM measurements. The cantilever was coated with gold with its spring constant of 0.06 N/m. To functionalize the tip and mimic $-CH_3$ and −COOH oil groups, 1-octadecanethiol ($C_{18}H_{38}S$) and 11-mercaptoundecanoic acid

($C_{11}H_{22}O_2S$) were used. We first cleaned a new AFM tip using a plasma cleaner for 30 min. The tip then was directly immersed in ethanol at room temperature to reduce the gold oxide formed by the plasma treatment to Au [199]. Subsequently, it was immersed into 1 mM of 1-octadecanethiol ($C_{18}H_{38}S$) or 11-mercaptoundecanoic acid ($C_{11}H_{22}O_2S$) ethanol solution for 24h. Finally, the functionalized tips were rinsed with pure ethanol and dried under a nitrogen stream [200].

A contact configuration mode was used in the AFM to obtain the adhesion force measurement. To obtain representative adhesion forces, we recorded roughly 1000 force−distance curves across the muscovite surface with 1000 data points for each of the force− distance curves. Aqueous solutions were prepared 1 day before AFM measurements, and the pH was calibrated using a pH meter.

6.3.4 Total Disjoining Pressure ($\Pi_{(Total)}$)

To gain a better isotherm thermodynamic understanding, DLVO theory was used to compute the intermolecular forces between the oil/brine and brine/rock interfaces as a sum [204].

$$\prod_{(Total)} = \prod_{(\mathrm{vdw})} + \prod_{(EDL)} \qquad \text{Eq } 6-1$$

We neglected the structural force because it is considered to be a short-range interaction over a distance less than 5 nm [206]. To better interpret the adhesion force measured using AFM, we computed the disjoining pressure using both flat/flat and sphere/flat geometry models under constant potential condition.

Van der Waals Forces: In the intermolecular forces, van der Waals force plays an important role in a small separation and large separation [206], and it is always attractive regardless of the charge sign of the surfaces [227]. In this study, the flat−flat and sphere−flat surface geometry models were used to compute the van der Waals intermolecular force.

For flat/flat surfaces model, the van der Waals force is given by [206]

$$\prod_{(\mathrm{vdw})} = -\frac{A}{6\pi h^3} \qquad \text{Eq } 6-2$$

Where A is the Hamaker constant (assume 8.14×10^{-21} J) [36], and h is the film thickness between the two surfaces (m).

For the sphere−flat surface model, the van der Waals force is given by [206]

$$\prod_{(\mathrm{vdw})} = -\frac{AR}{6h^2} \qquad \text{Eq } 6-3$$

Where A is the Hamaker constant (assume 8.14×10^{-21} J) [239], h is the film thickness between the two surfaces (m), and R is the radius of the sphere (m).

Electric Double Layer Force: The electric double layer force is a function of surface charges which significantly affects the total disjoining pressure. Moreover, geometry plays an important role in the electrical double layer forces. It is worth noting that we used the Debye−Huckel equation to calculate electrostatic potential although our zeta potential is greater than 50 mV in magnitude [207].

For flat−flat surface geometry, the electric double layer force is given by [204]

$$\prod_{(EDL)} = \frac{\varepsilon\varepsilon_w\, k^2[\,(e^{+kh} + e^{-kh})\psi_1\psi_2 - (\psi_1^2 + \psi_2^2)]}{(e^{+kh} - e^{-kh})^2} \qquad \text{Eq } 6-4$$

Where ψ_1 is zeta potential of the interface of brine/muscovite, and ψ_2 is zeta potential of the interface of oil/brine; ε_w is the permittivity of water (78.3 C/(V.m).); ε is the permittivity of vacuum (8.85×10^{-12} C/(V.m)), and k is the Debye length of solution (1/m).

The reciprocal of Debye length is described by [204]

$$k^{-1} = \sqrt{\frac{\varepsilon\varepsilon_w k_B T}{2e^2 z^2 n_b}} \qquad \text{Eq } 6-5$$

Where k_B is the Boltzmann constant (1.381×10^{-23} J/K); T is the temperature in kelvin; e is the electron charge (1.60×10^{-19} C); n_b is ion density in the bulk solution; and z is the valence of a symmetrical electrolyte solution.

For the sphere−flat surface model, the electric double layer force is given by [204]

$$\prod_{(EDL)} = \frac{2\pi R\varepsilon\varepsilon_w k[\,2\psi_1\psi_2 - (\psi_1^2 + \psi_2^2)e^{-kh}]}{(e^{+kh} - e^{-kh})} \qquad \text{Eq } 6-6$$

Where ψ_1 is zeta potential of the interface of brine/muscovite, ψ_2 is zeta potential of the interface of oil/brine, and R is the radius of the sphere (m).

6.4 Results and Discussion

6.4.1. Effect of pH on Zeta Potential of Brine−Muscovite.

Increasing the pH triggered a strongly negative zeta potential of brine−muscovite interfaces (Figure 6-1) in line with literature works [207, 255-259]. For example, an aqueous solution with pH 7 gave a zeta potential of −20 mV, but it became more negative (−28 mV) when pH increased to 11. This is in line with the work of Nishimura et al. [256] and Nosrati et al. [257] who observed a similar pH effect on the zeta potential of muscovite clays. For instance, Nishimura et al. [256] found that increasing the pH from 6 to 10 decreased the zeta potential from −25 to −45 mV. Also, Juhl et al. [207] reported that zeta potential of brine−muscovite (1 mM NaCl) decreased from −50 to −110 mV with increasing pH from 3 to 9. In addition, Chorom et al. [260] reported that zeta potential of smectite decreased from −37 to −44 mV

with increasing pH from 7 to 9.7. The increase of zeta potential in magnitude with pH is largely due to ion exchange in muscovite surfaces [255, 256]. Adsorption of K and Na into muscovite surfaces leads to zeta potential increase in magnitude [255]. Moreover, increasing pH compensates H^+ substitution of Na and K [76] and thus higher zeta potential.

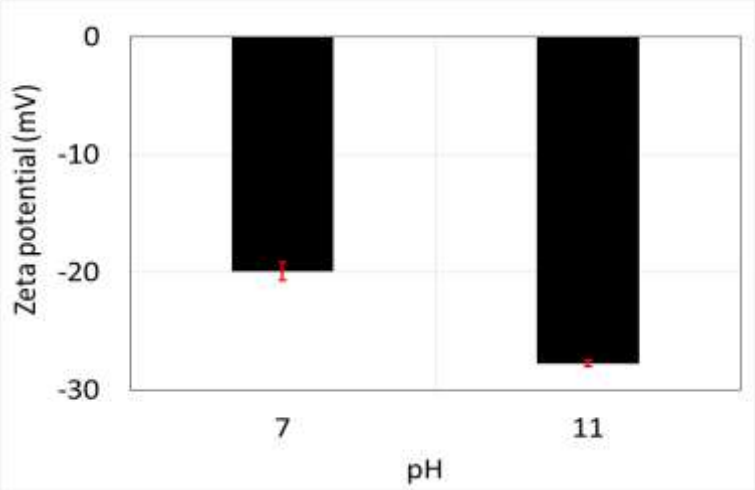

Figure 6-1. Zeta potential of muscovite powders as a function of pH at 10 000 ppm of NaCl solution

6.4.2. Effect of pH on Zeta Potential of −CH_3−Brine and −COOH−Brine.

Similar to brine−muscovite surfaces, increasing pH yielded strongly negative zeta potential for oil− brine (−CH_3/brine, −COOH/brine). For instance, the zeta potential of −COOH/NaCl brine decreased from −46 to −65 mV with increasing pH from 7 to 11 (Figure 6-2). This is largely because increasing pH increases $-COO^-$ ($-COOH = -COO^- + H^+$, $\log K_{25^oC} = -5.0$). For example, Brady et al. [76] modeled oil surface species variation with pH using PHREEQC, showing that $-COO^-$ increases from 4 to 6 μmol/m^2 with increasing pH from 4 to 9 in 1 M NaCl brine. This implies that high acidic oil likely triggers more low salinity EOR effects for a given pH increase due to the ion exchange process. Analogously, zeta potential of the −CH_3/NaCl brine decreased from −38 to −64 mV as pH increased from 7 to 11 (Figure 6-3). For the nonpolarized oil group (−CH_3), the decrease of the zeta potential of the −CH_3/NaCl brine interfaces with increasing pH is largely because of the adsorption of excess OH^- ions on the interfaces [217, 218].

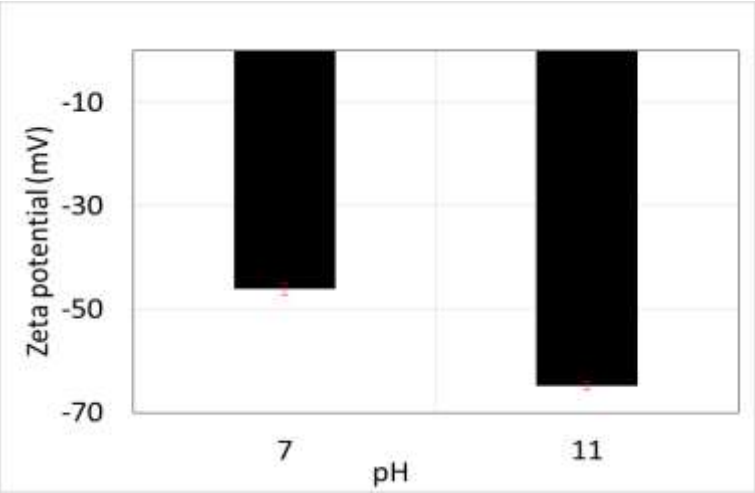

Figure 6-2. Zeta potential of the −COOH oil group droplets as a function of pH at 10 000 ppm of NaCl solution.

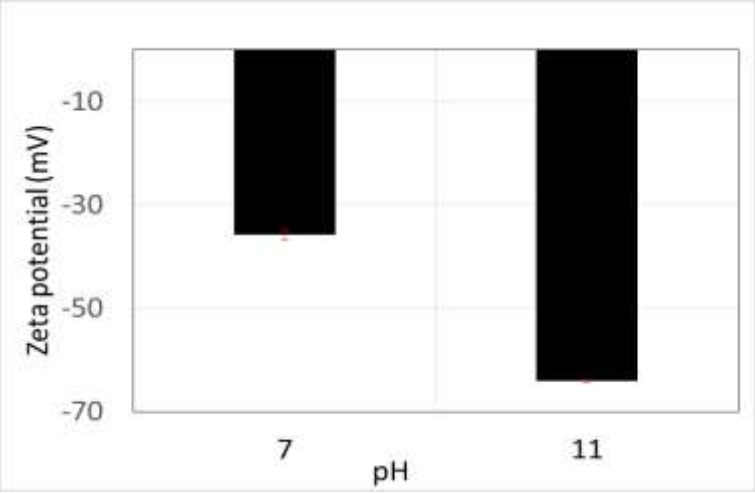

Figure 6-3. Zeta potential of the $-CH_3$ oil group droplets as a function of pH at 10 000 ppm of NaCl solution.

6.4.3. Effect of pH on Adhesion Force.

Figures 5-4 and 5-5 show the force-distance curves between different oil groups and muscovite, and Table 6-1 shows the average adhesion force for each of the system. AFM measurements show that increasing pH decreased adhesion force between oil−muscovite regardless of functional groups, confirming that low salinity effect can take place in sandstone reservoirs bearing basal-charged clays. For example, for nonpolar oil group ($-CH_3$), the adhesion forces decreased from about 890 to 180 pN (5 time decrease) with pH increasing from 7 to 11. Similarly, the adhesion forces between −COOH and muscovite decreased from 4950 to 500 pN (10 times decrease) when pH decreased from 7 to 11. Our results are in line with the work of Shi et al. [196] who reported that increasing pH from 4.5 to 7.5 decreases the adhesion force from 390 to 260 pN between −COOH and sandstone grains in the presence of

artificial seawater. Analogously, for the −CH_3 oil group, adhesion force decreases from 200 to 116 pN with increasing pH from 4.5 to 7.5 in artificial seawater. Moreover, they also observed the same pH effect on the adhesion between oil and sandstone in diluted seawater.

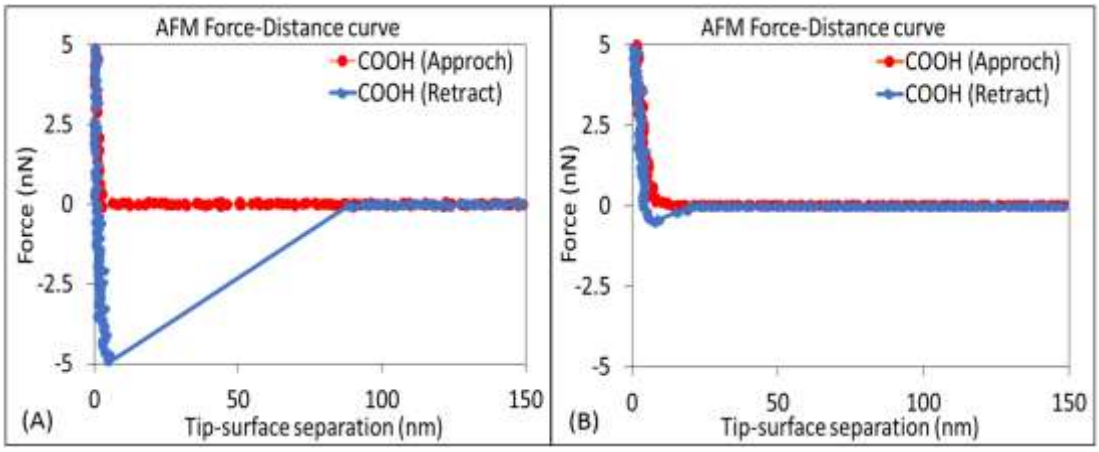

Figure 6-4. Force−distance curve of polar oil group (−COOH) and muscovite in NaCl solutions at (A) pH 7 and (B) pH 11.

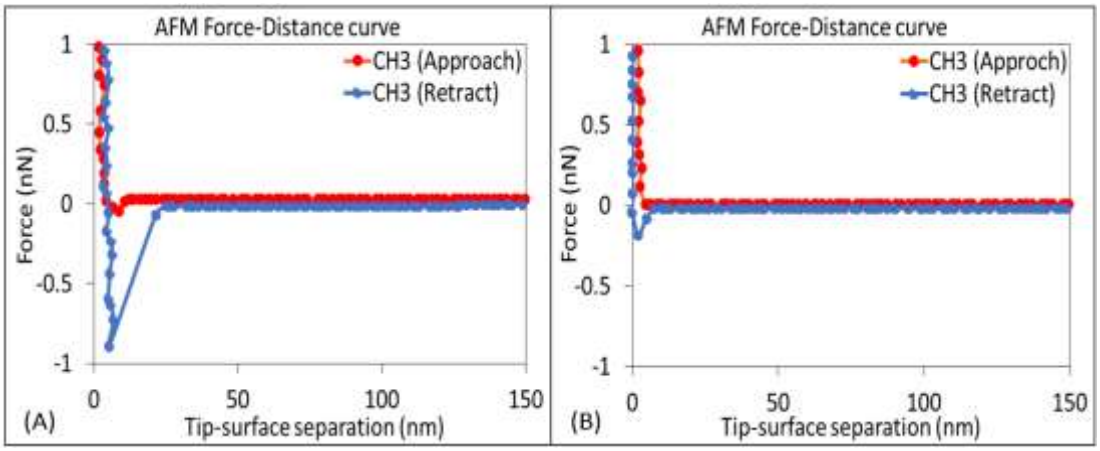

Figure 6-5. Force−distance curve of nonpolar oil group (−CH_3) and muscovite in NaCl solutions at (A) pH 7 and (B) pH 11.

Table 6-1. Average Adhesion Force between Oil Groups and Muscovite at pH 7 and 11.[a]

		Oil group	
		-CH_3	-COOH
$F_{adh}^{pH\ 7}$	(pN)	890	4950
$F_{adh}^{pH\ 11}$	(pN)	180	500

ΔF_{adh} (%)	80 %	90 %

[a] *To calculate the relative change in adhesion force due to pH increase, the equation below was used* $\Delta F_{adh} = \left(F_{adh}^{pH=7} - F_{adh}^{pH=11} \right) \Big/ F_{adh}^{pH=7} \times 100$ *).*

6.4.4. Effect of Functional Oil Groups on Adhesion Force

The polarized functional group (−COOH group) gave four times greater adhesion force than the nonpolar group ($-CH_3$) at pH = 7, implying that polarized functional groups play a significant role in the low salinity effect [150, 195]. For example, −COOH gave an adhesion force of 5000 pN, but $-CH_3$ yielded an adhesion force of 890 pN. Likewise, at pH = 11, −COOH gave an adhesion force of 500 pN, whereas $-CH_3$ showed an adhesion force of 180 pN. Our results are also in line with the work of Wu et al. [150] who investigated the adhesion force between different oil groups and mica in NaCl solutions. They reported that the adhesion force for –COOH and $-CH_3$ were 2541 and 1524 pN in the presence of 8000 ppm of NaCl solution, respectively. Besides, Liu et al. [166] reported that polarized functional groups (−COOH and $-NH_2$) give 6 to 10 times greater adhesion force than non-polarized oil groups ($-CH_3$ and $-C_6H_5$) at quartz surfaces regardless of salinity level. Moreover, Shi et al. [196] observed the same, showing that −COOH gives 200 pN adhesion force in low salinity artificial seawater at pH 4.5, whereas $-CH_3$ gives 140 pN at pH = 4.5. To better interpret the adhesion forces measured using AFM, we computed the disjoining pressure under the constant potential condition using flat−flat and sphere−flat surface thermodynamic models which are discussed in the section below.

6.4.5. Effect of pH and Functional Groups on Disjoining Pressure Using Flat−Flat and Sphere−Flat Models

Flat−flat model calculations show that all brines at different pH give positive disjoining pressure which exhibits a progressively more repulsive barrier on approach (Figure 6-6). Moreover, increasing the pH increases the disjoining pressure, meaning more repulsion, which agrees well with the adhesion forces obtained by the AFM. For example, brines with pH = 11 gave lower adhesion force compared to pH = 7 for both polar and nonpolar groups.

Sphere−flat model calculations predict the same trend as the flat−flat model, showing that all brine gives positive disjoining pressure (Figure 6-7). Moreover, increasing pH increases disjoining pressure, implying more repulsion in the oil− brine−muscovite systems in line with AFM measurements. For instance, the repulsion of −COOH−brine−muscovite increases with pH from 7 to 11. Also, the same trend is observed with the $-CH_3$−brine−muscovite interface. However, it appears that the disjoining pressure predicted by the sphere−flat model is almost hundred times lower than that in the flat−flat model in part due to the limited contact area

compared to the flat−flat model. We believe that the sphere−flat model can better represent the AFM experiments which measure the adhesion between a modified tip and a substrate. Also, the disjoining pressure difference at different pH can better represent the adhesion measured by AFM. For example, AFM measurements show that increasing the pH to 11, adhesion become 5 times less for $-CH_3$−brine−muscovite and 10 times for −COOH−brine−muscovite in line with the decrease of the energy barrier computed using a sphere−flat model. While disjoining pressure calculation predicts the same trend as AFM experiments in terms of the magnitude of adhesion force with different pH, disjoining pressure calculation fails to interpret the attraction force which was observed in AFM tests. For example, disjoining pressure calculation from two different geometry models gives positive disjoining pressure, implying repulsion force. Yet, the AFM measurements present attractive forces, shown as negative sign.

This would be attributed to the zeta potential of oil−brine and brine−muscovite powders not being representative of zeta potentials of functionalized tip−brine and brine−muscovite substrate. To be more specific, zeta potentials in AFM measurements should be lower than oil−brine and brine−muscovite powers which we used for disjoining pressure calculation due to the limited specific area. However, we did not measure the zeta potentials of functionalized tip−brine and brine−muscovite substrate due to the limitation of the equipment, and we therefore cannot confirm this mechanism.

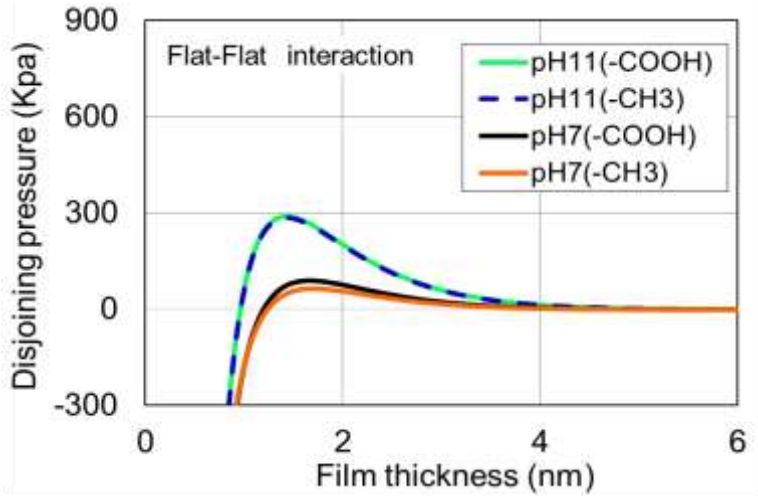

Figure 6-6. Total disjoining pressure from flat−flat model.

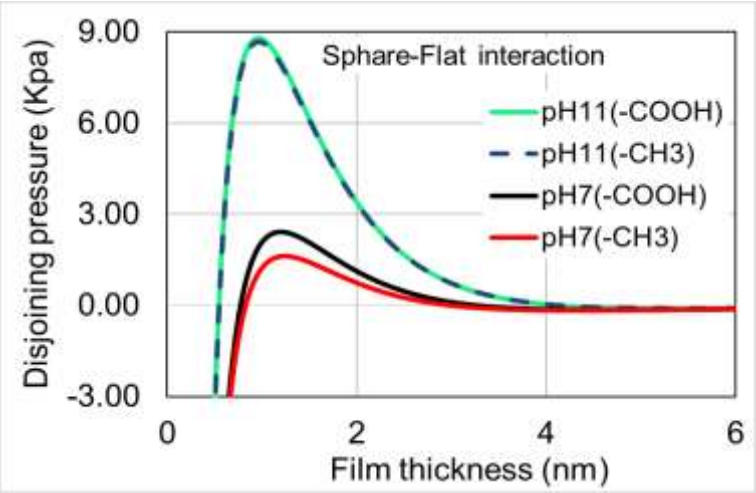

Figure 6-7. Total disjoining pressure from sphere−flat model.

Our AFM results show that increasing pH from 7 to 11 indeed decreased 80% of the adhesion force for both functional groups, confirming that low salinity water likely lifts off oil films from pore surfaces thus increasing water-wetting. Similar results were also observed by Hassenkam et al. [195, 261, 262] who measured adhesion force of a model oil on sandstone grains and model rocks using AFM. Their results show that low salinity water decreases the adhesion force between the model oil and both types of rock, implying that adhesion force reduction of oil and rock surface in the presence of low salinity water can be achieved at pore surfaces in reservoirs. However, it is worth noting that, as Bartels et al. (2017) [237] and (2019) [235] proposed, although low salinity brine triggers adhesion forces decrease at pore surfaces, this does not mean that an oil film would percolate at the pore network and core scale. This is because different length scale likely limits the low salinity effect as a result of wettability alteration. For example, existing spontaneous imbibition tests show that low salinity brine yields a much higher incremental oil recovery at secondary mode compared to tertiary mode [263, 264]. The same phenomenon has been also observed in core flooding experiments [250, 265, 266]. This proves that length scale does affect the low salinity effect which needs to be thoroughly constrained. However, we believe that an adhesion force decrease in the presence of low salinity water would serve as a predictive indicator of wettability alteration.

6.5 Implications and Conclusions

In this paper, we hypothesized that basal charged clays trigger pH increase due to ion exchange, which in return leads to strongly negative zeta potential at both oil−brine and brine−clay interfaces, thus decreasing oil−mineral adhesion force and oil saturation. To test our hypothesis, we measured adhesion force between functional groups (−CH_3 and −COOH) and muscovite in the presence of NaCl with a concentration of 10 000 mg/L NaCl at pH of 7

and 11. To gain a better isotherm thermodynamic understanding, we measured zeta potential of brine−muscovite and oil−brine and computed total disjoining pressure under constant potential conditions using surface−surface and sphere−surface thermodynamic models.

Zeta potential measurements show that increasing pH leads to strongly negative zeta potential for oil−brine and brine−muscovite, thus increasing electrical double layer expansion [37, 267, 268] as well as repulsive force [36]. Our AFM tests support our hypothesis, showing that increasing pH indeed significantly decreased adhesion force regardless of functional groups [196, 269]. Moreover, polarized functional group (−COOH group) gave four times greater adhesion force than nonpolar group ($-CH_3$), confirming that polarized functional groups play a significant role in low salinity effect [58, 60, 76]. We believe that the sphere−flat model (DLVO theory) can better interpret the AFM experiments which measure the adhesion between a modified tip (sphere) and a substrate (flat). Moreover, the sphere−flat model predicts the same degree of adhesion decrease with increasing pH in line with AFM measurements. This study reveals the significance of basal charged clays during low salinity waterflooding in sandstone reservoirs, thus expanding the application envelope of low salinity water in sandstone reservoirs bearing basal charged clays.

Chapter 7. Effect of Surface Roughness Induced by Calcite Dissolution on Contact Angle Measurement

7.1 Abstract

Low salinity waterflooding appears to be a promising means to improve oil recovery in carbonate reservoirs because of a wettability alteration process. Contact angle measurement is a direct approach to reveal the wettability alteration in an oil−brine−carbonate system. However, questions have been raised about using contact angle measurement to justify the wettability alteration. This is because the contact angle may be significantly affected by surface roughness variation in the presence of low salinity water because of calcite dissolution during the contact angle measurement. To clarify the cause and effect of wettability alteration during low salinity waterflooding, we measured the contact angle on two calcite substrates with similar surface roughness (7 and 4 nm) in the presence of high-salinity water (1 mol NaCl + 0.01 mol $CaCl_2$) and low salinity water (100 times diluted high-salinity water). Moreover, we measured the surface roughness of the substrates before and after the contact angle measurements using atomic force microscopy (AFM). Furthermore, we performed a geochemical study to quantify the amount of calcite dissolution in the presence of low- and high-salinity brines and compared it with surface roughness measurements. Our contact angle and AFM results reveal that surface roughness increase due to calcite dissolution in low salinity water plays a negligible role in the contact angle, rather confirming that oil−brine−rock interactions govern the system wettability. Furthermore, our geochemical study shows that low salinity water only dissolves 1.16×10^{-4} mol/mol of calcites in low salinity water during the contact angle measurement. We, therefore, eradicate the possibility that surface roughness variation due to calcite dissolution in low salinity water would affect contact angle results. Consequently, we argue that contact angle measurement remains a valid approach to directly examine the wettability alteration process in low salinity waterflooding.

7.2 Introduction

Low salinity water (LSW) flooding appears to be a cost effective and environmentally friendly means to enhance oil recovery in carbonate reservoirs (e.g., decreasing chemical injection thus low capital and operation costs). This is largely because LSW shifts the in situ oil−brine−carbonate reservoir system wettability [22, 25, 49, 68], which in return drives the relative permeability curves toward lower residual oil saturation [49, 68]. The wettability alteration during LSW flooding in carbonate reservoirs has been identified as the main physicochemical processes [83, 168, 174]. While the wettability alteration process at the core scale has been extensively reported in the lab by the aid of core-flooding experiments [14, 30, 49, 68] and spontaneous imbibition experiments [29-31], contact angle measurement of the oil− brine−carbonate system is a simple and direct approach to examine the wettability

alteration in the presence of brines with various ionic strengths. For example, Yousef et al. [14] conducted contact angle measurements to investigate the effect of smart water on low salinity (LS) EOR effect in carbonate reservoirs. Their contact angle results show that initial connate water (213 000 ppm salinity) gives a contact angle of 90°, whereas the twice diluted seawater (29 000 ppm) and 10 times diluted seawater (6000 ppm) give a contact angle of 80° and 69°, respectively, suggesting that decreasing the salinity shifts the wettability of the carbonate rock from intermediate-wet to slightly water-wet. Also, Alameri et al. [49] performed contact experiments to study the effect of the LSW on the wettability alteration of the carbonate reservoir rocks. Their contact angle results show that lowering the salinity of the seawater from 51 346 to 12 840 ppm decreases the contact angle from 133° to 117°, implying a less oil-wet system. In addition, AlQuraishi et al. [64] found that the contact angle of the oil−brine−carbonate system decreases from 98° to 65° by diluting the seawater 20 times, suggesting that lowering the salinity can shift the wettability of the carbonate rock from intermediate-wet to more water-wet zone. Moreover, Awolayo et al. [27] show that decreasing the salinity of the brine from 261 210 ppm (formation brine) to 48 280 ppm salinity (synthetic seawater) decreases the contact angle of the oil−brine−carbonate system from 135° to 120°.

To understand the contact angle change thus wettability alteration process in the presence of LSW in carbonate reservoirs, several mechanisms have been proposed such as change of carbonate surface charge [24, 43], combination of the mineral dissolution and change of surface charge [44, 45], in situ surfactant generation [50], variations in interface viscoelasticity [7, 33, 36, 41, 51] and formation of micro dispersion [39, 52], and dissolution of calcite [23, 42] and anhydrite [15]. However, it is worth noting that calcite dissolution will only occur nearby the injector during LSW flooding. For example, Nasralla et al. [270] coupled PHREEQC and reservoir model to investigate calcite dissolution at the core scale and field scale during LSW flooding in carbonate rocks. Their results show that the amount of dissolved calcite (wt %) almost decreases to zero at the 0.05 cm at the core scale and 5 m at the reservoir scale from the inject, implying that calcite dissolution is not relevant at the field scale.

To gain a deeper understanding of the controlling factor(s) of wettability alteration as shown by contact angle decrease with lowering salinity in carbonate reservoirs, electrostatic bridging [15, 25, 77], electrical double layer theory [42, 49, 54], and surface complexation modeling [58, 59] have been proposed and developed to quantify and predict the wettability alteration. Our previous work also show correlations between the contact angle of oil−calcite adhesion in the presence of various aqueous ionic solutions [28, 60, 61] and carbonated water [78, 271] using surface complexation modeling. However, until recently, questions have been raised about the reliability of contact angle results to indicate wettability alteration during LSW flooding. This is because calcite dissolution in the presence of LSW during contact angle measurement may yield surface roughness difference, which may significantly affect contact

angle measurements, thus wettability. For example, existing literature studies show increasing surface roughness in the gas−brine−rock system leads to an increase in the contact angle in the oil-wet system, whereas the contact angle decreases with increasing surface roughness in the water-wet system [103, 272]. AlRatrout et al. [180] also report that increasing surface roughness decreases the contact angle in the oil−brine−carbonate system. In addition, Rücker (2018) reported that surface roughness has a strong effect on the wettability alteration process which effects the wettability measurements of the oil−brine−rock system [181]. Therefore, to identify the cause and effect of wettability alteration in the oil−brine− calcite system, in particular, to examine if the surface roughness variation induced by calcite dissolution in the presence of LSW plays a certain role in contact angle, we measured the contact angle on two calcite substrates with similar surface roughness (7 and 4 nm) in the presence of high salinity (HS) water (1mol NaCl + 0.01 mol $CaCl_2$) and low salinity (LS) water (100 times diluted HS water). Moreover, we measured the surface roughness of the substrates before and after the contact angle measurements using atomic force microscopy (AFM). Furthermore, we performed a geochemical study to quantify the amount of calcite dissolution in the presence of LS and HS brines and compared with surface roughness measurements.

7.3 Experimental Procedures

7.3.1 Fluids

Brines

To examine surface roughness effect due to calcite dissolution in LSW on the contact angle, we designed two different brines for contact angle measurements. One was HS brine with 1 mol/L NaCl (AR, 99.9%) and 0.01 mol/L $CaCl_2$ (AR, 99.9%) and the other one was LS brine which was 100 times diluted HS brine using ultrapure water (resistivity 18.2 M Ω). To focus on the effect of the surface roughness due to calcite dissolution in LS brine on the contact angle, we only included Na^+ and Ca^{2+} components in two brines. It is worth noting that to experimentally simulate the LSW injection at in situ reservoir conditions, the pH of brines was not adjusted, thus allowing calcite dissolution to take place during contact angle measurements (Table 7-1). Surface roughness was measured using AFM (WITec alpha 300 SAR) before and after contact angle measurements.

Table 7-1. Brine Composition of HS and LS Brines with the Corresponding pH before and after Contact Angle Measurements

Brine	Concentration (ppm)		TDS (ppm)	pH before contact angle test	pH after contact angle test
	NaCl	$CaCl_2$			
HS brine	58 440	1111	59 551	6.76	8.18

LS brine	584	11	596	6.01	7.15

Oil

To test the contact angle, we used a crude oil with a density of 0.89 g/cm^3 at 20 °C, acid number of 1.7 mg KOH/g, and base number of 1.2 mg KOH/g. Also, the oil was contained 26.3% naphthenes, 3.9 wt% Sulphur, and 3.8 wt% wax.

7.3.2 Substrates

To better focus on the effect of surface roughness variation due to calcite dissolution in the LS brine on the contact angle, calcite crystals (Iceland spar; Ward's Science) were used to test the contact angle in the presence of LS and HS brines. Prior to contact angle measurements, calcite crystals were cleaved from a cleaned calcite sample to obtain a fresh calcite surface. Ultrapure water saturated with $CaCO_3$ was then used to flush the fresh surface to remove any existing small pieces of calcite on the new calcite surfaces. It is worth noting that we did not use the porous carbonate substrate to conduct contact angle measurements because in situ surface roughness likely affects contact angles [192], which prevent us from distinguishing the effect of surface roughness as a result of mineral dissolution on the contact angle thus wettability.

7.3.3 Surface Roughness Measurements

To measure the surface roughness of the substrate before and after contact angle measurements in the presence of brines, we used AFM (WITec alpha 300 SAR) to examine the surface roughness at ambient conditions of temperature and pressure,44 and WITec Project FOUR software was used to collect AFM topography data, background correction, and calculation of the surface roughness [198]. The AFM tips (NPG-10) supplied by Bruker Corporation were used in all AFM image scanning. It is worth noting that we used average roughness parameter to calculate the surface roughness. To be more specific, the software uses the 3D average roughness equation (Eq 7-1) to calculate the average roughness of the scanning image [273]:

$$Ra(N,M) = \frac{1}{NM}\sum_{x=1}^{N}\sum_{y=1}^{M}|z(x,y) - \bar{z}(N,M)| \qquad \text{Eq } 7-1$$

where $\bar{z}$ is the arithmetic average height [273]:

$$\bar{z}(N,M) = \frac{1}{NM}\sum_{x=1}^{N}\sum_{y=1}^{M} z(x,y) \qquad \text{Eq } 7-2$$

7.3.4 Contact Angle Measurements

Prior to contact angle measurements, calcite crystals were cleaved from a cleaned calcite sample to obtain a fresh new calcite surface. Ultrapure water saturated with $CaCO_3$ was then used to flush the fresh surface to remove any existing small pieces of calcite on the new calcite surfaces [48]. Subsequently, the surface roughness of the new calcite substrate was measured using AFM at ambient conditions. On the completion of surface roughness measurement prior to the contact angle test, the substrate was placed into the cell, which was filled with a certain brine in Figure 7-1. The contact angle was then recorded with time until a negligible change in the contact angle (usually up to 12 h). The pH of brine was measured before and after contact angle measurements. Finally, the ultrapure water saturated with $CaCO_3$ was used again to clean the calcite substrate before the AFM test.

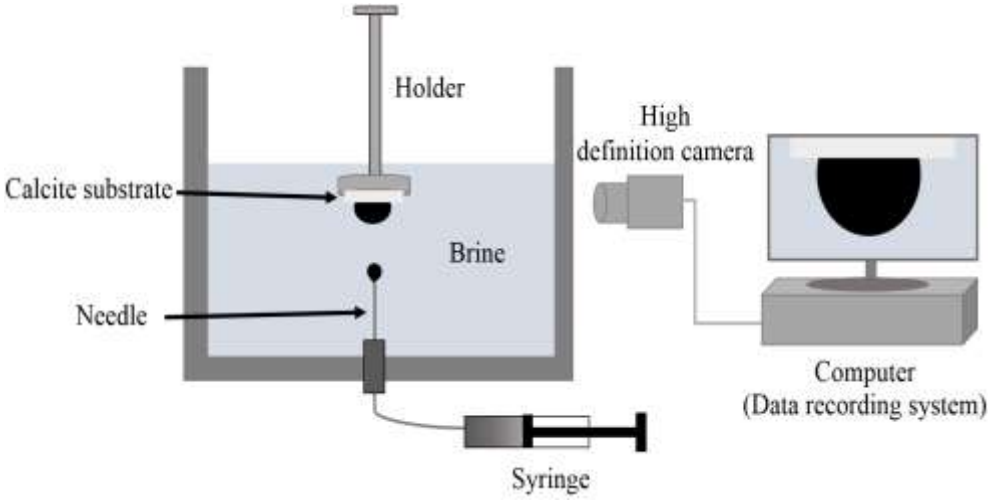

Figure 7-1. Schematic diagram of the contact angle experimental setup.

7.3.5 Experimental Scenarios

To understand the contribution of surface roughness effect on the contact angle due to calcite dissolution in the LS brine, we performed contact angle and AFM measurements in two scenarios which are shown below.

Scenario 1: sample #1 (AFM test) + contact angle measurement in HS + AFM test.

Scenario 2: sample #2 (AFM test) + contact angle measurement in LS + AFM test + contact angle measurement in HS + AFM test.

We measured the surface roughness of sample #1 and #2 prior to contact angle measurements. Subsequently, we measured the contact angle of oil on sample #1 in the presence of the HS brine and the contact angle of oil on sample #2 in the presence of the LS brine. Later, we measured the surface roughness of the two samples. On the completion of the surface roughness of sample #2, we put sample #2 in the HS brine and measured the contact angle of the same oil followed by surface roughness measurement.

7.4 Results

7.4.1 Effect of Salinity on the Contact Angle.

Lowering the salinity of the brine decreases the contact angle between the oil drop and calcite substrate (Figure 7-2), implying that LSW shifts oil−brine−carbonate wettability from oil-wet to intermediate-wet. For example, HS water gives a contact angle of 165°, while the contact angle decreased to 105° in the presence of LSW (Figure 7-2), in line with literature. For example, Yousef et al. [68] reported that lowering the salinity of the brine from 210 000 ppm (formation brine) to 29 000 ppm (twice diluted seawater) reduced the contact angle from 82° to 75° using porous carbonate rocks. Also, Alameri et al. [49] reported that decreasing the salinity of seawater fourfold shifts the contact angle from 133° to 117°, indicating a less oil-wet system. Moreover, Awolayo et al. [27] found that the contact angle decreases from 135° to 120° using porous carbonate rocks when decreasing the salinity from 261 210 (formation brine) to 48 280 ppm salinity (synthetic seawater). It is worth noting that using the porous carbonate rock for contact angle measurements may not cause significant contact angle decrease in the LS brine [25, 68] due to the accumulation of the water in the crevices at the rough surface between the oil drop and rock surfaces [180]. Contact angle decrease with lowering salinity can be interpreted using existing geochemical modeling [58, 60, 61, 78, 165, 271]. For example, Brady and Thyne [58] performed surface complexation modeling to quantify the electrostatic adhesion of the oil−calcite at different water salinities, and they found that decreasing the salinity decreases the bond product sum of the oil−calcite adhesion, thus altering the wettability of the oil− brine−carbonate system to less oil-wet. For instance, diluting the seawater 2 and 10 times decreases the bond product of [>CaSO4 −][−NH+] from 0.21 to 0.13 and 0.05 $(\mu mol/m^2)^2$, respectively.

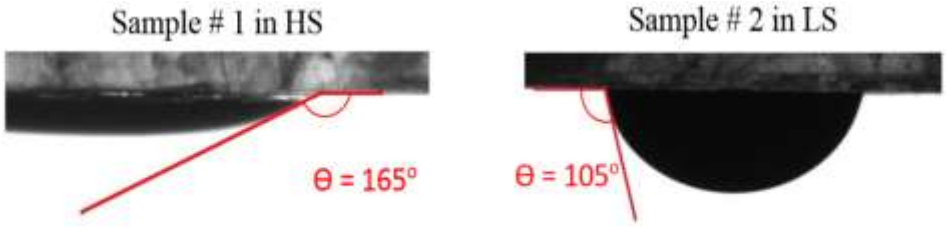

Figure 7-2. Contact angle of sample 1 and 2 in different salinity brines.

Given, we assumed that the surface roughness of sample #2 increases maybe due to calcite dissolution in the presence of the LS brine to examine the surface roughness effect on the contact angle, we measured the contact angle of oil on the reused substrate (sample #2) in the presence of the HS brine (Figure 7-3). Surprisingly, HS water gives a contact angle of 164° almost as same as the contact angle of oil on the sample #1, indicating that oil−brine−calcite

interactions govern system wettability rather surface roughness variation due to calcite dissolution. To gain a deeper understanding of this physicochemical process, we measured the surface roughness of the samples before and after contact angle measurements, which are discussed in the subsection below.

Figure 7-3. Contact angle of sample 1 and 2 in HS brines.

We also noticed that the contact angle reaches the equilibrium much faster in the HS brine compared to the LS brine (Figure 7-4). For example, the contact angle required only 5 min to reach 154° and stabilize at 165° in 70 min. However, in the presence of the LS brine, it takes 80 min to reach a contact angle of 90° and more than 300 min to stabilize at 105°. It is difficult to explain these results, but it might be related to the Ca^{2+} level increase in the LS brine as a result of the calcite dissolution process, which is time-dependent thus influencing oil−brine−calcite interactions [21]. However, this process might not apply to the HS brine because calcite dissolution is minor [25], thereby the equilibrium state of the oil− brine−calcite can be reached shortly.

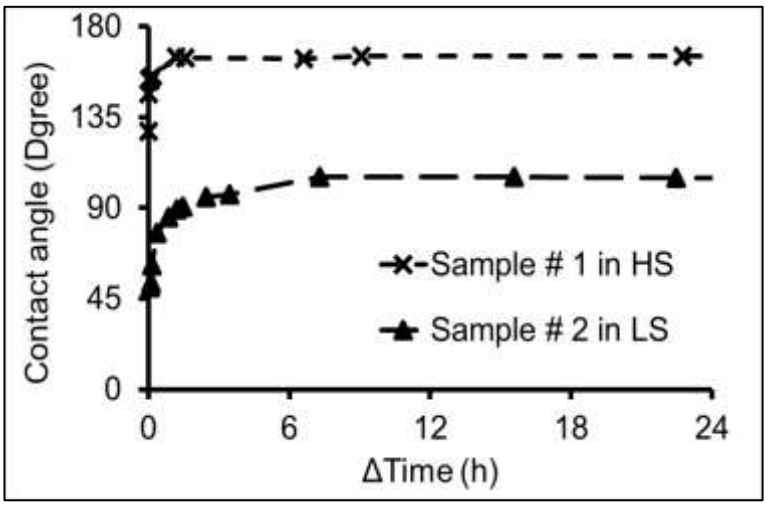

Figure 7-4. Change of contact angle in HS and LS brines.

7.4.2 Effect of Salinity on Calcite Surface Roughness

To quantify the surface roughness variation due to calcite dissolution in the LS brine, we measured surface roughness before and after contact angle measurements using AFM. Figure 7-5 shows that the HS brine gives a negligible roughness difference before and after contact

angle measurements, implying that calcite dissolution is minor in the presence of the HS brine. For example, Figure 7-5 shows that prior to the contact angle measurement, the surface roughness was 7 nm, and a smaller increase in surface roughness (12 nm) was observed after the contact angle measurement. However, the LS brine indeed increased the surface roughness from 4 to 17 nm (three folds increase), suggesting that calcite dissolution occurred in the presence of the LS brine (Figure 7-6), which would be discussed in the subsection with geochemical modeling.

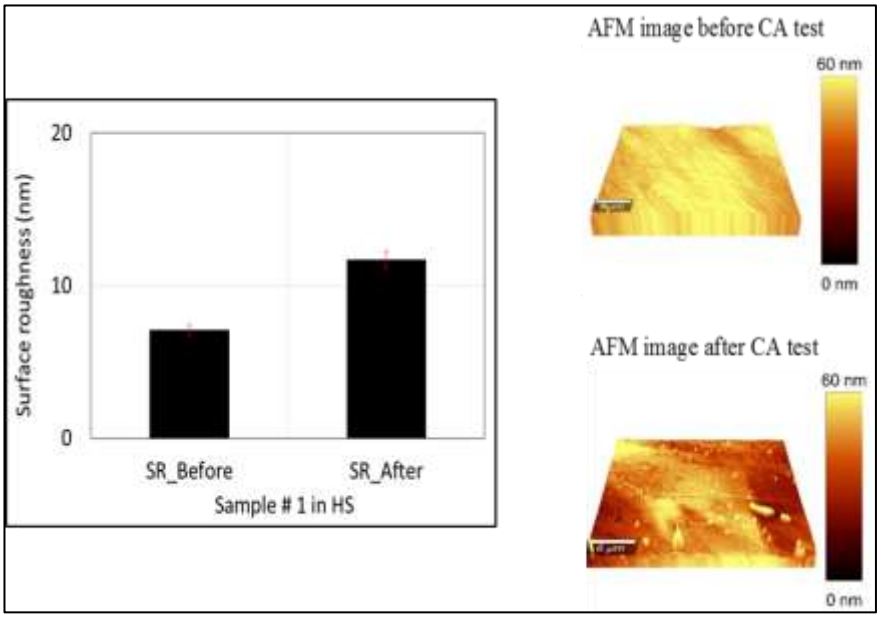

Figure 7-5. Change of the surface roughness of sample #1 due to HS.

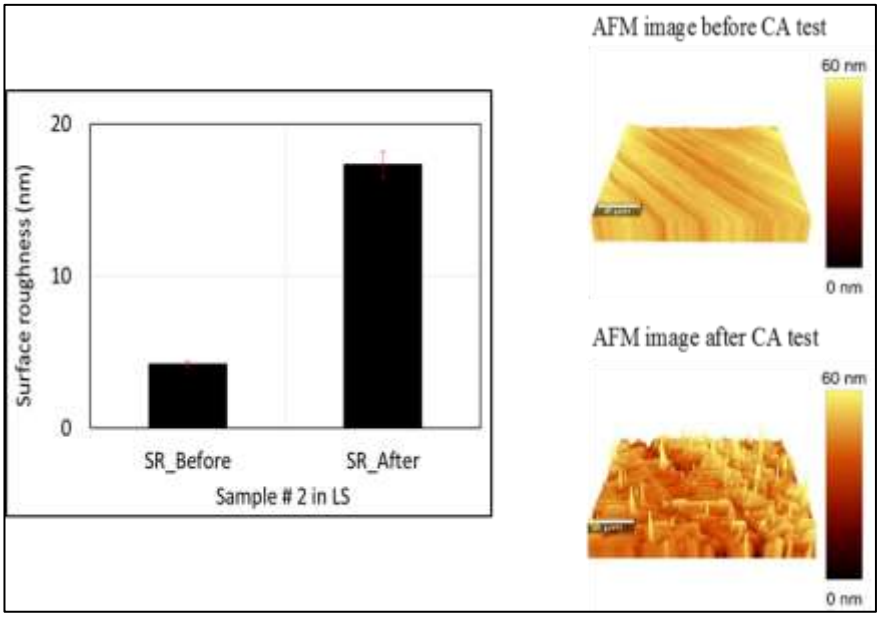

Figure 7-6. Change of the surface roughness of sample #2 due to LS.

7.5 Discussion

7.5.1 Response of Surface Roughness Change due to Calcite Dissolution on the Contact Angle

A combination of contact angle and surface roughness measurements before and after contact angle tests suggests that surface roughness increases as a result of calcite dissolution in LSW plays a negligible role in contact angle, confirming that the interaction of oil−brine−carbonate governs system wettability rather the surface roughness during the LSW flooding. For example, Figure 7-6 shows that the LS brine increases surface roughness from 4 to 17 nm due to calcite dissolution with a contact angle of 105°, whereas the HS brine gives a negligible surface roughness increase with a contact angle of 165°. This confirms that lowering salinity shifts oil−brine−carbonate system wettability toward less oil-wet, which has been reasonably characterized using geochemical modeling. To rule out the potential contribution of surface roughness increase due to calcite dissolution in the LS brine on contact angle decrease, we measured the contact angle of oil on the reused sample #2 in the presence of the HS brine, which yields a contact angle of 164°, confirming that surface roughness increases due to calcite dissolution in the presence of the LS brine plays a limited role in the contact angle. This confirms that contact angle measurement remains a direct and practical approach to indicate the wettability of the oil−brine−carbonate system, which would provide insights to characterize the oil−brine− carbonate interactions thus wettability using thermodynamic and electrostatic approaches.

7.5.2 Analytical Modeling Using the Wenzel Equation

To gain better understanding on the effect of surface roughness due to calcite dissolution on the contact angle thus wettability, we used the Wenzel [103] equation (Eq 7-3) to investigate the effect of surface roughness on the contact angle.

$$COS\,\theta_{rough} = r\,COS\,\theta_{smooth} \qquad \text{Eq } 7-3$$

where r is a roughness factor (Eq 6-4) [103] :

$$r = \frac{True\ surface\ area}{Reference\ surface\ \ area} \qquad \text{Eq } 7-4$$

Given the definition of the roughness factor in Eq 7-4, we calculated the r before and after the dissolutions (sample #2) using the true and reference surface area collected from our AFM data. Our calculation shows that the roughness factor is 1.0003 and 1.0040 before and after calcite dissolution in the LS brine. Subsequently, we used the Wenzel equation to calculate the contact angles at the rough surface as a function of roughness factor as shown in Figure 7-7. Figure 7-7 shows that the contact angle at a rough surface is always greater than the smooth surface. Also, for a given contact angle at a smooth surface, the contact angle at the rough

surface increases with the roughness factor. In particular, the contribution of the surface roughens on the contact angle at rough surfaces increases when the contact angle is greater than 120°. However, with the minor surface roughness change due to calcite dissolution in the LS brine, the contact angle difference at smooth and rough surfaces is limited. For example, the variation of the roughness factor of sample #2 was less than 0.01, suggesting a negligible effect on the contact angle in light of the Wenzel equation [103]. To be more specific, Figure 7-7 shows that at a given contact angle 160° in the HS brine, the contact angle increases only by 1.6° with increasing the roughness factor of 0.01. In the presence of the LS brine with a contact angle of 105°, increasing the roughness factor to 0.01 only leads to additional 0.2° contact angle increase. Together, we can conclude that surface roughness variation due to calcite dissolution is negligible to the oil−brine−carbonate system contact angle thus wettability.

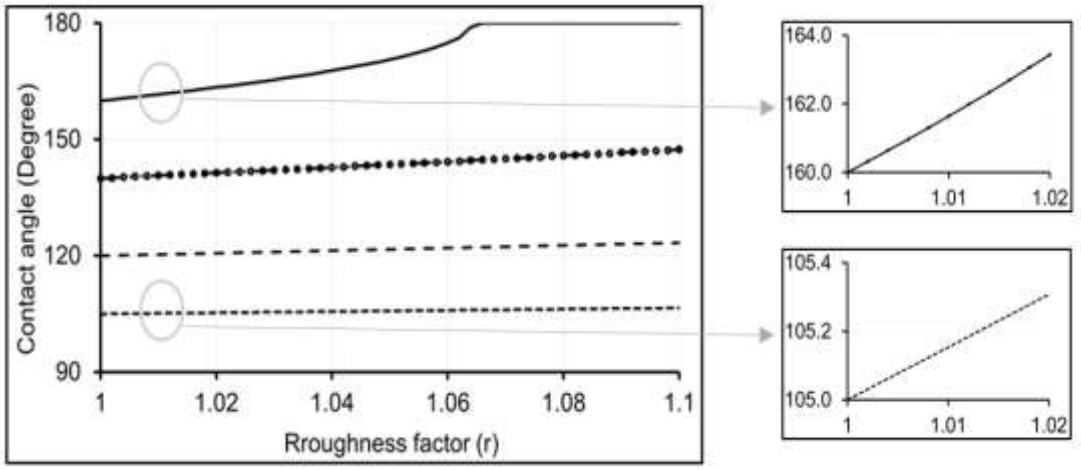

Figure 7-7. Effect of the roughness factor on the contact angle (Wenzel equation).

7.5.3 Geochemical Modeling

To further confirm that surface roughness increase due to mineral dissolution in LSW flooding plays a minor role in system wettability, we performed a geochemical study using PHREEQC software [274] to examine the calcite dissolution process in the presence of either HS brine or LS brine. The equilibrium condition for the bulk was calculated as the calcite substrate is brought in contact with the brine. To calculate how much calcite dissolved in the HS and LS brines, which might change the surface roughness of the calcite substrate, we assumed that the interaction of brines with the calcite reached an equilibrium with saturation index equivalent to 0 [28]. The geochemical results show that both HS and LS at pH = 6 can only dissolve very small amount of the calcite. For example, the HS brine dissolves 5.41×10^{-5} mol/mol of calcite and the LS brine dissolves 1.16×10^{-4} mol/mol of calcite, almost twofold calcite dissolution than HS, which is in line with previous literature studies. For example, Sari et al. [28] performed geochemical modelng to study the effect of water chemistry of the formation brine

and diluted formation brine on the calcite precipitation and dissolution. They reported that the formation brine with a salinity of 252 244 ppm and the 10 times diluted formation brine dissolve 3.966×10^{-3} and 4.091×10^{-3} mol/mol of calcite at low pH (<4.5), respectively. In addition, Nasralla et al. [22] used PHREEQC software to investigate the dissolution or precipitation of calcite due to injection of the seawater and diluted seawater to limestone core samples. They found that 25 times diluted seawater dissolved 2.13×10^{-4} mol/mol of calcite and 100 times diluted seawater dissolved 2.10×10^{-4} mol/mol of calcite. Taken together, LSW triggers minor calcite dissolution, which does not significantly affect surface roughness of the calcite substrate in line with our AFM measurements. This confirms that contact angle alteration in the presence of LSW is governed by oil−brine−carbonate interactions rather than surface roughness change due to the calcite dissolution on the substrate.

7.6 Implications and Conclusions

Contact angle measurement appears to be a direct and practical approach to describe the oil-brine-carbonate system interactions thus wettability in the presence of aqueous ionic solutions for enhanced oil recovery purposes. However, until recently, there has been an increasing concern that the contact angle may not be reliable because of the possible surface roughness variation as a result of calcite dissolution in the presence of the LS brine. To understand the relative contribution of surface roughness effect on the contact angle due to calcite dissolution in the LS brine, we thus measured the contact angle of oil droplets on calcite surfaces in the presence of HS water (1 mol NaCl + 0.01 mol $CaCl_2$) and LSW (100 times diluted HS water). We also measured the surface roughness of calcite substrates before and after contact angle measurements using AFM. Moreover, we performed a geochemical study to quantify the calcite dissolution in the presence of brines and compared our geochemical study with our AFM measurements.

Contact angle measurements show that the HS brine gives a contact angle of 165°, whereas LSW gives a contact angle of 105°, implying a less oil-wet or intermediate system. Surface roughness measurement shows that the HS brine leads to negligible surface roughness change, but LSW causes surface roughness increase from 4 to 17 nm. Geochemical modeling demonstrates that the surface roughness increase in LSW is induced by a small amount of calcite dissolution (1.16×10^{-4} mol/mol). Taken together, our results confirm that surface roughness variation due to calcite dissolution in LSW plays a negligible role in the contact angle. Therefore, the contact angle remains a direct and practical approach to indicate the wettability alteration in the presence of various aqueous ionic brines.

Chapter 8. Alcohol-Assisted Waterflooding in Carbonate Reservoirs*

8.1 Abstract

Low salinity waterflooding has been identified as a cost-effective and environmentally friendly means to enhance oil recovery in carbonate reservoirs by decreasing hydrophobicity. Published work shows that a low concentration of 1-pentanol can further decrease the hydrophobicity, although the mechanism(s) remain unclear. In this work, we aimed to decipher the controlling factor(s), which prevail the process of wettability alteration, by adding alcohols in injected water. To achieve this aim, we examined the effect of alcohol carbon chain length and number of −OH functional groups on the contact angle of oil−brine−carbonate using ethanol, isopropanol, 1-pentanol, and glycerol in high- and low salinity brines. Moreover, to interpret the contact angle results on the basis of a thermodynamic isotherm, we measured the ζ potential of brine−calcite and brine−oil with and without alcohols at ambient conditions. Contact angle results confirm that intermediate carbon chain alcohol (1-pentanol) shifts the wettability of the oil−brine−carbonate system to less oil-wet or more water-wet, implying greater hydrophilicity compared to other short carbon chain alcohols. Also, the number of −OH functional groups in an alcohol has a negligible effect on the contact angle and, thus, wettability alteration. However, the ζ potential at oil−brine and brine−calcite fails to explain the effect of alcohols on the wettability of the oil−brine−carbonate system, implying that the Derjaguin, Landau, Verwey, and Overbeek (DLVO) theory may not account for the effect of alcohol on the wettability alteration. We argue that increasing the length of the carbon chain likely increases −OH at oil−brine interfaces, which likely breaks the in situ bridges between oil and calcite surfaces, thus increasing hydrophilicity. Our finding shows that waterflooding efficiency may be boosted by adding 1-pentanol with a low concentration in high-salinity carbonate reservoirs, where conventional chemical-assisted enhanced oil recovery (e.g., polymer flooding and surfactant flooding) may not be viable.

8.2 Introduction

Most of the world's oil (>60%) was discovered in carbonate reservoirs , and less than 40% can be produced by the primary recovery stage (i.e., depletion process) and secondary recovery stages (e.g., waterflooding and gas flooding) [3]. Waterflooding has been widely used in fields to maintain reservoir pressure, thus improving oil recovery. To further improve the recovery factor achieved by conventional waterflooding in carbonate reservoirs, a concept targeting oil−brine−carbonate interactions from physiochemical processes have been proposed to decrease residual oil saturation by improving displacement efficiency of the injected water, namely, low salinity waterflooding , smart waterflooding [17], and designer waterflooding [8, 9]. To test the concept, contact angle measurements [25-28], spontaneous imbibition [29-31],

and core flooding experiments [14, 30, 49, 68] have been performed to show the potential of low salinity waterflooding in carbonate reservoirs by yielding 5−30% incremental oil recovery [11, 14, 15, 18, 19, 22, 23, 65]. Meanwhile, to predict and upscale the experimental results, a few mechanisms have been proposed, e.g., dissolution of calcite [23, 42] and anhydrite [15], change of carbonate surface charges [24, 43], a combination of the mineral dissolution and change of surface charge [44, 45], in situ surfactant generation [50], electrical double-layer theory, and surface complexation modeling.

To further assist low salinity waterflooding in carbonate reservoirs, a recent study shows that adding a small percentage of alcohol (0.5 and 1 wt% 1-pentanol) to high- and low salinity water can enhance the wettability alteration toward hydrophilicity in carbonate reservoirs [275]. For example, Lu et al. [275] report that adding 0.5 wt% 1-pentanol to low salinity water (0.1 M NaCl) decreases 80° of the contact angle in the oil−brine−calcite system. The proposed mechanism to account for the significant contact angle decrease is that 1-pentanol likely reduces the Ca^{2+} cation bridges between the acid oil group (e.g., $-COO^{-}$) and negative calcite surface species ($>CO_3^{-}$) [275]. This is largely attributed to the strong attraction between the negative −OH of 1-pentanol and Ca^{2+} cations in the water film between oil and calcite surfaces. While the mechanism of enhancing the hydrophilicity of calcite by adding 1-pentanol remains to be further identified, the promising shift of wettability toward hydrophilicity by adding alcohols likely expands the application envelop of low salinity enhanced oil recovery (EOR) in carbonate reservoirs in Western China and the Middle East.

In this work, we aimed to decipher the controlling factor(s), which prevail the process of wettability alteration, by adding alcohols in injected water. To be more specific, we further tested the hypothesis that increasing the number of −OH in alcohol would further facilitate the hydrophilicity of oil−brine−carbonate systems. To achieve this aim, we examined the effect of the number of −OH functional groups and the length of the carbon chain on the oil−brine−carbonate contact angle using ethanol, isopropanol, 1-pentanol, and glycerol in high- and low salinity brines. Moreover, to interpret the contact angle results on the basis of a thermodynamic isotherm, we measured the ζ potential of brine−calcite and brine−oil with and without alcohols at ambient conditions. Finally, a surface complexation model taking place at oil−brine interfaces in the presence of alcohols has been proposed to account for the hydrophilicity of oil−brine−carbonate systems with alcohols.

8.3 Experimental Procedures

8.3.1 Material

Brines.

Two different ionic aqueous solutions were prepared for contact angle and ζ potential measurements with and without alcohols. One was high-salinity brine (HS) with 1 mol/L sodium chloride (NaCl) and 0.01 mol/L calcium chloride ($CaCl_2$), and the second was low salinity brine (LS), which was prepared by diluting HS 100 times using deionized water. Ultrapure water with a resistivity of 18.2 MΩ was used in all preparations of the brines. It is worth noting that to avoid the complication and focus only on the impact of the alcohols on the wettability of the oil−brine−calcite system, we only used NaCl and $CaCl_2$ salts in the two brines to represent the mono- and divalent cations in formation brines.

Alcohols.

To test our hypothesis and obtain the objective of this research, we selected four different alcohols listed in Table 8-1. The elected alcohols contain different carbon chain lengths and a different number of functional groups (−OH) with a different molecular structure.

Table 8-1. Selection of Alcohols with Different Numbers of −OH, Lengths of the Carbon Chain, and Molecular Structures

Name	Chemical formula	Molecular structure	Solubility at water (g/L at 25°C)
Ethanol	C_2H_6O	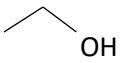	completely soluble
Isopropanol	C_3H_8O		completely soluble
Glycerol	$C_3H_8O_3$	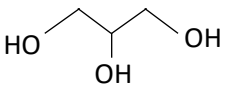	completely soluble
1-Pentanol	$C_5H_{12}O$	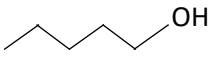	22.8

Oil.

Given that oil functional groups (e.g., $-COO^-$ and $-NH^+$) would play a significant role in oil adhesion on calcite surfaces [58, 78, 197], an oil with certain functional groups would be important to test the hypothesis. A crude oil with a density of 0.89 g/cm^3, acid number (AN) of 1.7 mg of KOH/g, and base number (BN) of 1.2 mg of KOH/g was used. Also, gas

chromatography−mass spectrometry (GC−MS) shows that the oil is rich in naphthenes with a mass concentration of 26.3%, followed by sulfur (3.9%), and wax (3.8%).

Calcite.

Given that calcium carbonate is the main component of the carbonate rocks, we used a calcite crystal supplied by Ward's Science in both contact angle and ζ potential measurements. Furthermore, to avoid the effect of the surface roughness on wettability measurements, a cleaved calcite crystal was used for contact angle measurements with a clean and smooth new surface. Prior to the contact angle measurements, the new calcite surface was flushed using ultrapure water saturated with $CaCO_3$ to remove any small calcite pieces [190]. It is worth noting that we did not use reservoir carbonate rock in this research because the heterogeneity of the surface roughness likely affects the contact angle results [180, 181, 192]. To prepare calcite powders for ζ potential measurements, the calcite crystals were cleaned using ultrapure water saturated with $CaCO_3$. Then, the clean calcite crystals were placed in an oven at 60° to remove remaining water for 24 h. Subsequently, the calcite crystal was crushed to a fine powder with a diameter in the range of 10−100 μm for ζ potential measurements [48].

8.3.2. Contact Angle Measurements.

The contact angle measurement remains as a direct approach to examine the oil−brine−carbonate system wettability with a negligible variation of surface roughness as a result of calcite dissolution [190]. A sessile drop method was used to examine the influence of different alcohols (e.g., number of −OH and length of the carbon chain) on the wettability of the oil−brine−carbonate system at ambient conditions. Because the pressure has a negligible effect on the contact angle of oil−brine−rock systems [191], the contact angle measurements were conducted at ambient conditions. To proceed with the contact angle measurement, a new calcite surface was glued at the holder of the contact angle measurement cell (Figure 8-1). Then, the holder was placed in the cell, which was filled with a certain brine. Subsequently, a syringe located at the bottom of the cell was used to introduce an oil droplet onto the calcite surface. A high-definition camera and computer system were used to monitor and record the contact angle variation until reaching the equilibrium.

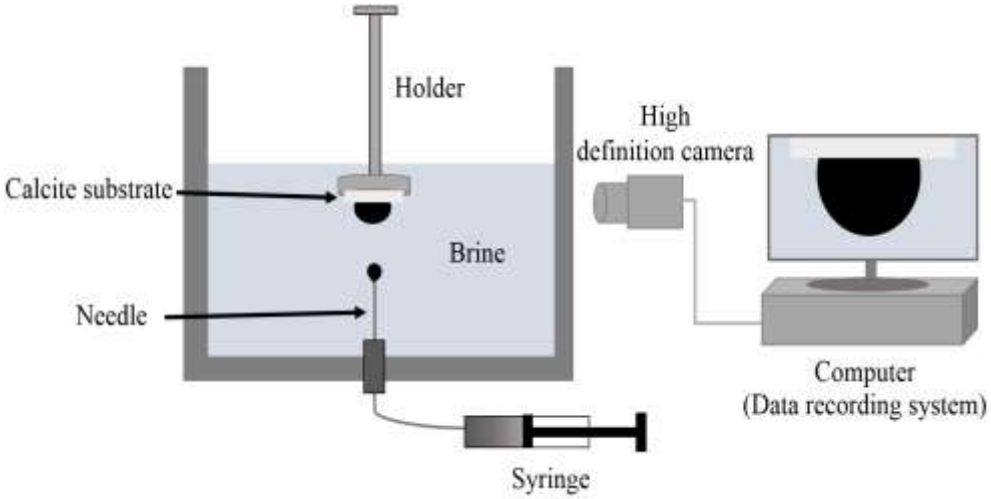

Figure 8-1. Schematic diagram of contact angle experimental setup [190].

8.3.3. ζ Potential Measurements.

ζ potential plays an important role in the electrical double layer force, which affects the disjoining pressure isotherm and, thus the wettability alteration of the oil−brine−rock system [48, 201, 202]. To gain a deeper understanding of how alcohols drive the shift of wettability, we examined the influence of different alcohols on the ζ potential of the two interfaces (oil−brine and brine−calcite) using a Malvern Zetasizer Nano ZS series. To measure the ζ potential of oil−brine and brine−calcite mixtures, the oil and brine were mixed at the ratio of 1:10 (v/v) and 0.4 g of calcite powder was added to 20 mL of brine [275]. Before the samples were loaded into the cuvette cell to measure ζ potential, all samples were stirred for 5 min using a magnetic stirrer to reach an equilibrium. To minimize the standard deviation of ζ potential results, three measurements were made for each of the samples and the average was used to represent the ζ potential for each of the samples.

8.4 Results and Discussion

8.4.1 Effect of Alcohol on the Contact Angle in High-Salinity Water.

Figure 8-2 shows that adding alcohols (ethanol, isopropanol, and glycerol) with a concentration of 1 wt% only slightly decreases the contact angle in high-salinity brine, whereas the same concentration of 1-pentanol significantly decreases the contact angle. For example, adding 1 wt% ethanol and isopropanol to high-salinity brine decreases the contact angle of the oil−brine−calcite system from 165° to 158° and 160°, respectively. Similarly, adding the same concentration of glycerol only decreases the contact angle from 165° to 160°. However, adding 1 wt% 1-pentanol yields a significant contact angle decrease from 165° to 125° in high-salinity brine, in line with Lu et al. [275] under similar conditions. Our results confirm that the length of the alcohol carbon chain likely plays an important role in shifting wettability from oil-wet to intermediate-wet [275]. For example, the intermediate carbon chain alcohol (1-pentanol) in

high-salinity brine reduces 40° (24%) of the contact angle of the oil−brine−calcite system, shifting wettability to the less oil-wet system. Nevertheless, adding short carbon chain alcohols (ethanol and isopropanol) to high-salinity brine only lowers the contact angle less than 8° (5%), implying a negligible effect on the wettability of the oil−brine−calcite system.

Given that long carbon chain alcohols exhibit more hydrophobic characteristics and are, thus, more soluble in oil [275, 276], the adsorption of the −OH group on the oil−brine interface would increase. It is plausible to assume that –OH from alcohols likely bridges with acidic functional groups ($-COO^-$ and $-COOCa^+$) at oil−brine surfaces, which, in return, breaks the bonds between oil and calcite surfaces. A more detailed explanation is given in section 3.5. Figure 8-2 also shows that increasing the number of –OH groups in alcohol for a given length of carbon chain does not contribute to the wettability alteration toward intermediate-wet in the oil−brine−calcite system. For instance, adding 1 wt% glycerol (alcohol with three −OH functional groups) to the oil−brine−calcite system decreases the contact angle from 165° to 160°, similar to the performance of ethanol and isopropanol (alcohol with one −OH). Rather, 1-pentanol (1 wt%, alcohol with one −OH functional group) decreases the contact angle from 165° to 125°. This is likely because 1-pentanol is less soluble in water compared to glycerol for a certain concentration of alcohol in the brine. Therefore, the excess −OH group likely adsorbs at oil−brine interfaces to bridge functional groups at oil surfaces, which, in return, likely breaks bridges originated from oil−brine−calcite, e.g.,$-COO^-$/(>Ca^+ at calcite) and $-COOCa^+$/(>CO_3^- at calcite) [58, 61, 78]. Consequently, the oil−brine−calcite system becomes less oil-wet.

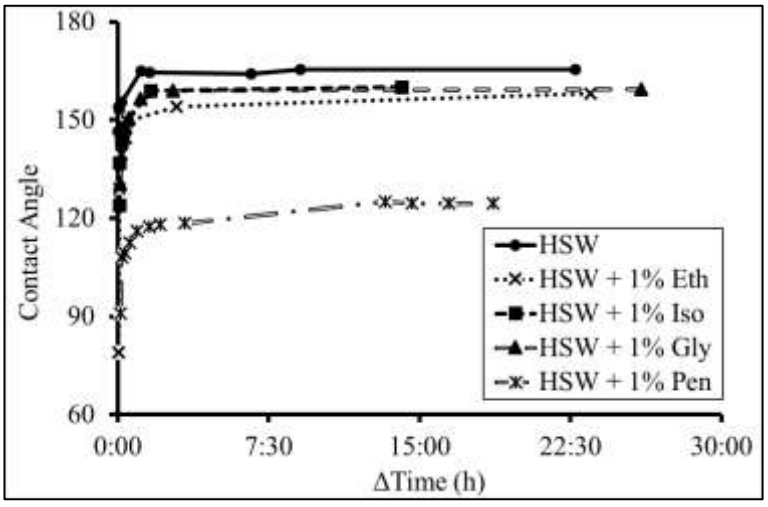

Figure 8-2. Contact angle of oil with calcite in the presence of highsalinity brine with different alcohols.

8.4.2 Effect of Alcohol on the Contact Angle in Low- Salinity Water.

Adding 1 wt% alcohols with a low carbon chain (e.g., ethanol and isopropanol) to low salinity brine did not decrease the contact angle. Rather, the contact angle increased from 105° to 136° compared to low salinity brine without adding alcohols. This implies that low carbon chain alcohols may not facilitate the low salinity effect pertaining to wettability alteration toward more hydrophilicity. For example, Figure 8-3 shows that adding 1 wt% ethanol and isopropanol to low salinity water increases the contact angle of the oil−brine−calcite system from 105° to 116° and 136°, respectively. Similarly, mixing 1 wt% glycerol to low salinity water increases the contact angle of the oil−brine−calcite system from 105° to 118°. We are uncertain why adding alcohols weakens the low salinity effect (increasing hydrophilicity); perhaps this is because the increase of −OH in a thin water film increases the bridges between oil and calcite surface species and, thus, more adhesion.

However, adding 1 wt% 1-pentanol alcohol leads to a decrease in the contact angle from 105° to 90°, implying that 1-pentanol likely shifts wettability from slightly oil-wet to intermediate-wet, favoring displacement efficiency and, thus, a lower residual oil saturation [277]. Taken collectively, Figure 8-3 shows that increasing the number of −OH functional groups in alcohol (glycerol) does not improve the low salinity effect in the oil−brine−calcite system, suggesting that accumulation of alcohol in the thin water film may not lead to a stronger water wetting state. For instance, mixing 1 wt% glycerol (alcohol with three −OH functional groups) to low salinity brine increases the contact angle from 105° to 118° and, thus, a more oil-wet system compared to low salinity brine without any alcohols. Rather, adding 1 wt% 1-pentanol (alcohol with one −OH functional group) to the low salinity brine shifts the wettability of the oil−brine−calcite system to a more water-wet system. This is likely because the solubility of 1-pentanol at low salinity brine is less than the solubility of glycerol, and thus, more 1-pentanol adsorbed at the oil−brine interfaces, which, in return, prompts the hydrophilicity of the oil−brine−calcite system. Therefore, we tentatively conclude that adsorption of −OH at the oil−brine interface likely determines the wettability of the oil−brine−carbonate system rather the accumulation of alcohol within the thin water film between oil and rock surfaces. In addition, the alcohol activity coefficient increases with increasing the salinity of the brine and, thus, decreases the solubility of alcohol in the brine phase [278, 279]. This process likely promotes the movement of alcohol from the thin water film to the oil−brine interface in the presence of high-salinity brine. Consequently, more −OH would be accumulated at the oil−brine interfaces, which leads to a stronger impact of alcohol on the wettability of the oil−brine−calcite system. This is also supported by the contact angle results, which show that 1-pentanol with 1 wt% significantly decreases the contact angle, thus increasing the

hydrophilicity of the oil−brine−carbonate system in high-salinity brine (Figure 8-2) compared to low salinity brine (Figure 8-3).

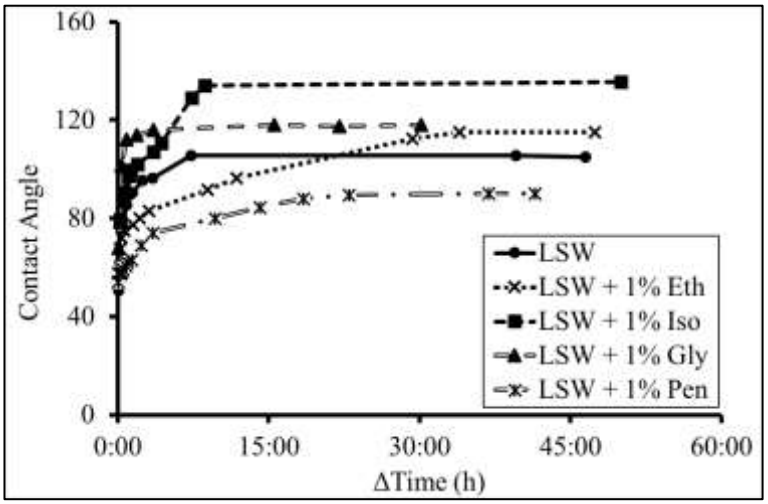

Figure 8-3. Contact angle of oil on calcite surfaces in the presence of low salinity brine with different alcohols.

8.4.3 Influence of Alcohol on ζ Potential in High-Salinity Water. Oil−Brine Interfaces

Figure 8-4A shows that adding alcohols to high-salinity brine has a minor effect on ζ potential of the oil−brine interface, suggesting that the electrical double-layer force may play a negligible role in oil− brine−calcite interactions and, thus, wettability. For example, adding 1 wt% ethanol, isopropanol, or 1-pentanol to high-salinity brine only slightly decreases the negativity of the ζ potential of the oil−brine interface from 4.5 to 5.9 mV compared to literature data [65, 146], while adding 1 wt% glycerol slightly increases the negativity of ζ potential likely as a result of the high number of −OH functional groups at oil−brine interfaces, the incremental ζ potential remains to be low (4.5 mV) compared to the ζ potential increase in low salinity brine in the literature [65, 146].

Although the length of the carbon chain in alcohol also plays a negligible role in the ζ potential of the oil−brine interface, 1-pentanol gives the lowest ζ potential compared to other short carbon chain alcohols. For example, a short carbon chain alcohol (e.g., ethanol and isopropanol) gives a less than 5.0 mV decrease comparable to those in other studies under similar conditions [275]. Adding 1-pentanol (intermediate carbon chain alcohol) to high-salinity brine decreases the magnitude of the ζ potential of the oil−brine interface from −24.2 to −18.3 mV. Our results imply that alcohol adsorbed at oil−brine interfaces have a minor effect on the ζ potential, which may be attributed to the low ionization equilibrium constant of −OH (pKa = 16−19 [280]).

Brine−Calcite Interfaces

Figure 8-4B shows that adding alcohols to high-salinity brine has a negligible influence on the ζ potential of the brine−calcite interfaces. For example, adding 1 wt% ethanol, isopropanol, or 1-pentanol to high-salinity brine decreases the ζ potential of the brine−calcite interfaces from 0.8 to 2.6 mV. Also, adding 1 wt% glycerol decreases 2.0 mV of the ζ potential of the brine−calcite interface, although with three −OH functional groups. This suggests that the number of −OH functional groups in alcohol plays a negligible role on the ζ potential of the brine−calcite interface.

The length of the carbon chain in alcohol also has a minor impact on the ζ potential of the brine−calcite interfaces. For example, adding ethanol and isopropanol (short carbon chain alcohols) to high-salinity water decreases only 1.3 and 2.6 mV of the magnitude of the ζ potential of the brine−calcite interfaces. Also, 1-pentanol (intermediate carbon chain alcohol) only yields minor reduction (0.8 mV) of the ζ potential at the brine−calcite interfaces, implying that the length of the carbon chain in alcohol plays a negligible role on the ζ potential of the brine−calcite interface.

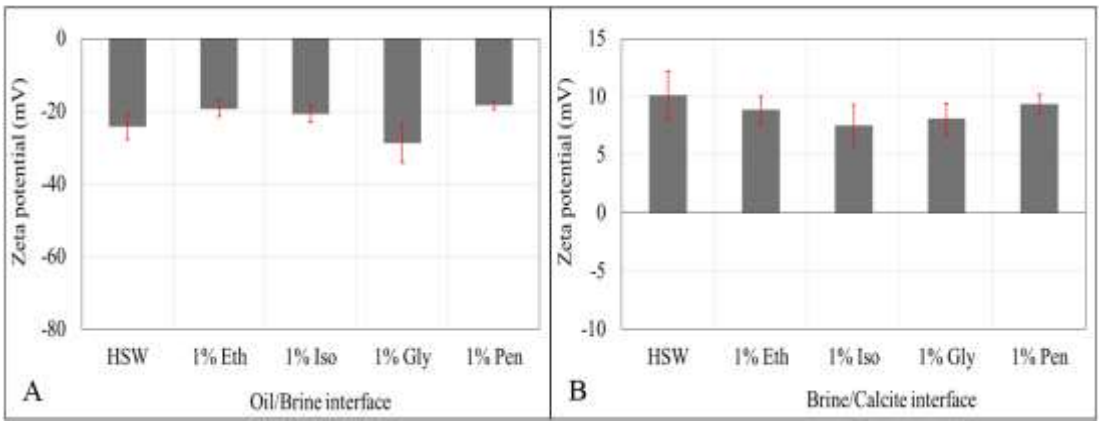

Figure 8-4. ζ potential at high-salinity brine of the (A) oil−brine interface and (B) brine−calcite interface. Error bars show the standard deviation.

8.4.4 Influence of Alcohol on the ζ Potential in Low salinity Water.

Oil−Brine Interface.

Figure 8-5A shows that adding alcohols to low salinity brine does not strongly affect the ζ potential of the oil−brine interfaces. For example, adding 1 wt% ethanol, isopropanol, or 1-pentanol to low salinity brine decreases the negativity of the ζ potential of the oil−brine interface from 0 to 21.5 mV, whereas adding 1 wt% glycerol decreases the negativity of the ζ potential of the oil− brine interface from −61.4 to −56.3 mV. However, Figure 8-5A confirms that lowering salinity shifts the ζ potential of oil− brine interfaces to strongly negative

compared to high-salinity brine largely as a result of an increase of $-COO^-$ at oil−brine interfaces [58, 60, 61, 78].

Figure 8-5A also shows that increasing the length of the carbon chain in alcohols likely decreases the ζ potential in magnitude. For example, adding 1-pentanol (intermediate carbon chain alcohol) to low salinity brine reduces 21.5 mV of the ζ potential compared to a short carbon chain. We assumed that this is possibly attributed to higher dissolution of 1-pentanol at the oil−brine interface with excess −OH, which likely links $-COO^-$ and $-COOCa^+$ and, thus, lowers the ζ potential in magnitude. As a consequence, this physiochemical process breaks the bridges between oil and calcite surfaces, forming a more water-wet system, in line with our contact angle measurement (Figure 8-3).

In addition, the number of −OH functional groups in alcohol does not affect the ζ potential of the oil−brine interface. For instance, adding 1 wt% glycerol (alcohol with three −OH functional groups) to high-salinity brine decreases only 5 mV of the magnitude of the ζ potential of the oil−brine interface. However, the magnitude of the ζ potential of the oil−brine interface decreases 21.4 mV with adding 1 wt% 1-pentanol (alcohol with one −OH functional group) to the high-salinity brine.

Brine−Calcite Interfaces.

Figure 8-5B shows that mixing alcohols to low salinity brine has a minor impact on the ζ potential of the brine−calcite interfaces. For example, adding 1 wt% ethanol, isopropanol, or 1-pentanol to low salinity brine shifts the ζ potential of the brine−calcite interface from −5.2 to −0.7, 0.9, and 0.2 mV, respectively. Also, adding 1 wt% glycerol decreases the ζ potential of the brine−calcite interface from −5.2 to −1.2 mV. However, Figure 8-5B confirms that lowering salinity decreases the magnitude of the ζ potential of brine−calcite compared to high-salinity brine (Figure 8-4B), in line with published experimental data at similar experimental conditions [27, 59].

Moreover, Figure 8-5B shows that the length of the carbon chain in alcohol has a minor impact on the ζ potential of the brine−calcite interface. For example, adding ethanol or isopropanol (short carbon chain alcohols) to low salinity water decreases the ζ potential of brine−calcite in a range of 4.6−6.2 mV in magnitude. Adding 1-pentanol (intermediate carbon chain alcohol) yields a comparable reduction of ζ potential (5.4 mV). This is likely because 1-pentanol was more concentrated at the oil−brine interfaces than the brine−calcite interfaces.

Additionally, the number of −OH functional groups in alcohol also plays a negligible role in the ζ potential of the brine−calcite interface. For instance, adding 1 wt% glycerol (alcohol with three −OH functional groups) to high-salinity brine decreases 4.0 mV of the magnitude of the

ζ potential of the oil−brine interface. Also, the magnitude of the ζ potential of the brine−calcite interface decreases 5.4 mV with adding 1 wt% 1-pentanol (alcohol with one −OH functional group) to the low salinity brine. This is in agreement with the work of Yingda et al. [275] who found that the ζ potential of the brine−calcite interface decreases when adding 1 wt% 1-pentanol to the low salinity brine.

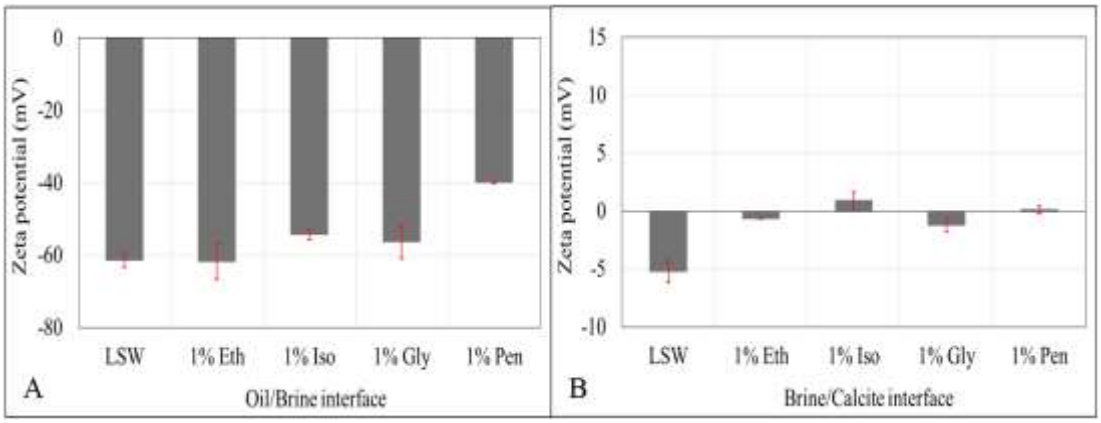

Figure 8-5. ζ potential at low salinity brine of the (A) oil−brine interface and (B) brine−calcite interface. Error bars show the standard deviation.

8.4.5 Proposed Mechanism.

With a combination of contact angle and ζ potential measurements, we provide one possible mechanism accounting for the significant impact of alcohols on wettability alteration as a function of salinity. Figure 8-2 shows that increasing the number of −OH functional groups in alcohols plays a minor role in the contact angle decrease in high-salinity brine, which implies that the accumulation of alcohols at the thin water film between oil and calcite surface may not increase hydrophilicity. However, 1-pentanol (1 wt %) significantly decreases the contact angle from 165° to 125°, implying that the length of the carbon chain likely determines in part the oil−brine−calcite wettability. To be more specific, increasing the number of carbon chains increases the dissolution of alcohols to the oil phase [276], in particular at oil−brine interfaces, thus increasing the number of −OH at oil−brine interfaces. We propose that the adsorption of −OH at the oil−brine interface likely forms an ion−dipole bond with oil surface species, such as $-NH^+$, $-COO^-$, and $-COOCa^+$, thus breaking the in situ bridges between oil and calcite surfaces (e.g., $[-NH^+]$ $[>CO_3^-]$,$[-NH^+]$ $[>CaCO_3^-]$, $[-COOCa^+]$ $[>CO_3^-]$, $[-COOCa^+]$ $[>CaCO_3^-]$, $[-COO^-]$ $[>CaOH_2^+]$, and $[-COO^-]$ $[>CO_3Ca^+]$) (Figure 8-6). This physicochemical process may be attributed to a shorter distance between −OH and functional groups at oil surfaces compared to the distance between oil and calcite through the thin water film thickness (5−30 nm), although the ion−dipole interaction is weaker than the original ionic bonding (electrostatic bonding) between chemical surface species at oil and calcite surfaces. It is worth noting that the ion−dipole intermolecular interaction may also be generated between

−OH and −$COOCa^+$ through $-O^{\delta-}$ and $-Ca^+$ (proposed in Figures 7-6 and 7-7) [281, 282]. For example, partially positive hydrogen in the alcohol functional group (−OH) forms an ion−dipole bond with anionic oxygens, and also partially negative oxygen in the alcohol functional group (−OH) forms an ion−dipole interaction with the calcium ion.

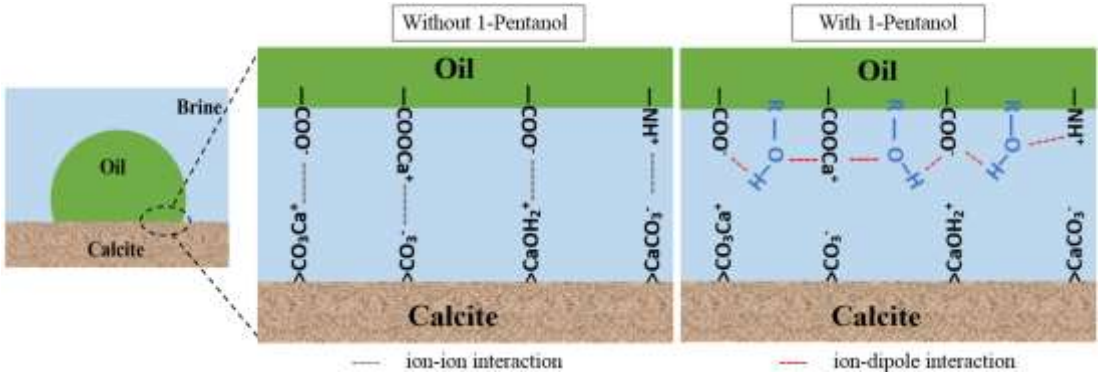

Figure 8-6. Effect of 1-pentanol on the wettability of oil−brine−calcite in the presence of high-salinity brine.

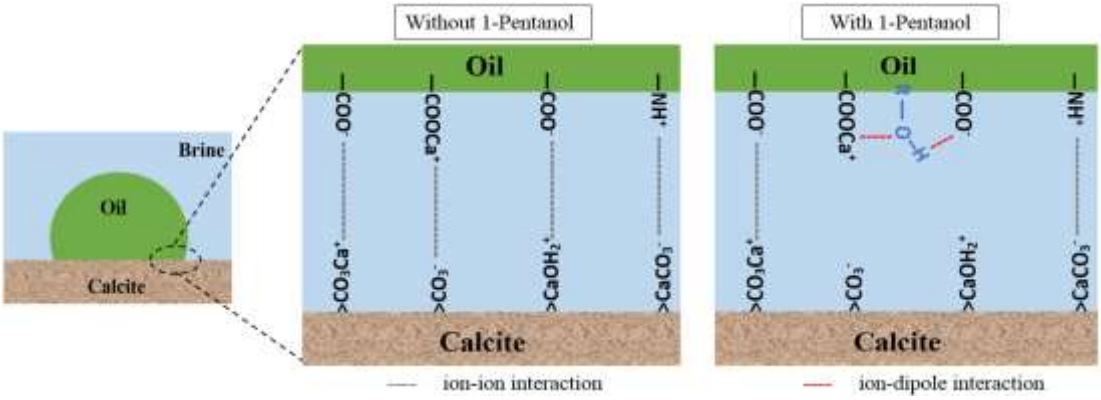

Figure 8-7. Effect of 1-pentanol on the wettability of oil−brine−calcite in the presence of low salinity brine.

This mechanism also accounts for the weak performance of alcohols in low salinity brine (Figure 8-3) compared to high-salinity brine. For example, Figure 8-3 shows that low salinity brine only achieves a 15° contact angle decrease with the presence of 1-pentanol. This is very likely due to a higher dissolution of 1-pentanol in low salinity brine and, thus, less −OH attached at oil−brine interfaces (Figure 8-7). Consequently, less bridges between oil−brine−calcite would be broken by −OH attached at oil−brine interfaces and, thereby, less hydrophilicity (Figure 8-7), although low salinity brine likely increases the water film thickness.

In addition, Figure 8-3 shows that, in low salinity brine, short carbon chain alcohols increase the hydrophobicity of the oil−brine−calcite system, indicating that increasing dissolution of alcohols in the thin water film (i.e., increasing accumulation of −OH in the thin water film)

does not promote hydrophilicity. This observation further validates the proposed mechanism that increasing −OH at oil−brine interfaces likely increases ion−dipole interactions occurring at oil−brine interfaces, breaking the original electrostatic bridges between oil and calcite and, thus, promoting the hydrophilicity.

The proposed mechanism is also supported by ζ potential measurements, which show that the ζ potential of oil−brine and brine−calcite does not change significantly with and without alcohols for a given salinity, in line with Lu et al. [275] We also tentatively believe that increasing the Ca^{2+} and Mg^{2+} level in the formation brine (less than 0.01 mol/L) likely weakens the performance of 1-pentanol due to the fact that –OH adsorbed at oil−brine interfaces may not be able to bridge $-COOCa^{+}$ and $-COOMg^{+}$ together. However, further increasing the Ca^{2+} and Mg^{2+} level results in an increase of −OH at oil−brine interfaces, which, in return, may help to break the bridge between oil and calcite surfaces. This may explains why Lu et al. [275] observed a contact angle increase with increasing $MgCl_2$ (up to 0.01 mol/L) but a decrease with further increasing $MgCl_2$. However, to gain a deeper understanding, more quantitative work remains to be made with a combination of molecular simulations and atomic force microscopy at the molecular level.

8.5 Implications and Conclusions

We aimed to decipher the controlling factor(s), which prevail the process of wettability alteration, by adding alcohols in injected water. In particular, we further tested the hypothesis that increasing the number of −OH in alcohol would further facilitate the hydrophilicity of oil−brine−carbonate systems. To achieve this aim, we examined the effect of the number of −OH functional groups and the length of the carbon chain on the oil−brine−carbonate contact angle using ethanol, isopropanol, 1-pentanol, and glycerol in high- and low salinity brines. Moreover, to interpret the contact angle results on the basis of a thermodynamic isotherm, we measured the ζ potential of brine−calcite and brine−oil with and without alcohols at ambient conditions.

Our results confirm that intermediate carbon chain alcohol (1-pentanol) increases the hydrophilicity of oil−brine−calcite systems in both high- and low salinity brines, but high-salinity brine further boosts the effect of 1-pentanol on wettability alteration. Short carbon chain alcohols (e.g., ethanol and isopropanol) play a minor effect on wettability characteristics of oil−brine−calcite in high-salinity brine, whereas adding short carbon chain alcohols likely increases hydrophobicity in low salinity brines. Also, increasing the number of –OH functional groups does not decrease the contact angle and, thus, hydrophilicity. Alcohols play a minor effect on the ζ potential of the oil−brine and brine−rock interfaces compared to salinity, implying that the Derjaguin, Landau, Verwey, and Overbeek (DLVO) theory cannot explain

the impact of alcohol on the wettability of the oil−brine−carbonate system. However, we suggest that the selection of an appropriate alcohol to increase the hydrophilicity of the oil−brine−carbonate system should follow two principles. First, the alcohol should be water-soluble, which enables the alcohol to penetrate the thin water film, thus accumulating at oil−brine interfaces. Second, the alcohol may need to have medium-level long carbon chains (C5−C10), which would help the accumulation of alcohol at oil−brine interfaces. We also suggest that alcohol with multi −OH groups (two to three −OH) and a long carbon chain (10−15) would likely further promote the hydrophilicity. Besides, we also believe that 1-pentanol may be a good candidate to assist waterflooding in high-temperature and high-salinity carbonate reservoirs, where conventional chemical-assisted EOR (e.g., polymer flooding and surfactant flooding) may not be viable.

Chapter 9. 1-Pentanol-Assisted Waterflooding in High Salinity Brine up to 140°C in Carbonate Reservoirs*

9.1 Abstract

A primary challenge of chemical enhanced oil recovery (CEOR) in high temperature (>100°C) carbonate fields is to obtain viable and cost-effective chemicals that can survive at such critical reservoir conditions. Our previous work shows that alcohol-assisted waterflooding shifts wettability in contact angle measurements (subpore level), which can be deciphered from a geochemical perspective. In this work, we aimed to examine if the wettability alteration process at the subpore level would trigger oil detachment, coalescence, and transport, and thus, enhance oil recovery for high temperature and high salinity carbonate reservoirs. To achieve this objective, we examined the influence of 1-pentanol alcohol (1 wt%) on the contact angle of the oil-brine-calcite system at different temperatures (60, 100, 140°C) and pressures (10, 20, 30, 40 MPa) in low (596 mg/L) and high salinity brines (59600 mg/L). Furthermore, we conducted four core flooding experiments to investigate the application of adding a small percentage of 1-pentanol alcohol (0.4 wt%) at secondary and tertiary modes. Our results show that adding 1-pentanol alcohol (1 wt %) alters the wettability of the oil-brine-carbonate system from a strongly oil-wet system to an intermediate-wet or weakly water-wet system, suggesting a more hydrophilic system compared to brines without 1-pentanol. Increasing the temperature increases the contact angle, whereas the temperature effect becomes minor while the temperature is greater than 100 °C, implying that 1-pentanol alcohol may be applied to high temperature carbonate reservoirs. Also, increasing the salinity increases the wettability shift toward hydrophilicity by adding 1-pentanol, expanding the application envelope of 1-pentanol alcohol to high temperature and high salinity carbonate reservoirs. Core flooding experiments show that adding 0.4 wt % of 1-pentanol to the injected brine results in a 16% incremental oil recovery in the secondary mode compared with waterflooding without 1-pentanol at high temperature and high pressure. This study sheds light on the significant influence of 1-pentanol alcohol-assisted waterflooding on the wettability alteration process, which can lead to oil detachment, coalescence, and transport and, thus, enhance oil recovery even in high temperature, high pressure carbonate reservoirs.

9.2 Introduction

Fossil fuel resources, in particular oils, will remain the primary geo-energy resource for the rest of the century [283]. Carbonate reservoir reserves of more than 60% of the world's original oil in place (OOIP) [1, 2], a huge amount of the proved reserves, are stored in a deep subsurface where they are exposed to high temperatures up to 170 °C. For example, the depth of the Halahatang oil field, Tarim Basin in China, ranges from 7000 to 8000 m at subsurface, with temperature from 140 and 172 °C [284]. Depletion and waterflooding together with gas

injection have been widely used to enhance the oil recovery from such reservoirs. However, the recovery factor remains low, usually less than 40% of the OOIP [3]. To further unlock the remaining resources (60% of OOIP), various chemically enhanced oil recovery (CEOR) techniques have been investigated in the laboratory, such as surfactant flooding [285], polymer injection [286, 287], and alkaline flooding [288]. However, given the high temperature and high salinity condition of such carbonate reservoirs, reservoir engineers have been struggling to find viable and cost-effective chemicals that can survive and thus enhance oil recovery with such reservoir conditions. Although there are some existing commercial surfactants that could work in high salinity and high temperature carbonate reservoirs, the high cost of the surfactants together with the measurable adsorption of the surfactant on carbonate rocks maybe not be viable for field application, in particular in the period of low oil prices [285, 289-291]. Therefore, there is a pressing need to develop a cost-effective approach to achieve carbonate reservoirs in particular at high temperature and high salinity conditions.

Although the low salinity waterflooding technique seems to be a leading technique to lower residual oil saturation by increasing hydrophilicity in such carbonate fields, the lack of freshwater resources in most carbonate reservoirs (e.g., Oman, other Middle East countries, Western China, and the offshore oil fields) points to a limitation of low salinity waterflooding. For example, 70% of carbonate fields in the world are located in the Middle East [2], where there is a lack of freshwater. Therefore, there is a pressing need to develop a cost-effective approach to unlock remaining oils in carbonate reservoirs at high temperature and high salinity conditions where low salinity water (i.e., freshwater resources) is not available.

Recently, Lu et al. [275] reported that a small concentration of 1- pentanol alcohol can trigger a significant reduction in the contact angle of the oil-brine-carbonate system, suggesting a more hydrophilic system. For instance, they show that the contact angle of the carbonate system reduces to 80° by adding 1-pentanol alcohol (0.5 wt %) to 0.1 M NaCl brine. They also proposed a plausible hypothesis to interpret the contact angle reduction, assuming that −OH from 1-pentanol alcohol would capture divalent cations within the water film, thereby breaking bridges between the acidic oil groups ($-COO^-$) and calcite surfaces through divalent cations (see Figure 10 in ref [275]). In our previous work [292], we tested the hypothesis using alcoholbased chemicals with various hydrocarbon-chain lengths and various numbers of hydroxyl functional groups (−OH) using ethanol, isopropanol, glycerol, and 1-pentanol in low salinity and high salinity brines at ambient conditions. Our results show that mixing 1-pentanol alcohol (1 wt %) with 1 mol NaCl + 0.01 mol $CaCl_2$ brine reduces the contact angle of the oil droplet on the calcite surface from 165° to 125° [292]. However, our contact angle experimental results with a range of alcohol-based chemicals cannot be interpreted with Lu's hypothesis. We therefore hypothesized that ion-dipole interactions between alcohols (−OH)

and polar oil species (e.g.,$-COOCa^+$, $-COO^-$, $-NH^+$) at the oil surfaces may be the main force to break the initial adhesion between polar oil species and calcite surface species (see Figure 6 in ref [292]). In this work, we aimed to test our hypothesis that 1-pentanol would trigger wettability alteration in porous media during fluid transport, which also adapts to the high temperature and high salinity carbonate reservoirs. In this context, we selected 1-pentanol alcohol because its intermediate-carbon chain would increase the absorption of 1-pentanol alcohol into oil-brine interfaces, which allows 1-pentanol hydroxyl functional groups (–OH) to break the electrostatic bridges between polar oil species and calcite surface species. To achieve this objective, we measured the contact angles of oil droplets on the calcite substrate in the presence of 1-pentanol alcohol (1 wt%) in low and high salinity brines (596, 59600 ppm) at different temperatures (60, 100, 140 ^oC), and pressures (10, 20, 30, 40 MPa). Moreover, to confirm that the wettability alteration process achieved by 1-pentanol alcohol can lead to oil detachment, coalescence, and transport, and thus enhance oil recovery, we performed four core flooding experiments to quantify the incremental oil recovery by injecting 1-pentanol (0.4 wt%) assisted water at secondary and tertiary modes at high temperature and high salinity.

9.3 Materials and Experimental Procedures

9.3.1 Materials

Brines

In this study, we used two brine solutions for contact angle experiments with and without 1-pentanol alcohol. The high salinity (HS) brine contains 1 mol/L NaCl and 0.01 mol/L $CaCl_2$, and low salinity (LS) brine was prepared by diluting the high salinity brine 100 times using ultrapure water. All the brines were prepared using ultrapure water (resistivity of 18.2 MΩ). It is worth noting that NaCl and $CaCl_2$ salts widely exist in reservoir brine, which simulates the divalent and monovalent cations in reservoir brines.

The formation brine (194 450 ppm) used in the core flooding experiments was synthesized based on the salt concentrations provided by Al Harrasi et al. [18] as listed in Table 9-1 below. It is worth noting that we used FB and FBP as shorthand for the formation brine alone and formation brine with 0.4 wt % 1-pentanol, respectively. Also, it is important to mention that increasing the salinity of the solution decreases the solubility of 1-pentanol alcohol in the solution [278, 279]. We therefore added a relatively low weight percentage of 1-pentanol alcohol (0.4 wt %) to the formation brine for the core flooding experiments.

Table 9-1: Salt concentration in FB

Salt	NaCl	$CaCl_2$	$MgCl_2$	Na_2SO_4	$NaHCO_3$

Concentration (mg/L)	151600	32170	18010	1010	12

1-Pentanol Alcohol

Given that in our previous work 1-pentanol alcohol shows the highest ability to shift the wettability of carbonate rock from an oil-wet system toward a weakly water-wet or intermediate-wet system compared with other types of alcohols (e.g., ethanol, isopropanol, and glycerol) [292], in this work, we used commercially available analytical grade (100%) of 1-pentanol alcohol in all the experiments. 1-Pentanol (n-amyl alcohol, pentyl alcohol) is an intermediate-chain-length alcohol with a straight carbon chain () and molecular formula of $C_5H_{12}O$. The relative density of 1-pentanol alcohol is 0.811 g/mL at 25 °C, and the solubility in water is 22.8 g/L at 25 °C.

Oil

Given that adhesion of oil on rock surfaces is largely governed by the polar oil component such as $-COO^-$ and $-NH^+$ [58, 190, 197, 201, 241, 271, 293], the crude oil used in all the experiments had a density of 0.89 g/cm^3 at 20^{o}C, with base number (BN) and acid number (AN) of 1.2 and 1.7 mg KOH/g , respectively. In addition, the gas chromatograph-mass spectrometer analysis test indicates that crude oil contains a mass concentration of 3.9% sulfur, 26.3% naphthenes, and 3.8% wax.

Calcite Substrates

In this study, we used Iceland spar calcite crystal from Ward's science to represent the carbonate rock in all the contact angle experiments. In addition, the Iceland spar calcite crystals were cleated to acquire smooth and clean new calcite surfaces. This would help to limit the calcite surface roughness effect on the contact angle experiments [180, 181, 189, 190], Before the contact angle experiments, the new calcite surfaces were rinsed by ultrapure water equilibrated with calcite ($CaCO_3$) to remove all the small calcite pieces from the new calcite surfaces [190, 224]. It is noteworthy that we did not use porous substrates from a carbonate reservoir in the contact angle experiments because of avoiding the potential uncertainty of surface mineral heterogeneity on contact angle results [180, 181, 192].

Core Samples

Four carbonate core samples sourced from a carbonate reservoir in Oman were selected for core flooding experiments. The core samples (L= 6.2−6.7 cm, D=3.8 cm) are rich in calcite (99.1%) with minor dolomite (0.6%) according to the X-ray diffraction test. Table 9-2 shows petrophysical properties of the core samples and the injected fluids for each of the core flooding experiment.

Table 9-2: Petrophysical Properties of Core Plugs and the Corresponding Core Flooding Fluids[a]

Core flooding test	Core sample	Porosity (%)	Permeability (mD)	Pore Volume	Core flooding fluids
CF1	C1	27.2	5.1	19.1	FB → FBP
CF2	C2	25.7	1.8	18.4	FB
CF3	C3	29.7	5.6	22.6	FBP
CF4	C4	25.9	4.0	18.0	FBP

[a]FB: formation brine, FBP: formation brine with 0.4 wt % 1-pentanol.

9.3.2 Experimental Procedures

Contact Angle Measurements

The sessile droplet technique was used in all the contact angle measurements (measured through the brine phase) using the Vinic IFT-700 apparatus (Figure 1). It is worth noting that while published works show that fluid-calcite interaction likely leads to calcite dissolution especially in low salinity brine [58, 61, 72], our previous work shows that calcite surface roughness variation caused by dissolution of calcite in low salinity brine has a minimal effect on contact angle measurements [190]. However, in this work, the influence of 1-pentanol alcohol on the contact angle of the oil-brine-calcite system was examined as a function of temperature (60, 100, and 140 °C) and pressure (10, 20, 30, and 40 MPa) in both LS and HS brines.

To measure the contact angles, a new calcite surface was attached to the substrate holder in the Vinic IFT-700 apparatus; thereafter, the system was vacuumed for 2 h until the pressure in the IFT cell was below 0.1 bar. Then, the system was filled with brine, and the temperature and pressure of the system were adjusted to the desired values. After the system was stabilized with the desired temperature and pressure, a drop of the oil was injected on the calcite surface using a hand pump through a needle with a diameter of 0.88 mm. Finally, the contact angle variation was monitored and recorded using a high definition camera and a computer system until the contact angle reaches equilibrium, usually within 4 h. On the completion of the test at the desired temperature, the contact angle was measured with increasing pressure for each temperature.

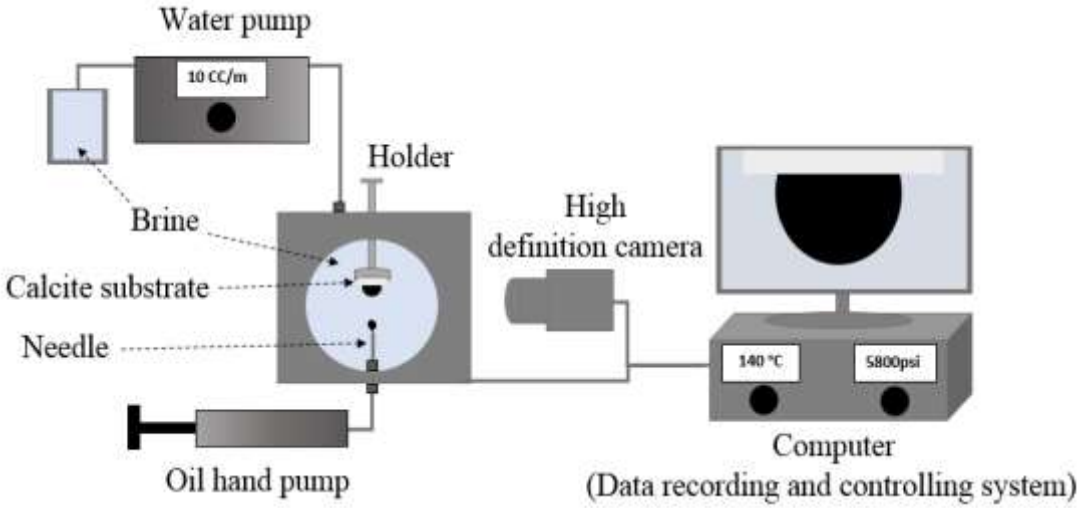

Figure 9-1. Schematic diagram of the high temperature-high pressure apparatus for the contact angle experiments.

Core Flooding Experiments

To examine whether the wettability alteration process occurring at subpore scale leads to oil detachment, coalescence, and transport in porous media, we performed four core flooding (CF) experiments to investigate the application of 1-pentanol to assist the secondary and tertiary waterflooding in high-salinity and high-temperature carbonate reservoirs. The following steps were taken to conduct the core flooding experiments. First, each core sample was cleaned using organic solvents (toluene and methanol) in a Dean-Stark apparatus to remove any organic and inorganic contaminants from its pores. After completing the cleaning step, the core sample was dried by placing it in the oven at 60 °C until completely dried. Next, the gas permeability and porosity of the core sample was measured using an automatic porosi-permeameter equipment. Subsequently, the core sample was wrapped, first with a heat shrink sleeve, and then with a rubber sleeve to prevent the crossflow between the pore pressure and confining pressure. Later, the core sample was placed in the core holder, and the inlet and outlet of the core holder were connected to the core flooding system. Upon the completion of loading the sample to the system, the confining pressure was increased and maintained at 600 psi by using a syringe pump. A temperature controller was used to raise the temperature of the system to 100 °C. Afterward, the core sample was vacuumed for 24 h to reduce the air in the pores, and the temperature was gradually increased to 140 °C for the water saturation process. The water saturation process was started by injecting the FB into the core sample which leads to an increase in the pore pressure, so the confining pressure was increased gradually at the same time to maintain the pressure difference between the pore pressure and the confining pressure. When the confining pressure, pore pressure, and temperature stabilized at the desired values, the FB injection was continued for 5 PV to ensure that the core sample was fully

saturated with the FB. During this process, the absolute permeability of the core sample was measured through three different flow rates (0.1, 0.2, and 0.4 cm^3/min). However, to promote the water saturation step, the core sample was left for 2 days at 350 psi. The core sample was then flooded with the crude oil to obtain the irreducible water saturation at a flow rate of 0.1−0.3 cm^3/min until the fraction flow of water reached almost 0 (99.99%). The produced FB and crude oil were collected and recorded carefully to calculate the irreducible water saturation (S_{wi}) and the oil saturation (S_o) in the core sample. Thereafter, the sample was kept for 4 weeks for the aging process to restore the wettability. After completing the aging time, we started the oil recovery step by injecting FB or FBP at a flow rate of 0.15 cm^3/min until the water cut reached above 99%, and then the injection flow rate was increased to 0.5 cm^3/min to minimize the end effect during the oil recovery step. During the recovery stage, all the inlet and outlet pressures and the volume of the effluent were recorded. It is worth noting that experiments CF1 and CF2 were conducted with FB to obtain the reference oil recovery from the conventional secondary waterflooding, while CF3 and CF4 were done with FBP to observe the effect of adding 1-pentanol to FB on the oil recovery. Additionally, to examine the effectiveness of adding 1-pentanol alcohol to enhance the oil recovery at the tertiary mode after the conventional waterflooding, we flooded the CF1 with FBP after obtaining the reference oil recovery from the conventional FB waterflooding. A schematic diagram of the core flooding experiment is shown in Figure 9-2.

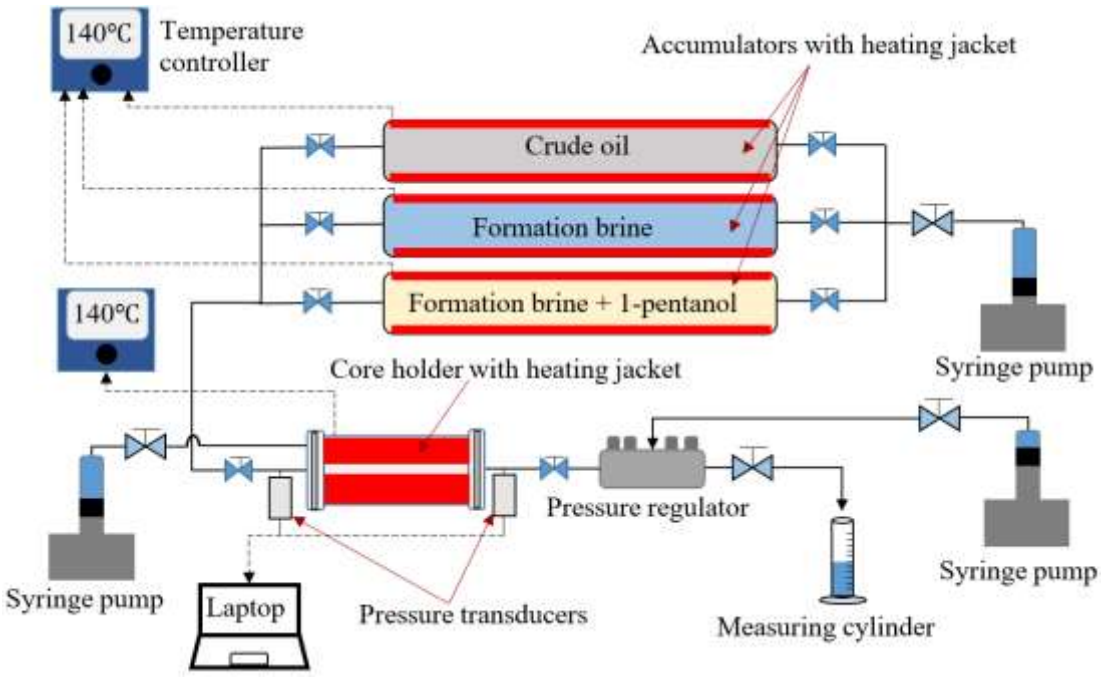

Figure 9-2: Schematic diagram of the core flooding setup.

9.4 Results and Discussion

9.4.1 Effect of Salinity, Temperature, and Pressure on the Contact Angle of the Oil-Brine-Calcite System

Decreasing the salinity reduces the contact angle of the oil-brine-carbonate system without 1-pentanol alcohol, confirming that LS brine increases hydrophilicity of carbonate rock (Figures 3 and 4). For example, at a given temperature (100ºC) and pressure (10 MPa), HS brines gives a contact angle of 160°, implying a strongly oil-wet system, whereas LS brine gives a contact angle of 88° suggesting an intermediate-wet system. This is in line with our previous work [190], which shows that decreasing the salinity from 59 551 to 596 ppm reduces the contact angle of the oil droplet on the calcite surface from 165° to 105°. This is also in agreement with Alameri et al. [49] who found that lowering the seawater salinity four times decreases the contact angle on carbonate rock from 133° to 117°, implying a less oil-wet system. Our contact angle reduction in LS brine can be also interpreted using the existing geochemical models [58, 61, 78]. For example, LS water in our experiment likely decreases [$–COO^-$] at oil surfaces, and also reduces of [$>CaOH_2^+$] and [$>CO_3Ca^+$] at calcite surfaces compared with high salinity water [58, 61, 78]. This process likely decreases the bonds (e.g., [COO^-][$>CaOH_2^+$] and [$–COO^-$][$>CO_3Ca^+$]) between the polar oil species and calcite surface species and thus lowers the contact angle.

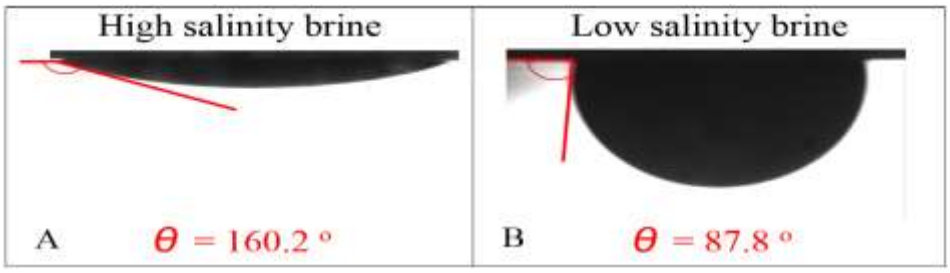

Figure 9-3. Contact angle of the oil droplet on the calcite surface at 10 MPa and 100 °C: (A) in HS brine and (B) in LS brine.

In addition, our contact angle experiments (Figure 9-4) indicate that the temperature has a slight influence on the wettability of the oil-brine-calcite system without 1-pentanol. For example, for each of the brines (HS or LS brine) we found almost similar contact angles (±2°) for the oil droplet on the calcite surface at different temperatures. This is in agreement with Wang and Gupta [191] who show that increasing the temperature from 55 to 93 °C slightly varies the contact angle (±3°) of the oil-brine-calcite system. Also, Xie et al. [165] and Sari et al. [48] found that the impact of temperature on the contact angle becomes minor after the temperature increases above 60 °C (Figure 2 in ref [165] and Figure 2 in ref [48]). On the contrary, published works also show that temperature plays a certain role in the wettability of

the oil-brine-carbonate system [69, 294]. For instance, Alotaibi et al. [69] reported that, in seawater brine (54 Kppm), the contact angle of the oil droplet on the calcite surface reduces from 146° to 116° with increasing the temperature from 50 to 90 °C. In addition, Lu et al. [294] found a similar temperature effect in the presence of 1 mol of NaCl; the contact angle of the oil droplet on the calcite surface reduces from 150° to 80° with increasing the temperature from 25 to 65 °C. The two potential explanations likely interpret the discrepancy as the following. First, increasing the temperature up to 100 °C decreases [$>CO_3^-$][$-COOMg^+$] and [$>CaCO_3^-$][$-COOMg^+$] electrostatic bridges between the polar oil species and calcite surface species and thus decreases the contact angle [72]. This is in agreement with Lu et al. [294] who observed a contact angle decrease using brine with Mg^{2+}. Second, increasing the temperature up to 100 °C decreases [$>CaSO_4^-$][$-COOCa^+$],[$>CaSO_4^-$][$-COOMg^+$], and [$>CaSO_4^-$][$-NH^+$] electrostatic bridges between polar oil species and calcite surface species and therefore decreases the contact angle [72]. Both explanations are in agreement with Alotaibi et al. [69] who observed contact angle decrease using brine with SO_4^{2-} and Mg^{2+}.

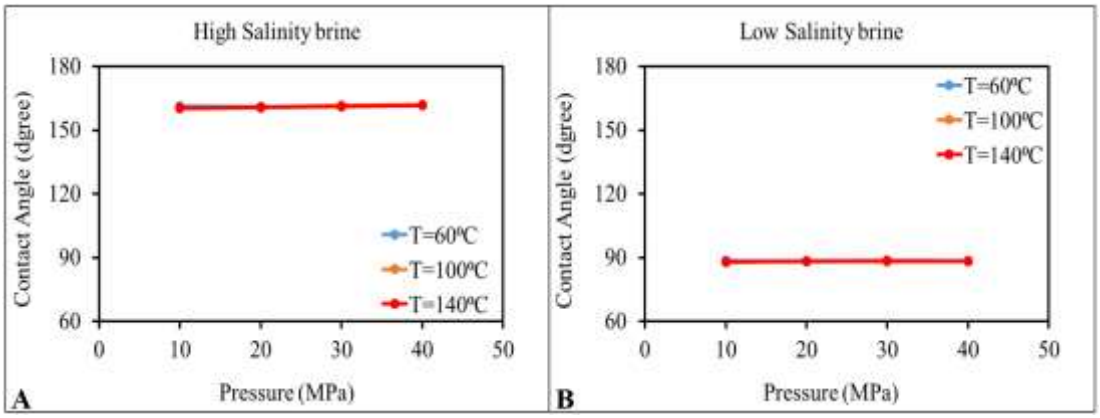

Figure 9-4. Contact angle results of the oil droplet on calcite surface at different temperatures and pressures: (A) HS brine and (B) LS brine.

Pressure has a minor influence on the contact angle and, thus, the wettability of the oil-brine-carbonate system (Figure 9-4). For instance, Figure 9-4 illustrates that increasing the pressure from 10 to 40 MPa only varies the contact angle in a 0.2 to 1% change, confirming that the pressure has a minimal influence on the wettability of carbonate rock in line with the literature [67, 69, 191, 253, 295, 296]. For instance, Alotaibi et al. [69] reported that raising the pressure from 200 to 2000 psi reduced only 2° of the contact angle of oil-seawater-calcite from 142° to 140°. Additionally, Hansen et al. [253] report that increasing the pressure from 0.1 to 30 MPa at 25 °C had a slight effect on the wettability of the decane-water-(calcite + stearic acid) system. Collectively together, these experimental observations rule out the wettability alteration caused by any pressure variation during the development of oil reservoirs.

9.4.2 Effect of 1-Pentanol Alcohol on the Contact Angle in High Salinity Brine

1-Pentanol alcohol (1 wt %) in HS brine significantly decreases the contact angle of the oil droplet on the calcite surface, suggesting a more hydrophilic system. For instance, Figure 9-5 indicates that mixing 1 wt % of 1-pentanol alcohol to HS brine (at 60 °C and 10 MPa) reduces the contact angle from 162° to 84°, shifting the wettability from the strongly oil-wet system toward the slightly water-wet system (or intermediate-wet). Similarly, the contact angle of the oil droplet on the calcite surface reduces from 162° to 103° at 140 °C and 40 MPa. This observation is in line with the work of Lu et al. [275] who report that adding 1-pentanol alcohol (1 wt %) to high salinity brine (1 M NaCl) reduces the contact angle of the oil droplet on the calcite surface from 135° (without 1-pentanol) to 70°, a 65° reduction, with a strong shift of the wettability from a strongly oil-wet system toward a weakly water-wet system, although they did not test at high temperature and high pressure. This observation is also in agreement with our previous study [292], showing that the contact angle of oil-brine-calcite reduces from 165° to 125° while mixing 1-pentanol alcohol (1 wt %) to high salinity brine (1 mol NaCl + 0.01 mol $CaCl_2$) at ambient conditions. We assume that increasing the salinity increases the accumulation of 1-pentanol alcohol in the oil-brine interface, which allows a 1-pentanol hydroxyl group (−OH) to bridge $-COO^-$, $-COOCa^+$, and $-NH^+$ through ion-dipole interactions (see Figure 6 in ref [292]), hence breaking the electrostatic bridges between polar oil species and calcite surface species. This process accounts for the shift toward hydrophilicity by adding 1-pentanol alcohol [292].

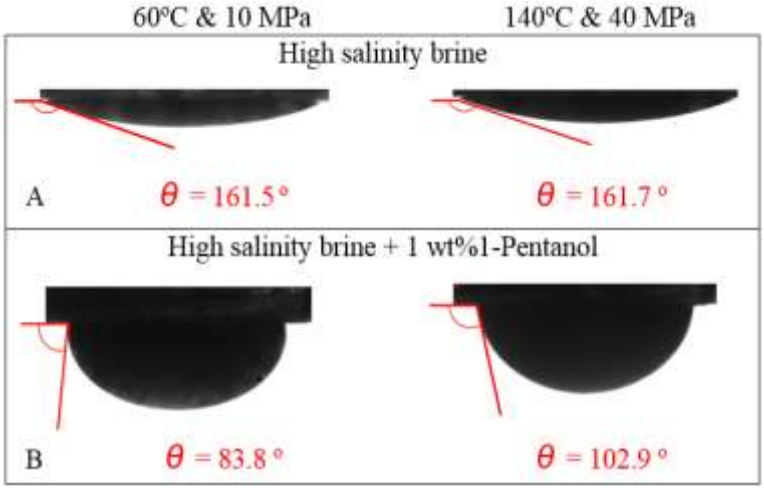

Figure 9-5. Contact angle of the oil droplet on calcite at 60 °C and 10 MPa and 140 °C and 40 MPa: (A) in HS brine; and (B) in HS brine with 1 wt % of 1-pentanol.

Figure 9-6B demonstrates that increasing the temperature increases the contact angle of the oil droplet on the calcite substrate in the presence of HS brines with 1-pentanol alcohol (1 wt %). For instance, Figure 9-6B indicates that increasing the temperature of the system from 60 to

100 °C increases the contact angle the oil droplet on the calcite substrate from 85° to 100°. This is largely because the solubility of 1-pentanol alcohol in the aqueous phase increases with increasing the temperature [297], and in return, less 1-pentanol alcohol would dissolve into oil and accumulate at the oil-brine interfaces. This physiochemical process would prevent 1-pentanol alcohol from bridging chemical surface species at oil-brine surfaces such as $-COO^-$, $-COOCa^+$, and $-NH^+$), thus, less hydrophilicity [292]. Figure 9-6B also shows that further increasing the temperature from 100 to 140 °C has a minimal impact on the contact angle increase, thereby expanding the application of 1-pentanol alcohol in high temperature carbonate reservoirs. For example, increasing the temperature of the oil-(HS)-brine-calcite system from 100 to 140 °C has a minor impact on the contact angle (+3°). We are uncertain why increasing temperature further above 100 °C only causes a minor effect on the wettability; perhaps this is because high temperature weakens the intermolecular hydrogen bonds between alcohol and the water molecule. This process decreases the solubility of alcohol in the brine while increasing its concentration at oil-brine interfaces [298, 299]. Figure 9-6 also confirms that pressure does not affect the contact angle in the presence of 1-pentanol alcohol in line with the contact angle results without 1-pentanol (Figure 9-4). Taken together, our results clearly show that 1-pentanol alcohol can trigger a shift of wettability from the oil-wet system toward an intermediate-wet system on calcite surfaces. While increasing the temperature up to 100 °C likely increases contact angle thus lowers the hydrophilicity (from water-wet to slightly water-wet), the negative effect of temperature above 100 °C on wettability becomes minor. More importantly, at a temperature of 140 °C, 1-pentanol alcohol (1 wt %) in HS brine remains to shift the wettability from a strongly oil-wet system (CA = 162°) toward the intermediate-wet system (CA = 103°), suggesting that 1-pentanol alcohol may be a practical alternative to enhance the oil recovery in high salinity and high temperature carbonate formations as a result of the wettability alteration.

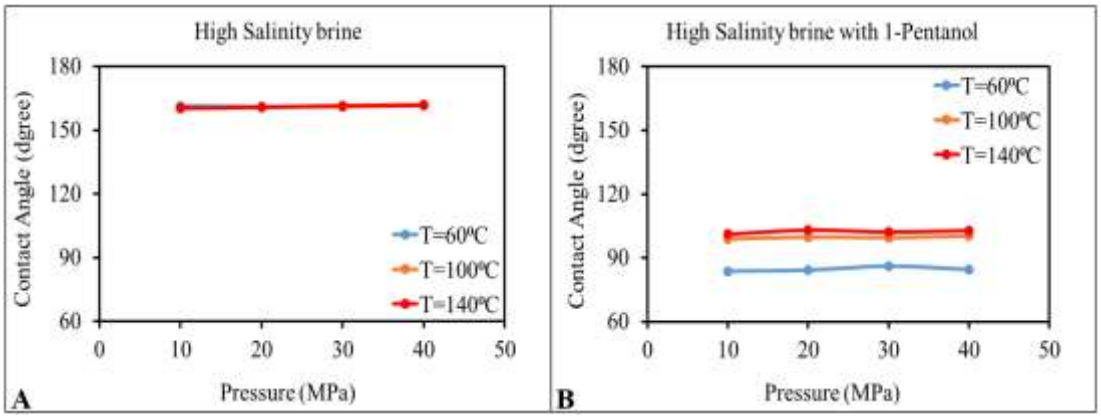

Figure 9-6. Contact angle results of the oil droplet on calcite surface at different temperature and pressure:(A) HS brine only (B) HS brine with 1-pentanol.

9.4.3 The Effect of 1-Pentanol Alcohol on the Contact Angle in Low Salinity Brine

Adding 1-pentanol alcohol slightly reduces the contact angle and, thus, hydrophilicity in the presence of LS brine at a low temperature (60 °C), while the contact angle increases with increasing temperature (Figures 9-7 and 9-8) in line with the performance of 1-pentanol alcohol in the HS brine. For instance, Figure 9-7 indicates that mixing 1-pentanol alcohol (1 wt %) with LS brine at 60 °C and 40 MPa reduces the contact angle of the oil droplet on the calcite surface from 88° to 81°. This is likely at low temperature; a fraction of 1-pentanol alcohol absorbs in the oil-brine interface and thus increases the hydrophilicity of the calcite surface as discussed in the above section. This is also in line with our previous work [292], which illustrates that the contact angle of the oil droplet on the calcite surface reduces from 105° to 90°. Analogously, Lu et al. [275] reported that the contact angle of the oil droplet on the calcite surface reduces to 23° when mixing 1-pentanol alcohol (1 wt %) with low salinity brine (0.01 M NaCl). Moreover, similar to HS brine, Figure 9-8 demonstrates that increasing the temperature increases the contact angle and, thus, the hydrophobicity in LS brine with 1-pentanol alcohol (1 wt %). For instance, Figure 9-7 presents that contact angle of the oil-(LS)brine-calcite increases from 88° to 101° with increasing the temperature from 60 to 100 °C, increasing the hydrophobicity. This is likely due to the fact that increasing the temperature increases the solubility of 1-pentanol alcohol in the brine, which yields an increase of the accumulation of 1-pentanol hydroxyl groups (−OH) inside the thin water film. This physical process likely increases the electrostatic bridges between polar oil species and calcite surface species through ion-dipole interactions, therefore, increasing the hydrophobicity of the system, although more quantitative validation remains to be made to understand this process.

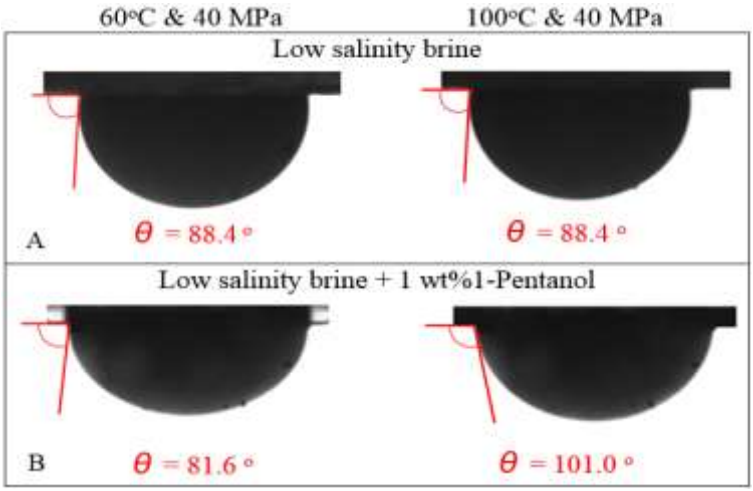

Figure 9-7. Contact angle of the oil droplet on the calcite surface at 60 oC and 40 MPa and 100 °C and 40 MPa: (A) in LS brine and (B) in LS brine with 1 wt % of 1-pentanol.

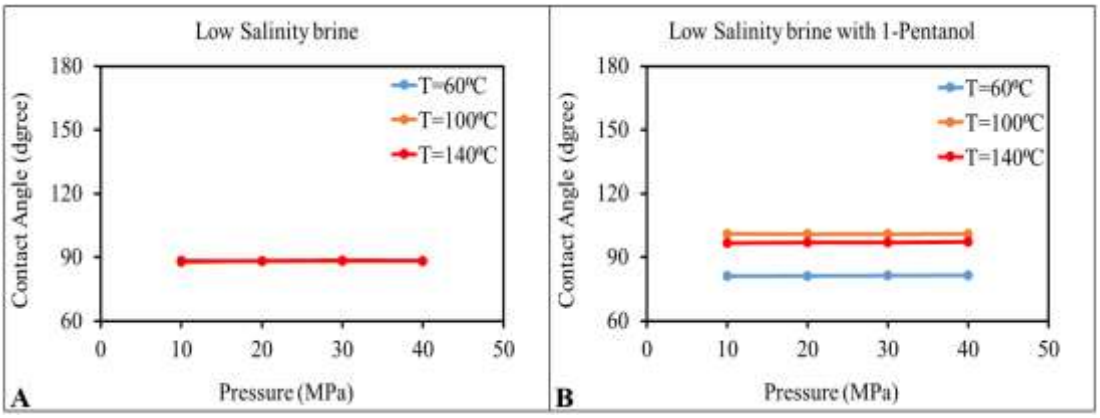

Figure 9-8. Contact angle results of the oil droplet on the calcite surface in LS water at different temperatures and pressures: (A) LS brine only and (B) LS brine with 1-pentanol.

9.4.4 Confirmation of Our Previous Proposed Mechanism for 1-Pentanol Increasing Hydrophilicity in High Salinity and High Temperatures

Figure 9-9 shows our proposed mechanism (modified based on our previous proposed mechanism in Figure 6 in ref [292]), accounting for the wettability shift toward hydrophilicity by adding 1-pentanol alcohol as a function of temperature. At in situ reservoir conditions, the interaction among oil-brine-calcite can be interpreted using a number of bonds generated from chemical surface species at polar oil-brine and brine-carbonate surfaces [58, 60, 61], After adding 1-pentanol alcohol in the brine regardless of salinity, 1-pentanol alcohol is mainly soluble in the brine phase, and the concentration of 1-pentanol alcohol in the oil phase is small [275]. However, the accumulation of 1-pentanol alcohol at the oil-brine interface likely breaks the original electrostatic bridges between polar oil species and calcite surface species through the thin water film (e.g., [$-COO^-$] [$>CaOH_2^+$], [$-NH^+$] [$>CaCO_3^-$], [$-NH$][$>CO_3^-$], [$-COO^-$] [$>CO_3Ca^+$], [$-COOCa^+$] [$>CaCO_3^-$], and [$-COOCa^+$] [$>CO_3^-$]). This is likely achieved by bridging $-COO^-$, $-COOCa^+$, and $-NH^+$ through the hydroxyl functional group ($-OH$) provided by 1-pentanol alcohol (Figure 9-9) with ion-dipole interactions. This physiochemical process likely breaks the bridges between polar oil species and calcite surface species, accounting for the shift toward hydrophilicity by adding 1-pentanol alcohol [292]. This hypothesis is supported by Figure 9-6 which shows that 1-pentanol alcohol (1 wt %) alters the wettability of the calcite surface from a strongly oil-wet system toward an intermediate-wet system in HS brine. Increasing the temperature increases the solubility of 1-pentanol alcohol in the aqueous phase [297], thus likely decreasing the accumulation of 1-pentanol alcohol in the oil-brine interface (Figure 9-9). Consequently, this would decrease the number of bridges between the hydroxyl functional group ($-OH$) and polar oil groups at oil-brine interfaces, which results in a slight shift from water-wet system toward a less water-wet system with increasing temperature up to 100 °C. This hypothesis is also supported by Figure 9-6B which

shows that increasing the temperature from 60 to 100°C increases the contact angle of the oil-(HS)brine-calcite system from 85° to 100°. However, this negative effect of temperature above 100 °C on wettability becomes negligible, possibly because desorption of 1-pentanol alcohol from the oil-brine interface to the HS brine decreases with increasing the temperature further above 100 °C.

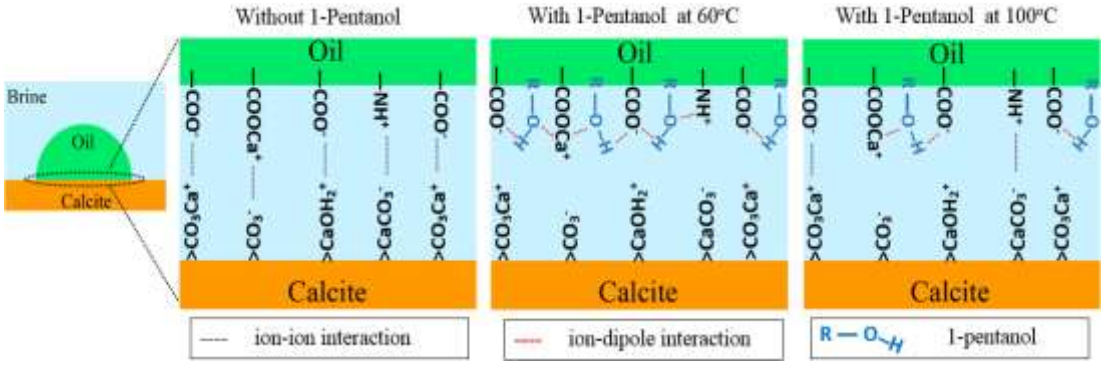

Figure 9-9. Influence of the temperature on the 1-pentanol hydrophilicity effect in the oil-brine-carbonate system in HS brine.

9.4.5 Effect of 1-Pentanol Assisted Waterflooding at the Secondary Mode

1-Pentanol (0.4 wt %) assisted waterflooding yields almost 16% (original oil in place, OOIP) of additional oil recovery at the secondary mode compared with waterflooding without 1-pentanol, confirming that the wettability alteration process achieved by 1-pentanol can lead to the oil detachment, coalescence, and transport and, thus, enhance oil recovery. For example, conventional waterflooding yields about 55% of the OOIP, while the conventional waterflooding with 0.4 wt % of 1-pentanol achieves an average of 71% of the OOIP (Figure 9-10). To be more specific, CF1 (waterflooding without 1-pentanol) shows about 32.7% of oil recovery before water breakthrough, whereas CF3 (waterflooding with 1-pentanol) gives 45.9% of oil recovery prior to water breakthrough, as shown in Table 9-3 and Figure 9-10A. This shows that 1-pentanol delays the breakthrough oil recoveries, indicating a wettability alteration toward less hydrophobicity during the injection of FBP [164, 277]. In addition, the results of the CF1 and CF3 experiments in Table 9-3 show that residual oil saturation (S_{or}) was reduced from 0.46 during FB injection to 0.31 during FBP injection. Furthermore, the water relative permeabilities at the residual oil saturation ($K_{rw}(S_{orw})$) of CF1 and CF3 show that adding1-pentanol (0.4 wt %) to the waterflooding lowers the $K_{rw}(S_{orw})$ from 0.26 during FB injection to 0.17 during FBP injection. This decrease in the S_{or} and $K_{rw}(S_{orw})$ caused by the 1-pentanol effect further confirms the in situ wettability shift during the FBP, hence, increasing the hydrophilicity of carbonate and enhancing the oil recovery.

Table 9-3: Core flooding results

Coreflooding	Coreflooding fluid	S_{wi}	$RF_{Breakthrough}$ (%)	$K_{rw}(S_{or})$	S_{or}	RF_{Total} (%)
CF1	FB	0.21	32.7	0.26	0.46	54.3
CF2	FB	0.17	46.4	0.33	0.45	54.9
CF3	FBP	0.20	45.9	0.17	0.31	68.9
CF4	FBP	0.22	49.1	0.23	0.35	72.3

A similar performance of 1-pentanol was observed from CF2 and CF4 as shown in Table 9-3 and Figure 9-10B, further confirming that waterflooding with 1-pentanol can enhance the wettability alteration during secondary oil recovery, increasing the total oil recovery from carbonate reservoirs. For instance, Table 9-3 shows that 1-pentanol (CF4) lowers the S_{or} and $K_{rw}(S_{orw})$ to 0.35 and 0.23, respectively, whereas without 1-pentanol, conventional waterflooding (CF2) gives S_{or} = 0.45 and $K_{rw}(S_{orw})$ = 0.33, confirming that the wettability alteration was toward a less oil-wet system with 1-pentanol.

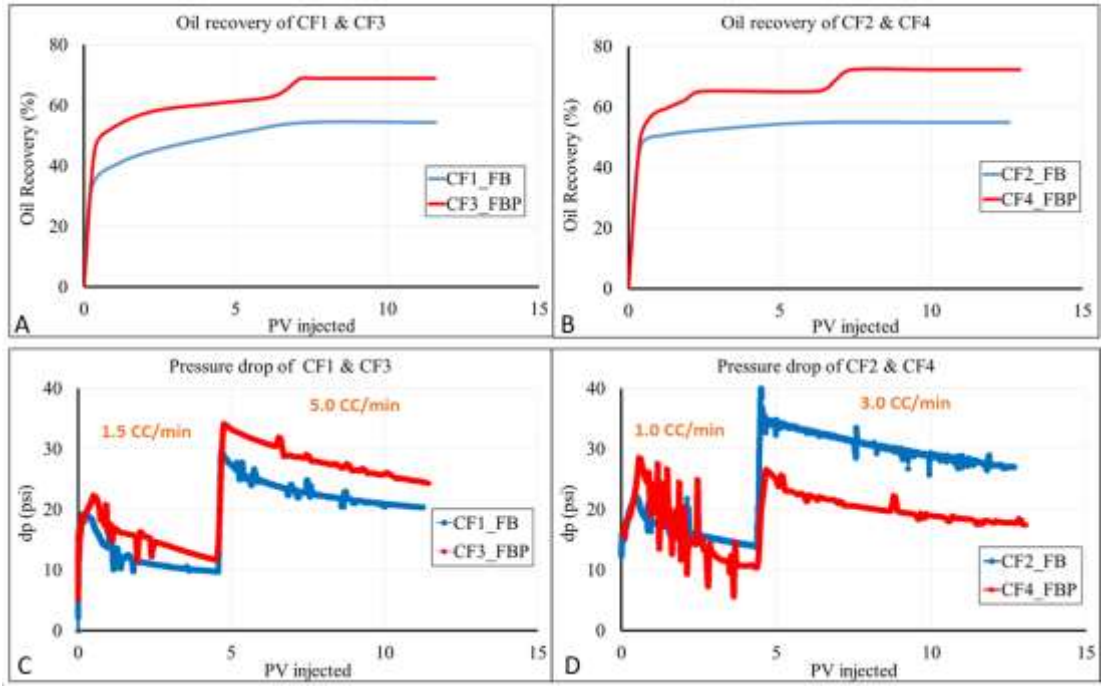

Figure 9-10: Oil recovery from core flooding experiments: (A) CF1 vs CF3 and (B) CF2 vs CF4. Pressure drop from core flooding experiments: (C) CF1 vs CF3 and (D) CF2 vs CF4.

9.4.6 Effect of 1-Pentanol Assisted Waterflooding in the Tertiary Mode

Figure 9-11 shows that 1-pentanol assisted waterflooding in the tertiary mode only gives 5.4% additional oil recovery in the tertiary mode, which is far less than the incremental oil recovery made in the secondary mode. For example, FB in CF1 yields a total oil recovery of 54.3% of

OOIP after 12 PV FB injection, whereas FBP slightly increases the oil recovery to 59.7% of OOIP after the same amount of pore volume injection and reduced the S_{or} from 0.46 after FB injection to 0.40. Moreover, the incremental oil recovery was obtained after injecting 7 PV of FBP, indicating that the effect of 1-pentanol on the wettability alteration may take a longer time to occur at high water saturation. The similar phenomena can be seen from low salinity waterflooding in the tertiary mode as well, which usually gives a lower incremental oil recovery compared to the secondary mode [20, 234, 250, 263, 300]. This is most likely attributed to the flow path created by the conventional FB flooding in the secondary mode which decreases the displacement efficiency even at the pore network [20]. In this context, 1-pentanol likely passes through the pores easily in the tertiary mode. Therefore, limiting the penetration of 1-pentanol alcohol into the thin water film between the oil and the carbonate surface thus lowers the effectiveness of 1-pentanol alcohol to alter the wettability of carbonate toward the less oil-wet system. The lower incremental oil recovery in the tertiary mode also implies an uncertainty of the timing for the application of 1-pentanol alcohol-assisted waterflooding. We tentatively believe that the incremental oil recovery (from 1-pentanol assisted waterflooding) would decrease with increasing in situ water saturation. However, more core flooding experiments with pore network modeling may need to be done to relate the incremental oil recovery with the in situ water saturation.

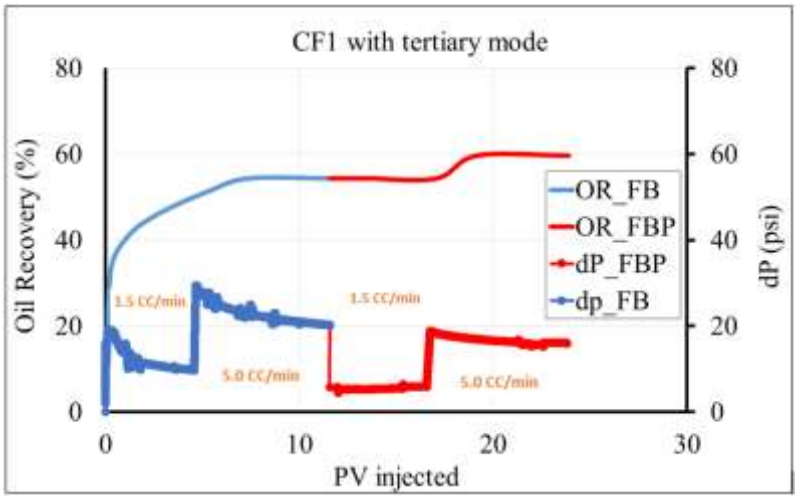

Figure 9-11: Oil recovery and pressure drop from core flooding experiments CF1 under tertiary mode.

9.5 Summary and Conclusions

On the basis of our previous work, [292] in this paper, we aimed to examine the wettability alteration process achieved by 1-pentanol alcohol at the subpore level that would trigger oil detachment, coalescence, and transport and thus enhance oil recovery for high temperature and high salinity carbonate reservoirs. To achieve this aim, we examined the influence of 1-

pentanol alcohol (1 wt %) on the contact angle of oil-brine-calcite at different temperatures (60, 100, 140 °C) and pressures (10, 20, 30, 40 MPa) in HS and LS brines. Furthermore, we conducted four core flooding experiments to examine the application of adding a small percentage of 1-pentanol alcohol (0.4 wt %) to assist the conventional secondary waterflooding in the carbonate reservoir under high temperature and high salinity conditions.

Our contact angle experiments confirm that 1-pentanol alcohol (1 wt %) alters the wettability of the oil-brine-carbonate system from a strongly oil-wet system (without 1-pentanol) toward a weakly water-wet or an intermediate-wet system, favoring a reduction of residual oil saturation and thus incremental oil recovery. More interestingly, HS brine would further improve the performance of 1-pentanol alcohol with respect to shifting the wettability from a strongly oil-wet system toward an intermediate-wet system. This finding brings a practical application of 1-pentanol-assisted waterflooding to enhance the oil recovery in high salinity carbonate formations. Moreover, while increasing the temperature up to 100 °C increases the contact angle (20%) with the presence of 1-pentanol alcohol in HS brine, the temperature effect becomes negligible with further increasing the temperature to 140 °C (4%). Additionally, our core flooding results support the contact angle results and show that adding 0.4 wt % of 1-pentanol to the injected brine yields 16% of additional oil recovery at the secondary mode. This study would likely expand the application of 1-pentanol-assisted waterflooding in harsh reservoir conditions which are widely found in Oman and other Middle Eastern countries, as well as in the western part of China. Taken together, 1-pentanol-assisted waterflooding maybe a viable and cost-effective means to enhance the oil recovery in high temperature and high salinity carbonate formations where freshwater is not available.

Chapter 10. Conclusions, Recommendations and Outlook for Future Work

10.1 Conclusions

Low salinity waterflooding appears to be a cost-effective and environmentally friendly means for enhanced oil recovery (EOR) in carbonate reservoirs, in particular in the period of low oil prices. However, the low salinity waterflooding technique has not been widely applied in carbonate oil reservoirs due to the remaining uncertainties. For example, while the wettability alteration process has been identified as an important physicochemical process behind low salinity waterflooding, the effect of oil composition, calcite dissolution process, and pH on oil adhesion remains unclear, especially at the nano and sub-pore scale. Also, the effect of the mineralogy of carbonate reservoirs, in particular clay-rich carbonate reservoirs on the wettability alteration process has been received little attention. To address the above issues, this research was conducted with a combination of atomic force microscopy, contact angle measurements, disjoining pressure isotherm, and geochemical modeling as a function of salinity, ion type, and ionic strength.

In addition, given the fact that not every carbonate reservoir would have access to low salinity water, such as reservoirs in the Middle East and Western China, a new EOR approach was examined through multi-scale experimental approaches. To be more specific, in light of existing knowledge in the oil-brine-rock interactions, this research also investigated the mechanisms and potential of 1-pentanol-assisted enhanced oil recovery from sub-pore scale to core scale with a combination of contact angle measurements, zeta potential measurements, and coreflooding experiments.

The conclusions from this thesis can be categorized into three aspects as followings:

1. Oil-brine-calcite interactions at nanoscale as a function of oil composition, pH and its implications to low salinity waterflooding in carbonate reservoirs.
2. Role of clay impurities on low salinity effect in clay-rich carbonate reservoirs at the molecular level, and validity of contact angle measurements associated with calcite dissolution to show the wettability alteration.
3. Influence of 1-pentanol on oil-brine-calcite interaction at sub-pore, and core-scale, and its implications to enhanced oil recovery.

10.1.1 Oil-brine-calcite interactions at nanoscale as a function of oil composition, pH and its implications to low salinity waterflooding in carbonate reservoirs.

Given that wettability is mainly governed by oil-brine-rock interactions, oil composition would play an important role in wettability alteration during low salinity waterflooding in carbonate reservoirs. While the effect of polar oil components on wettability alteration has been well examined using contact angles measurements and coreflooding experiments as a function of pH, but researchers have not evaluated the response of non-polar oil on wettability alteration in much detail. Also, while geochemical modeling together with contact angle measurement have been performed to understand the nature of the wettability alteration during low salinity water injection, there has been little experimental evidence associating acidic oil groups (-COOH) with wettability at a molecular level as a function of pH. To address the above knowledge gaps, a combination of atomic force microscopy (AFM), zeta potential measurements, disjoining pressure isotherm estimation were conducted with non-polar oil group ($–CH_3$) and acidic oil groups (-COOH) as a function of pH.

AFM adhesion force measurements between the non-polar oil group ($–CH_3$) and calcite show that the adhesion force decreases with an increase in pH from 9.5 to 11, accounting for the decrease of contact angle with pH, hence increasing hydrophilicity. The zeta potential data shows that increasing pH shifts the zeta potential of the non-polar oil ($–CH_3$)-brine and calcite-brine interfaces towards more negative values, resulting in an increase in the electrical double layer force. The total disjoining pressure and AFM adhesion tests follow the same trend, showing that adhesion force decreases with increasing pH due to electrical double layer expansion, thus leading to a water-wet system. Taken together, our results confirm that detachment of non-polar oil from carbonate rock continues to take place during low salinity water injection. Also, this work sheds further light on the significance of pH increase on non-polar oil-calcite adhesion during low salinity water injection, and provides insights into the quantification of carbonate reservoir wettability.

Similar to non-polar oil groups ($-CH_3$), polar oil groups with –COOH exhibit a similar response to calcite adhesion with respect to pH. For example, the AFM measurements support contact angle results, showing that the adhesion force between the -COOH oil group and calcite reduces from 1.26 to 1.05 nN as the pH of the sodium chloride brine increasing from 9.5 to 11. Zeta potential results show that raising the pH increases the negativity of the zeta potential of the acidic oil-brine and calcite-brine interfaces, thus elevating the electrical double layer force. Furthermore, the disjoining pressure calculation shows a shift of thermodynamic isotherm from strongly negative to less negative, supporting the results of AFM and contact angle experiments, confirming that the increase of local pH caused by calcite dissolution during low salinity water injection likely contributes to wettability alteration hence

incremental oil recovery. This study sheds light on the significant influence of a local pH increase caused by calcite dissolution on the performance of low salinity waterflooding in particular for high acidic oil bearing carbonate reservoirs.

10.1.2 Role of clay impurities on low salinity effect in clay-rich carbonate reservoirs at the molecular level, and validity of contact angle measurements associated with calcite dissolution to show the wettability alteration.

Given that clay minerals play an important role in local pH variation, it is important to understand how clay minerals in particular basal-charged minerals, respond to oil-mineral adhesion. Also, contact angle measurement appears to be a direct and practical approach to describe the oil-brine-carbonate system interactions thus wettability in the presence of aqueous ionic solutions for enhanced oil recovery purposes. However, until recently, there has been an increasing concern that the contact angle may not be reliable because of the possible surface roughness variation as a result of calcite dissolution in the presence of the LS brine. To address the above issues, AFM, zeta potential measurements, and disjoining pressure isotherm were combined to investigate the effect of low salinity water in clay-rich carbonate reservoirs on the adhesion between the clay and different oil groups ($-CH_3$ and –COOH) as a function of pH. Also, AFM, contact angle measurements, and geochemical modeling were combined to examine if the surface roughness variation induced by calcite dissolution in the presence of LSW plays a certain role in contact angle.

Zeta potential measurements show that increasing pH leads to strongly negative zeta potential for oil−brine and brine−muscovite, thus increasing electrical double layer expansion [37, 267, 268] as well as repulsive force [36]. AFM tests support the hypothesis, showing that increasing pH indeed significantly decreased adhesion force regardless of functional groups [196, 269]. Moreover, the polarized functional group (−COOH group) gives four times greater adhesion force than nonpolar group ($-CH_3$), confirming that polarized functional groups play a significant role in the low salinity effect [58, 60, 76]. Sphere−flat model (DLVO theory) can better interpret the AFM experiments which measure the adhesion between a modified tip (sphere) and a substrate (flat). Moreover, the sphere−flat model predicts the same degree of adhesion decrease with increasing pH in line with AFM measurements. This study reveals the significance of basal charged clays during low salinity waterflooding in sandstone reservoirs, thus expanding the application envelope of low salinity water in sandstone reservoirs bearing basal charged clays.

Surface roughness measurement shows that the high salinity water (HSW) leads to negligible surface roughness change, but low salinity water (LSW) causes a surface roughness increase from 4 to 17 nm. Geochemical modeling demonstrates that the surface roughness increase in

LSW is induced by a small amount of calcite dissolution (1.16×10^{-4} mol/mol). Taken together, our results confirm that surface roughness variation due to calcite dissolution in LSW plays a negligible role in the contact angle. Therefore, the contact angle remains a direct and practical approach to indicate the wettability alteration in the presence of various aqueous ionic brines.

10.1.3 Influence of 1-pentanol on oil-brine-calcite interaction at sub-pore, and core-scale, and its implications to enhanced oil recovery

Low salinity waterflooding has been identified as a cost-effective and environmentally friendly means to enhance oil recovery in carbonate reservoirs by decreasing hydrophobicity. However, low salinity waterflooding may not be practical for reservoirs without access to freshwater resources such as reservoirs in Western China and the Middle East. Therefore, it is of vital importance to develop a new cost-effective EOR technique with a deep understanding of oil-brine-rock interaction. In this context, adding various alcohols (with various numbers of the carbon chain and -OH) in injected water was examined to explore the potential of the wettability alteration process in carbonate reservoirs. This investigation was conducted with a combination of contact angle measurement, zeta potential measurements, disjoining pressure isotherm calculation. Moreover, the influence of 1-pentanol alcohol (1 wt%) on the wettability alteration process was examined through the measurement of contact angle of oil-brine-calcite at different temperatures (60, 100, 140^{o}C) and pressures (10, 20, 30, 40 MPa) in high and low salinity water. Furthermore, four core flooding experiments were conducted to examine the application of adding a small percentage of 1-pentanol alcohol (0.4 wt%) to assist waterflooding at high temperature and high salinity conditions.

Results show that intermediate carbon chain alcohol (1-pentanol) increases the hydrophilicity of oil−brine−calcite systems in both high- and low salinity brines, but high-salinity brine further boosts the effect of 1-pentanol on wettability alteration. Short carbon chain alcohols (e.g., ethanol and isopropanol) play a minor effect on wettability characteristics of oil−brine−calcite in high-salinity brine, whereas adding short carbon chain alcohols likely increases hydrophobicity in low salinity brines. Also, increasing the number of –OH functional groups does not decrease the contact angle and hydrophilicity. Alcohols play a minor effect on the ζ potential of the oil−brine and brine−rock interfaces compared to salinity, implying that the Derjaguin, Landau, Verwey, and Overbeek (DLVO) theory cannot explain the impact of alcohol on the wettability of the oil−brine−carbonate system.

Moreover, contact angle experiments further confirm that 1-pentanol alcohol (1wt %) alters the wettability of the oil-brine-carbonate system from strongly oil-wet system (without 1-pentanol) toward weakly water-wet or an intermediate-wet system, favoring a reduction of residual oil saturation thus incremental oil recovery. More interestingly, high salinity water

would further improve the performance of 1-pentanol alcohol with respect to shifting the wettability from strongly oil-wet system toward an intermediate-wet system. This finding brings a practical application of 1-pentanol-assisted waterflooding to enhance the oil recovery in high salinity carbonate formations. Additionally, the coreflooding results support the contact angle results and show that adding 0.4 wt% of 1-pentanol to the injected brine yields 16% of additional oil recovery at the secondary mode. This study would likely expand the application of 1-pentanol-assisted waterflooding in harsh reservoir conditions which are widely found in Oman, other Middle Eastern countries, as well as in the Western part of China. Taken together, 1-pentanol-assisted waterflooding maybe a viable and cost-effective means to enhance the oil recovery in high temperature and high salinity carbonate formations where freshwater is not available.

10.2 Recommendations and Outlook for Future Work

While this research experimentally reveals the impact of oil composition and local pH variation, surface roughness on in-situ wettability alteration, some quantitative work remains to be done to better model the low salinity waterflooding performance at both core- and reservoir-scale. For example, the oil detachment process may be characterized using thermodynamics and electrostatics (including both polar- and non-polar components). Then an analytical model may need to be proposed to be incorporated into the existing reservoir simulator and thus better model the physics behind the low salinity waterflooding.

In addition, the contact angle measurements and the core flooding experiments confirm that adding intermediate carbon chain alcohol (1-pentanol) to the injected brines can shift the wettability of carbonate rock from a strong oil-wet state toward the less oil-wet state. However, further work is required to achieve a deeper understanding of the alcohol effect to improve the confidence in applying the Alcohol-Assisted waterflooding to enhance the oil recovery in carbonate formations under harsh conditions. For example, the mechanism behind the wettability alteration still needs to be further investigated. Also, how 1-pentanol affects the wettability alteration at the pore-scale requires further evaluation, and the optimum concentration of 1-pentanol to enhance the oil recovery at different temperatures and different salinities (provide a framework for petroleum industry with respect to the optimal concentration of 1-pentanol to use at certain temperature and salinity) needs to be assessed. Therefore the following research activities are recommended for future work:

- Coupling AFM adhesion measurements and surface complexation modeling or molecular dynamic simulation to understand the mechanism(s) behind the effect of intermediate carbon chain alcohol on the wettability of the oil-brine-carbonate system.

- Using a micro-model and micro-CT scanning advantage to understand how 1-pentanol alcohol affects the wettability alteration at the pore-scale flow in carbonate rocks.
- Combining the contact angle and core flooding experiments to provide a framework to help the petroleum industry determining the minimum concentration of 1-pentanol that can be used to enhance the oil recovery from carbonate reservoirs at certain temperatures and certain salinities.
- Using the core flooding results together with numerical modeling to predict the relative permeability curves, which will be helpful to upscale the 1-pentanol alcohol effect from lab-scale to the reservoir-scale and evaluate the economic value of the application of 1-pentanol-assisted waterflooding to enhance the oil recovery in carbonate formations.

REFERENCES

1. Klemme, H. and G.F. Ulmishek, *Effective petroleum source rocks of the world: stratigraphic distribution and controlling depositional factors (1).* AAPG Bulletin, 1991. **75**(12): p. 1809-1851.
2. Schlumberger. *Carbonate Reservoirs*. 2019; Available from: https://www.slb.com/technical-challenges/carbonates.
3. Downs, H.H. and P.D. Hoover, *Enhanced Oil Recovery by Wettability Alteration*, in *Oil-Field Chemistry*. 1989, American Chemical Society. p. 577-595.
4. Lager, A., K. J. Webb, C. J. J. Black, M. Singleton, and K. S. Sorbie, *Low Salinity Oil Recovery - An Experimental Investigation*. 2006.
5. Jerauld, G.R., K.J. Webb, C.-Y. Lin, and J.C. Seccombe, *Modeling Low-Salinity Waterflooding.* SPE Reservoir Evaluation & Engineering, 2013. **11**(06): p. 1000-1012.
6. Seccombe, J.C., A. Lager, K.J. Webb, G. Jerauld, and E. Fueg, *Improving Wateflood Recovery: LoSalTM EOR Field Evaluation*. 2008, Society of Petroleum Engineers.
7. Alvarado, V., M. Moradi Bidhendi, G. Garcia-Olvera, B. Morin, and J.S. Oakey, *Interfacial Visco-Elasticity of Crude Oil - Brine: An Alternative EOR Mechanism in Smart Waterflooding*, in *SPE Improved Oil Recovery Symposium*. 2014, Society of Petroleum Engineers: Tulsa, Oklahoma, USA. p. 17.
8. Ayirala, S.C., E. Uehara-Nagamine, A.N. Matzakos, R.W. Chin, P.H. Doe, and P.J. van den Hoek, *A Designer Water Process for Offshore Low Salinity and Polymer Flooding Applications*, in *SPE Improved Oil Recovery Symposium*. 2010, Society of Petroleum Engineers: Tulsa, Oklahoma, USA.
9. Cense, A., S. Berg, K. Bakker, and E. Jansen, *Direct Visualization of Designer Water Flooding in Model Experiments*. 2011, Society of Petroleum Engineers.
10. Strand, S., T. Austad, T. Puntervold, E.J. Høgnesen, M. Olsen, and S.M.F. Barstad, *"Smart Water" for Oil Recovery from Fractured Limestone: A Preliminary Study.* Energy & Fuels, 2008. **22**(5): p. 3126-3133.
11. RezaeiDoust, A., T. Puntervold, S. Strand, and T. Austad, *Smart water as wettability modifier in carbonate and sandstone: A discussion of similarities/differences in the chemical mechanisms.* Energy & fuels, 2009. **23**(9): p. 4479-4485.
12. Fathi, S.J., T. Austad, and S. Strand, *"Smart Water" as a Wettability Modifier in Chalk: The Effect of Salinity and Ionic Composition.* Energy & Fuels, 2010. **24**(4): p. 2514-2519.
13. Yousef, A.A., S. Al-Saleh, and M.S. Al-Jawfi, *Smart WaterFlooding for Carbonate Reservoirs: Salinity and Role of Ions*, in *SPE Middle East Oil and Gas Show and Conference*. 2011, Society of Petroleum Engineers: Manama, Bahrain. p. 11.
14. Yousef, A.A., S.H. Al-Salehsalah, and M.S. Al-Jawfi, *New Recovery Method for Carbonate Reservoirs through Tuning the Injection Water Salinity: Smart WaterFlooding*. 2011, Society of Petroleum Engineers.
15. Austad, T., S.F. Shariatpanahi, S. Strand, C.J.J. Black, and K.J. Webb, *Conditions for a Low-Salinity Enhanced Oil Recovery (EOR) Effect in Carbonate Oil Reservoirs.* Energy & Fuels, 2012. **26**(1): p. 569-575.
16. Zahid, A., E.H. Stenby, and A.A. Shapiro, *Smart Waterflooding (High Sal/Low Sal) in Carbonate Reservoirs*, in *SPE Europec/EAGE Annual Conference*. 2012, Society of Petroleum Engineers: Copenhagen, Denmark. p. 21.
17. Al-sofi, A.M. and A.A. Yousef, *Insight into Smart-Water Recovery Mechanism through Detailed History Matching of Coreflood Experiments*, in *SPE Reservoir Characterization and Simulation Conference and Exhibition*. 2013, Society of Petroleum Engineers: Abu Dhabi, UAE. p. 12.

18. Al Harrasi, A., R.S. Al-maamari, and S.K. Masalmeh. *Laboratory investigation of low salinity waterflooding for carbonate reservoirs*. in *Abu Dhabi International Petroleum Conference and Exhibition*. 2012. Society of Petroleum Engineers.
19. Al-Shalabi, E.W., K. Sepehrnoori, G. Pope, and K. Mohanty, *A Fundamental Model for Predicting Oil Recovery Due to Low Salinity Water Injection in Carbonate Rocks*, in *SPE Energy Resources Conference*. 2014, Society of Petroleum Engineers: Port of Spain, Trinidad and Tobago. p. 24.
20. Chandrasekhar, S., *Wettability alteration with brine composition in high temperature carbonate reservoirs.* 2013.
21. Chandrasekhar, S., H. Sharma, and K.K. Mohanty, *Wettability Alteration with Brine Composition in High Temperature Carbonate Rocks*, in *SPE Annual Technical Conference and Exhibition*. 2016, Society of Petroleum Engineers: Dubai, UAE. p. 21.
22. Nasralla, R.A., E. Sergienko, S.K. Masalmeh, H.A. van der Linde, N.J. Brussee, H. Mahani, B.M.J.M. Suijkerbuijk, and I.S.M. Al-Qarshubi, *Potential of Low-Salinity Waterflood To Improve Oil Recovery in Carbonates: Demonstrating the Effect by Qualitative Coreflood.* SPE Journal, 2016. **21**(05): p. 1643-1654.
23. Yousef, A.A., S.H. Al-Saleh, A. Al-Kaabi, and M.S. Al-Jawfi, *Laboratory Investigation of the Impact of Injection-Water Salinity and Ionic Content on Oil Recovery From Carbonate Reservoirs.* SPE Reservoir Evaluation & Engineering, 2013. **14**(05): p. 578-593.
24. Zhang, P.M. and T. Austad, *Wettability and oil recovery from carbonates: Effects of temperature and potential determining ions.* Colloids and Surfaces a-Physicochemical and Engineering Aspects, 2006. **279**(1-3): p. 179-187.
25. Mahani, H., A.L. Keya, S. Berg, W.B. Bartels, R. Nasralla, and W.R. Rossen, *Insights into the Mechanism of Wettability Alteration by Low-Salinity Flooding (LSF) in Carbonates.* Energy & Fuels, 2015. **29**(3): p. 1352-1367.
26. Karimi, M., R.S. Al-Maamari, S. Ayatollahi, and N. Mehranbod, *Mechanistic study of wettability alteration of oil-wet calcite: The effect of magnesium ions in the presence and absence of cationic surfactant.* Colloids and Surfaces a-Physicochemical and Engineering Aspects, 2015. **482**: p. 403-415.
27. Awolayo, A., H. Sarma, and A.M. AlSumaiti, *A Laboratory Study of Ionic Effect of Smart Water for Enhancing Oil Recovery in Carbonate Reservoirs*. 2014, Society of Petroleum Engineers.
28. Sari, A., Q. Xie, Y.Q. Chen, A. Saeedi, and E. Pooryousefy, *Drivers of Low Salinity Effect in Carbonate Reservoirs.* Energy & Fuels, 2017. **31**(9): p. 8951-8958.
29. Hognesen, E.J., S. Strand, and T. Austad, *Waterflooding of preferential oil-wet carbonates: Oil recovery related to reservoir temperature and brine composition*. 2005, Society of Petroleum Engineers.
30. Ligthelm, D.J., J. Gronsveld, J. Hofman, N. Brussee, F. Marcelis, and H. van der Linde, *Novel Waterflooding Strategy By Manipulation Of Injection Brine Composition*. 2009, Society of Petroleum Engineers.
31. Tie, H. and N.R. Morrow, *Oil recovery by spontaneous imbibition before and af-ter wettability alteration of three carbonate rocks by a moderately asphaltic crude oil.* Proceedings of society of core analysts held in Toronto, Canada, SCA20, 2005: p. 05-11.
32. Brady, P.V., C.R. Bryan, G. Thyne, and H.N. Li, *Altering wettability to recover more oil from tight formations.* Journal of Unconventional Oil and Gas Resources, 2016. **15**: p. 79-83.
33. Chavez-Miyauchi, T.E., A. Firoozabadi, and G.G. Fuller, *Nonmonotonic Elasticity of the Crude Oil-Brine Interface in Relation to Improved Oil Recovery.* Langmuir, 2016. **32**(9): p. 2192-8.

34. Lashkarbolooki, M., M. Riazi, F. Hajibagheri, and S. Ayatollahi, *Low salinity injection into asphaltenic-carbonate oil reservoir, mechanistical study.* Journal of Molecular Liquids, 2016. **216**: p. 377-386.
35. Lee, S.Y., K.J. Webb, I. Collins, A. Lager, S. Clarke, apos, M. Sullivan, A. Routh, and X. Wang, *Low Salinity Oil Recovery: Increasing Understanding of the Underlying Mechanisms*. 2010, Society of Petroleum Engineers.
36. Morin, B., Y. Liu, V. Alvarado, and J. Oakey, *A microfluidic flow focusing platform to screen the evolution of crude oil–brine interfacial elasticity.* Lab on a Chip, 2016. **16**(16): p. 3074-3081.
37. Nasralla, R.A. and H.A. Nasr-El-Din, *Double-Layer Expansion: Is It a Primary Mechanism of Improved Oil Recovery by Low-Salinity Waterflooding?* SPE Reservoir Evaluation & Engineering, 2014. **17**(01): p. 49-59.
38. Sandengen, K. and O. Arntzen. *Osmosis during low salinity water flooding*. in *IOR 2013-17th European Symposium on Improved Oil Recovery*. 2013.
39. Sohrabi, M., P. Mahzari, S.A. Farzaneh, J.R. Mills, P. Tsolis, and S. Ireland, *Novel Insights Into Mechanisms of Oil Recovery by Use of Low-Salinity-Water Injection.* SPE Journal, 2017. **22**(02): p. 407-416.
40. Tang, G.Q. and N.R. Morrow, *Influence of brine composition and fines migration on crude oil/brine/rock interactions and oil recovery.* Journal of Petroleum Science and Engineering, 1999. **24**(2-4): p. 99-111.
41. Wang, X. and V. Alvarado, *Effects of low-salinity waterflooding on capillary pressure hysteresis.* Fuel, 2017. **207**: p. 336-343.
42. Hiorth, A., L.M. Cathles, and M.V. Madland, *The Impact of Pore Water Chemistry on Carbonate Surface Charge and Oil Wettability.* Transport in Porous Media, 2010. **85**(1): p. 1-21.
43. Rezaei Gomari, K.A., O. Karoussi, and A.A. Hamouda, *Mechanistic Study of Interaction between Water and Carbonate Rocks for Enhancing Oil Recovery*, in *SPE Europec/EAGE Annual Conference and Exhibition*. 2006, Society of Petroleum Engineers: Vienna, Austria. p. 8.
44. Zaretskiy, Y., *Towards modelling physical and chemical effects during wettability alteration in carbonates at pore and continuum scales*. 2012, Heriot-Watt University.
45. Al-Shalabi, E.W., K. Sepehrnoori, and G. Pope, *Geochemical Interpretation of Low-Salinity-Water Injection in Carbonate Oil Reservoirs.* SPE Journal, 2015. **20**(06): p. 1212-1226.
46. Alotaibi, M.B., H.A. Nasr-El-Din, and J.J. Fletcher, *Electrokinetics of Limestone and Dolomite Rock Particles.* SPE Reservoir Evaluation & Engineering, 2013. **14**(05): p. 594-603.
47. Alshakhs, M.J. and A.R. Kovscek, *An Experimental Study of the Impact of Injection Water Composition on Oil Recovery from Carbonate Rocks*, in *SPE Annual Technical Conference and Exhibition*. 2015, Society of Petroleum Engineers: Houston, Texas, USA. p. 21.
48. Sari, A., Y.Q. Chen, Q. Xie, and A. Saeedi, *Low salinity water flooding in high acidic oil reservoirs: Impact of pH on wettability of carbonate reservoirs.* Journal of Molecular Liquids, 2019. **281**: p. 444-450.
49. Alameri, W., T.W. Teklu, R.M. Graves, H. Kazemi, and A.M. AlSumaiti, *Wettability Alteration During Low-Salinity Waterflooding in Carbonate Reservoir Cores*, in *SPE Asia Pacific Oil & Gas Conference and Exhibition*. 2014, Society of Petroleum Engineers: Adelaide, Australia. p. 18.
50. McGuire, P.L., J.R. Chatham, F.K. Paskvan, D.M. Sommer, and F.H. Carini, *Low Salinity Oil Recovery: An Exciting New EOR Opportunity for Alaska's North Slope*. 2005, Society of Petroleum Engineers.

51. Alves, D.R., J.S.A. Carneiro, I.F. Oliveira, F. Façanha, A.F. Santos, C. Dariva, E. Franceschi, and M. Fortuny, *Influence of the salinity on the interfacial properties of a Brazilian crude oil–brine systems.* Fuel, 2014. **118**: p. 21-26.
52. Mahzari, P. and M. Sohrabi, *Crude Oil/Brine Interactions and Spontaneous Formation of Micro-Dispersions in Low Salinity Water Injection*, in *SPE Improved Oil Recovery Symposium*. 2014, Society of Petroleum Engineers: Tulsa, Oklahoma, USA. p. 15.
53. Flori1, H.N.A.-S.R.E. and P.V. Brady2, *Insights into Low Salinity Water Flooding.* This paper was prepared for presentation at the International Symposium of the Society of

Core Analysts held in Trondheim, Norway, 27-30 August 2018, 2018.
54. Al Mahrouqi, D., J. Vinogradov, and M.D. Jackson, *Zeta potential of artificial and natural calcite in aqueous solution.* Adv Colloid Interface Sci, 2017. **240**: p. 60-76.
55. Austad, T., S. Strand, E.J. Høgnesen, and P. Zhang, *Seawater as IOR Fluid in Fractured Chalk*, in *SPE International Symposium on Oilfield Chemistry*. 2005, Society of Petroleum Engineers: The Woodlands, Texas. p. 10.
56. Zhang, P. and T. Austad, *Waterflooding in chalk: Relationship between oil recovery, new wettability index, brine composition and cationic wettability modifier*, in *SPE Europec/EAGE Annual Conference*. 2005, Society of Petroleum Engineers: Madrid, Spain. p. 7.
57. Strand, S., E.J. Høgnesen, and T. Austad, *Wettability alteration of carbonates—Effects of potential determining ions (Ca2+ and SO42−) and temperature.* Colloids and Surfaces A: Physicochemical and Engineering Aspects, 2006. **275**(1-3): p. 1-10.
58. Brady, P.V. and G. Thyne, *Functional Wettability in Carbonate Reservoirs.* Energy & Fuels, 2016. **30**(11): p. 9217-9225.
59. Mahani, H., A.L. Keya, S. Berg, and R. Nasralla, *Electrokinetics of carbonate/brine interface in low-salinity waterflooding: Effect of brine salinity, composition, rock type, and pH on ζ-potential and a surface-complexation model.* SPE Journal, 2016.
60. Xie, Q., A. Sari, W.F. Pu, Y.Q. Chen, P.V. Brady, N. Al Maskari, and A. Saeedi, *pH effect on wettability of oil/brine/carbonate system: Implications for low salinity water flooding.* Journal of Petroleum Science and Engineering, 2018. **168**: p. 419-425.
61. Chen, Y.Q., Q. Xie, A. Sari, P.V. Brady, and A. Saeedi, *Oil/water/rock wettability: Influencing factors and implications for low salinity water flooding in carbonate reservoirs.* Fuel, 2018. **215**: p. 171-177.
62. Qiao, C., L. Li, R.T. Johns, and J. Xu, *A Mechanistic Model for Wettability Alteration by Chemically Tuned Water Flooding in Carbonate Reservoirs*, in *SPE Annual Technical Conference and Exhibition*. 2014, Society of Petroleum Engineers: Amsterdam, The Netherlands. p. 29.
63. Shehata, A.M., M.B. Alotaibi, and H.A. Nasr-El-Din, *Waterflooding in Carbonate Reservoirs: Does the Salinity Matter?* SPE Reservoir Evaluation & Engineering, 2014. **17**(03): p. 304-313.
64. AlQuraishi, A.A., S.N. AlHussinan, and H.Q. AlYami, *Efficiency and Recovery Mechanisms of Low Salinity Water Flooding in Sandstone and Carbonate Reservoirs*, in *Offshore Mediterranean Conference and Exhibition*. 2015, Offshore Mediterranean Conference: Ravenna, Italy. p. 14.
65. Mahani, H., A.L. Keya, S. Berg, W.-B. Bartels, R. Nasralla, and W. Rossen, *Driving Mechanism of Low Salinity Flooding in Carbonate Rocks*, in *EUROPEC 2015*. 2015, Society of Petroleum Engineers: Madrid, Spain. p. 27.
66. Buckley, J.S., C. Bousseau, and Y. Liu, *Wetting Alteration by Brine and Crude Oil: From Contact Angles to Cores.* SPE Journal, 1996. **1**(03): p. 341-350.

67. Hjelmeland, O.S. and L.E. Larrondo, *Experimental Investigation of the Effects of Temperature, Pressure, and Crude Oil Composition on Interfacial Properties.* SPE Reservoir Engineering, 2013. **1**(04): p. 321-328.
68. Yousef, A.A., S. Al-Saleh, and M.S. Al-Jawfi. *Improved/enhanced oil recovery from carbonate reservoirs by tuning injection water salinity and ionic content*. in *SPE Improved Oil Recovery Symposium*. 2012. Society of Petroleum Engineers.
69. Alotaibi, M.B., R. Azmy, and H.A. Nasr-El-Din, *Wettability Challenges in Carbonate Reservoirs*, in *SPE Improved Oil Recovery Symposium*. 2010, Society of Petroleum Engineers: Tulsa, Oklahoma, USA. p. 20.
70. Chilingar, G.V. and T.F. Yen, *Some Notes on Wettability and Relative Permeabilities of Carbonate Reservoir Rocks, II.* Energy Sources, 2007. **7**(1): p. 67-75.
71. Heidari, M.A., A. Habibi, S. Ayatollahi, M. Masihi, and S. Ashoorian, *Effect of Time and Temperature on Crude Oil Aging to do a Right Surfactant Flooding with a New Approach*, in *Offshore Technology Conference-Asia*. 2014, Offshore Technology Conference: Kuala Lumpur, Malaysia. p. 7.
72. Brady, P.V., J.L. Krumhansl, and P.E. Mariner, *Surface Complexation Modeling for Improved Oil Recovery*. 2012, Society of Petroleum Engineers.
73. Zhang, P. and T. Austad, *The Relative Effects of Acid Number and Temperature on Chalk Wettability*, in *SPE International Symposium on Oilfield Chemistry*. 2005, Society of Petroleum Engineers: The Woodlands, Texas. p. 7.
74. Strand, S., T. Puntervold, and T. Austad, *Effect of temperature on enhanced oil recovery from mixed-wet chalk cores by spontaneous imbibition and forced displacement using seawater.* Energy & Fuels, 2008. **22**(5): p. 3222-3225.
75. Standnes, D.C. and T. Austad, *Wettability alteration in chalk: 1. Preparation of core material and oil properties.* Journal of Petroleum Science and Engineering, 2000. **28**(3): p. 111-121.
76. Brady, P.V., N.R. Morrow, A. Fogden, V. Deniz, N. Loahardjo, and Winoto, *Electrostatics and the Low Salinity Effect in Sandstone Reservoirs.* Energy & Fuels, 2015. **29**(2): p. 666-677.
77. Zhang, P., M.T. Tweheyo, and T. Austad, *Wettability alteration and improved oil recovery by spontaneous imbibition of seawater into chalk: Impact of the potential determining ions Ca 2+, Mg 2+, and SO 4 2−.* Colloids and Surfaces A: Physicochemical and Engineering Aspects, 2007. **301**(1): p. 199-208.
78. Chen, Y., A. Sari, Q. Xie, P.V. Brady, M.M. Hossain, and A. Saeedi, *Electrostatic Origins of CO2-Increased Hydrophilicity in Carbonate Reservoirs.* Sci Rep, 2018. **8**(1): p. 17691.
79. Romanuka, J., J. Hofman, D.J. Ligthelm, B. Suijkerbuijk, F. Marcelis, S. Oedai, N. Brussee, H. van der Linde, H. Aksulu, and T. Austad, *Low Salinity EOR in Carbonates*. 2012, Society of Petroleum Engineers.
80. Zahid, A., A.A. Shapiro, and A. Skauge, *Experimental Studies of Low Salinity Water Flooding Carbonate: A New Promising Approach*, in *SPE EOR Conference at Oil and Gas West Asia*. 2012, Society of Petroleum Engineers: Muscat, Oman. p. 14.
81. Shalabi, E.W.A., K. Sepehrnoori, and M. Delshad, *Mechanisms behind low salinity water injection in carbonate reservoirs.* Fuel, 2014. **121**: p. 11-19.
82. Den Ouden, L., R. Nasralla, H. Guo, H. Bruining, and C. van Kruijsdijk. *Calcite dissolution behaviour during low salinity water flooding in carbonate rock*. in *IOR 2015-18th European Symposium on Improved Oil Recovery*. 2015.
83. Al-Shalabi, E.W. and K. Sepehrnoori, *A comprehensive review of low salinity/engineered water injections and their applications in sandstone and carbonate rocks.* Journal of Petroleum Science and Engineering, 2016. **139**: p. 137-161.

84. Nasralla, R.A., H.A. van der Linde, F.H.M. Marcelis, H. Mahani, S.K. Masalmeh, E. Sergienko, N.J. Brussee, S.G.J. Pieterse, and S. Basu, *Low Salinity Waterflooding for a Carbonate Reservoir Experimental Evaluation and Numerical Interpretation*, in *Abu Dhabi International Petroleum Exhibition & Conference*. 2016, Society of Petroleum Engineers: Abu Dhabi, UAE.
85. Kilybay, A., B. Ghosh, and N. Chacko Thomas, *A Review on the Progress of Ion-Engineered Water Flooding.* Journal of Petroleum Engineering, 2017. **2017**: p. 7171957.
86. Emadi, A. and M. Sohrabi. *Visual investigation of low salinity waterflooding*. in *International Symposium of the Society of Core Analysts, Aberdeen, Scotland, UK*. 2012.
87. Emadi, A. and M. Sohrabi, *Visual Investigation of Oil Recovery by LowSalinity Water Injection: Formation of Water Micro-Dispersions and WettabilityAlteration*, in *SPE Annual Technical Conference and Exhibition*. 2013, Society of Petroleum Engineers: New Orleans, Louisiana, USA. p. 15.
88. Austad, T., *Chapter 13 - Water-Based EOR in Carbonates and Sandstones: New Chemical Understanding of the EOR Potential Using "Smart Water" A2 - Sheng, James J*, in *Enhanced Oil Recovery Field Case Studies*. 2013, Gulf Professional Publishing: Boston. p. 301-335.
89. Schön, J.H., *Physical properties of rocks: Fundamentals and principles of petrophysics*. 2015: Elsevier.
90. Abdallah, W., J.S. Buckley, A. Carnegie, J. Edwards, B. Herold, E. Fordham, A. Graue, T. Habashy, N. Seleznev, and C. Signer, *Fundamentals of wettability.* Technology, 1986. **38**(1125-1144): p. 268.
91. Anderson, W.G., *Wettability Literature Survey- Part 1: Rock/Oil/Brine Interactions and the Effects of Core Handling on Wettability.* Journal of Petroleum Technology, 1986. **38**(10): p. 1125-1144.
92. Brown, R.J.S. and I. Fatt, *Measurements Of Fractional Wettability Of Oil Fields' Rocks By The Nuclear Magnetic Relaxation Method*, in *Fall Meeting of the Petroleum Branch of AIME*. 1956, Society of Petroleum Engineers: Los Angeles, California. p. 4.
93. Donaldson, E.C. and W. Alam, *Wettability*. 2013: Elsevier.
94. Masalmeh, S.K., *The effect of wettability heterogeneity on capillary pressure and relative permeability.* Journal of Petroleum Science and Engineering, 2003. **39**(3): p. 399-408.
95. Salathiel, R.A., *Oil Recovery by Surface Film Drainage in Mixed-Wettability Rocks.* Journal of Petroleum Technology, 1973. **25**(Oct): p. 1216-1224.
96. Israelachvili, J.N., *Intermolecular and surface forces*. 2011: Academic press.
97. Raina, G., *Atomic Force Microscopy as a Nanometrology Tool: Some Issues and Future Targets.* MAPAN, 2013. **28**(4): p. 311-319.
98. Anderson, W., *Wettability Literature Survey- Part 2: Wettability Measurement.* Journal of Petroleum Technology, 1986. **38**(11): p. 1246-1262.
99. Cassie, A. and S. Baxter, *Wettability of porous surfaces.* Transactions of the Faraday society, 1944. **40**: p. 546-551.
100. Dettre, R.H. and R.E. Johnson Jr, *Contact angle hysteresis. IV. Contact angle measurements on heterogeneous surfaces1.* The journal of physical chemistry, 1965. **69**(5): p. 1507-1515.
101. Israelachvili, J.N., *Adhesion and wetting phenomena.* Intermolecular and surface forces, 2011. **3**: p. 415-467.
102. Morrow, N.R., *The Effects of Surface Roughness On Contact: Angle With Special Reference to Petroleum Recovery.* Journal of Canadian Petroleum Technology, 2013. **14**(04): p. 13.

103. Wenzel, R.N., *Resistance of Solid Surfaces to Wetting by Water.* Industrial & Engineering Chemistry, 1936. **28**(8): p. 988-994.
104. Xie, X., N.R. Morrow, and J.S. Buckley, *Contact angle hysteresis and the stability of wetting changes induced by adsorption from crude oil.* Journal of Petroleum Science and Engineering, 2002. **33**(1): p. 147-159.
105. Andrew, M., B. Bijeljic, and M.J. Blunt, *Pore-scale contact angle measurements at reservoir conditions using X-ray microtomography.* Advances in Water Resources, 2014. **68**: p. 24-31.
106. AlRatrout, A., A.Q. Raeini, B. Bijeljic, and M.J. Blunt, *Automatic measurement of contact angle in pore-space images.* Advances in Water Resources, 2017. **109**: p. 158-169.
107. Scanziani, A., K. Singh, M.J. Blunt, and A. Guadagnini, *Automatic method for estimation of in situ effective contact angle from X-ray micro tomography images of two-phase flow in porous media.* Journal of Colloid and Interface Science, 2017. **496**: p. 51-59.
108. Alhammadi, A.M., A. AlRatrout, K. Singh, B. Bijeljic, and M.J. Blunt, *In situ characterization of mixed-wettability in a reservoir rock at subsurface conditions.* Scientific Reports, 2017. **7**(1): p. 10753.
109. Bultreys, T., Q. Lin, Y. Gao, A.Q. Raeini, A. AlRatrout, B. Bijeljic, and M.J. Blunt, *Validation of model predictions of pore-scale fluid distributions during two-phase flow.* Physical Review E, 2018. **97**(5): p. 053104.
110. Al-Raoush, R.I., *Impact of Wettability on Pore-Scale Characteristics of Residual Nonaqueous Phase Liquids.* Environmental Science & Technology, 2009. **43**(13): p. 4796-4801.
111. Iglauer, S., M.A. Fernø, P. Shearing, and M.J. Blunt, *Comparison of residual oil cluster size distribution, morphology and saturation in oil-wet and water-wet sandstone.* Journal of Colloid and Interface Science, 2012. **375**(1): p. 187-192.
112. Singh, K., B. Bijeljic, and M.J. Blunt, *Imaging of oil layers, curvature and contact angle in a mixed-wet and a water-wet carbonate rock.* Water Resources Research, 2016. **52**(3): p. 1716-1728.
113. Armstrong, R.T., M.L. Porter, and D. Wildenschild, *Linking pore-scale interfacial curvature to column-scale capillary pressure.* Advances in Water Resources, 2012. **46**: p. 55-62.
114. Berg, S., M. Rücker, H. Ott, A. Georgiadis, H. van der Linde, F. Enzmann, M. Kersten, R.T. Armstrong, S. de With, J. Becker, and A. Wiegmann, *Connected pathway relative permeability from pore-scale imaging of imbibition.* Advances in Water Resources, 2016. **90**: p. 24-35.
115. Donaldson, E.C., R.D. Thomas, and P.B. Lorenz, *Wettability Determination and Its Effect on Recovery Efficiency.* Society of Petroleum Engineers Journal, 1969. **9**(01): p. 13-20.
116. Amott, E., *Observations Relating to the Wettability of Porous Rock.* Transactions of the AIME, 1959. **216**(01): p. 156-162.
117. Mattax, C.C. and J.R. Kyte, *Imbibition Oil Recovery from Fractured, Water-Drive Reservoir.* Society of Petroleum Engineers Journal, 1962. **2**(02): p. 177-184.
118. Ma, S., N.R. Morrow, and X. Zhang, *Generalized Scaling Of Spontaneous Imbibition Data For Strongly Water-Wet Systems*, in *Technical Meeting / Petroleum Conference of The South Saskatchewan Section*. 1995, Petroleum Society of Canada: Regina. p. 19.
119. Schmid, K.S. and S. Geiger, *Universal scaling of spontaneous imbibition for arbitrary petrophysical properties: Water-wet and mixed-wet states and Handy's conjecture.* Journal of Petroleum Science and Engineering, 2013. **101**: p. 44-61.

120. Leverett, M.C., *Capillary Behavior in Porous Solids.* Transactions of the AIME, 1941. **142**(01): p. 152-169.
121. Zou, S. and R. Armstrong, *Multiphase Flow Under Heterogeneous Wettability Conditions Studied by Special Core Analysis and Pore-Scale Imaging.* SPE Journal, 2019. **24**(03): p. 1234-1247.
122. Blunt, M.J., *Multiphase flow in permeable media: A pore-scale perspective*. 2017: Cambridge University Press.
123. Evje, S. and A. Hiorth, *A mathematical model for dynamic wettability alteration controlled by water-rock chemistry.* Networks & Heterogeneous Media, 2010. **5**(2): p. 217.
124. Hamouda, A.A. and S. Gupta, *Enhancing oil recovery from chalk reservoirs by a low-salinity water flooding mechanism and fluid/rock interactions.* Energies, 2017. **10**(4): p. 576.
125. Bagci, S., M.V. Kok, and U. Turksoy, *Effect of brine composition on oil recovery by waterflooding.* Petroleum Science and Technology, 2001. **19**(3-4): p. 359-372.
126. Gandomkar, A. and M.R. Rahimpour, *Investigation of Low-Salinity Waterflooding in Secondary and Tertiary Enhanced Oil Recovery in Limestone Reservoirs.* Energy & Fuels, 2015. **29**(12): p. 7781-7792.
127. Pu, H., X. Xie, P. Yin, and N.R. Morrow, *Low-Salinity Waterflooding and Mineral Dissolution*. 2010, Society of Petroleum Engineers.
128. Austad, T., S.F. Shariatpanahi, S. Strand, H. Aksulu, and T. Puntervold, *Low salinity EOR effects in limestone reservoir cores containing anhydrite: a discussion of the chemical mechanism.* Energy & Fuels, 2015. **29**(11): p. 6903-6911.
129. Jiang, H., C.G. Chopping, C. Forsman, and X. Xie. *Lab observation of low salinity waterflooding for a phosphoria reservoir rock*. in *SPE Western North American and Rocky Mountain Joint Meeting*. 2014. Society of Petroleum Engineers.
130. Uetani, T., H. Kaido, and H. Yonebayashi, *Investigation of Anhydrite Dissolution as a Potential Low Salinity Waterflooding Mechanism Using Carbonate Reservoir Rocks*, in *International Petroleum Technology Conference*. 2019, International Petroleum Technology Conference: Beijing, China. p. 10.
131. RezaeiDoust, A., T. Puntervold, and T. Austad, *Chemical Verification of the EOR Mechanism by Using Low Saline/Smart Water in Sandstone.* Energy & Fuels, 2011. **25**(5): p. 2151-2162.
132. Curbelo, F.D.S., V.C. Santanna, E.L.B. Neto, T.V. Dutra, T.N.C. Dantas, A.A.D. Neto, and A.I.C. Garnica, *Adsorption of nonionic surfactants in sandstones.* Colloids and Surfaces A: Physicochemical and Engineering Aspects, 2007. **293**(1): p. 1-4.
133. Okasha, T.M. and A. Alshiwaish, *Effect of Brine Salinity on Interfacial Tension in Arab-D Carbonate Reservoir, Saudi Arabia*, in *SPE Middle East Oil and Gas Show and Conference*. 2009, Society of Petroleum Engineers: Manama, Bahrain. p. 9.
134. Mohsenzadeh, A., P. Pourafshary, and Y. Al-Wahaibi, *Oil Recovery Enhancement in Carbonate Reservoirs Via Low Saline Water Flooding in Presence of Low Concentration Active Ions; A Case Study*, in *SPE EOR Conference at Oil and Gas West Asia*. 2016, Society of Petroleum Engineers: Muscat, Oman. p. 14.
135. Al-Attar, H.H., M.Y. Mahmoud, A.Y. Zekri, R. Almehaideb, and M. Ghannam, *Low-salinity flooding in a selected carbonate reservoir: experimental approach.* Journal of Petroleum Exploration and Production Technology, 2013. **3**(2): p. 139-149.
136. Darvish Sarvestani, A., S. Ayatollahi, and M. Bahari Moghaddam, *Smart water flooding performance in carbonate reservoirs: an experimental approach for tertiary oil recovery.* Journal of Petroleum Exploration and Production Technology, 2019. **9**(4): p. 2643-2657.

137. Generosi, J., M. Ceccato, M.P. Andersson, T. Hassenkam, S. Dobberschütz, N. Bovet, and S.L.S. Stipp, *Calcite Wettability in the Presence of Dissolved Mg2+and SO42–.* Energy & Fuels, 2016. **31**(1): p. 1005-1014.
138. Bai, S., J. Kubelka, and M. Piri, *A positively charged calcite surface model for molecular dynamics studies of wettability alteration.* Journal of Colloid and Interface Science, 2020. **569**: p. 128-139.
139. Mahmoud, M.A., *Evaluating the Damage Caused by Calcium Sulfate Scale Precipitation During Low- and High-Salinity-Water Injection.* Journal of Canadian Petroleum Technology, 2014. **53**(03): p. 141-150.
140. BinMerdhah, A.B., A.A.M. Yassin, and M.A. Muherei, *Laboratory and prediction of barium sulfate scaling at high-barium formation water.* Journal of Petroleum Science and Engineering, 2010. **70**(1): p. 79-88.
141. Merdhah, A.B.B. and A.A.M. Yassin, *Scale formation in oil reservoir during water injection at high-salinity formation water.* Journal of applied sciences, 2007. **7**(21): p. 3198-3207.
142. Merdhah, A.B.B. and A.A.M. Yassin, *Barium sulfate scale formation in oil reservoir during water injection at high-barium formation water.* J. Appl. Sci, 2007. **7**(17): p. 2393-2403.
143. Khatib, Z.I. and J.R. Salanitro, *Reservoir Souring: Analysis of Surveys and Experience in Sour Waterfloods*, in *SPE Annual Technical Conference and Exhibition*. 1997, Society of Petroleum Engineers: San Antonio, Texas. p. 11.
144. Holmberg, K., D.O. Shah, and M.J. Schwuger, *Handbook of applied surface and colloid chemistry*. Vol. 1. 2002: John Wiley & Sons.
145. Alroudhan, A., J. Vinogradov, and M.D. Jackson, *Zeta potential of intact natural limestone: Impact of potential-determining ions Ca, Mg and SO4.* Colloids and Surfaces A: Physicochemical and Engineering Aspects, 2016. **493**: p. 83-98.
146. Mahani, H., R. Menezes, S. Berg, A. Fadili, R. Nasralla, D. Voskov, and V. Joekar-Niasar, *Insights into the Impact of Temperature on the Wettability Alteration by Low Salinity in Carbonate Rocks.* Energy & Fuels, 2017. **31**(8): p. 7839-7853.
147. Alotaibi, M.B. and H.A. Nasr-El-Din, *Electrokinetics of Limestone Particles and Crude-Oil Droplets in Saline Solutions.* SPE Reservoir Evaluation & Engineering, 2011. **14**(05): p. 604-611.
148. Hadia, N.J., T. Hansen, M.T. Tweheyo, and O. Torsaeter, *Influence of Crude Oil Components on Recovery by High and Low Salinity Waterflooding.* Energy & Fuels, 2012. **26**(7): p. 4328-4335.
149. Hopkins, P.A., I. Omland, F. Layti, S. Strand, T. Puntervold, and T. Austad, *Crude Oil Quantity and Its Effect on Chalk Surface Wetting.* Energy & Fuels, 2017. **31**(5): p. 4663-4669.
150. Wu, J.Z., F.H. Liu, H. Yang, S.J. Xu, Q. Xie, M.H. Zhang, T. Chen, G.X. Hu, and J.B. Wang, *Effect of specific functional groups on oil adhesion from mica substrate: Implications for low salinity effect.* Journal of Industrial and Engineering Chemistry, 2017. **56**: p. 342-349.
151. Puntervold, T. and T. Austad, *Injection of seawater and mixtures with produced water into North Sea chalk formation: Impact of fluid–rock interactions on wettability and scale formation.* Journal of Petroleum Science and Engineering, 2008. **63**(1): p. 23-33.
152. Quan, X., W. Jiazhong, Q. Jishun, L. Qingjie, M. Desheng, L. Li, and L. Manli. *Investigation of electrical surface charges and wettability alteration by ions matching waterflooding*. in *International Symposium of the Society of Core Analysts, Aberdeen, Scotland*. 2012.

153. Van Cappellen, P., L. Charlet, W. Stumm, and P. Wersin, *A surface complexation model of the carbonate mineral-aqueous solution interface.* Geochimica et Cosmochimica Acta, 1993. **57**(15): p. 3505-3518.
154. Song, J., Y. Zeng, L. Wang, X. Duan, M. Puerto, W.G. Chapman, S.L. Biswal, and G.J. Hirasaki, *Surface complexation modeling of calcite zeta potential measurements in brines with mixed potential determining ions (Ca(2+), CO3(2-), Mg(2+), SO4(2-)) for characterizing carbonate wettability.* J Colloid Interface Sci, 2017. **506**: p. 169-179.
155. Ahmadi, A. and M. Moosavi, *Investigation of the effects of low-salinity waterflooding for improved oil recovery in carbonate reservoir cores.* Energy Sources Part a-Recovery Utilization and Environmental Effects, 2018. **40**(9): p. 1035-1043.
156. Purswani, P. and Z.T. Karpyn, *Laboratory investigation of chemical mechanisms driving oil recovery from oil-wet carbonate rocks.* Fuel, 2019. **235**: p. 406-415.
157. Shirazi, M., J. Farzaneh, S. Kord, and Y. Tamsilian, *Smart water spontaneous imbibition into oil-wet carbonate reservoir cores: Symbiotic and individual behavior of potential determining ions.* Journal of Molecular Liquids, 2019: p. 112102.
158. Joonaki, E., J. Buckman, R. Burgass, and B. Tohidi, *Water versus Asphaltenes; Liquid–Liquid and Solid–Liquid Molecular Interactions Unravel the Mechanisms behind an Improved Oil Recovery Methodology.* Scientific Reports, 2019. **9**(1): p. 11369.
159. Abed, J., C. Aubry, M. Zaidani, N. El Hadri, R. Devarapalli, and M. Jouiad, *Determination of Dead-Oil Wetting and Adhesive Forces on Carbonate Rocks Using Colloidal-Probe Atomic Force Microscopy.* Energy & Fuels, 2018. **32**(9): p. 9182-9190.
160. Buckley, J.S., *Effective wettability of minerals exposed to crude oil.* Current Opinion in Colloid & Interface Science, 2001. **6**(3): p. 191-196.
161. Jackson, M.D., D. Al-Mahrouqi, and J. Vinogradov, *Zeta potential in oil-water-carbonate systems and its impact on oil recovery during controlled salinity water-flooding.* Sci Rep, 2016. **6**: p. 37363.
162. Dubey, S.T. and P.H. Doe, *Base Number and Wetting Properties of Crude Oils.* SPE Reservoir Engineering, 1993. **8**(03): p. 195-200.
163. Sanaei, A., S. Tavassoli, and K. Sepehrnoori, *Investigation of modified Water chemistry for improved oil recovery: Application of DLVO theory and surface complexation model.* Colloids and Surfaces A: Physicochemical and Engineering Aspects, 2019. **574**: p. 131-145.
164. Qiao, C.H., R. Johns, and L. Li, *Modeling Low-Salinity Waterflooding in Chalk and Limestone Reservoirs.* Energy & Fuels, 2016. **30**(2): p. 884-895.
165. Xie, Q., Y.Q. Chen, A. Sari, W.F. Pu, A. Saeedi, and W. Liao, *A pH-Resolved Wettability Alteration: Implications for CO2-Assisted EOR in Carbonate Reservoirs.* Energy & Fuels, 2017. **31**(12): p. 13593-13599.
166. Liu, F.H., H. Yang, J.Y. Wang, M.H. Zhang, T. Chen, G.X. Hu, W. Zhang, J.Z. Wu, S.J. Xu, X. Wu, and J.B. Wang, *Salinity-dependent adhesion of model molecules of crude oil at quartz surface with different wettability.* Fuel, 2018. **223**: p. 401-407.
167. Fernø, M.A., R. Grønsdal, J. Åsheim, A. Nyheim, M. Berge, and A. Graue, *Use of Sulfate for Water Based Enhanced Oil Recovery during Spontaneous Imbibition in Chalk.* Energy & Fuels, 2011. **25**(4): p. 1697-1706.
168. Alotaibi, M.B., R.A. Nasralla, and H.A. Nasr-El-Din, *Wettability Studies Using Low-Salinity Water in Sandstone Reservoirs.* SPE Reservoir Evaluation & Engineering, 2013. **14**(06): p. 713-725.
169. Tang, G. and N. Morrow, *Effect of temperature, salinity and oil composition on wetting behavior and oil recovery by waterflooding*. 1996, Society of Petroleum Engineers (SPE), Inc., Richardson, TX (United States).

170. Sincock, K.J. and C.J.J. Black, *Validation of Water/Oil Displacement Scaling Criteria Using Microvisualization Techniques*, in *SPE Annual Technical Conference and Exhibition*. 1988, Society of Petroleum Engineers: Houston, Texas.
171. Sutanto, E., H.T. Davis, and L.E. Scriven, *Liquid Distributions in Porous Rock Examined by Cryo Scanning Electron Microscopy*, in *SPE Annual Technical Conference and Exhibition*. 1990, Society of Petroleum Engineers: New Orleans, Louisiana.
172. Rueslatten, H., P.E. Oren, M. Robin, and E. Rosenberg, *A Combined Use of CRYO-SEM and NMR-Spectroscopy for Studying the Distribution of Oil and Brine in Sandstones*, in *SPE/DOE Improved Oil Recovery Symposium*. 1994, Society of Petroleum Engineers: Tulsa, Oklahoma.
173. Jerauld, G.R. and J.J. Rathmell, *Wettability and Relative Permeability of Prudhoe Bay: A Case Study in Mixed-Wet Reservoirs.* SPE Reservoir Engineering, 2013. **12**(01): p. 58-65.
174. Berg, S., A.W. Cense, E. Jansen, and K. Bakker, *Direct Experimental Evidence of Wettability Modification by Low Salinity.* Petrophysics, 2010. **51**(5): p. 314-322.
175. Seccombe, J., A. Lager, G. Jerauld, B. Jhaveri, T. Buikema, S. Bassler, J. Denis, K. Webb, A. Cockin, and E. Fueg, *Demonstration of Low-Salinity EOR at Interwell Scale, Endicott Field, Alaska*, in *SPE Improved Oil Recovery Symposium*. 2010, Society of Petroleum Engineers: Tulsa, Oklahoma, USA.
176. Fassi-Fihri, O., M. Robin, and E. Rosenberg, *Wettability Studies at the Pore Level: A New Approach by the Use of Cryo-Scanning Electron Microscopy.* SPE Formation Evaluation, 2013. **10**(01): p. 11-19.
177. Kareem, R., P. Cubillas, J. Gluyas, L. Bowen, S. Hillier, and H.C. Greenwell, *Multi-technique approach to the petrophysical characterization of Berea sandstone core plugs (Cleveland Quarries, USA).* Journal of Petroleum Science and Engineering, 2017. **149**: p. 436-455.
178. Aoyagi, K. and Chilinga.Gv, *Clay-Minerals in Carbonate Reservoir Rocks and Their Significance in Porosity Studies.* Sedimentary Geology, 1972. **8**(4): p. 241-249.
179. Strand, S., M.L. Hjuler, R. Torsvik, J.I. Pedersen, M.V. Madland, and T. Austad, *Wettability of chalk: impact of silica, clay content and mechanical properties.* Petroleum Geoscience, 2007. **13**(1): p. 69-80.
180. AlRatrout, A., M.J. Blunt, and B. Bijeljic, *Wettability in complex porous materials, the mixed-wet state, and its relationship to surface roughness.* Proc Natl Acad Sci U S A, 2018. **115**(36): p. 8901-8906.
181. Rücker, M., *Wettability and wettability alteration at the pore- and nano- scales (PhD thesis)*, in *Earth Science and Engineering*. 2018, Imperial College London: London,UK.
182. Council, W.E. *WORLD ENERGY SCENARIOS: COMPOSING ENERGY FUTURES TO 2050*. World Energy Scenarios_Composing energy futures to 2050_Full report 2013; Available from: https://www.worldenergy.org/assets/downloads/World-Energy-Scenarios_Composing-energy-futures-to-2050_Full-report1.pdf.
183. Gupta, R., G.G. Smith, L. Hu, T. Willingham, M. Lo Cascio, J.J. Shyeh, and C.R. Harris, *Enhanced Waterflood for Carbonate Reservoirs - Impact of Injection Water Composition*. 2011, Society of Petroleum Engineers.
184. Buckley, J.S. and Y. Liu, *Some mechanisms of crude oil/brine/solid interactions.* Journal of Petroleum Science and Engineering, 1998. **20**(3): p. 155-160.
185. Xie, Q., S. He, and W. Pu, *The effects of temperature and acid number of crude oil on the wettability of acid volcanic reservoir rock from the Hailar Oilfield.* Petroleum Science, 2010. **7**(1): p. 93-99.

186. Gaboriaud, F. and Y.F. Dufrene, *Atomic force microscopy of microbial cells: application to nanomechanical properties, surface forces and molecular recognition forces.* Colloids Surf B Biointerfaces, 2007. **54**(1): p. 10-9.
187. Barattin, R. and N. Voyer, *Chemical modifications of AFM tips for the study of molecular recognition events.* Chem Commun (Camb), 2008(13): p. 1513-32.
188. Arif, M., M. Lebedev, A. Barifcani, and S. Iglauer, *CO2 storage in carbonates: Wettability of calcite.* International Journal of Greenhouse Gas Control, 2017. **62**: p. 113-121.
189. Sari, A., N.S. Al Maskari, A. Saeedi, and Q. Xie, *Impact of surface roughness on wettability of oil-brine-calcite system at sub-pore scale.* Journal of Molecular Liquids, 2019: p. 112107.
190. Al Maskari, N.S., A. Sari, A. Saeedi, and Q. Xie, *Influence of Surface Roughness on the Contact Angle due to Calcite Dissolution in an Oil–Brine–Calcite System: A Nanoscale Analysis Using Atomic Force Microscopy and Geochemical Modeling.* Energy & Fuels, 2019. **33**(5): p. 4219-4224.
191. Wang, W. and A. Gupta, *Investigation of the Effect of Temperature and Pressure on Wettability Using Modified Pendant Drop Method*, in *SPE Annual Technical Conference and Exhibition*. 1995, Society of Petroleum Engineers: Dallas, Texas. p. 10.
192. Alnili, F., A. Al-Yaseri, H. Roshan, T. Rahman, M. Verall, M. Lebedev, M. Sarmadivaleh, S. Iglauer, and A. Barifcani, *Carbon dioxide/brine wettability of porous sandstone versus solid quartz: An experimental and theoretical investigation.* J Colloid Interface Sci, 2018. **524**: p. 188-194.
193. Hassenkam, T., L.L. Skovbjerg, and S.L.S. Stipp, *Probing the intrinsically oil-wet surfaces of pores in North Sea chalk at subpore resolution.* Proceedings of the National Academy of Sciences of the United States of America, 2009. **106**(15): p. 6071-6076.
194. Derkani, M.H., A.J. Fletcher, W. Abdallah, B. Sauerer, J. Anderson, and Z.Y.J. Zhang, *Low Salinity Waterflooding in Carbonate Reservoirs: Review of Interfacial Mechanisms.* Colloids and Interfaces, 2018. **2**(2): p. 20.
195. Hassenkam, T., M.P. Andersson, E. Hilner, J. Matthiesen, S. Dobberschütz, K.N. Dalby, N. Bovet, S.L.S. Stipp, P. Salino, C. Reddick, and I.R. Collins, *Could Atomic-Force Microscopy Force Mapping Be a Fast Alternative to Core-Plug Tests for Optimizing Injection-Water Salinity for Enhanced Oil Recovery in Sandstone?* SPE Journal, 2016. **21**(03): p. 0720-0729.
196. Shi, L., M.H.M. Olsson, T. Hassenkam, and S.L.S. Stipp, *A pH-Resolved View of the Low Salinity Effect in Sandstone Reservoirs.* Energy & Fuels, 2016. **30**(7): p. 5346-5354.
197. Al Maskari, N.S., Q. Xie, and A. Saeedi, *Role of Basal-Charged Clays in Low Salinity Effect in Sandstone Reservoirs: Adhesion Force on Muscovite using Atomic Force Microscope.* Energy & Fuels, 2019. **33**(2): p. 756-764.
198. Yu, H.A., T. Becker, N. Nic Daeid, and S.W. Lewis, *Fundamental studies of the adhesion of explosives to textile and non-textile surfaces.* Forensic Sci Int, 2017. **273**: p. 88-95.
199. Ron, H., S. Matlis, and I. Rubinstein, *Self-assembled monolayers on oxidized metals. 2. Gold surface oxidative pretreatment, monolayer properties, and depression formation.* Langmuir, 1998. **14**(5): p. 1116-1121.
200. Fujihira, M., Y. Tani, M. Furugori, U. Akiba, and Y. Okabe, *Chemical force microscopy of self-assembled monolayers on sputtered gold films patterned by phase separation.* Ultramicroscopy, 2001. **86**(1-2): p. 63-73.

201. Xie, Q., F. Liu, Y. Chen, H. Yang, A. Saeedi, and M.M. Hossain, *Effect of electrical double layer and ion exchange on low salinity EOR in a pH controlled system.* Journal of Petroleum Science and Engineering, 2019. **174**: p. 418-424.
202. Tian, H., F. Liu, X. Jin, and M. Wang, *Competitive effects of interfacial interactions on ion-tuned wettability by atomic simulations.* J Colloid Interface Sci, 2019. **540**: p. 495-500.
203. Yang, G., T. Chen, J. Zhao, D. Yu, F. Liu, D. Wang, M. Fan, W. Chen, J. Zhang, H. Yang, and J. Wang, *Desorption Mechanism of Asphaltenes in the Presence of Electrolyte and the Extended Derjaguin–Landau–Verwey–Overbeek Theory.* Energy & Fuels, 2015. **29**(7): p. 4272-4280.
204. Israelachvili, J.N., *14 - Electrostatic Forces between Surfaces in Liquids*, in *Intermolecular and Surface Forces (Third Edition)*, J.N. Israelachvili, Editor. 2011, Academic Press: Boston. p. 291-340.
205. Israelachvili, J.N., *15 - Solvation, Structural, and Hydration Forces*, in *Intermolecular and Surface Forces (Third Edition)*, J.N. Israelachvili, Editor. 2011, Academic Press: San Diego. p. 341-380.
206. Israelachvili, J.N., *Chapter 13 - Van der Waals Forces between Particles and Surfaces*, in *Intermolecular and Surface Forces (Third Edition)*, J.N. Israelachvili, Editor. 2011, Academic Press: Boston. p. 253-289.
207. Juhl, K.M., C.S. Pedersen, N. Bovet, K.N. Dalby, T. Hassenkam, M.P. Andersson, D. Okhrimenko, and S.L. Stipp, *Adhesion of alkane as a functional group on muscovite and quartz: dependence on pH and contact time.* Langmuir, 2014. **30**(48): p. 14476-85.
208. Churaev, N.V. and B.V. Derjaguin, *Inclusion of Structural Forces in the Theory of Stability of Colloids and Films.* Journal of Colloid and Interface Science, 1985. **103**(2): p. 542-553.
209. Dehghan Monfared, A., M.H. Ghazanfari, M. Kazemeini, M. Jamialahmadi, and A. Helalizadeh, *Wettability Alteration Modeling for Oil-Wet Calcite/Silica Nanoparticle System Using Surface Forces Analysis: Contribution of DLVO versus Non-DLVO Interactions.* Industrial & Engineering Chemistry Research, 2018. **57**(43): p. 14482-14492.
210. Kilpatrick, J.I., S.-H. Loh, and S.P. Jarvis, *Directly Probing the Effects of Ions on Hydration Forces at Interfaces.* Journal of the American Chemical Society, 2013. **135**(7): p. 2628-2634.
211. Tabor, R.F., F. Grieser, R.R. Dagastine, and D.Y. Chan, *The hydrophobic force: measurements and methods.* Physical Chemistry Chemical Physics, 2014. **16**(34): p. 18065-18075.
212. Rezaei Gomari, K.A. and A.A. Hamouda, *Effect of fatty acids, water composition and pH on the wettability alteration of calcite surface.* Journal of Petroleum Science and Engineering, 2006. **50**(2): p. 140-150.
213. Siffert, D. and P. Fimbel, *Parameters affecting the sign and magnitude of the eletrokinetic potential of calcite.* Colloids and Surfaces, 1984. **11**(3-4): p. 377-389.
214. Thompson, D.W. and P.G. Pownall, *Surface Electrical-Properties of Calcite.* Journal of Colloid and Interface Science, 1989. **131**(1): p. 74-82.
215. Vdović, N., *Electrokinetic behaviour of calcite—the relationship with other calcite properties.* Chemical Geology, 2001. **177**(3-4): p. 241-248.
216. Heberling, F., T.P. Trainor, J. Lutzenkirchen, P. Eng, M.A. Denecke, and D. Bosbach, *Structure and reactivity of the calcite-water interface.* J Colloid Interface Sci, 2011. **354**(2): p. 843-57.
217. Stachurski, J. and M. MichaLek, *The Effect of the zeta Potential on the Stability of a Non-Polar Oil-in-Water Emulsion.* J Colloid Interface Sci, 1996. **184**(2): p. 433-6.

218. Marinova, K.G., R.G. Alargova, N.D. Denkov, O.D. Velev, D.N. Petsev, I.B. Ivanov, and R.P. Borwankar, *Charging of Oil–Water Interfaces Due to Spontaneous Adsorption of Hydroxyl Ions.* Langmuir, 1996. **12**(8): p. 2045-2051.
219. Beattie, J.K. and A.M. Djerdjev, *The pristine oil/water interface: surfactant-free hydroxide-charged emulsions.* Angew Chem Int Ed Engl, 2004. **43**(27): p. 3568-71.
220. Mohammadi, M. and H. Mahani, *Direct insights into the pore-scale mechanism of low-salinity waterflooding in carbonates using a novel calcite microfluidic chip.* Fuel, 2020. **260**: p. 116374.
221. Adegbite, J.O., E.W. Al-Shalabi, and B. Ghosh, *Geochemical modeling of engineered water injection effect on oil recovery from carbonate cores.* Journal of Petroleum Science and Engineering, 2018. **170**: p. 696-711.
222. Zaeri, M.R., H. Shahverdi, R. Hashemi, and M. Mohammadi, *Impact of water saturation and cation concentrations on wettability alteration and oil recovery of carbonate rocks using low-salinity water.* Journal of Petroleum Exploration and Production Technology, 2019. **9**(2): p. 1185-1196.
223. Xie, Y., M. Khishvand, and M. Piri, *Wettability of Calcite Surfaces: Impacts of Brine Ionic Composition and Oil Phase Polarity at Elevated Temperature and Pressure Conditions.* Langmuir, 2020. **36**(22): p. 6079-6088.
224. Maskari, N.S.A., A. Sari, M.M. Hossain, A. Saeedi, and Q. Xie, *Response of Non-Polar Oil Component on Low Salinity Effect in Carbonate Reservoirs: Adhesion Force Measurement Using Atomic Force Microscopy.* Energies, 2019. **13**(1): p. 77.
225. Almehaideb, R.A., M.T. Ghannam, and A.Y. Zekri, *Experimental investigation of contact angles under oil-microbial solution on carbonate rocks.* Petroleum Science and Technology, 2004. **22**(3-4): p. 423-438.
226. Liu, Z.L., T. Rios-Carvajal, M.P. Andersson, M. Ceccato, S.L.S. Stipp, and T. Hassenkam, *Insights into the Pore-Scale Mechanism for the Low-Salinity Effect: Implications for Enhanced Oil Recovery.* Energy & Fuels, 2018. **32**(12): p. 12081-12090.
227. Schembre, J.M., G.Q. Tang, and A.R. Kovscek, *Wettability alteration and oil recovery by water imbibition at elevated temperatures.* Journal of Petroleum Science and Engineering, 2006. **52**(1-4): p. 131-148.
228. Xie, Q., P.V. Brady, E. Pooryousefy, D. Zhou, Y. Liu, and A. Saeedi, *The low salinity effect at high temperatures.* Fuel, 2017. **200**: p. 419-426.
229. Chen, Y., A. Sari, Q. Xie, P.V. Brady, M.M. Hossain, and A. Saeedi, *Electrostatic Origins of CO2-Increased Hydrophilicity in Carbonate Reservoirs.* Scientific Reports, 2018. **8**(1): p. 17691.
230. Xie, Y., M. Khishvand, and M. Piri, *Impact of Connate Brine Chemistry on In Situ Wettability and Oil Recovery: Pore-Scale Experimental Investigation.* Energy & Fuels, 2020. **34**(4): p. 4031-4045.
231. Pierre Gadonneix, A.S., Liu,Tie'nan, *2013 World Energy Issues Monitor*, in *Pierre Gadonneix*. 2013, World Energy Council: London W1B 5LT, United Kingdom.
232. Ding, H.N. and S. Rahman, *Experimental and theoretical study of wettability alteration during low salinity water flooding-an state of the art review.* Colloids and Surfaces a-Physicochemical and Engineering Aspects, 2017. **520**: p. 622-639.
233. Lashkarbolooki, M., S. Ayatollahi, and M. Riazi, *Mechanistical study of effect of ions in smart water injection into carbonate oil reservoir.* Process Safety and Environmental Protection, 2017. **105**: p. 361-372.
234. Xie, Q., Y.Z. Liu, J.Z. Wu, and Q.J. Liu, *Ions tuning water flooding experiments and interpretation by thermodynamics of wettability.* Journal of Petroleum Science and Engineering, 2014. **124**: p. 350-358.

235. Bartels, W.B., H. Mahani, S. Berg, and S.M. Hassanizadeh, *Literature review of low salinity waterflooding from a length and time scale perspective.* Fuel, 2019. **236**: p. 338-353.
236. Liu, Z.S., A. Herring, C. Arns, S. Berg, and R.T. Armstrong, *Pore-Scale Characterization of Two-Phase Flow Using Integral Geometry.* Transport in Porous Media, 2017. **118**(1): p. 99-117.
237. Bartels, W.-B., H. Mahani, S. Berg, R. Menezes, J.A. van der Hoeven, and A. Fadili, *Oil Configuration Under High-Salinity and Low-Salinity Conditions at Pore Scale: A Parametric Investigation by Use of a Single-Channel Micromodel.* SPE Journal, 2017. **22**(05): p. 1362-1373.
238. Pooryousefy, E., Q. Xie, Y.Q. Chen, A. Sari, and A. Saeedi, *Drivers of low salinity effect in sandstone reservoirs.* Journal of Molecular Liquids, 2018. **250**: p. 396-403.
239. Xie, Q., A. Saeedi, E. Pooryousefy, and Y.B. Liu, *Extended DLVO-based estimates of surface force in low salinity water flooding.* Journal of Molecular Liquids, 2016. **221**: p. 658-665.
240. Austad, T., A. Rezaeidoust, and T. Puntervold, *Chemical Mechanism of Low Salinity Water Flooding in Sandstone Reservoirs*. 2010, Society of Petroleum Engineers.
241. Brady, P.V. and J.L. Krumhansl, *A surface complexation model of oil–brine–sandstone interfaces at 100°C: Low salinity waterflooding.* Journal of Petroleum Science and Engineering, 2012. **81**: p. 171-176.
242. Cissokho, M., S. Boussour, P. Cordier, H. Bertin, and G. Hamon, *Low Salinity Oil Recovery on Clayey Sandstone: Experimental Study.* Petrophysics, 2010. **51**(5): p. 305-313.
243. Al-Saedi, H.N., P.V. Brady, R. Flori, and P. Heidari, *Novel Insights into Low Salinity Water Flooding Enhanced Oil Recovery in Sandstone: The Clay Role Study*, in *SPE Improved Oil Recovery Conference*. 2018, Society of Petroleum Engineers: Tulsa, Oklahoma, USA. p. 18.
244. Chen, Y.Q., Q. Xie, W.F. Pu, and A. Saeedi, *Drivers of pH increase and implications for low salinity effect in sandstone.* Fuel, 2018. **218**: p. 112-117.
245. Nasralla, R.A. and H.A. Nasr-El-Din, *Impact of Electrical Surface Charges and Cation Exchange on Oil Recovery by Low Salinity Water*. 2011, Society of Petroleum Engineers.
246. Chen, Y.Q., Q. Xie, and A. Saeedi, *Role of ion exchange, surface complexation, and albite dissolution in low salinity water flooding in sandstone.* Journal of Petroleum Science and Engineering, 2019. **176**: p. 126-131.
247. Bailey, G.W., J.L. White, and T. Rothberg, *Adsorption of Organic Herbicides by Montmorillonite: Role of pH and Chemical Character of Adsorbate1.* Soil Science Society of America Journal, 1968. **32**(2): p. 222.
248. Farooq, U., S. Simon, M. Tweheyo, G. Øye, and J. Sjöblom, *Interfacial Tension Measurements Between Oil Fractions of a Crude Oil and Aqueous Solutions with Different Ionic Composition and pH*. Vol. 34. 2013.
249. Kelesoglu, S., P. Meakin, and J. Sjoblom, *Effect of Aqueous Phase pH on the Dynamic Interfacial Tension of Acidic Crude Oils and Myristic Acid in Dodecane.* Journal of Dispersion Science and Technology, 2011. **32**(11): p. 1682-1691.
250. Zhang, Y., X. Xie, and N.R. Morrow, *Waterflood Performance By Injection Of Brine With Different Salinity For Reservoir Cores*. 2007, Society of Petroleum Engineers.
251. Meier, L.P., R.A. Shelden, W.R. Caseri, and U.W. Suter, *Polymerization of Styrene with Initiator Ionically Bound to High-Surface-Area Mica - Grafting Via an Unexpected Mechanism.* Macromolecules, 1994. **27**(6): p. 1637-1642.
252. Xiao, Y., *Reactive Transport Modeling: Applications in Subsurface Energy and Environmental Problems*. 2018: Wiley.

253. Hansen, G., A.A. Hamouda, and R. Denoyel, *The effect of pressure on contact angles and wettability in the mica/water/n-decane system and the calcite plus stearic acid/water/n-decane system.* Colloids and Surfaces a-Physicochemical and Engineering Aspects, 2000. **172**(1-3): p. 7-16.
254. Zhao, H., S. Bhattacharjee, R. Chow, D. Wallace, J.H. Masliyah, and Z. Xu, *Probing surface charge potentials of clay basal planes and edges by direct force measurements.* Langmuir, 2008. **24**(22): p. 12899-910.
255. Newman, A.C.D., *Cation Exchange Properties of Micas.* Journal of Soil Science, 1969. **20**(2): p. 357-372.
256. Nishimura, S., H. Tateyama, K. Tsunematsu, and K. Jinnai, *Zeta-Potential Measurement of Muscovite Mica Basal-Plane Aqueous-Solution Interface by Means of Plane Interface Technique.* Journal of Colloid and Interface Science, 1992. **152**(2): p. 359-367.
257. Nosrati, A., J. Addai-Mensah, and W. Skinner, *Muscovite clay mineral particle interactions in aqueous media.* Powder Technology, 2012. **219**: p. 228-238.
258. Scales, P.J., F. Grieser, and T.W. Healy, *Electrokinetics of the Muscovite Mica Aqueous-Solution Interface.* Langmuir, 1990. **6**(3): p. 582-589.
259. Scales, P.J., T.W. Healy, and D.F. Evans, *The Zeta-Potential of Muscovite Mica - Counterion Complexation by a Macrocyclic Ligand.* Journal of Colloid and Interface Science, 1988. **124**(2): p. 391-395.
260. Chorom, M. and P. Rengasamy, *Dispersion and zeta potential of pure clays as related to net particle charge under varying pH, electrolyte concentration and cation type.* European Journal of Soil Science, 1995. **46**(4): p. 657-665.
261. Hassenkam, T., M. Andersson, E. Hilner, J. Matthiesen, S. Dobberschutz, K.N. Dalby, N. Bovet, S.L.S. Stipp, P. Salino, C. Reddick, and I.R. Collins, *A Fast Alternative to Core Plug Tests for Optimising Injection Water Salinity for EOR*. 2014, Society of Petroleum Engineers.
262. Hassenkam, T., A.C. Mitchell, C.S. Pedersen, L.L. Skovbjerg, N. Bovet, and S.L.S. Stipp, *The low salinity effect observed on sandstone model surfaces.* Colloids and Surfaces a-Physicochemical and Engineering Aspects, 2012. **403**: p. 79-86.
263. Sorop, T.G., S.K. Masalmeh, B.M.J.M. Suijkerbuijk, H.A. van der Linde, H. Mahani, N.J. Brussee, F.A.H.M. Marcelis, and A. Coorn, *Relative Permeability Measurements to Quantify the Low Salinity Flooding Effect at Field Scale*, in *Abu Dhabi International Petroleum Exhibition and Conference*. 2015, Society of Petroleum Engineers: Abu Dhabi, UAE. p. 15.
264. Liu, Y., T. Jiang, D. Zhou, J. Zhao, Q. Xie, and A. Saeedi, *Evaluation of the Potential of Low Salinity Water Flooding in the High Temperature and High Salinity Dong-He-Tang Reservoir in the Tarim Oilfeild, China: Experimental and Reservoir Simulation Results*, in *SPE Asia Pacific Oil & Gas Conference and Exhibition*. 2016, Society of Petroleum Engineers: Perth, Australia. p. 15.
265. Fjelde, I., S.M. Asen, and A.V. Omekeh, *Low Salinity Water Flooding Experiments and Interpretation by Simulations*, in *SPE Improved Oil Recovery Symposium*. 2012, Society of Petroleum Engineers: Tulsa, Oklahoma, USA. p. 12.
266. Xie, Q., D. Ma, J. Wu, Q. Liu, N. Jia, and M. Luo. *Potential Evaluation of Ion Tuning Waterflooding for a Tight Oil Reservoir in Jiyuan OilField: Experiments and Reservoir Simulation Results*. in *SPE Asia Pacific Enhanced Oil Recovery Conference*. 2015. Society of Petroleum Engineers.
267. Nasralla, R.A. and H.A. Nasr-El-Din, *Impact of cation type and concentration in injected brine on oil recovery in sandstone reservoirs.* Journal of Petroleum Science and Engineering, 2014. **122**: p. 384-395.
268. Xie, Q., P.V. Brady, E. Pooryousefy, D.Y. Zhou, Y.B. Liu, and A. Saeedi, *The low salinity effect at high temperatures.* Fuel, 2017. **200**: p. 419-426.

269. Røyne, A., K.N. Dalby, and T. Hassenkam, *Repulsive hydration forces between calcite surfaces and their effect on the brittle strength of calcite-bearing rocks.* Geophysical Research Letters, 2015. **42**(12): p. 4786-4794.
270. Nasralla, R.A., J.R. Snippe, and R. Farajzadeh, *Coupled Geochemical-Reservoir Model to Understand the Interaction Between Low Salinity Brines and Carbonate Rock*, in *SPE Asia Pacific Enhanced Oil Recovery Conference*. 2015, Society of Petroleum Engineers: Kuala Lumpur, Malaysia. p. 21.
271. Chen, Y.Q., A. Sari, Q. Xie, and A. Saeedi, *Insights into the wettability alteration of CO2-assisted EOR in carbonate reservoirs.* Journal of Molecular Liquids, 2019. **279**: p. 420-426.
272. Cassie, A., *Contact angles.* Discussions of the Faraday society, 1948. **3**: p. 11-16.
273. Raposo, M., Q. Ferreira, and P. Ribeiro, *A guide for atomic force microscopy analysis of soft-condensed matter.* Modern research and educational topics in microscopy, 2007. **1**: p. 758-769.
274. Appelo, C.A.J. and D. Postma, *Geochemistry, groundwater and pollution*. 2004: CRC press.
275. Lu, Y., N.F. Najafabadi, and A. Firoozabadi, *Effect of Low-Concentration of 1-Pentanol on the Wettability of Petroleum Fluid-Brine-Rock Systems.* Langmuir, 2019. **35**(12): p. 4263-4269.
276. Lipton, P.M. *Purdue CHM 26505: Organic Chemistry for Chemistry Majors (1st Semester)*. 2014; Available from: https://chem.libretexts.org/Courses/Purdue/Purdue%3A_Chem_26505%3A_Organic_Chemistry_I_(Lipton)/Chapter_4._Intermolecular_Forces_and_Physical_Properties/4.4_Solubility.
277. Hadia, N.J., A. Ashraf, M.T. Tweheyo, and O. Torsaeter, *Laboratory investigation on effects of initial wettabilities on performance of low salinity waterflooding.* Journal of Petroleum Science and Engineering, 2013. **105**: p. 18-25.
278. Long, F.A. and W.F. McDevit, *Activity Coefficients of Nonelectrolyte Solutes in Aqueous Salt Solutions.* Chemical Reviews, 1952. **51**(1): p. 119-169.
279. Malinowski, J.J. and A.J. Daugulis, *Salt Effects in Extraction of Ethanol, 1-Butanol and Acetone from Aqueous-Solutions.* Aiche Journal, 1994. **40**(9): p. 1459-1465.
280. Steiner, E.C. and J.M. Gilbert, *The acidities of weak acids in dimethyl sulfoxide.* Journal of the American Chemical Society, 1963. **85**(19): p. 3054-3055.
281. Bissada, K.K., W. Johns, and F. Cheng, *Cation-dipole interactions in clay organic complexes.* Clay Minerals, 1967. **7**(2): p. 155-166.
282. Weng, L. and G.D. Elliott, *Polymerization effect of electrolytes on hydrogen-bonding cryoprotectants: ion-dipole interactions between metal ions and glycerol.* J Phys Chem B, 2014. **118**(49): p. 14546-54.
283. Gadonneix, P., A. Sambo, Z. Guobao, Y.D. Kim, J. Teyssen, J.A.V. Lleras, A.A. Naqi, K. Meyers, H.C. Shin, and M.-J. Nadeau, *World Energy Issues Monitor.* World Energy Council, 2012.
284. Zhu, G.Y., A.V. Milkov, Z.Y. Zhang, C.H. Sun, X.X. Zhou, F.R. Chen, J.F. Han, and Y.F. Zhu, *Formation and preservation of a giant petroleum accumulation in superdeep carbonate reservoirs in the southern Halahatang oil field area, Tarim Basin, China.* Aapg Bulletin, 2019. **103**(7): p. 1703-1743.
285. Pal, S., M. Mushtaq, F. Banat, and A.M. Al Sumaiti, *Review of surfactant-assisted chemical enhanced oil recovery for carbonate reservoirs: challenges and future perspectives.* Petroleum Science, 2018. **15**(1): p. 77-102.
286. Alfazazi, U., W. AlAmeri, and M.R. Hashmet, *Experimental investigation of polymer flooding with low-salinity preconditioning of high temperature–high-salinity carbonate reservoir.* Journal of Petroleum Exploration and Production Technology, 2018. **9**(2): p. 1517-1530.

287. El-hoshoudy, A.N., *Quaternary ammonium based surfmer-co-acrylamide polymers for altering carbonate rock wettability during water flooding.* Journal of Molecular Liquids, 2018. **250**: p. 35-43.
288. Bortolotti, V., G. Gottardi, P. Macini, and F. Srisuriyachai, *Intermittent Alkali Flooding in Vertical Carbonate Reservoirs*, in *EUROPEC/EAGE Conference and Exhibition*. 2009, Society of Petroleum Engineers: Amsterdam, The Netherlands. p. 11.
289. Zulkifli, N.N., S.M. Mahmood, S. Akbari, A.A.A. Manap, N.I. Kechut, and K.A. Elrais, *Evaluation of new surfactants for enhanced oil recovery applications in high-temperature reservoirs.* Journal of Petroleum Exploration and Production Technology, 2020. **10**(2): p. 283-296.
290. Hosseini, E., F. Hajivand, and R. Tahmasebi, *The effect of alkaline–surfactant on the wettability, relative permeability and oil recovery of carbonate reservoir rock: experimental investigation.* Journal of Petroleum Exploration and Production Technology, 2019. **9**(4): p. 2877-2891.
291. Ghosh, P. and K.K. Mohanty, *Study of Surfactant–Polymer Flooding in High-Temperature and High-Salinity Carbonate Rocks.* Energy & Fuels, 2019. **33**(5): p. 4130-4145.
292. Al Maskari, N.S., A. Saeedi, and Q. Xie, *Alcohol-Assisted Waterflooding in Carbonate Reservoirs.* Energy & Fuels, 2019. **33**(11): p. 10651-10658.
293. Chen, Y.Q., Q. Xie, and A. Saeedi, *Electrostatic characterization of -NH+-brine-kaolinite system: Implications for low salinity waterflooding in sandstone reservoirs.* Journal of Petroleum Science and Engineering, 2019. **179**: p. 539-545.
294. Lu, Y.D., N.F. Najafabadi, and A. Firoozabadi, *Effect of Temperature on Wettability of Oil/Brine/Rock Systems.* Energy & Fuels, 2017. **31**(5): p. 4989-4995.
295. Mccaffery, F.G., *Measurement of Interfacial Tensions and Contact Angles at High-Temperature and Pressure.* Journal of Canadian Petroleum Technology, 1972. **11**(3): p. 26-+.
296. Saner, S., H.K. Asar, H. Okaygun, and H.J. Abdul, *Wettability Study of Saudi-Arabian Carbonate Reservoir Core Samples.* Arabian Journal for Science and Engineering, 1991. **16**(3): p. 357-371.
297. Yalkowsky, S.H., Y. He, and P. Jain, *Handbook of aqueous solubility data*. 2016: CRC press.
298. Feng, Z., J.Q. Li, X. Sun, L. Sun, and J. Chen, *Liquid–liquid equilibria of aqueous systems containing alcohol and ammonium sulfate.* Fluid Phase Equilibria, 2012. **317**: p. 1-8.
299. Katayama, H. and M. Miyahara, *Liquid−Liquid Phase Equilibria of (Ethanol or Methanol + Water) Containing either Dipotassium Hydrogen Phosphate or Sodium Dihydrogen Phosphate.* Journal of Chemical & Engineering Data, 2006. **51**(3): p. 914-918.
300. Alotaibi, M.B., R. Azmy, and H.A. Nasr-El-Din, *A Comprehensive EOR Study Using Low Salinity Water in Sandstone Reservoirs*, in *SPE Improved Oil Recovery Symposium*. 2010, Society of Petroleum Engineers: Tulsa, Oklahoma, USA. p. 20.

Appendix 1

In this section, attribution tables for all publications are presented here to illustrate contribution from all co-authors.

Paper title: "**Response of Non-Polar Oil Component on Low Salinity Effect in Carbonate Reservoirs: Adhesion Force Measurement Using Atomic Force Microscopy**" *Energies* **2019,** 13, (1), 77.

Nasser S. Al Maskari [1,2,*], Ahmad Sari [1], Md Mofazzal Hossain [1], Ali Saeedi [1] and Quan Xie [1,*]

[1] Discipline of Petroleum Engineering, WA School of Mines: Minerals, Energy and Chemical Engineering, Curtin University, 26 Dick Perry Avenue, Kensington, WA 6151, Australia

[2] Petroleum Development Oman LLC, P.O. Box 81, Code 100, Muscat, Sultanate of Oman

Name	Conception & design	Acquisition of data & method	Data conditioning & manipulation	Analysis & statistical method	Interpretation & discussion	Final approval
Nasser AL Maskari (First author)	X	X	X	X	X	X
I acknowledge that these represent my contribution to the above research output. Signature:						
Ahmad Sari (Co-author 1)		X			X	X
I acknowledge that these represent my contribution to the above research output. Signature:						
Mofazzal Hossain (Co-author 2)						X
I acknowledge that these represent my contribution to the above research output. Signature:						
Ali Saeedi (Co-author 3)					X	X
I acknowledge that these represent my contribution to the above research output. Signature:						
Quan Xie (Co-author 4)	X	X			X	X
I acknowledge that these represent my contribution to the above research output. Signature:						

Paper title: "**Influence of pH on Acidic Oil-Brine-Carbonate Adhesion: Adhesion Force Measurement Using Atomic Force Microscopy**" *Energy & Fuels,* **(Under review).**

Nasser S. Al Maskari *†‡, Mohamed Almobarak †, Ali Saeedi †, Quan Xie *†

† Discipline of Petroleum Engineering, WA School of Mines: Minerals, Energy and Chemical Engineering, Curtin University, 26 Dick Perry Avenue, Kensington, WA 6151, Australia

‡ Petroleum Development Oman LLC, P.O. Box 81, Code 100, Muscat, Sultanate of Oman

Name	Conception & design	Acquisition of data & method	Data conditioning & manipulation	Analysis & statistical method	Interpretation & discussion	Final approval
Nasser AL Maskari (First author)	X	X	X	X	X	
I acknowledge that these represent my contribution to the above research output. Signature:						
Mohamed Almobarak (Co-author 1)		X				
I acknowledge that these represent my contribution to the above research output. Signature:						
Ali Saeedi (Co-author 2)					X	X
I acknowledge that these represent my contribution to the above research output. Signature:						
Quan Xie (Co-author 3)	X	X			X	X
I acknowledge that these represent my contribution to the above research output. Signature:						

Paper title: "**Role of Basal-Charged Clays in Low Salinity Effect in Sandstone Reservoirs: Adhesion Force on Muscovite using Atomic Force Microscope**" *Energy & Fuels,* 2019, 33, (2), 756-764.

Nasser S. Al Maskari *†‡, Quan Xie *†, Ali Saeedi †

† Discipline of Petroleum Engineering, WA School of Mines: Minerals, Energy and Chemical Engineering, Curtin University, 26 Dick Perry Avenue, Kensington, WA 6151, Australia

‡ Petroleum Development Oman LLC, P.O. Box 81, Code 100, Muscat, Sultanate of Oman

Name	Conception & design	Acquisition of data & method	Data conditioning & manipulation	Analysis & statistical method	Interpretation & discussion	Final approval
Nasser AL Maskari (First author)	X	X	X	X	X	
I acknowledge that these represent my contribution to the above research output. Signature:						
Quan Xie (Co-author 1)	X	X			X	X
I acknowledge that these represent my contribution to the above research output. Signature:						
Ali Saeedi (Co-author 2)						X
I acknowledge that these represent my contribution to the above research output. Signature:						

Paper title: "**Influence of Surface Roughness on the Contact Angle due to Calcite Dissolution in an Oil−Brine−Calcite System: A Nanoscale Analysis Using Atomic Force Microscopy and Geochemical Modeling**" *Energy & Fuels,* 2019, 33, (5), 4219-4224.

Nasser S. Al Maskari *†‡, Ahmad Sari †, Ali Saeedi †, Quan Xie *†

† Discipline of Petroleum Engineering, WA School of Mines: Minerals, Energy and Chemical Engineering, Curtin University, 26 Dick Perry Avenue, Kensington, WA 6151, Australia

‡ Petroleum Development Oman LLC, P.O. Box 81, Code 100, Muscat, Sultanate of Oman

Name	Conception & design	Acquisition of data & method	Data conditioning & manipulation	Analysis & statistical method	Interpretation & discussion	Final approval
Nasser AL Maskari (First author)	X	X	X	X	X	
I acknowledge that these represent my contribution to the above research output. Signature:						
Ahmad Sari (Co-author 1)		X			X	
I acknowledge that these represent my contribution to the above research output. Signature:						
Ali Saeedi (Co-author 2)						X
I acknowledge that these represent my contribution to the above research output. Signature:						
Quan Xie (Co-author 3)	X	X			X	X
I acknowledge that these represent my contribution to the above research output. Signature:						

Paper title: "**Alcohol-Assisted Waterflooding in Carbonate Reservoirs**" *Energy & Fuels,* 2019, 33, (11), 10651-10658.

Nasser S. Al Maskari *†‡, Ali Saeedi †, Quan Xie *†

† Discipline of Petroleum Engineering, WA School of Mines: Minerals, Energy and Chemical Engineering, Curtin University, 26 Dick Perry Avenue, Kensington, WA 6151, Australia

‡ Petroleum Development Oman LLC, P.O. Box 81, Code 100, Muscat, Sultanate of Oman

Name	Conception & design	Acquisition of data & method	Data conditioning & manipulation	Analysis & statistical method	Interpretation & discussion	Final approval
Nasser AL Maskari (First author)	X	X	X	X	X	
I acknowledge that these represent my contribution to the above research output. Signature:						
Ali Saeedi (Co-author 1)						X
I acknowledge that these represent my contribution to the above research output. Signature:						
Quan Xie (Co-author 2)	X	X			X	X
I acknowledge that these represent my contribution to the above research output. Signature:						

Paper title: "**1-Pentanol-Assisted Waterflooding in High Salinity Brine up to 140°C in Carbonate Reservoirs**" *Energy & Fuels,* **(Revised version submitted)**

Nasser S. Al Maskari *†‡, Eghan Arjomand †, Mohamed Almobarak †, Ali Saeedi †, Quan Xie *†

† Discipline of Petroleum Engineering, WA School of Mines: Minerals, Energy and Chemical Engineering, Curtin University, 26 Dick Perry Avenue, Kensington, WA 6151, Australia

‡ Petroleum Development Oman LLC, P.O. Box 81, Code 100, Muscat, Sultanate of Oman

Name	Conception & design	Acquisition of data & method	Data conditioning & manipulation	Analysis & statistical method	Interpretation & discussion	Final approval
Nasser AL Maskari (First author)	X	X	X	X	X	
I acknowledge that these represent my contribution to the above research output. Signature:						
Eghan Arjomand (Co-author 1)		X				
I acknowledge that these represent my contribution to the above research output. Signature:						
Mohamed Almobarak (Co-author 2)		X				
I acknowledge that these represent my contribution to the above research output. Signature:						
Ali Saeedi (Co-author 3)					X	X
I acknowledge that these represent my contribution to the above research output. Signature:						
Quan Xie (Co-author 4)	X	X			X	X
I acknowledge that these represent my contribution to the above research output. Signature:						

Appendix 2

In this section, the copyright agreements between the author and journals are included to reuse the author's own publication in this thesis.

Chapter 4, Article: "Response of Non-Polar Oil Component on Low Salinity Effect in Carbonate Reservoirs: Adhesion Force Measurement Using Atomic Force Microscopy"

energies

an Open Access Journal by MDPI

Indexed in: EI Compendex | CITESCORE 3.18 SCOPUS | IMPACT FACTOR 2.707

CERTIFICATE OF PUBLICATION

Certificate of publication for the article titled:

Response of Non-Polar Oil Component on Low Salinity Effect in Carbonate Reservoirs: Adhesion Force Measurement Using Atomic Force Microscopy

Authored by:

Nasser S. Al Maskari; Ahmad Sari; Md Mofazzal Hossain; Ali Saeedi; Quan Xie

Published in:

Energies 2020, Volume 13, Issue 1, 77

MDPI Academic Open Access Publishing since 2008

Basel, April 2020

Chapter 5, Article: “Influence of pH on Acidic Oil−Brine−Carbonate Adhesion Using Atomic Force Microscopy”

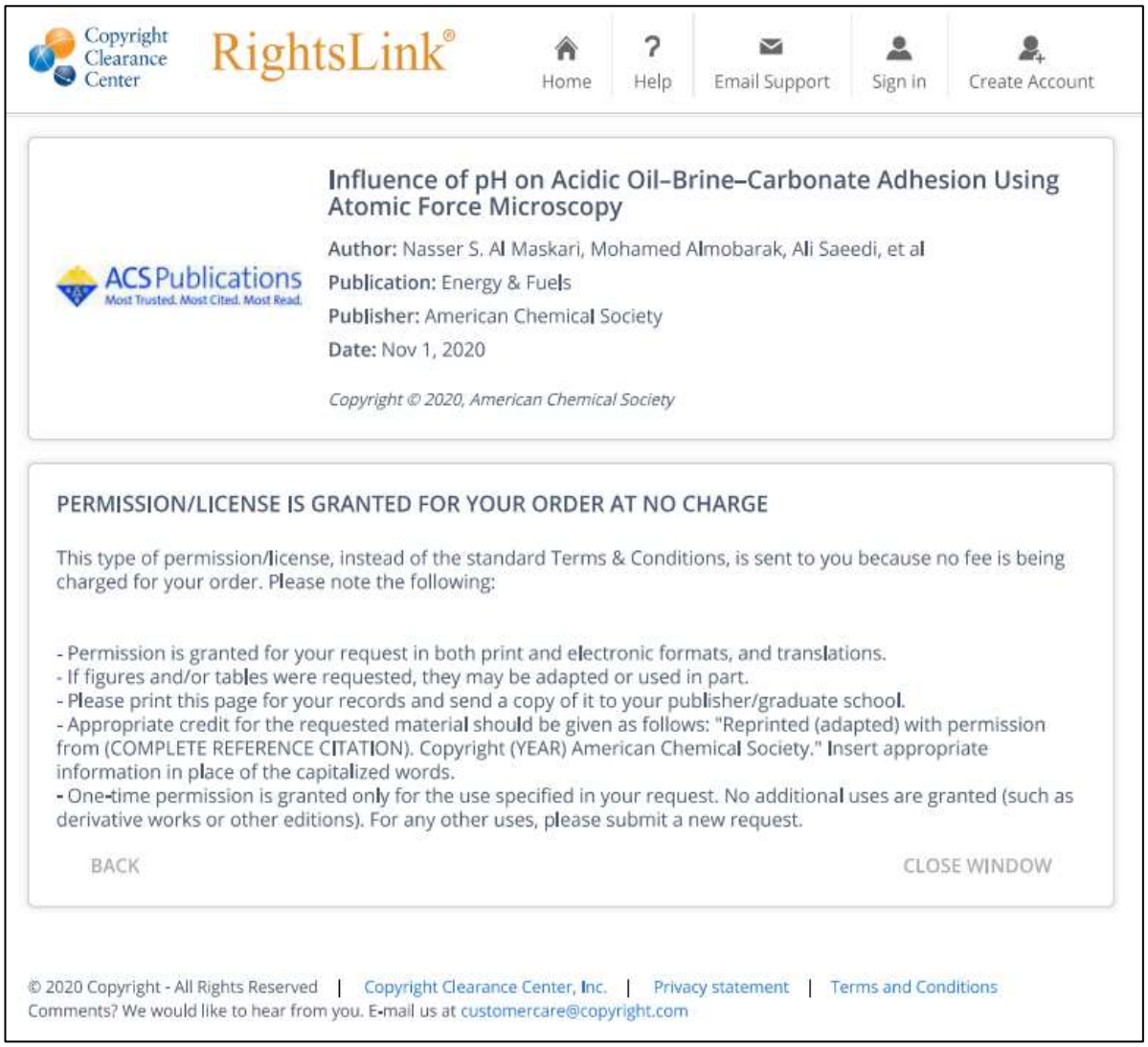

Copyright Clearance Center RightsLink®

Home | Help | Email Support | Sign in | Create Account

ACS Publications
Most Trusted. Most Cited. Most Read.

Influence of pH on Acidic Oil–Brine–Carbonate Adhesion Using Atomic Force Microscopy

Author: Nasser S. Al Maskari, Mohamed Almobarak, Ali Saeedi, et al

Publication: Energy & Fuels

Publisher: American Chemical Society

Date: Nov 1, 2020

Copyright © 2020, American Chemical Society

PERMISSION/LICENSE IS GRANTED FOR YOUR ORDER AT NO CHARGE

This type of permission/license, instead of the standard Terms & Conditions, is sent to you because no fee is being charged for your order. Please note the following:

- Permission is granted for your request in both print and electronic formats, and translations.
- If figures and/or tables were requested, they may be adapted or used in part.
- Please print this page for your records and send a copy of it to your publisher/graduate school.
- Appropriate credit for the requested material should be given as follows: "Reprinted (adapted) with permission from (COMPLETE REFERENCE CITATION). Copyright (YEAR) American Chemical Society." Insert appropriate information in place of the capitalized words.
- One-time permission is granted only for the use specified in your request. No additional uses are granted (such as derivative works or other editions). For any other uses, please submit a new request.

BACK CLOSE WINDOW

Chapter 6, Article: “Role of Basal-Charged Clays in Low Salinity Effect in Sandstone Reservoirs: Adhesion Force on Muscovite using Atomic Force Microscope”

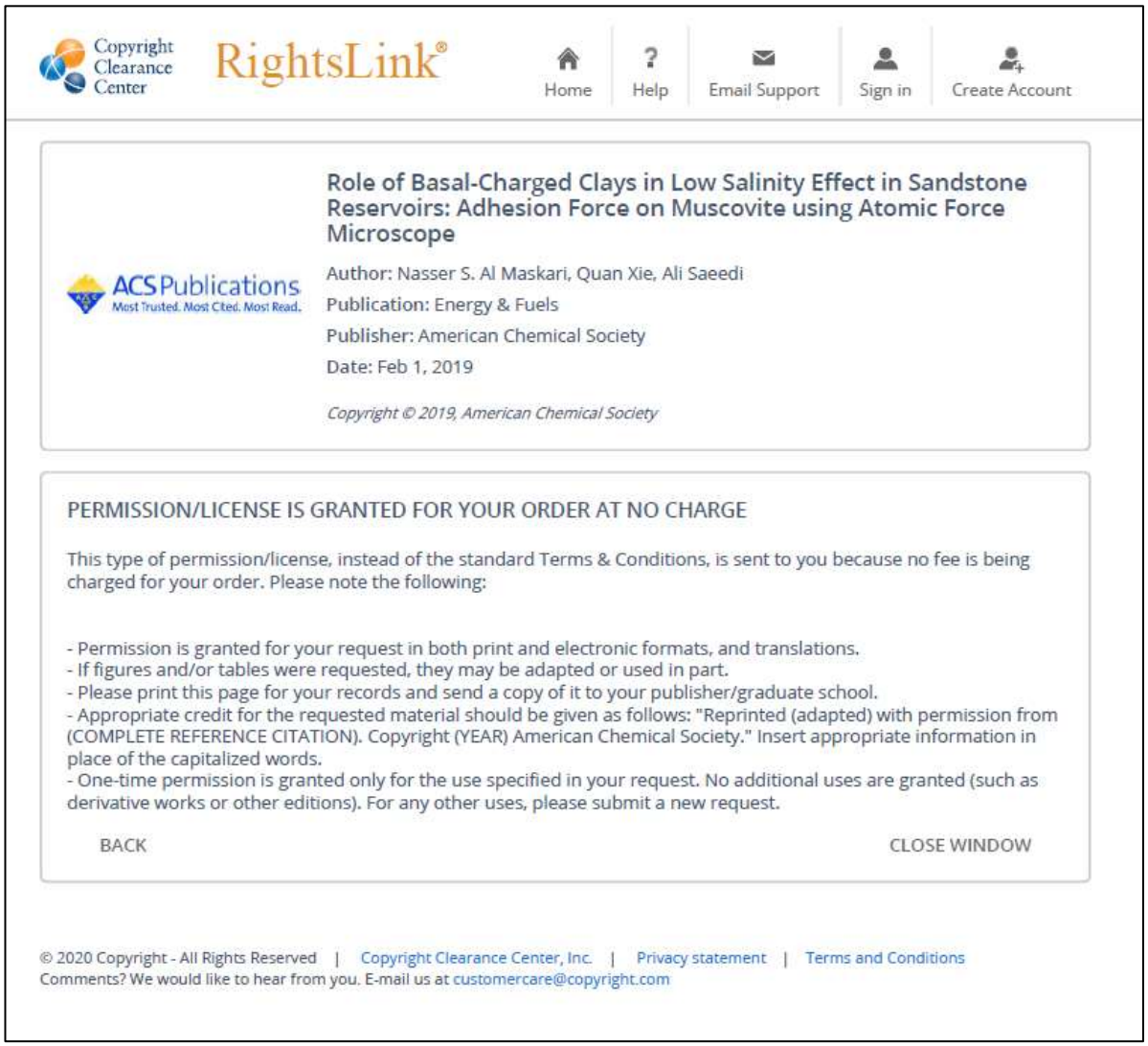

Copyright Clearance Center RightsLink®

Home | Help | Email Support | Sign in | Create Account

Role of Basal-Charged Clays in Low Salinity Effect in Sandstone Reservoirs: Adhesion Force on Muscovite using Atomic Force Microscope

ACS Publications
Most Trusted. Most Cited. Most Read.

Author: Nasser S. Al Maskari, Quan Xie, Ali Saeedi
Publication: Energy & Fuels
Publisher: American Chemical Society
Date: Feb 1, 2019

Copyright © 2019, American Chemical Society

PERMISSION/LICENSE IS GRANTED FOR YOUR ORDER AT NO CHARGE

This type of permission/license, instead of the standard Terms & Conditions, is sent to you because no fee is being charged for your order. Please note the following:

- Permission is granted for your request in both print and electronic formats, and translations.
- If figures and/or tables were requested, they may be adapted or used in part.
- Please print this page for your records and send a copy of it to your publisher/graduate school.
- Appropriate credit for the requested material should be given as follows: "Reprinted (adapted) with permission from (COMPLETE REFERENCE CITATION). Copyright (YEAR) American Chemical Society." Insert appropriate information in place of the capitalized words.
- One-time permission is granted only for the use specified in your request. No additional uses are granted (such as derivative works or other editions). For any other uses, please submit a new request.

BACK CLOSE WINDOW

Chapter 7, Article: “Influence of Surface Roughness on the Contact Angle due to Calcite Dissolution in an Oil−Brine−Calcite System: A Nanoscale Analysis Using Atomic Force Microscopy and Geochemical Modeling”

Copyright Clearance Center RightsLink®

Home | Help | Email Support | Sign in | Create Account

Influence of Surface Roughness on the Contact Angle due to Calcite Dissolution in an Oil–Brine–Calcite System: A Nanoscale Analysis Using Atomic Force Microscopy and Geochemical Modeling

ACS Publications
Most Trusted. Most Cited. Most Read.

Author: Nasser S. Al Maskari, Ahmad Sari, Ali Saeedi, et al
Publication: Energy & Fuels
Publisher: American Chemical Society
Date: May 1, 2019

Copyright © 2019, American Chemical Society

PERMISSION/LICENSE IS GRANTED FOR YOUR ORDER AT NO CHARGE

This type of permission/license, instead of the standard Terms & Conditions, is sent to you because no fee is being charged for your order. Please note the following:

- Permission is granted for your request in both print and electronic formats, and translations.
- If figures and/or tables were requested, they may be adapted or used in part.
- Please print this page for your records and send a copy of it to your publisher/graduate school.
- Appropriate credit for the requested material should be given as follows: "Reprinted (adapted) with permission from (COMPLETE REFERENCE CITATION). Copyright (YEAR) American Chemical Society." Insert appropriate information in place of the capitalized words.
- One-time permission is granted only for the use specified in your request. No additional uses are granted (such as derivative works or other editions). For any other uses, please submit a new request.

BACK CLOSE WINDOW

© 2020 Copyright - All Rights Reserved | Copyright Clearance Center, Inc. | Privacy statement | Terms and Conditions
Comments? We would like to hear from you. E-mail us at customercare@copyright.com

Chapter 8, Article: “Alcohol-Assisted Waterflooding in Carbonate Reservoirs”

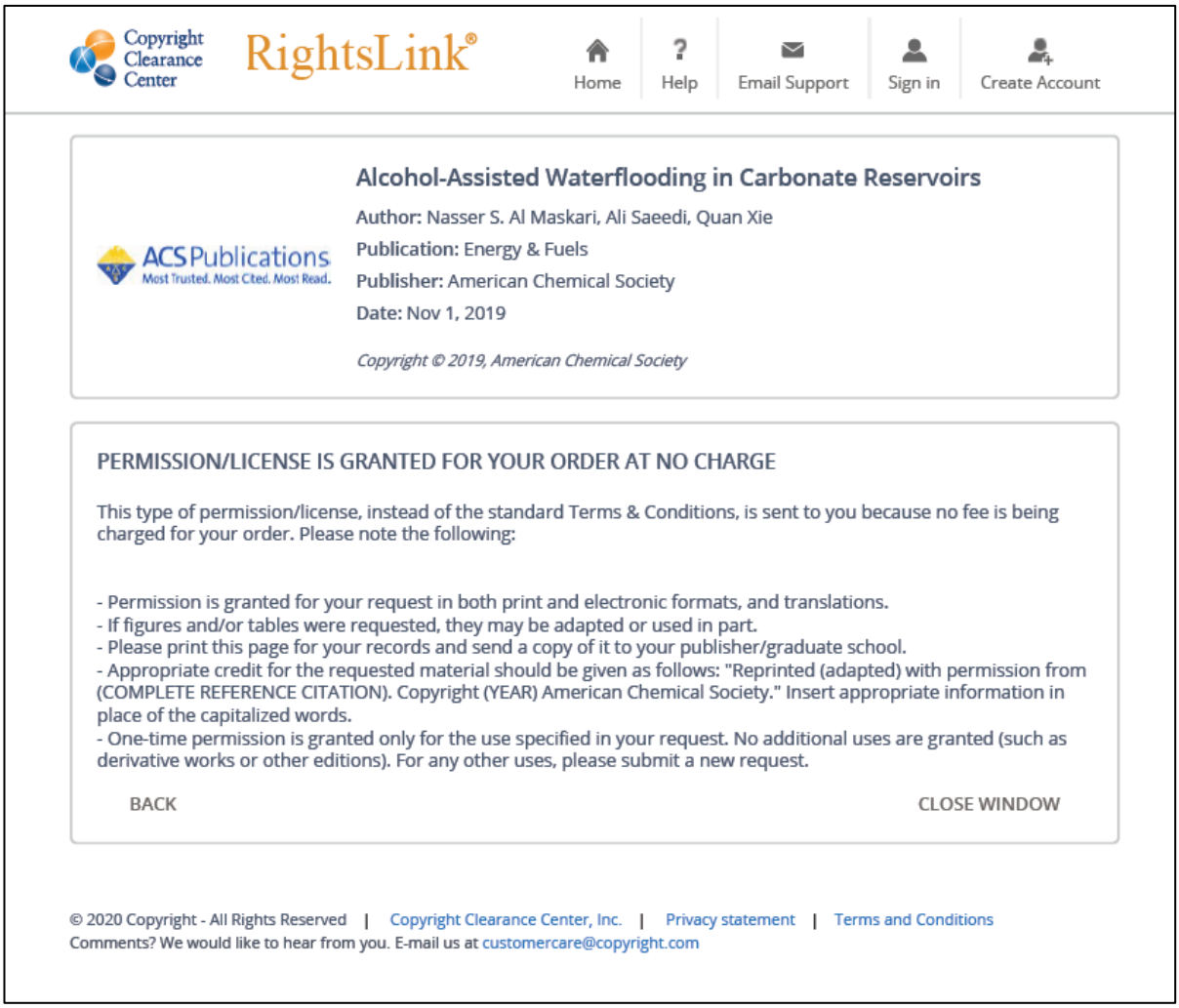

Copyright Clearance Center RightsLink®

Home | Help | Email Support | Sign in | Create Account

ACS Publications
Most Trusted. Most Cited. Most Read.

Alcohol-Assisted Waterflooding in Carbonate Reservoirs

Author: Nasser S. Al Maskari, Ali Saeedi, Quan Xie
Publication: Energy & Fuels
Publisher: American Chemical Society
Date: Nov 1, 2019

Copyright © 2019, American Chemical Society

PERMISSION/LICENSE IS GRANTED FOR YOUR ORDER AT NO CHARGE

This type of permission/license, instead of the standard Terms & Conditions, is sent to you because no fee is being charged for your order. Please note the following:

- Permission is granted for your request in both print and electronic formats, and translations.
- If figures and/or tables were requested, they may be adapted or used in part.
- Please print this page for your records and send a copy of it to your publisher/graduate school.
- Appropriate credit for the requested material should be given as follows: "Reprinted (adapted) with permission from (COMPLETE REFERENCE CITATION). Copyright (YEAR) American Chemical Society." Insert appropriate information in place of the capitalized words.
- One-time permission is granted only for the use specified in your request. No additional uses are granted (such as derivative works or other editions). For any other uses, please submit a new request.

BACK CLOSE WINDOW

Chapter 9, Article: “1-Pentanol-Assisted Waterflooding in High Salinity Brine up to 140 °C in Carbonate Reservoirs

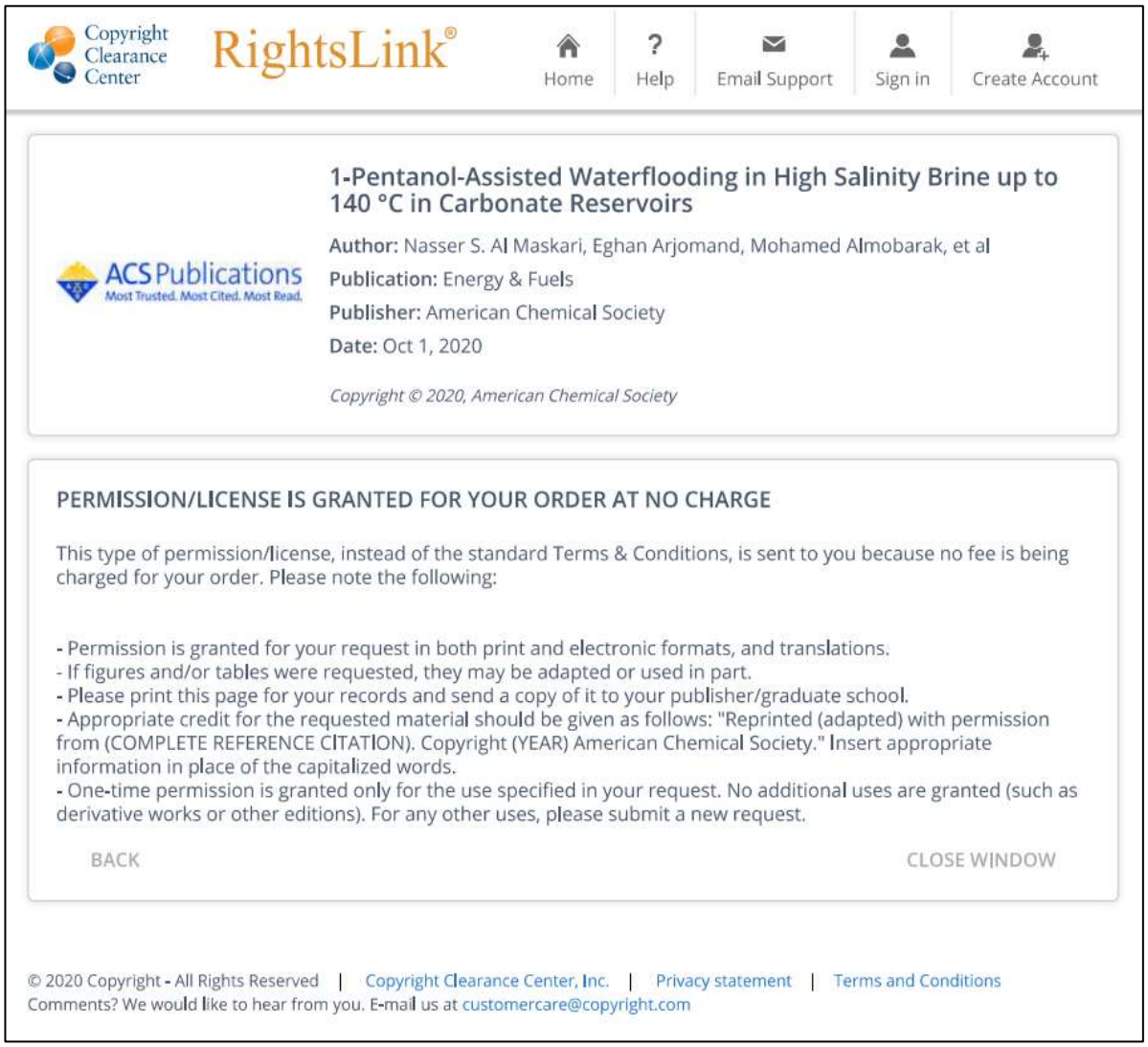

Appendix 3

In this section, the photographs of the main devices are presented here:

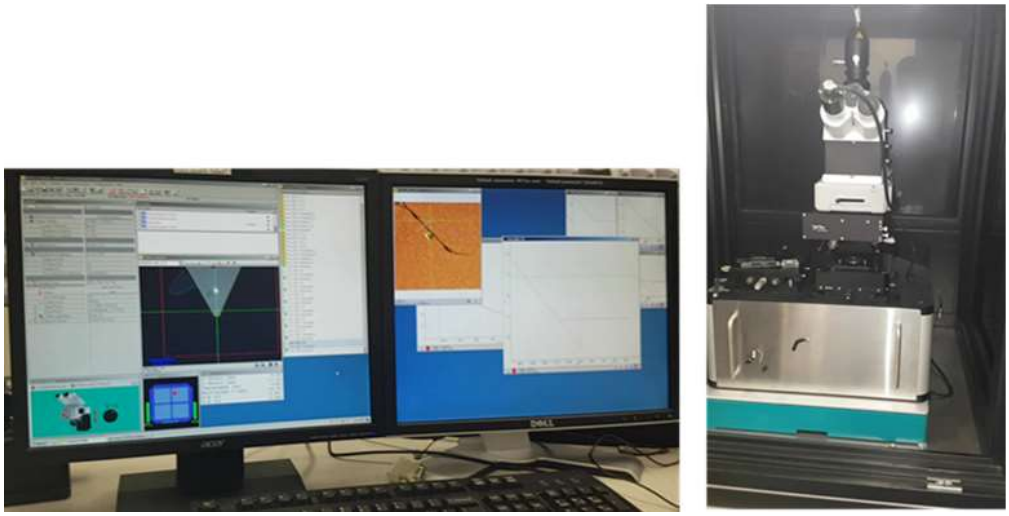

Figure A-1: Photograph of Atomic force microscopy (WITec alpha 300 SAR)

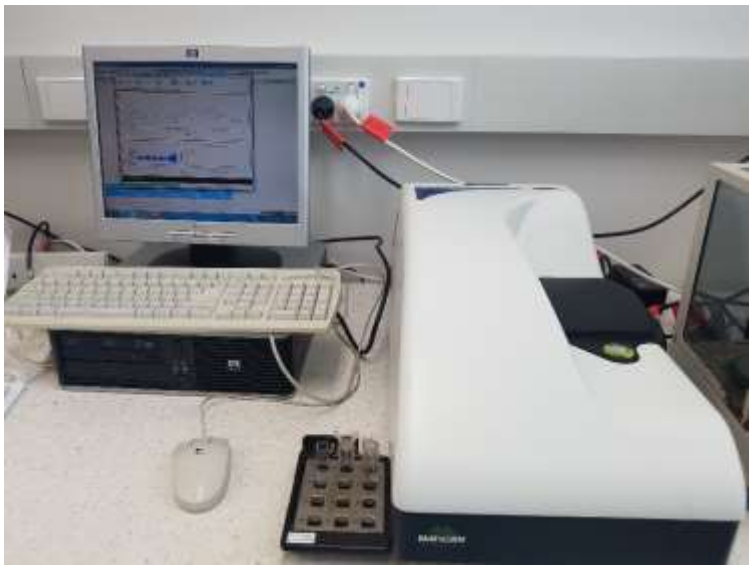

Figure A-2: Photograph of Malvern Zetasizer ZS Nano series

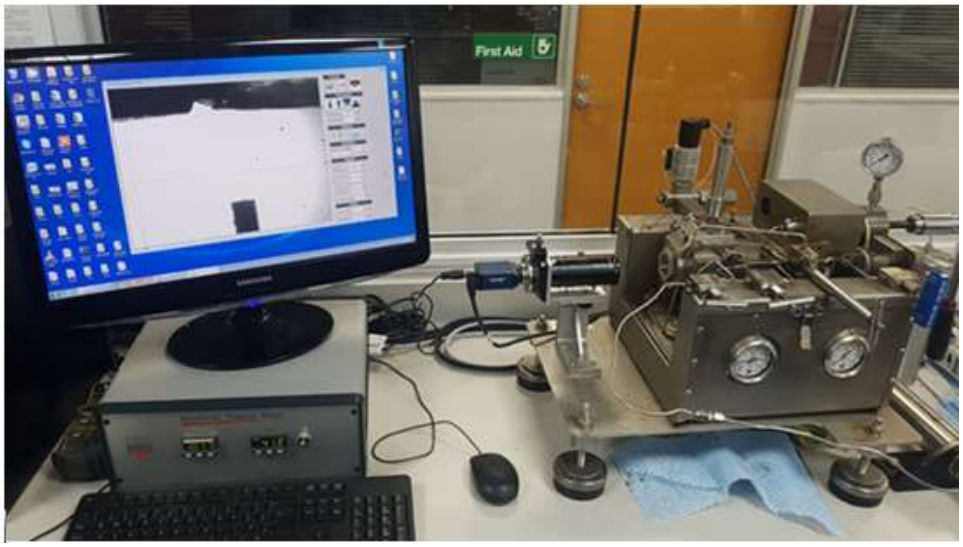

Figure A-3: Photograph of Vinic IFT-700 apparatus

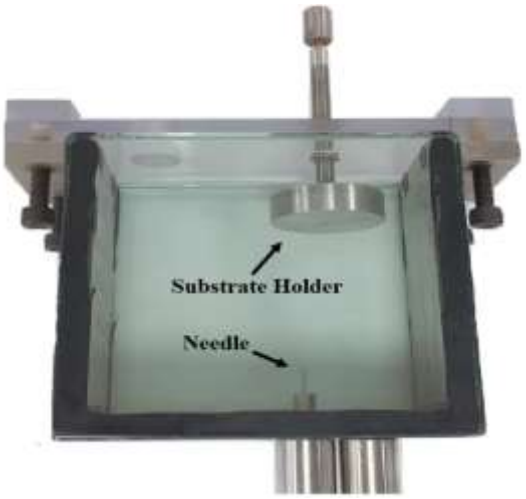

Figure A-4: Photograph of Our labs contact angle cell

Figure A-5: Porosi-permeameter instrument (AP-608)

Figure A-6: Photograph of plasma device

Appendix 4

In this section, the results and additional information are presented here:

Chapter 4,5&6:

❖ Stages of force distance curve

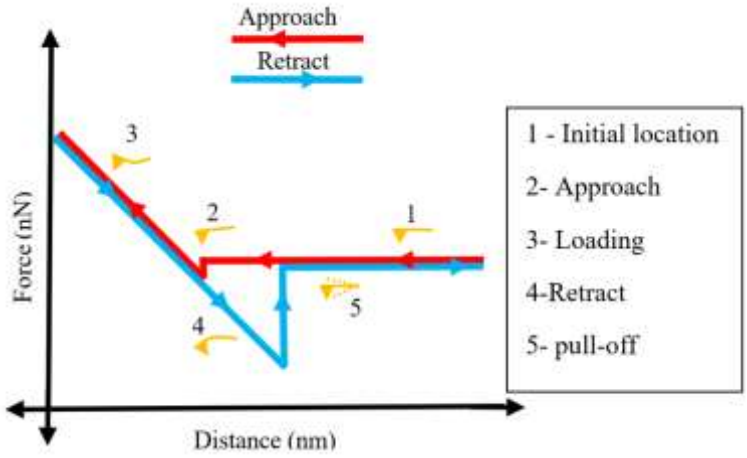

Figure A-9: Change of contact angle in HS and LS brines.

Chapter 7:

❖ Table A-1: Contact angle results

Sample	Brine	Contac Angle (°)
1	High salinity brine	165
2	High salinity brine	164
2	Low salinity brine	105

❖ Change of contact angle in high and low salinity brines

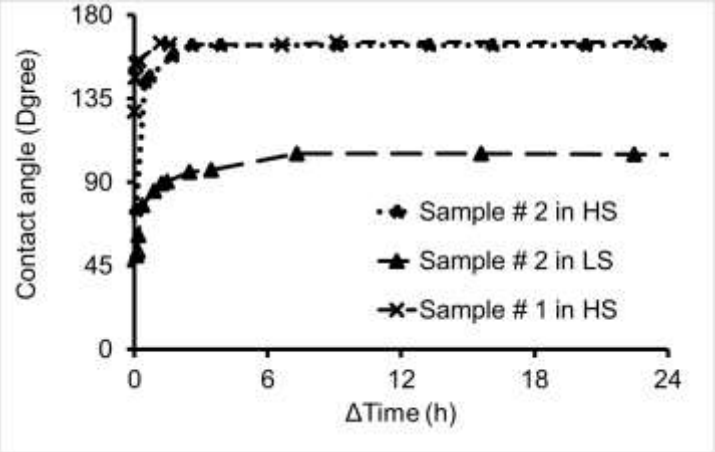

Figure A-7: Change of contact angle in HS and LS brines.

❖ The difference between the true surface area and reference surface area in roughness factor equation:

$$r = \frac{True\ surface\ area}{Reference\ surface\ \ area} \qquad \text{Eq } 7-4$$

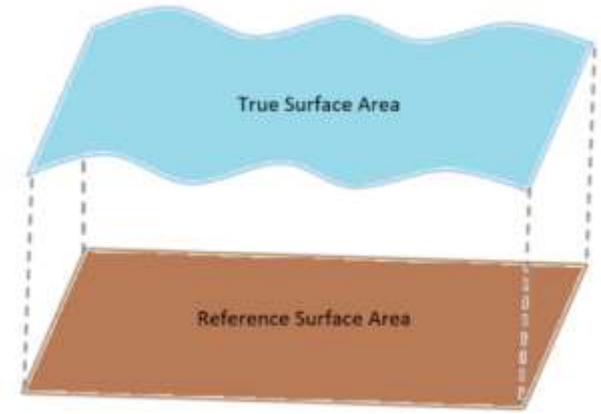

Figure A-8: True surface area and reference surface area.

Chapter 8:

❖ Table A-2: Contact angle in the presence of high salinity brine

	Contact Angle (°)
HSW	165.0
HSW+1% Ethanol	158.0
HSW+1% Isopropanol	160.0
HSW+1% Glycerol	160.0
HSW+1% Pentanol	125.0

❖ Table A-3: Contact angle in the presence of low salinity brine

	Contact Angle (°)
LSW	105.0
LSW+1% Ethanol	116.0
LSW+1% Isopropanol	135.0
LSW+1% Glycerol	118.0
LSW+1% Pentanol	90.0

❖ Table A-4: Zeta potential in the presence of high salinity brine

	Zeta potential (mV)	
	oil/brine	brine/Calcite
HSW	-24.2	10.1
HSW+1% Ethanol	-19.3	8.8
HSW+1% Isopropanol	-20.7	7.5
HSW+1% Glycerol	-28.7	8.1
HSW+1% Pentanol	-18.3	9.3

- Table A-5: Zeta potential in the presence of low salinity brine

	Zeta potential (mV)	
	oil/brine	brine/Calcite
LSW	-61.4	-5.2
LSW+1% Ethanol	-61.8	-0.7
LSW+1% Isopropanol	-54.2	0.9
LSW+1% Glycerol	-56.3	-1.2
LSW+1% Pentanol	-39.9	0.2

Chapter 9:

- Table A-6: Contact angle results of the oil droplet on the calcite surface at different temperatures and pressures in the presence of the HS brine only.

	Pressure (MPa)			
Temperature (C)	10	20	30	40
60	161.5	161.1	161.6	162.0
100	160.2	160.7	161.7	162.1
140	160.5	160.9	161.3	161.7

- Table A-7: Contact angle results of the oil droplet on the calcite surface at different temperatures and pressures in the presence of the HS brine with 1% 1-pentanol

	Pressure (MPa)			
Temperature (C)	10	20	30	40
60	83.8	84.3	86.2	84.6
100	98.9	99.9	99.6	100.3
140	101.2	103.1	102.2	102.9

❖ Table A-8: Contact angle results of the oil droplet on the calcite surface at different temperatures and pressures in the presence of the LS brine only

	Pressure (MPa)			
Temperature (C)	10	20	30	40
60	88.6	88.3	88.5	88.4
100	87.8	88.5	88.3	88.4
140	88.3	88.4	88.6	88.5

❖ Table A-9: Contact angle results of the oil droplet on the calcite surface at different temperatures and pressures in the presence of the LS brine with 1% 1-pentanol

	Pressure (MPa)			
Temperature (C)	10	20	30	40
60	81.2	81.3	81.4	81.6
100	101.1	100.9	100.9	101.0
140	96.7	97.0	96.9	97.3

❖ Table A-10: Some Petrophysical Properties of Core Plugs

Core sample	Porosity (%)	Gas Permeability (mD)	Pore Volume (CC)
C1	27.2	7.4	19.1
C2	25.7	4.5	18.4
C3	29.7	8.2	22.6
C4	25.9	5.4	18.0